

(NASA-CR-120184) LINEAR TEST BED.
VOLUME 1: TEST BED NO. 1 Final Report
(Rocketdyne) 252 p HC \$15.75 CSCL 14B

N74-19892

G3/11 Unclass
34957

R-9049

LINEAR TEST BED
FINAL REPORT
VOLUME I: TEST BED NO. 1

30 August 1972

Contract NAS8-25156

Rocketdyne Engineering
Canoga Park, California

APPROVED BY


P. N. Fuller
J-2 Program Manager



Rocketdyne
North American Rockwell

8833 Canoga Avenue.
Canoga Park, California 91304



1X224-12/2/71-S1*

Frontispiece: Linear Test Bed Firing

PRECEDING PAGE BLANK NOT FILLED

R-9049

iii/iv

CONTENTS

Introduction	1
Summary	1
Concept Selection	11
Design and Fabrication	13
Fluorine Ignition System	13
Combustion Wave Ignition System	14
Control System	14
Purge System	24
Ground Support Equipment	27
Delta-2B Facility Modification	28
Combustor Design	29
Injector Design	44
Nozzle Assembly Design	49
Coolant Tube Design	53
Thrust Chamber Fabrication and Assembly	55
Combustor Flow Distribution and Calibration	57
Base Seal	60
System Operation and Performance	71
Test Summary	71
Start and Cutoff	71
Ignition System Operation	90
Ignition Systems Problem Resolution	94
Mainstage Performance	97
Thrust Vector Measurements	98
Thrust Chamber Performance	118
Hardware Durability	135
Nozzle Tube Durability	135
End Fence Durability	146
Injectors and Igniter Elements Durability	146
Nozzle Assembly Durability	148
Turbine Exhausts and Base Seal Durability	148
Combustor Erosion	151

Component Development Program	177
Ignition Systems	177
Single-Segment C01 Testing	203
Injector Element Mixing Tests	207
C06 Single-Segment Test Program	216
High-Frequency Stability Analysis	221
Segment and Multisegment	221
Discussion	222
Characterization of Stability for a Typical Test	222
Feed-System-Coupled Oscillations	225
001 Segment Stability Results	237
Breadboard No. 1 High-Frequency Results	238

ILLUSTRATIONS

Frontispiece: Linear Test Bed Firing	iii
1. Test Bed	2
2. General Arrangement, End View	3
3. General Arrangement, Side View	4
4. General Arrangement, Top View	5
5. Test Bed Prior to Shipment of Delta-2B	6
6. Test Bed Installation at Delta-2B	7
7. Breadboard Thrust Chamber Evaluation Gaseous Fluorine Ignition System	15
8. Linear Test Bed Program Combustion Wave Ignition System	16
9. Linear Engine, Breadboard No. 1 Combustion Wave Ignition Unit	17
10. Combustion Wave Igniter Elements Posttest	18
11. Linear Engine Schematic	19
12. Electrical Control Ground Box	22
13. Purge Systems Sequence of Operation	25
14. NARloy Cast Liner	31
15. Breadboard Engine Combustor Assembly	33
16. Cast Liner Breadboard Design	35
17. Breadboard Engine Contour Wall Channel Parameters vs Axial Length	37
18. Breadboard Engine End Plate Channel Parameters vs Axial Length	38
19. Final Combustor Segment Assembly	41
20. Oxidizer Manifold Geometry	47
21. Oxidizer Post Geometry	48
22. Oxidizer Post, Fuel Cup Installation	50
23. Nozzle Wall Pressure Profile	52
24. Lines of Maximum OD/T_w for 347 CRES and INCO 625 With 2160-psia Internal Pressure	54
25. Flow Resistance for the Parallel System	58
26. Base Seal Engine Installation	63
27. Maximum Base Seal Shear Deformation	64
28. Waffle Pattern Seal Sample After Forming to Simulate Engine Seal Configuration	67

29.	Base Seal Corner Segment Mechanical Cycling Test Setup.	68
30.	Double Exposure of Corner Section of Base Seal During Mechanical Cycling	69
31.	Test Bed No. 1 Start Sequence (Fluorine Ignition)	81
32.	Linear Test Bed Program, Test Bed No. 1 Start Sequence Combustion Wave Ignition	83
33.	Linear Test Bed Program Chamber Pressure vs Time, Test 012	84
34.	Linear Test Bed Program Fuel Turbine Inlet Pressure, Test 012	85
35.	Linear Test Bed Program Fuel Turbine Inlet Temperature, Test 012	86
36.	Linear Test Bed Program, Mark 29 Fuel Pump Start Transient Head vs Flow, Test 012	87
37.	Linear Test Bed Program, Composite of 19 Chamber Pressures, Test 011	88
38.	Test Bed No. 1 Start Transient Main Thrust, Test 024-027	89
39.	Linear Test Bed Program, Test Bed No. 1 Cutoff Sequence	91
40.	Test Bed No. 1 Cutoff Transients, Main Thrust	92
41.	Combustion Wave Ignition Sequence	95
42.	Linear Test Bed Program, Site Engine Specific Impulse vs Chamber Pressure and Mixture Ratio	105
43.	Linear Test Bed Program, Test Bed No. 1 Performance Trends, Test 624-028	106
44.	Linear Test Bed Program, Test Bed No. 1 Performance Trends, Test 624-028	107
45.	Linear Test Bed Program, Test Bed No. 1 Performance Trends, Test 624-028	108
46.	Linear Test Bed Program, Test Bed No. 1 Performance vs Mixture Ratio, Test 624-028	109
47.	Linear Test Bed Program, Test Bed No. 1 Performance vs Mixture Ratio, Test 624-028	110
48.	Linear Test Bed Program, Test Bed No. 1 Performance vs Mixture Ratio, Test 624-028	111
49.	Linear Test Bed Program, Test Bed No. 1 Performance vs Mixture Ratio, Test 624-028	112
50.	Linear Test Bed Program, Test Bed No. 1 Performance vs Mixture Ratio, Test 624-028	113

51.	Load Cell Locations and Axis Definitions	114
52.	Linear Test Bed Program Thrust Vector Analysis; Pierce Point Displacement in the X-Z Plane	119
53.	Breadboard No. 1 Engine Mixture Ratio vs Chamber Pressure	120
54.	Engine Performance vs Chamber Pressure	121
55.	Wind Tunnel Test Data	124
56.	Breadboard Engine No. 1 Nozzle Pressure Profile	125
57.	Breadboard Engine No. 1 Nozzle Pressure Profile	126
58.	Breadboard Engine No. 1 Nozzle Pressure Profile	127
59.	Nozzle Heat Load vs Pressure Ratio	128
60.	Average Base Pressure vs Nozzle Pressure Ratio	130
61.	Estimated Base Pressure Profiles	131
62.	Linear Breadboard No. 1 Combustor Flow Balance Studies, Inner Temperature vs Outer Contour Wall Temperature (Test 016-029)	132
63.	Linear Breadboard No. 1 Combustor Flow Balance Studies, Inner Temperature vs Outer Contour Wall Temperature (Test 016-029)	133
64.	Location of Segments Which Exhibited Eroded Nozzle Tubes	139
65.	Typical Tube Erosion (Posttest 623-001)	140
66.	Number and Location of Eroded Tubes	
67.	Initial 3-Inch-Wide Zirconium Oxide Coating Prior to Test (623-002)	143
68.	Typical Nozzle Zirconium Oxide Coating Chipping	144
69.	End Fence Buckling	147
70.	Nozzle Tube Wall Ripples (Posttest 624-010)	149
71.	Turbine Exhaust and Base Seal Damage Following Test 624-007	150
72.	Combustor Erosion	155
73.	Combustion Erosion Rework	156
74.	Combustor Wall Erosions, Breadboard No. 1	162
75.	Comparison of Combustor Erosion Characteristics	163
76.	Linear Breadboard No. 1 Combustor Heat Flux Parameter	165
77.	Heat Flux Parameter vs Test Number	167
78.	Theoretical Wall Temperature	169
79.	Average Wall Temperature Parameter History Breadboard No. 1	171
80.	Maximum Gas Side-Wall Temperature Breadboard Engine No. 1	172
81.	Wall Temperature History Three Segment Testing	173

82.	Combustor Surface Roughness Analysis	175
83.	Multisegment Test Stand Cell 18A, CTL-3 Santa Susana Field Laboratory (Front View)	178 179
84.	Igniter Element	179
85.	Ignition Sequence Comparison Component and Simulated Engine Start Sequence	180 182
86.	Fluorine Ignition, Oxygen/Hydrogen Ignition Limits	184
87.	Combustion Wave Ignition Sequence	187
88.	High-Pressure Test Fixture	188
89.	Fluorine-Combustion Wave Interchangeable Ignition System	189
90.	Combustion Wave Igniter Configuration for Segment Testing	190
91.	Combustion Wave Ignition System Test Setup	193
92.	Combustion Wave Ignition System Spark Igniter Unit	193
93.	Research Area Test Data, Mixer Mixture Ratio Versus Element Mixture Ratio, Combustion Wave Igniter	194 194
94.	Combustion Wave Ignition System Simultaneous Ignition, 10 Elements	196
95.	Combustion Wave Ignition System Simultaneous Ignition, 20 Elements	196
96.	Oscillograph Trace, Test No. 975-085	200
97.	Operating Region for the Development Model Mixer	201
98.	Operating Region for the Breadboard No. 1 Mixer (20-Element Mixer)	202
99.	Element Mixing Test Apparatus	210
100.	Normalized Mass Flux vs Inches From Centerline (Run No. 13)	211
101.	Normalized Mass Flux vs Inches From Centerline	212
102.	Normalized Mass Flux vs Inches From Centerline (Run No. 7)	213
103.	Effect of Fuel Velocity on Mixture Ratio Distribution (Transient Conditions)	214 215
104.	Effects of Recess on Mixture Ratio Distribution	215
105.	Mixing Results, Transient	224
106.	Stability Characteristics, Multisegment Test 975-008	226
107.	Injector Element Feedback	228
108.	Linear Engine Combustion Response	229
109.	Oxidizer Injection Pressure, Test No. 975-008	231
110.	Hydraulic Response	233
111.	Effect of Oxidizer Post Inserts	234
112.	Real Time Spectral Analysis	234

TABLES

1.	Operating Parameters for Combustor Design	32
2.	Combustor Design Parameter	32
3.	Cast Segment Injector Parameters	45
4.	Combustor Flow Analysis	61
4a.	Linear Test Bed Program, Test Summary	72
5.	Linear Test Bed Program, Mainstage Test Summary	99
6.	Test Bed No. 1 Mainstage Performance Test 624-029 and Rated	103
7.	Linear Test Bed Program Test Bed No. 1, Thrust Vector Data	115
8.	Comparison of Design and Test Operating Conditions	134
9.	Breadboard Engine No. 1 Posttest Hardware Conditions	136
10.	Differences Observed in the Breadboard Engine Versus Component Testing	152
11.	Breadboard Engine No. 1 Mainstage Test Combustor Erosion Summary	157
12.	Combustor Erosion Summary, Breadboard Engine No. 1 Posttest 624-005	160
13.	Breadboard Test Bed No. 1 Erosion Summary Posttest 624-031	161
14.	Combustion Wave Tests on Multisegment Hardware	198
15.	Stabilized Test Conditions	205
16.	Summary of Cold-Flow Tests Conducted	209
17.	Single Segment Test Summary, SSFL, CTL-3, Cell 18A	218

INTRODUCTION

The Linear Test Bed program objectives were to design, fabricate, and evaluation test an advanced aerospike test bed which employed the segmented combustor concept. The program started in April 1970 with the release of a work statement by NASA-MSFC and was finished in June 1972 with the successful completion of 44 tests on the linear test bed. This report describes the complete program including concept selection, design, fabrication, component test, system test, supporting analysis, and posttest hardware inspection.

SUMMARY

The Linear Test Bed was evaluated during the Saturn System O&FS program. An isometric drawing and three views of the general arrangement drawings of the test bed are shown in Fig. 1 through 4.

The system is designated as a linear aerospike system and consists of a thrust chamber assembly, a power package, and a thrust frame. It was designed as an experimental system to demonstrate the feasibility of the linear aerospike-segmented combustor concept. The overall dimensions are 120 inches long by 120 inches wide by 96 inches in height. Photos of the completed test bed are shown in Fig. 5 and 6.

The propellants are liquid oxygen/liquid hydrogen. The system was designed to operate at 1200-psia chamber pressure, at a mixture ratio of 5.5. At the design conditions, the sea level thrust is 200,000 pounds.

The thrust chamber assembly consists of 20 combustors, 2 nozzle assemblies, a turbine exhaust base manifold, and the supporting rib structure and tie linkages. The combustors are made from precision investment-cast NARloy (silver-copper alloy) which undergoes a process in which nickel is electroplated to the outside of the liner to provide coolant channel closeout and for structural purposes. An aluminum

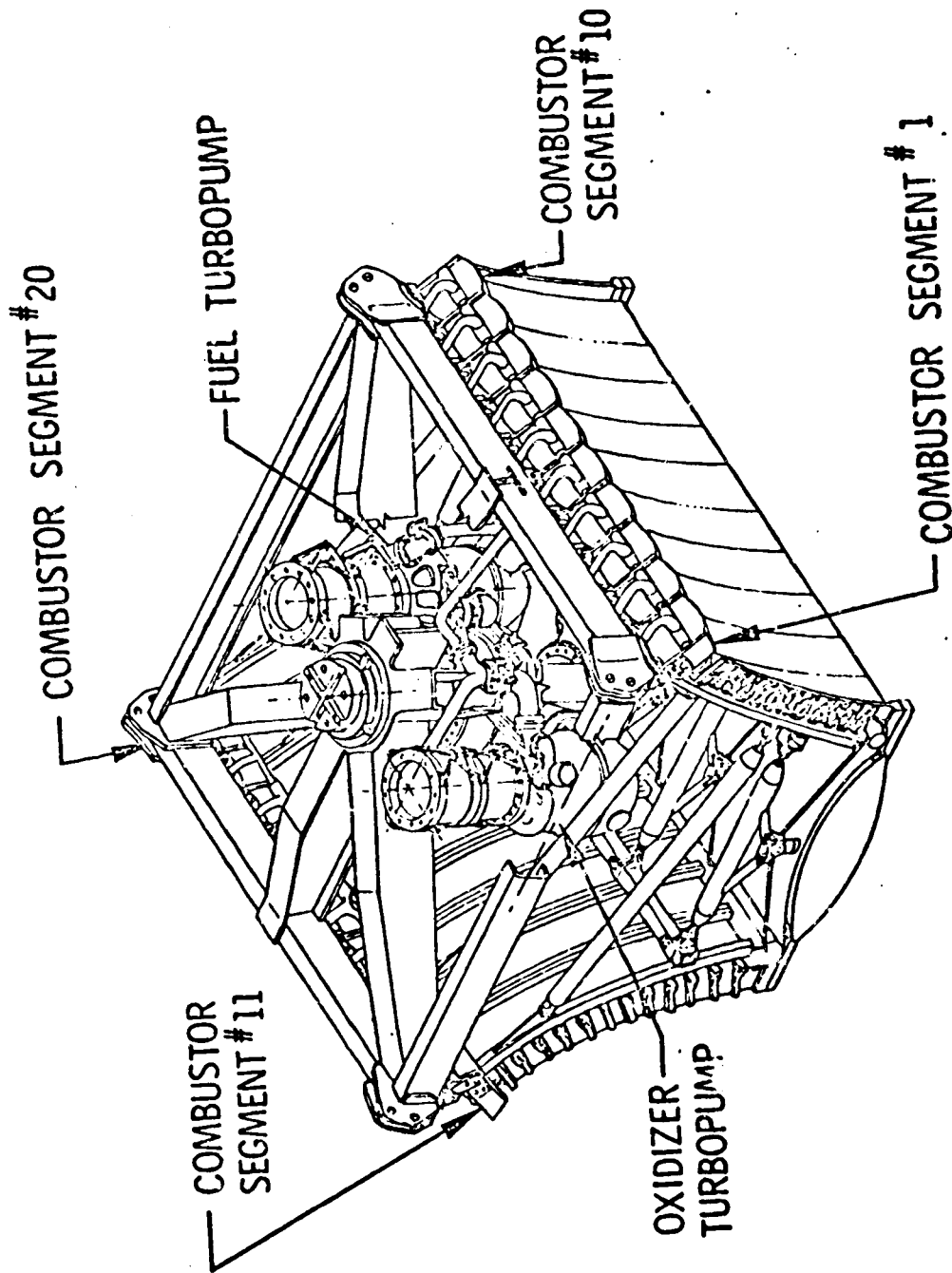


Figure 1. Test Bed

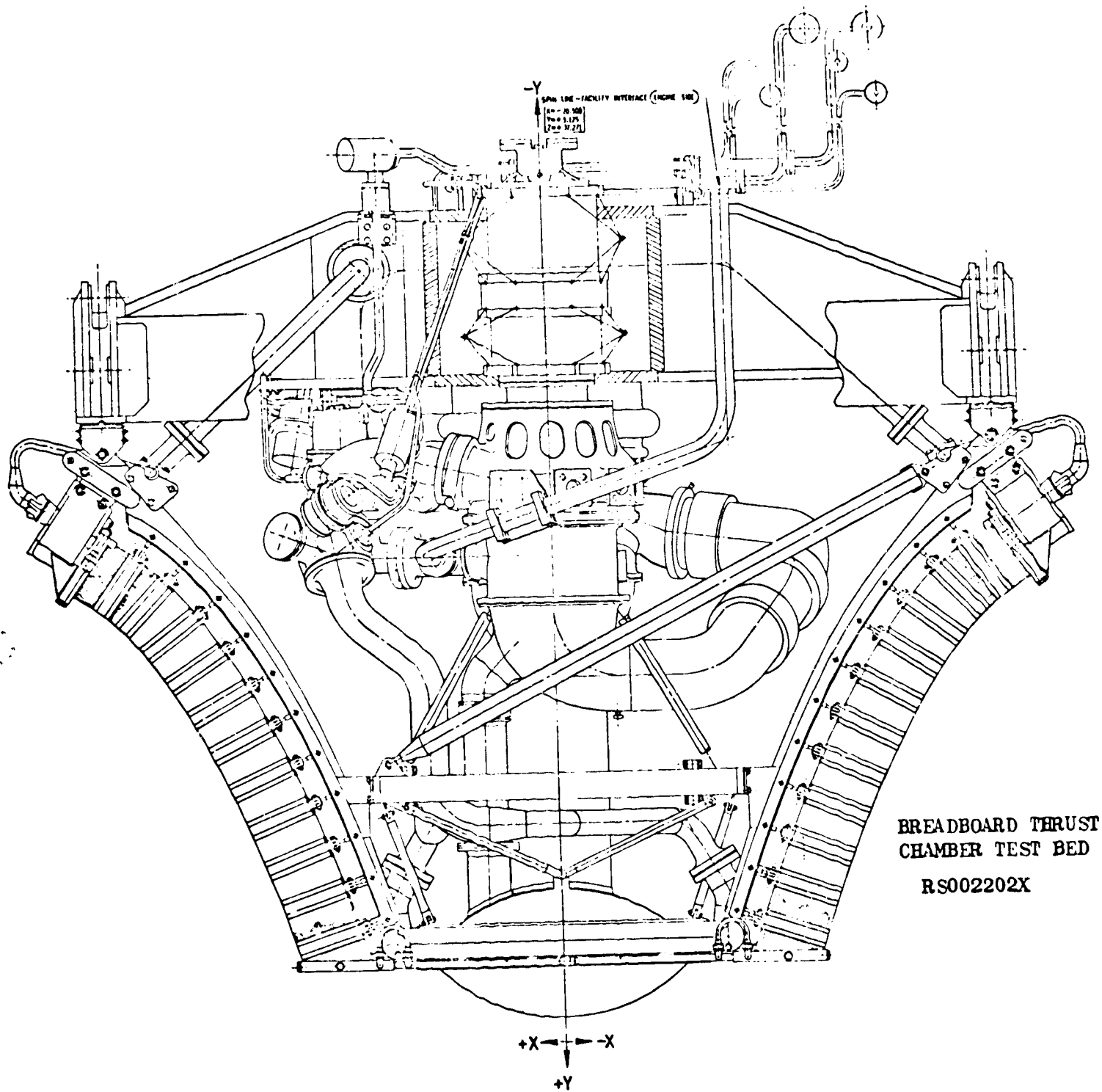


Figure 2. General Arrangement, End View

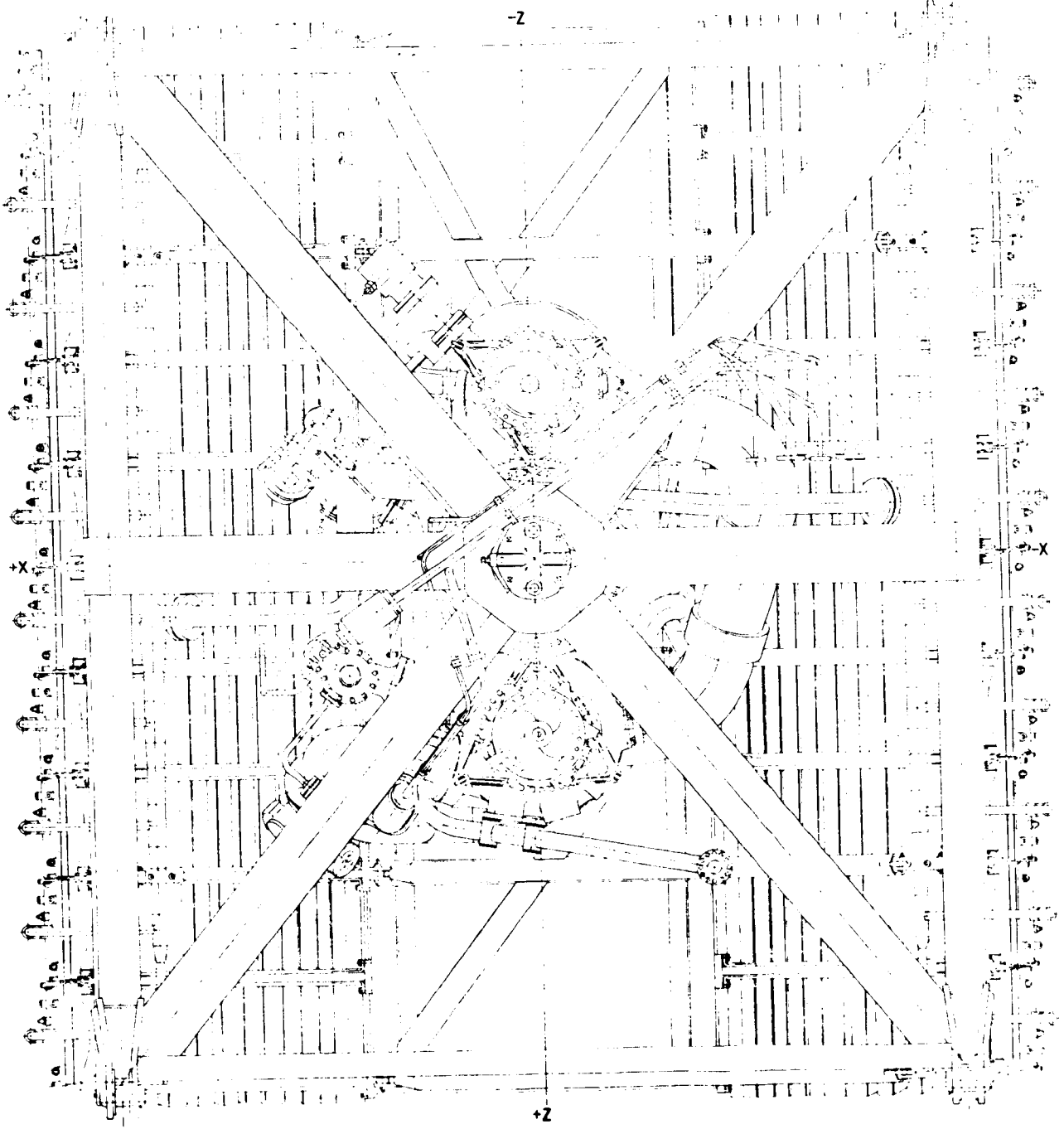
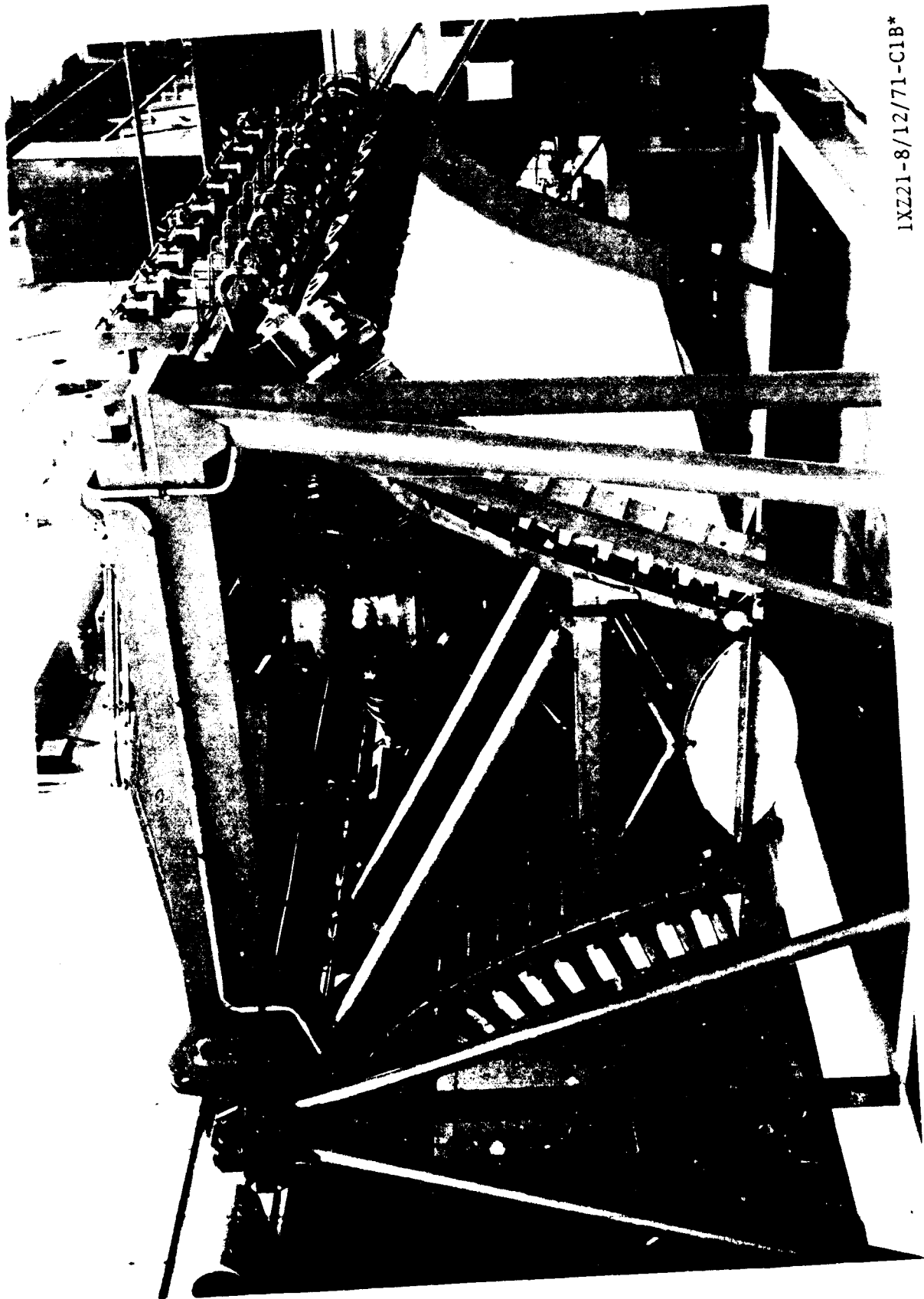
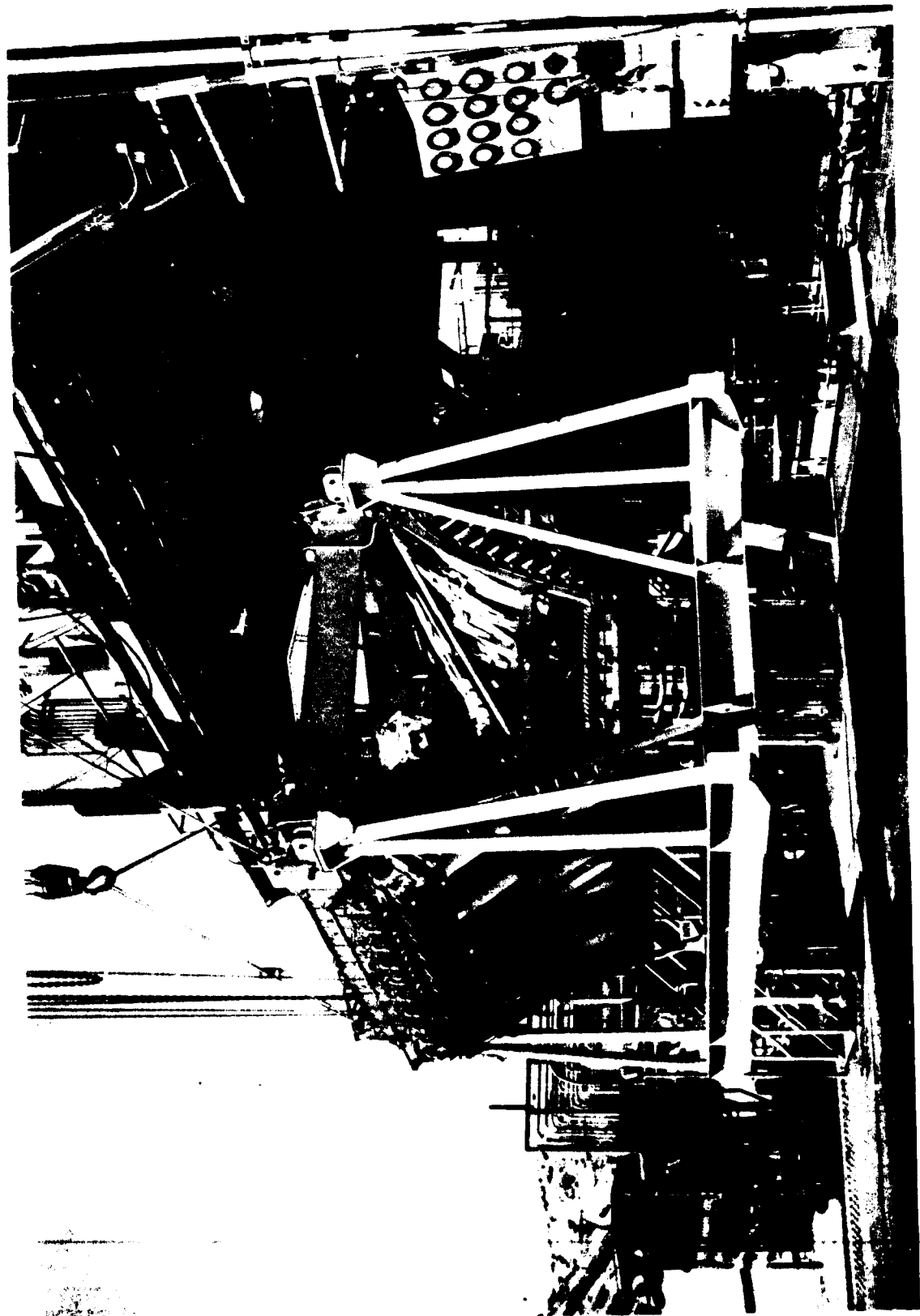


Figure 4. General Arrangement, Top View



1XZ21-8/12/71-C1B*

Figure 5. Test Bed Prior to Shipment to Delta-2B



1XZ17-6/5/72-S1D

Figure 6. Test Bed Installation at Delta-2B

backup structure is then bolted to the combustor. The nozzle is a furnace-brazed tubular structure, contoured to provide an expansion contour for the gases as they emit from the combustor.

Ten combustors are welded to each nozzle assembly. The exhaust manifold is of semimonocoque construction whose primary purpose is to provide for uniform distribution of turbine exhaust gas across the base of the thrust chamber.

The power package consists of a Mark 29-F fuel turbopump, a Mark 29-0 oxidizer turbopump, a gas generator, J-2S propellant valves, a J-2S pneumatic control package, and associated electrical and pneumatic lines. All components of the power package were spares from the J-2 or J-2S program and, at most, required only minor modifications for use on the linear test bed program.

The thrust frame is of heavy I-beam and box beam construction. Thrust frame weight was not considered important to the program objectives so the beam was designed for strength and low cost. The thrust is transmitted from the thrust frame through a central J-2S gimbal bearing into the facility thrust measurement system.

The objectives of the program were as follows:

- Demonstrate the feasibility of design, fabrication, and assembly of a full-scale linear aerospike test bed which employs the segmented combustor concept
- Perform component tests and supporting analysis, as required, to develop subsystems prior to their use on the test bed
- Perform hot-fire tests on the linear test bed to demonstrate performance, design integrity, satisfactory start and cutoff, and system stability
- Develop advanced ignition systems suitable for multiple ignition application which also are suitable for future advanced engine applications

All program objectives were achieved. Some of the significant accomplishments of the program are as follows:

- Fabrication of all components required for the test bed was successfully accomplished. Problems were encountered during fabrication that could have had major impact upon the program. These problems were discovered early enough to permit corrective action to be taken, to redesign where necessary, and to redirect engineering and manufacturing resources to find proper solutions and get back on schedule.
- Component testing of single and multisegment combustors was accomplished prior to completion of the test bed assembly. These tests were run to verify combustor structural integrity, to check performance, heat transfer, pressure drop, and to develop a test bed ignition system and an ignition detect system. Problems and design deficiencies were discovered during these tests. They were discovered early enough to permit corrective action on the test bed hardware and contributed greatly to the successful and relatively trouble-free test program run on the linear test bed.
- The test bed was tested 44 times for 3113 seconds total accumulated duration. Tests were run over a chamber pressure range from 670 psia to 1248 psia and mixture ratios from 3.3 to 5.6. The program was highlighted by test 624-028 which was run for 592 seconds mainstage duration.
- Combustor performance, heat transfer, pressure drops, nozzle pressure profiles, and base pressure data were acquired over the complete operating range. Combustion efficiency and specific impulse were higher than predicted and performance was satisfactory over the complete operating range. Test data evaluation indicated that the linear test bed will deliver between 450 and 455 seconds specific impulse at altitude.
- Two ignition systems were evaluated: the fluorine ignition system and the combustion wave ignition system. Ignition limits, start sequences, and performance characteristics were determined for both systems. This was the first multiple-ignition application of the combustion wave system. Satisfactory combustion wave system operation was repeatedly demonstrated during the test program.

- Combustor wall erosion was experienced during the test program. The causes and proposed solution to the erosion problem are discussed in detail in the body of the report.

CONCEPT SELECTION

At the onset of the Linear Test Bed Program, studies were conducted to determine the size, configuration, power cycle, and general arrangement of the test bed. The ground rules were to use existing components where possible, to use the combustor design that evolved from the CSE program, and to conduct a meaningful advanced experimental aerospike program within the imposed budget and time constraints. A low-cost experimental program to demonstrate the segmented aerospike concept was the prime objective of the program.

J-2S Mark 29-F and Mark 29-0 turbopumps, main propellant valves, and pneumatic control packages were available and it was decided these would be used. Slave gas generators used for Mark 29-F component tests also were available.

The combustors were designed for operation at 1200-psia chamber pressure and 6.0 mixture ratio. In matching the turbomachinery capability to the thrust chamber requirements, it was found that between 20 and 24 combustors would best match the turbopump H-Q and horsepower design capability. The thrust chamber fuel-side pressure drop was calculated and the required fuel pump discharge pressure was found to be on the upper limit of the Mark 29-F capability, and a best horsepower match was obtained with 20 combustors. (Twenty were selected to provide margin below the maximum design capability of the fuel turbopump.)

In selecting the thrust chamber configuration, several arrangements were considered including a round aerospike, linear one-sided, linear-two sided, and curved segments of a large-diameter aerospike. High expansion ratio was considered desirable. A round aerospike with 20 combustors would provide an expansion ratio of approximately 50. The nozzle fabrication cost would be high because of the need for tapered tubes and complex tooling.

The one-sided linear and the curved segment configuration would have very high expansion ratios, but they would be 20 feet long. The long length would not fit existing test stand flame deflectors and would entail complex structures and manifolding.

The two-sided linear would have high expansion ratio (119:1) symmetrical thrust vectors, simplified manifolding and structure, and the lowest fabrication cost. The nozzle could be fabricated with untapered tubes, and furnace brazing of the nozzle could be accomplished in 5-foot linear panels. With symmetrical nozzles, a conventional J-2S gimbal bearing could be used for transmitting thrust into a single main load cell. For these reasons the two-sided linear concept was selected.

Power cycles considered included tapoff turbine drive and gas generator turbine drive. The gas generator drive was selected because of availability of gas generator components and the complexities involved in developing a tapoff system for the segmented combustors.

DESIGN AND FABRICATION

FLUORINE IGNITION SYSTEM

Design of the fluorine ignition system manifold followed with strict adherence the design practices recommended in the NASA SP-3037, "Handling and Use of Fluorine and Fluorine-Oxygen Mixtures in Rocket Systems", H. W. Schmidt, 1967. Specific design criteria followed were:

1. The manifold was fabricated from pure nickel tubing to ensure the maximum material capability.
2. Tubing was X-ray inspected prior to fabrication to identify tungsten and other foreign inclusions.
3. The manifold was all-welded assembly with specially designed machined fittings.
4. All sharp edges in the machined fittings were rolled with a specially designed tool.
5. The automatic butt welds were X-ray inspected for droptrough and inclusions after fabrication.

The manifold tubing was sized with the aid of a computerized Fanno flow analysis developed for this purpose. The igniter elements also were fabricated from pure nickel, and were designed following the same practices as the manifold.

A special specification, RA0610-048, was written to maintain the cleanliness of the manifold and igniter elements during fabrication and engine test. Passivation procedures developed by the Rocketdyne Research Department were specified and strictly followed prior to each engine ignition test. Compatible metallic seals and valve seats were used during ignition system buildup. Annin valves controlling gaseous fluorine were repacked with copper chevron shaft seals, and passivated prior to engine testing.

The engine manifold was designed to include a -100 F dewpoint nitrogen purge which was operational on a 24 hour-per-day basis as recommended in NASA SP-3037. As a result of the design criteria, cleanliness procedures, passivation techniques, and purge precautions, no fluorine "incidents" were encountered on this program. A schematic of the fluorine ignition system is presented in Fig. 7.

COMBUSTION WAVE IGNITION SYSTEM

The combustion wave ignition system (Fig. 8) was designed using the existing fluorine manifold as the combustion wave manifold. Miniaturized 1/4-inch solenoid valves with optically flat sealing surfaces (Valcor) were procured to control propellant flow to a Rocketdyne-designed premixer assembly. A specially designed integrated spark plug and exciter unit was provided to supply ignition energy to the premixer unit. The entire ignition system was engine mounted and engine controlled. The adequacy of the fluorine manifold to serve as the combustion wave manifold was proved on a full-size mockup during testing in the research area. The combustion wave panel installed on test bed No. 1 is shown in Fig. 9 . The posttest condition of the 20 igniter elements is shown in Fig. 10.

CONTROL SYSTEM

Since the engine was to use oxygen and hydrogen as propellants, J-2 and J-2S hardware were utilized. Design requirements followed those of J-2 and J-2S electrical sequencing for pneumatic controls. The segmented concept precluded the use of a hot-gas tapoff drive for the turbomachinery, so a gas generator was incorporated. Figure 11 shows the complete system schematically, including control systems.

A J-2S pneumatic regulator controlled J-2S main propellant valves and J-2 bleed valves and gas generator control valve. Helium was supplied at 3000 psia from the facility; no bottle was utilized on the engine. Electrical sequencing was accomplished using relays rather than solid-state circuitry.

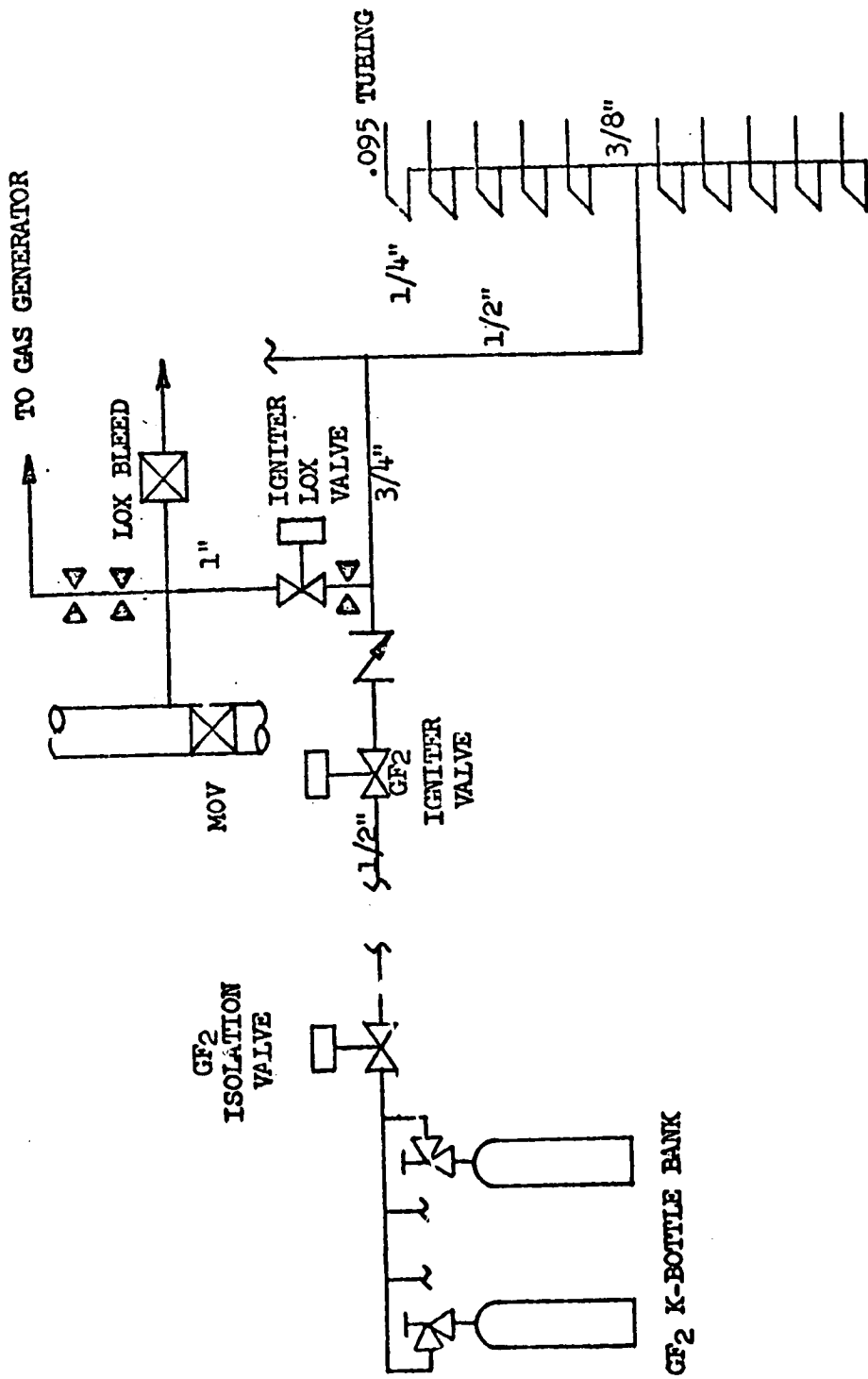


Figure 7. Breadboard Thrust Chamber Evaluation Gaseous Fluorine Ignition System

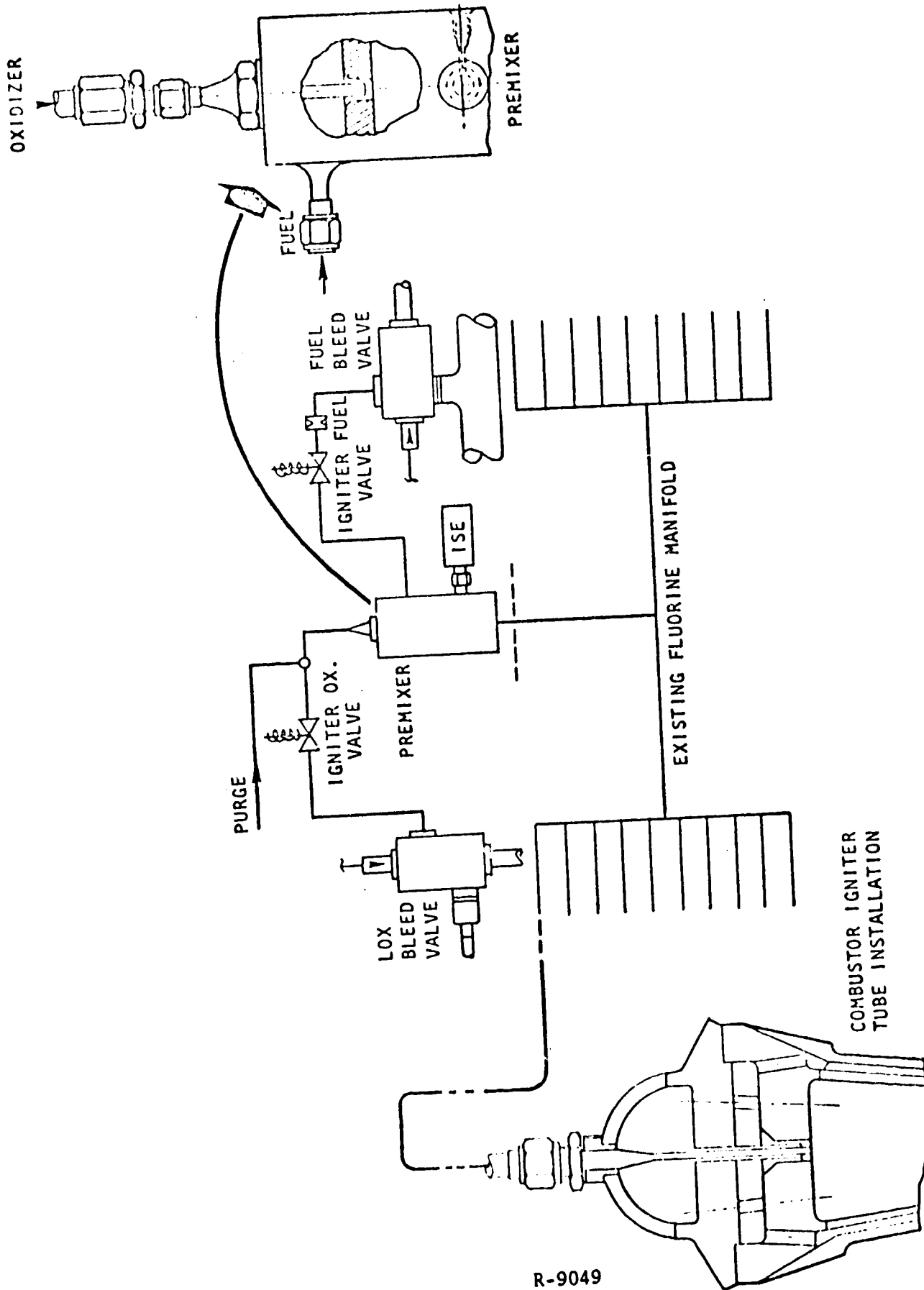


Figure 8. Linear Test Bed Program Combustion Wave Ignition System

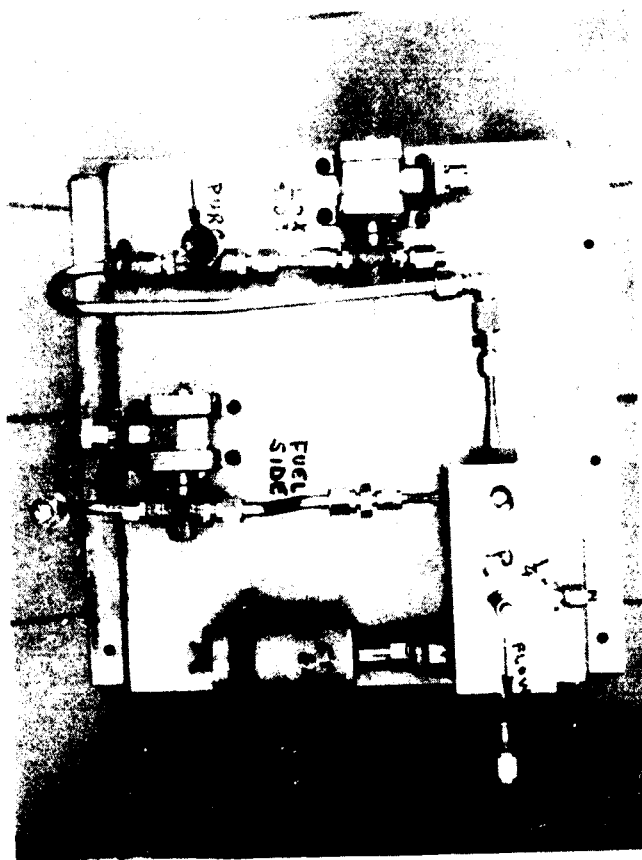


Figure 9. Linear Engine, Breadboard No. 1
Combustion Wave Ignition Unit

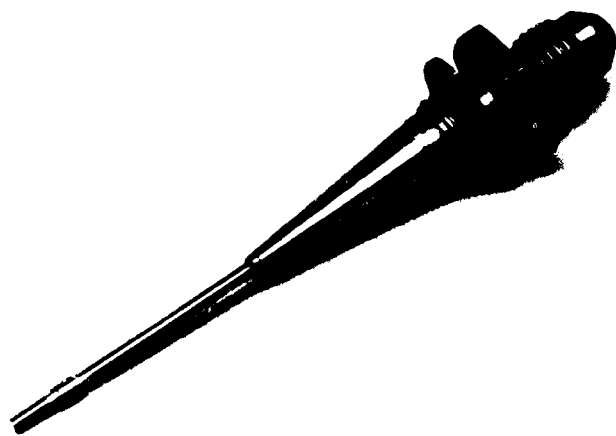
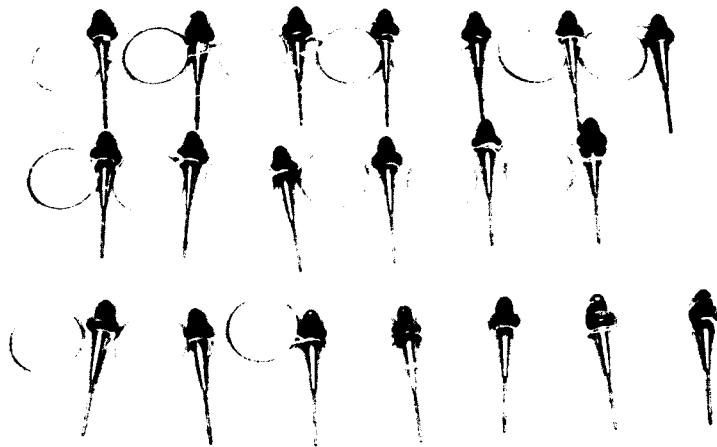
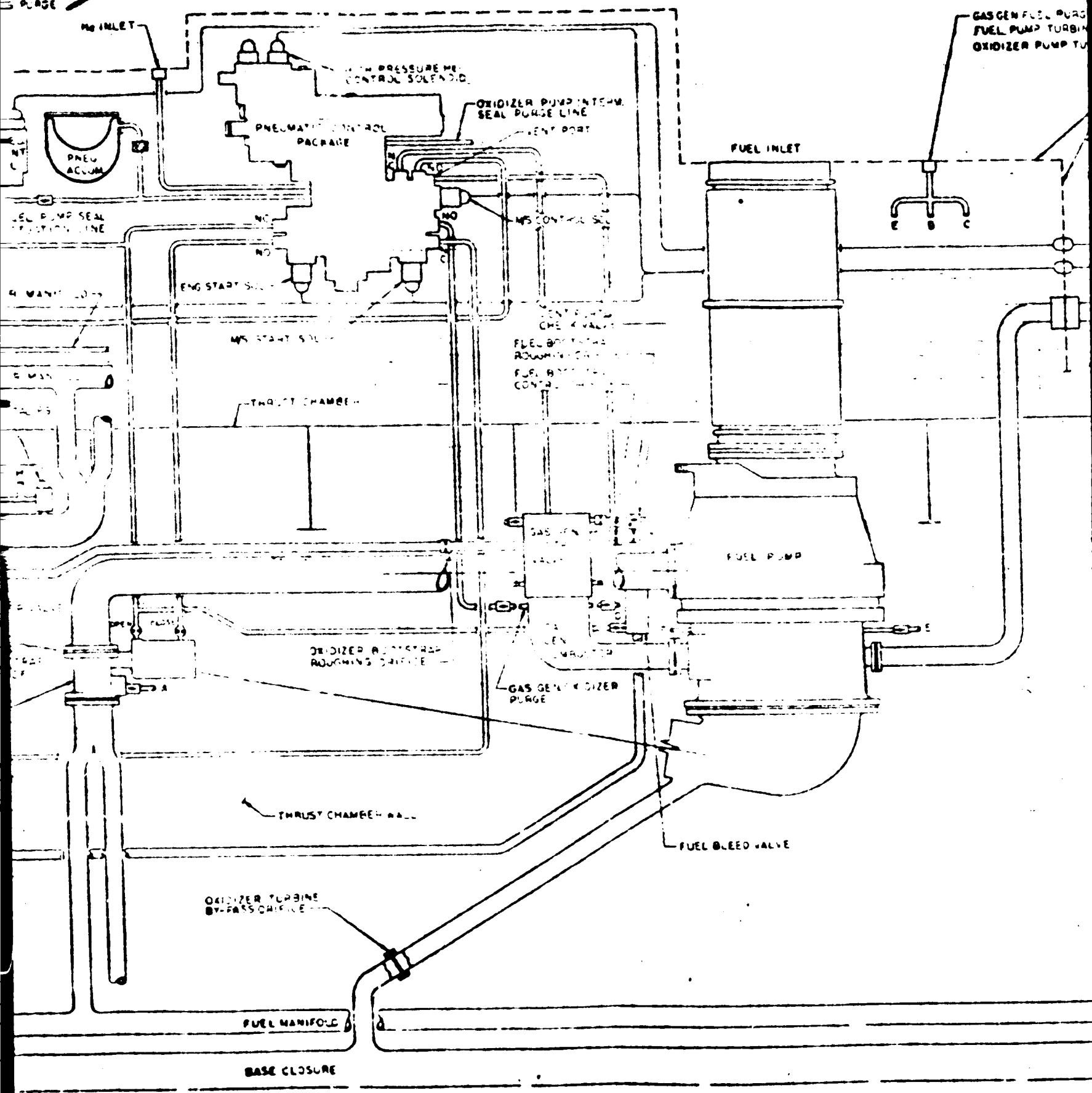


Figure 10. Combustion Wave Igniter Elements Posttest

PLAGE 2

3



FOLLOUT FRAME

3
GAS GEN FUEL PURGE (N)
FUEL PUMP TURBINE SEAL PURGE (E)
OXIDIZER PUMP TURBINE SEAL PURGE (S)

ENGINE-FACILITY INTERFACE

ELECTRICAL CONTROL ASSEMBLY

GN₂ SPIN START PRESSURE

SPIN START VALVE (ANNON)

SPIN START INTERLOCK VALVE

IGNITOR MANIFOLD

OXIDIZER MANIFOLD

END PLATE

COOLANT INLET

FUEL MANIFOLD

OXIDIZER TURBINE BYPASS DUCT

OXIDIZER TURBINE EXHAUST DUCT

BASE CLOSURE

THRUST CHAMBER SECTION

COOLANT OUTLET

R-9

19

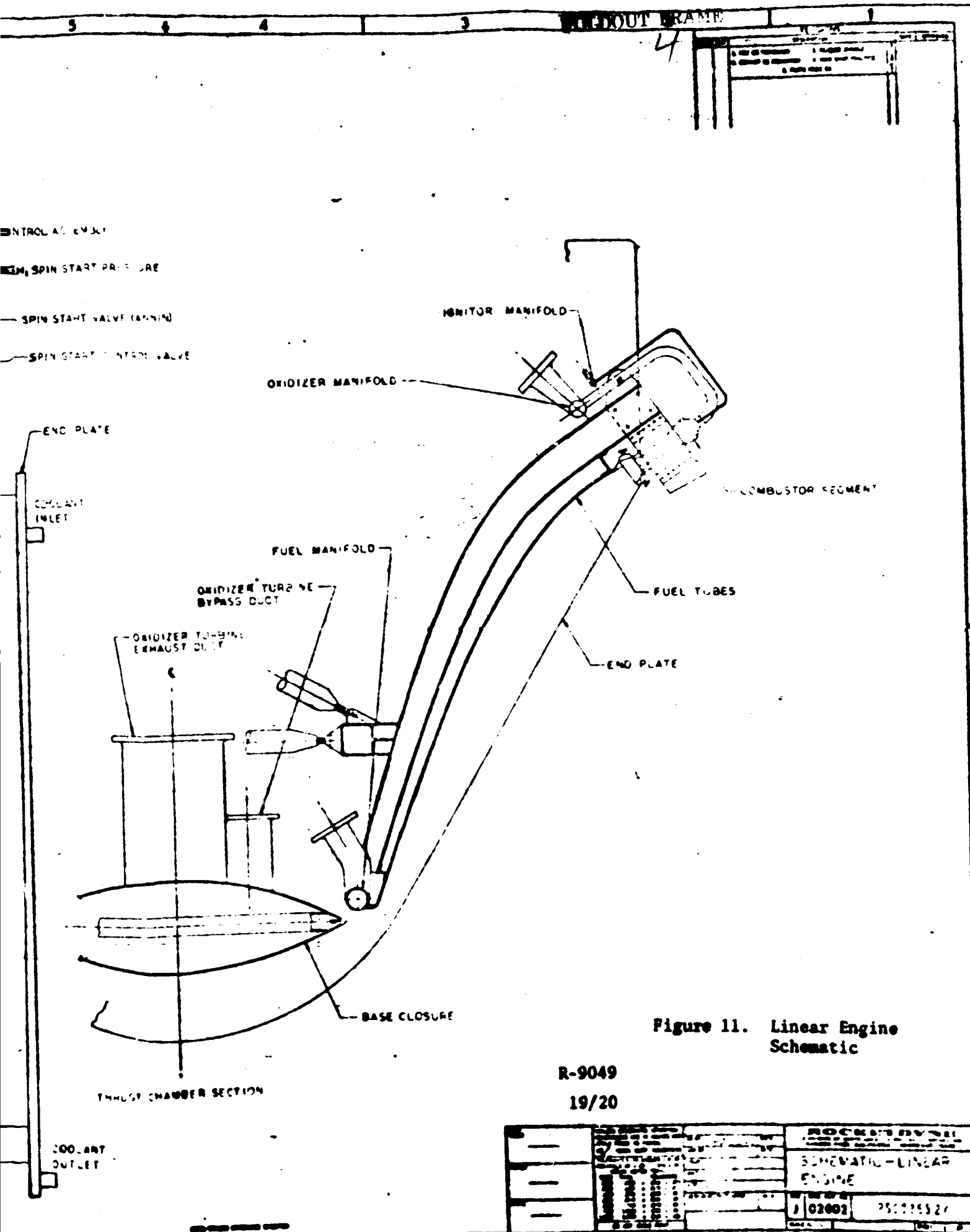


Figure 11. Linear Engine Schematic

ROCKETDYNE	
SCHEMATIC - LINEAR ENGINE	
7 02002	25000527

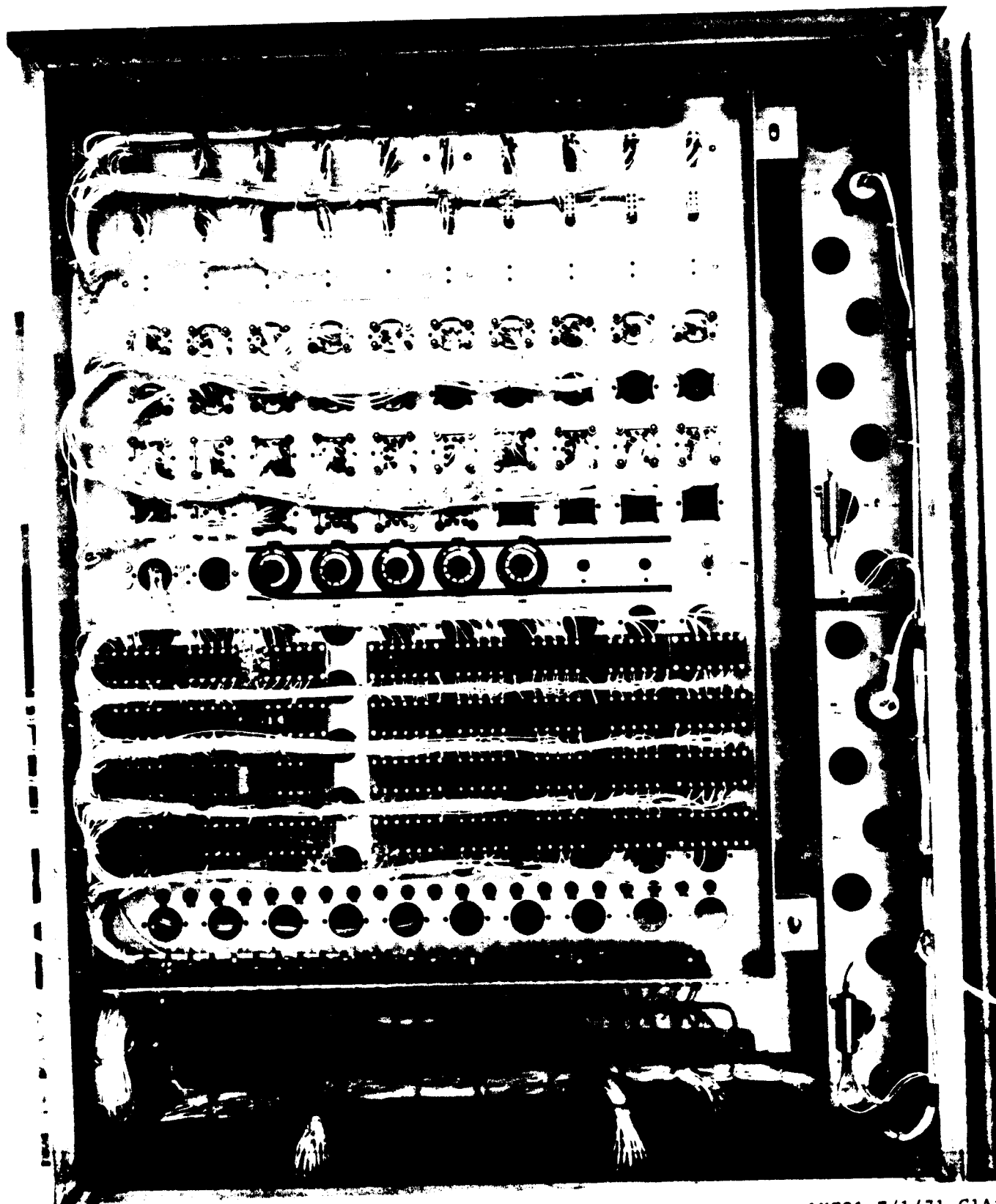
Use of a gas generator required modification of the normal plumbing procedure to the control solenoid. To prevent opening of the gas generator control valve by cryopumping while deactivated, the pneumatic actuator cavity and the valve housing are plumbed together to equalize pressures. Connection of the gas generator equalization port and the control solenoid vent port with an overboard vent provided both pressurization evaluation and provided solenoid venting capability. An 0.061-inch orifice in the equalization port prevented overpressurization at the case when control pressures were vented through the solenoid.

Overall, the pneumatic system performed satisfactorily. No design errors became apparent and no major problems were encountered. All J-2 hardware performed as expected with the J-2S system.

In the electrical control system, solid-state microcircuitry was abandoned in favor of relay logic and hard wiring to facilitate anticipated problems and routine changes in the electrical control system. The control "package" was assembled in a small control cabinet (Fig. 12) which was installed remotely from the engine on the test facility.

Computer start modeling provided the basis for engine sequencing logic. After modeling a satisfactory start sequence, basic logic and safety interlock circuits were established. A failure effects analysis was conducted to analyze engine hardware reliability and effectiveness of safety circuits.

Initial checkouts at Canoga Park revealed only minor problems, but post-installation sequences with the engine and facility encountered several problems involving circuit errors and interfacing conditions not anticipated during design. Following minor modifications to correct these problems and incorporate sequence changes, the system checked out satisfactorily.



1XZ91-7/1/71-C1A*

Figure 12. Electrical Control Ground Box

R-9049

Subsequent operation encountered no problems resulting from system deficiencies. Changes incorporated throughout the program were accomplished with few problems and minimum system downtime. Engine logic proved flexible and easily modifiable.

The fuel and oxidizer feed systems were designed as a hybrid of the J-2 and J-2S. High operating pressures required the use of J-2S main valves, while thrust chamber heat transfer dictated the need for engine bleeds. A J-2 gas generator was utilized to provide turbine power.

J-2S main propellant valves were used as is, the fuel valve having the sequence ports capped. Both bleed valves were modified by a closeout weld between the discharge flange and the valve seat to prevent structural failure at the flange in the event the valve opened during high-pressure operation.

A J-2 gas generator control valve was proof tested to linear test bed operating requirements, then functionally checked and serviced for use. A pit slave combustor assembly used for turbopump testing at SSFL was reconditioned and mated with the control valve to form an assembly capable of providing the higher power requirements of the J-2S turbomachinery.

Because of low reliability in a high-pressure hydrogen atmosphere, spark igniter for the gas generator was abandoned in favor of pyrotechnics. An R&D igniter used for component test and hyperflow gas generators was chosen due to its availability, high reliability, and potential burn time at high pressures.

No control system problems were encountered during the test program. All valves performed satisfactorily, providing adequate engine control. The pyrotechnic gas generator igniters proved 100 percent reliable, providing an excellent ignition source. The gas generator operated as predicted, with no problems, and exhibited no physical deterioration.

PURGE SYSTEM

The initial purge system requirements for the linear test bed were based largely on experience gained from the J-2 and J-2S, since components from these engines were those used to form the linear power package. Four purge subsystems were originally outlined: (1) turbopump and gas generator, (2) fuel manifold, (3) ignition system, and (4) oxidizer manifold. Nitrogen was to be used on (3) and (4), while helium was required for (1) and (2).

Turbopump and gas generator purge requirements of J-2 and J-2S were adopted without change for use on the linear, as their application to the linear was, for all practical purposes, identical to their original applications. Satisfactory operation was achieved and no problems were encountered.

Critical to the fluorine system was removal of all moisture to prevent a GF_2-H_2O reaction. Preliminary studies indicated that periodic purging would not provide complete assurance that the system was completely dry. Continuous purging, however, offered the advantage of providing a dry, inert atmosphere within the manifold at all times. This approach was determined to be more acceptable. Facility-supplied nitrogen was used, with an interface requirement of 100 ± 25 psig and -100 F dew point to provide 5 ± 1 scfm flowrate. Figure 13 shows the purge sequencing.

This continuous purging proved to be completely successful. No problems were encountered and the program was entirely free of the problems that can occur using fluorine.

In late January 1972, the fluorine system was replaced with the newly developed combustion wave ignition system. Total dryness was not critical as with fluorine, so the purge requirements were modified. Pre- and posttest purging was determined to be sufficient. Nitrogen (-78 F dew point) again was used. An interface pressure of 100 ± 25 psig supplied 25 - scfm flowrate.

Purge Parameters		Propellant Drop	Engine Start	Spin Start	Cutoff
System	Fluid				
Turbopumps and Gas Generator Fuel	Helium: 150 ±25 psig 50 -150 F	30 min	45 min **	15 min	15 min
Fuel Manifold	Helium: 2 Minutes *600 ±25 psig 100 -150 F 28 Minutes 150 ±25 psig 100 -150 F	2 min	1 min	1 Sec. (Approx)	High Vol. C/O Purge
Igniter System	Nitrogen: -78 F Dew Pt. 100 ±25 psig 25 ±5 SCFM				
LOX Manifold	Nitrogen: 150 ±25 psig 100 -150 F				5 min
Engine Compartment	Nitrogen: 1000 psig min. 50 -150 F				

*This 2 minute prepurge is only a surge pressure used to blow out any water bridging of the fuel annuli. Existing facility plumbing shall dictate maximum prepurge pressure.

**The turbopumps and gas generator purge will be turned on 1 minute prior to engine start as part of Facility Ready, and will be turned off at Spin Start

Figure 13. Purge Systems Sequence of Operation

The pretest LOX manifold purge requirements were essentially the same as J-2 and J-2S: a 30-minute predrop heated purge to ensure complete drying of the oxidizer system, continuing to engine start (125 ±25 F nitrogen at 150 ±25 psig was used).

Cutoff purging presented problems not previously encountered on J-2/J-2S. Inherent to the design of the linear test bed are large "trapped" volumes in both propellant systems. These volumes of residual propellants represent a serious hazard when considering the cutoff transient, since uncontrolled expulsion of either (particularly the oxidizer) could result in high mixture ratio and subsequent hardware damage. Considerable effort was expended prior to initial testing to determine optimum purge sequencing.

Since the residual oxidizer presented, by far, the greater hazard at cutoff, it was considered that immediate removal of residual fuel, while allowing natural boiloff of residual oxidizer, would result in a lower transient mixture ratio at cutoff. Posttest purging of the oxidizer manifold was, therefore, delayed until approximately 5 minutes after cutoff.

Also, the fuel manifold presented no major pretest purging problems. A preconditioning purge was not an engine requirement. A 2-minute, high-flow purge was used to ensure removal of any water bridging the injector fuel annuli. A low-flow predrop helium purge was used to dry and inert the fuel system, and was terminated at propellant drop.

The initial configuration of the fuel manifold purge was identical to that used on the J-2S: 1/2-inch line to the main thrust chamber purge check valve located in the main fuel valve housing. Evaluation of early test data indicated that a higher purge flow was desirable. Removal of the check valve did not significantly decrease system resistance, so a high volume purge was installed, bypassing the restriction of the customer connect plumbing through a 1-inch Annin valve to the main fuel valve. The existing purge feeds into the purge manifold upstream of the Annin (pretest 624003).

Subsequent test data indicated that purge operation was still unsatisfactory. Therefore, the drain screws were removed from the ends of each fuel manifold and 1/2-inch line was plumbed to these points. Referred to as the "super purge," it, too, proved inadequate. Prior to test 624010, a 4000 cu-in. J-2S helium tank was plumbed into the system to provide a momentary purge "blast" to clear the fuel manifold.

The purge tank was pressurized from the 3000-psi facility supply. At cutoff, both the "super purge" valve and the thrust chamber purge valve open, and the 3000-psi flow checks off the thrust chamber purge until the tank pressure decays below 1500 psi (thrust chamber purge supply pressure). Thrust chamber purge flow continues to assure complete purging of the fuel manifold and thrust chamber.

Subsequent tests exhibited satisfactory cutoff transients, and no further hardware changes were deemed necessary. Minor changes in sequencing of the purge tank were periodically made to attempt to improve cutoff cooling. No further problems were encountered.

GROUND SUPPORT EQUIPMENT

Test bed ground support equipment consisted primarily of new items and components modified for use with the new engine. J-2 and J-2S test plates and fixtures were the only items used requiring no modification.

The engine handling fixture was the first GSE item designed and constructed. It was used for both transportation and as a holding fixture during engine build.

The acceleration safety cutoff system (ASCOS) is a 12-channel vibration detection device, designed and constructed by Santa Susana Field Laboratory Test Group. Alternate combustors plus two end combustors were monitored to initiate cutoff if detected vibration exceeded 150 g rms for 100 milliseconds. The ASCOS performed satisfactorily, data showing the test bed to be free of damaging acoustical combustion instabilities.

Ignition detection was provided by a 20-channel system, also designed and built by SSFL test group. Fuel injection temperature was chosen as the most practical indicator of main chamber ignition, and a 40-degree per second rise was indicative of satisfactory combustion. The technique proved adequate, although the implementation (i.e., utilizing an instrumentation signal near the level of signal noise, instrumentation failures, etc.) proved somewhat awkward. Overall system performance was, however, satisfactory.

Minor modification allowed use of J-2S engine control panels with the test bed. Facility instrumentation, monitoring, recording, and automatic cutoff devices all proved satisfactory throughout the program.

DELTA-2B FACILITY MODIFICATION

Testing of the linear test bed was carried out at test stand Delta-2B, SSFL. Test stand capabilities and crew availability were the primary considerations used in choosing this test facility.

Delta stand had previously been used for J-2 acceptance and J-2 and J-2S R&D testing, so primary structure was not a problem. The main structure diagonal members at the engine deck level were boxed in and water cooled to provide protection from the open main exhaust. Stand structure at the horizontal load cell attach points was reinforced while vertical load cell attach points were installed on existing main structure.

To provide for higher thrust, the existing thrust mount was removed, the main thrust flexure assembly was updated, and the VTS-3B main load cell was installed.

A surplus lift table was obtained from CTL-3, updated to 24,000-pound capacity and installed in the test stand. The engine platform and decking also were modified to provide clearance for, and access to, the engine.

The flame bucket hole pattern was modified to provide coolant for the rectangular flame pattern, while the bucket blowback shield was cut back to clear the main exhaust plume.

A complete high-pressure water system was installed to provide coolant for the nozzle end fences. A surplus 8000-gallon water tank was placed opposite the test stand. Tank fill was accomplished manually. Water coolant feed was provided by GN_2 pressurization of the tank. Flowrate was monitored using a venturi-type flowmeter.

The fluorine ignition supply required a completely new installation, and introduction of necessary safety procedures. A bottle bank was located off the test stand, along with isolation valving. All plumbing was passivated for a 24-hour period before an engine-facility connection was made. The ignition system "engine valves" also were facility mounted due to their physical size, but were the only valves in this system to be controlled by the engine control system.

Engine spinup capability was provided by the facility gaseous hydrogen system. An Annin valve served as the facility pre valve, separating the main spin valve from the 3000-psi supply. The servocontrolled main valve provided a constant 400-psi spin pressure to the fuel turbine to initiate bootstrapping.

In general, instrumentation capabilities were adequate. However, additional thermocouple capability was required. No modifications were required to provide satisfactory recording capabilities.

COMBUSTOR DESIGN

The primary objective of the breadboard thrust chamber program was to improve the technology of advanced liquid propulsion systems. Gaining experience in the fabrication and development of low-cost combustors was a significant part of this program. Previous investigations have indicated that reduced costs and weight could be realized by investment casting a relatively simple combustor design with the potential for mass production. This led to the initiation of the Cast Segment Evaluation Program.

The Cast Segment Evaluation Program (Contract NAS8-30182) was initiated to investigate fabrication techniques and establish design criteria associated with the use of investment cast combustors. Cast segment technology developed on the CSE program has been utilized on the breadboard thrust chamber program. Improvements have been incorporated into the breadboard design based, in part, on CSE fabrication and testing experience. Areas of the CSE segment assembly that were complex to fabricate or caused operational difficulties were redesigned to improve the configuration and tailor it for breadboard thrust chamber application.

The CSE program demonstrated that a simplified combustor assembly using an investment-cast NARloy liner could be designed, fabricated, and successfully tested. Segment technology developed on this program provided the criteria to design a simplified combustor assembly with increased cycle life and reliability for the breadboard thrust chamber program.

The basic breadboard combustor design was defined on the Cast Segment Evaluation program. Emphasis was placed on a simplified design with high reliability which could be easily fabricated. This criterion resulted in a one-piece NARloy investment-cast liner with electroformed nickel used to close out the coolant channels (Fig. 14). Structural support for the electroform assembly was provided by two lightweight aluminum sand castings.

The combustor assembly was designed to be capable of being combined into a 20-segment, 248K thrust chamber assembly. Operating pressures and flowrates of the 20-segment assembly were required to be within the capability of J-2S turbomachinery. Table 1 summarizes the significant parameters that were the basis for the combustor design.

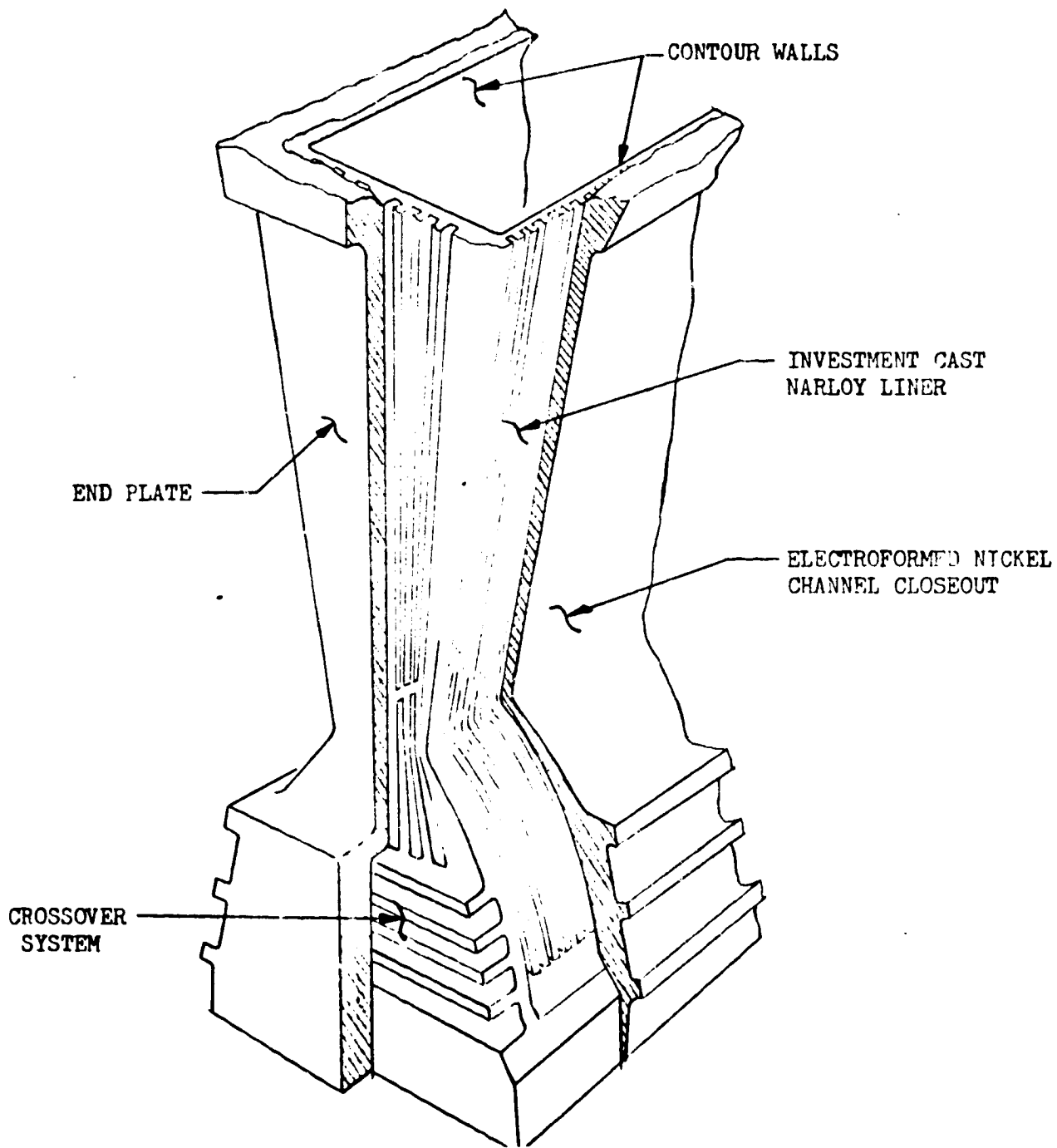


Figure 14. NARloy Cast Liner

TABLE 1. OPERATING PARAMETERS FOR COMBUSTOR DESIGN

Propellants	LOX-Hydrogen
Injector End Chamber Pressure, psia	1224
Engine Mixture Ratio	5.50
Segment Mixture Ratio	5.85
Maximum Combustor Inlet Fuel Pressure, psia	2032
*Maximum Thrust Chamber Fuel Inlet Pressure, psia	2144
Maximum Oxidizer Inlet Pressure, psia	1697
Fuel Flow, lb/sec	80.62 (20 segments)
Oxidizer Flow, lb/sec	471.39 (20 segments)
Design Life	30 starts, 10,000 seconds

*Approximate maximum of J-2S turbomachinery

The combustor assembly design was based on aerodynamic, stress, heat transfer, and pressure drop considerations. Major emphasis was placed on design simplicity and ease of fabrication.

The segment hot-gas contour is symmetrical. The combustion zone was a 6-degree straight wall convergence angle from the injector to the throat. The throat gap is 0.456 inch (as cast). The combustor nozzle contour was based on an ideal plane flow bell nozzle designed with a 4.3:1 expansion ratio and truncated to a 3.88:1 expansion ratio.

Table 2 summarizes the significant combustor design parameters.

TABLE 2. COMBUSTOR DESIGN PARAMETERS

Throat Gap, in.	0.456 (as cast)
Throat Area, in. ²	5.13
Contraction Ratio	3.25:1
Expansion Ratio	3.88:1
Injector Face to Throat (axial), in.	5.0
Throat to Exit Plane (axial), in.	2.55
Transverse Chamber Length, in.	11.250
Combustion Zone Convergence Angle, degrees	6

Cast Liner Thermal Analysis

Design studies indicated a regeneratively cooled chamber utilizing a single uppass coolant circuit would provide the most optimum heat transfer characteristics with minimum pressure loss. A simplified configuration was designed in which coolant enters the nozzle end of the inner contour wall and is distributed to the two end plates and outer contour wall via a crossover system (Fig. 15). Coolant then flows in all four circuits in a single uppass and is discharged into the injector fuel manifold. Flow distribution in the parallel circuits is controlled by drilled orifice holes at the coolant exit end of the inner contour wall. The drilled orifices provide the capability to cold-flow calibrate the segment and resize the orifice holes to redistribute the flow if necessary.

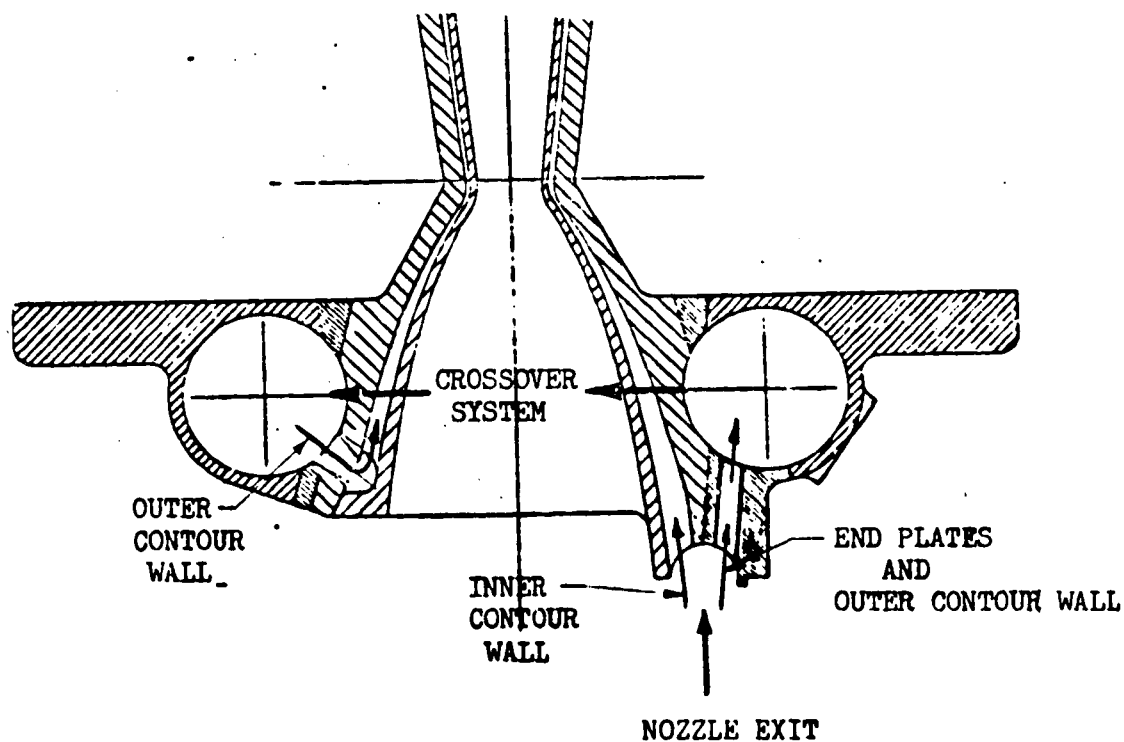


Figure 15. Breadboard Engine Combustor Assembly

The basic coolant channel geometry was defined on the Cast Segment Evaluation Program (CSE) after conducting a parametric thermal analysis. Channel width and depth, hot-gas wall thickness, land width, and coolant mass flux were varied to study their effect on hot-gas wall temperature. The investigation was limited to study channel dimensions which were within the casting capability of investment casting technology.

Several hydraulic modifications of the CSE segment design were incorporated into the breadboard segment design as a result of CSE test results. The cast liner dies were revised to optimize hydraulic and heat transfer characteristics. This effort primarily involved reducing pressure loss in the outer contour wall and end plate coolant circuits. In addition, the cast liner wall thickness was reduced to decrease the hot-gas wall temperature.

CSE segment testing indicated the end plate pressure loss was substantially higher than predicted. As a result, the end plate coolant flow was reduced considerably below the design value. Laboratory tests indicated that the chevron which transfers coolant from five to seven channels contributed a major part of the total end plate pressure loss. Therefore, the end plate was modified to eliminate the chevron and redesigned to contain seven channels traversing its entire length. The entrances to the seven channels were enlarged and rounded to prevent the loss of the entire crossover velocity head at the channel entrance and thereby minimize entrance losses.

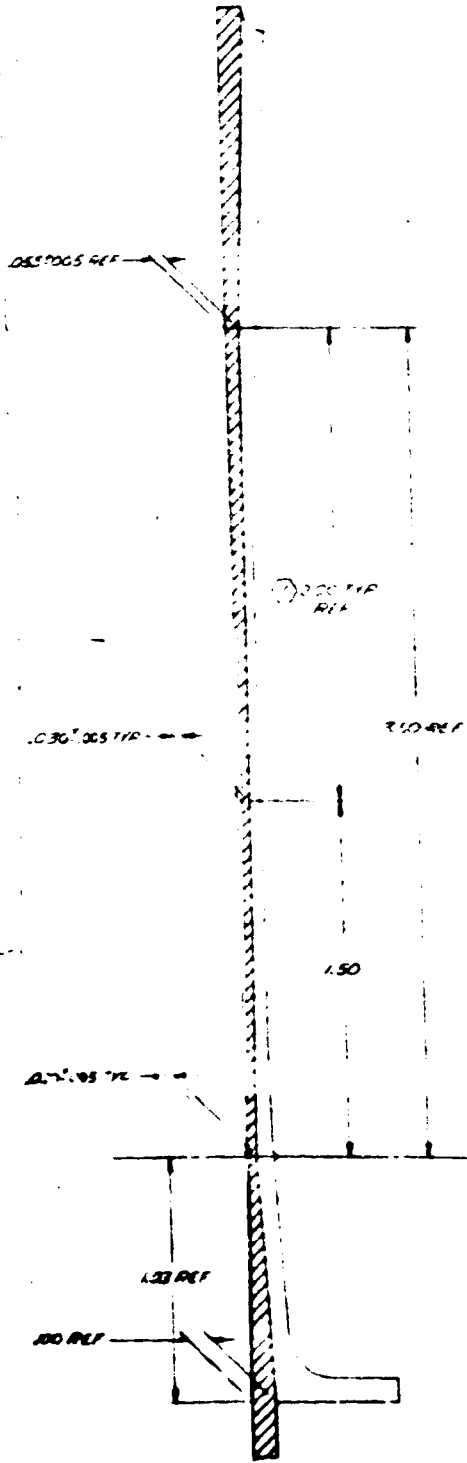
The released breadboard design of the cast liner is presented as Fig. 16. The channel geometry, coolant mass flux, and predicted maximum wall temperature versus axial length for the contour walls and end plates are shown in Fig. 17 and 18.

Combustor Assembly Stress Analysis

Analysis and CSE test results indicate the NARloy cast liner with the EFNi closeout and cast aluminum backup structure is structurally adequate for engine operation at a chamber pressure of 1200 psi. The CSE combustor was originally designed for possible uprating to a chamber pressure of 2000 psi; EFNi thickness and the cast

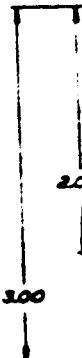
FOLDOUT FRAME

REPRODUCIBILITY OF THE ORIGINAL PAGE IS POOR.



X	Y	Z	H	T
4.850	1.474	1.045	1.45	
3.50			1.77	
1.50				
13				
00	1.45	1.005	1.2	1.210
017	1.60	1.025	1.1	
114	1.44		0.9	
178	1.40			
297	1.59			
392	1.75			
601	1.07	7		
844	1.2			
-1.20	1.12			
-1.70	1.00		1.28	
-2.08	1.72		1.80	
-2.25	1.769			
-3.00	1.20		1.50	

DETAIL E
FOR -5



FOLDOUT DRAWING

1/2 CHANNELS EQUALLY SPACED
WITHIN .002 OF TRUE POSITION
& PLACES

FOLD

.075 ± .005
4 PLCS

B 17

2
A B C D

11.25

A B C D

104 2 PLCS (ALL END PLATE PLACES
UNCHANGED)

.095 ± .002 TYP

.011 ± .005 TYP

WIRE ON 1/2 TIP

E

① 2.25

① .50 TIP

.067 ± .002 TIP
CHANNEL MOUNT

① WALL THICKNESS

.100 2 PLCS

.051 ± .002 TYP

.045 ± .002 TYP

.067 ± .002 TYP

.19 2 PLCS

.19 4 PLCS

.15 ± .005 2 PLCS

.200 4 PLCS

.15 ± .005 TYP
WIRE ON 1/2 TIP (GENT)
200 4 PLCS

① .44

① .26 2 PLCS

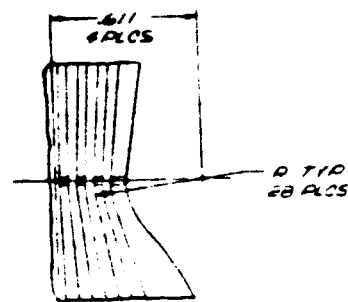
.585 8 PLCS

.100 8 PLCS

A 2

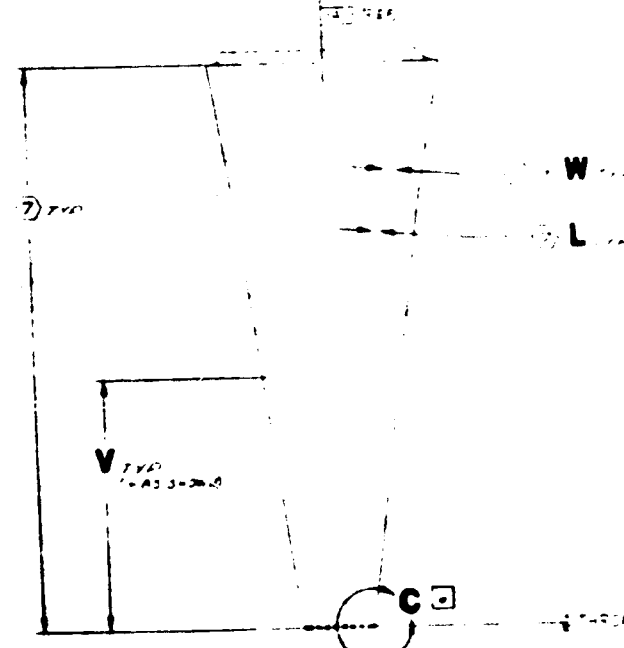
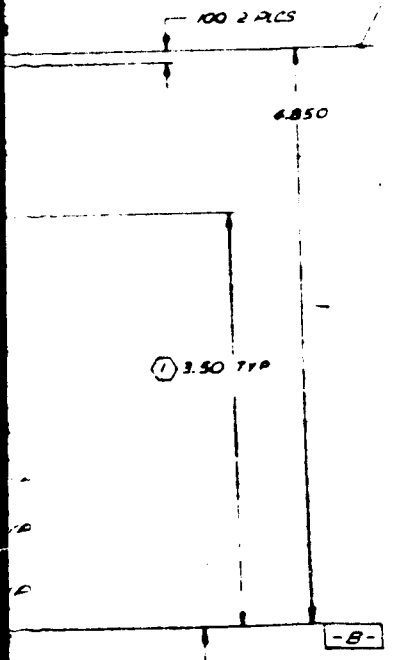
FOLD

V	W	L
4.75	1.00	1.00
.00	0.10	0.10
-.93	0.7100	0.7100

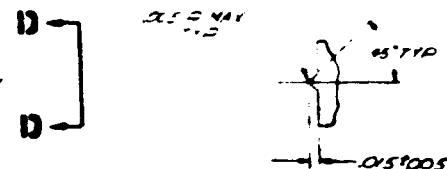


DETAIL C
SCALE 4/1

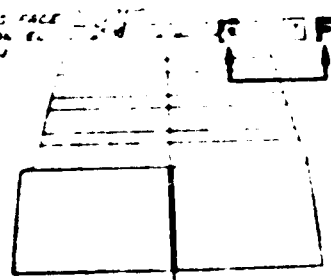
PLATE AND...
... (FOLDOUT FRA)



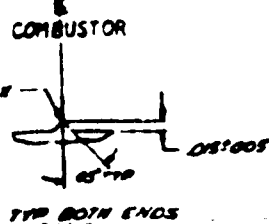
2.00 2.00 TYP
14 PLS
(NOTE: CURVED SURFACES SHALL
BE FROM LINE C IN FIG. 1
CONTAINED WALL ON
FREE END)



VIEW D-D
BOTH ENDS
SCALE 10/1



SECTION F-F



TYP BOTH ENDS

2.13 2 PLS
2.13 2 PLS
2.13 2 PLS

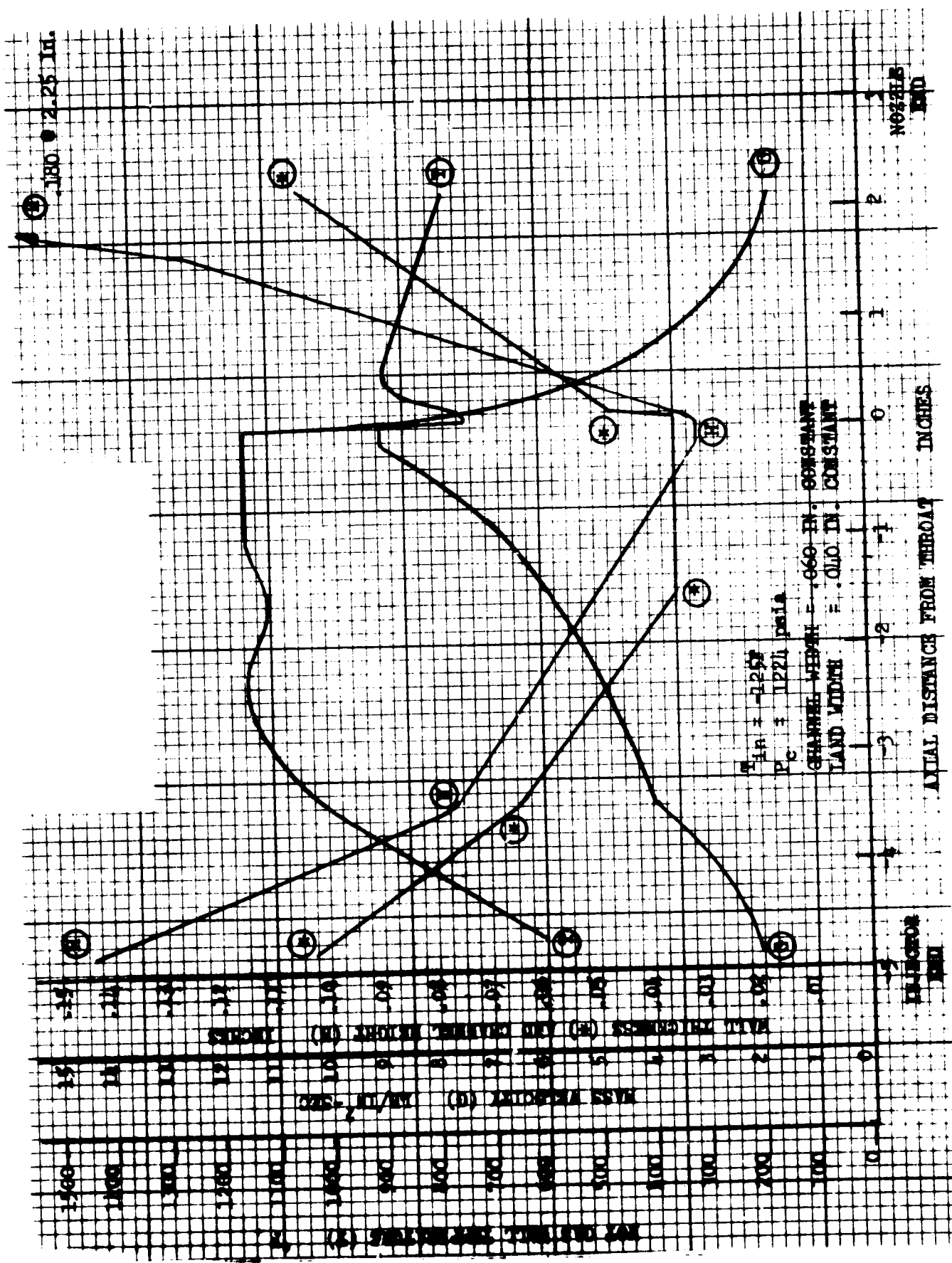


Figure 17. Breadboard Engine Contour Wall Channel Parameters vs Axial Length

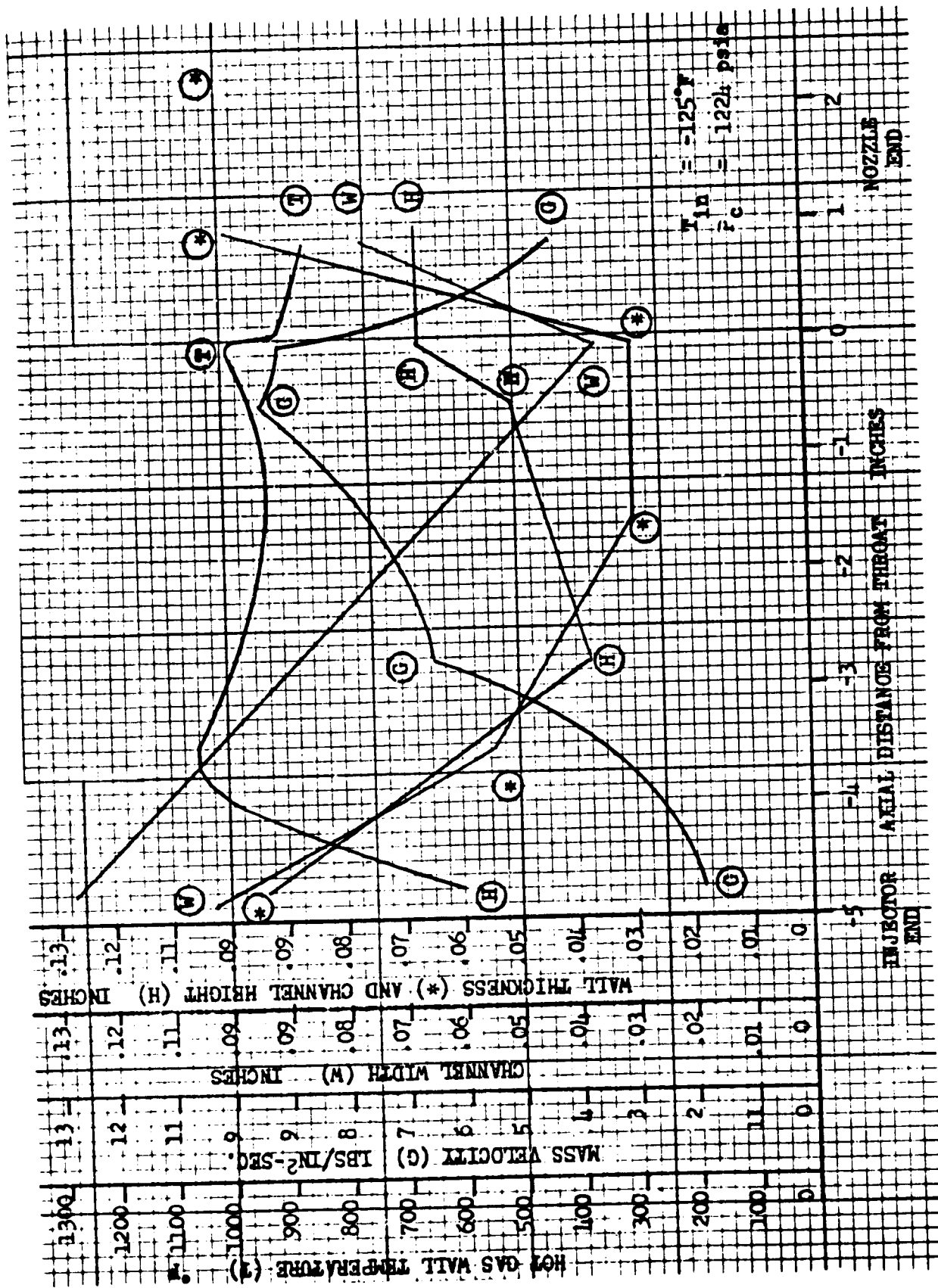


Figure 18. Breadboard Engine End Plate Channel Parameters vs Axial Length

aluminum backup structure were designed to withstand loads consistent with the higher chamber pressure. The EFNi thickness was made sufficient to withstand coolant pressure loads and transmit chamber pressure loads from the injector end to the aft combustor manifolds. The manifolds then transmit the total thrust load into the cast aluminum backup structure. The cast aluminum structures are attached together at each end by INCO 718 tension tie plates which transmit the load into the segment thrust mount. The final combustor segment assembly is presented as Fig. 19.

Several axial locations of the CSE cast liner design were investigated using a finite element computer analysis. The analysis, which accounts for both plastic and elastic strain, was performed to determine the strain levels resulting from thermal and pressure loads at 1200-psi and 2000-psi chamber pressure levels.

The most critical stress location for the hot-gas wall is at the throat. The minimum hot-gas wall thickness for the CSE design (0.040 inch) was dictated by casting capabilities. However, the breadboard liner hot-gas wall was reduced by machining to a minimum thickness of 0.025 inch in the throat. The minimum thickness was determined to provide the maximum allowable stress to meet chamber life requirements.

During CSE testing, cracks appeared in the EFNi closeout at the combustor-injector attachment location. Analysis indicated the cracks were probably due to hydrogen embrittlement of the nickel. Extensive laboratory testing of channel closeout samples verified that as-deposited EFNi was susceptible to hydrogen embrittlement and cracking in plastically strained areas. The tests also indicated that annealing the EFNi provided partial protection against hydrogen embrittlement. However, the most effective protection was provided by isolating the EFNi from the hydrogen with a thin layer of electrodeposited copper. Therefore, the breadboard combustor design was modified to include a thin electrodeposited copper layer (≈ 0.020 in.) to close out the channels prior to electroforming nickel. In addition, sufficient EFNi thickness was added to the released design to provide the capability to anneal the entire assembly if subsequent test results indicated it was desirable.

Segment Fabrication

Twent-one breadboard combustor assemblies were successfully fabricated in a sequence similar to the CSE combustor. Furthermore, additional manufacturing steps, i.e., thinning the hot-gas wall to reduce temperature and protecting against hydrogen embrittlement, became necessary due to combustor modifications.

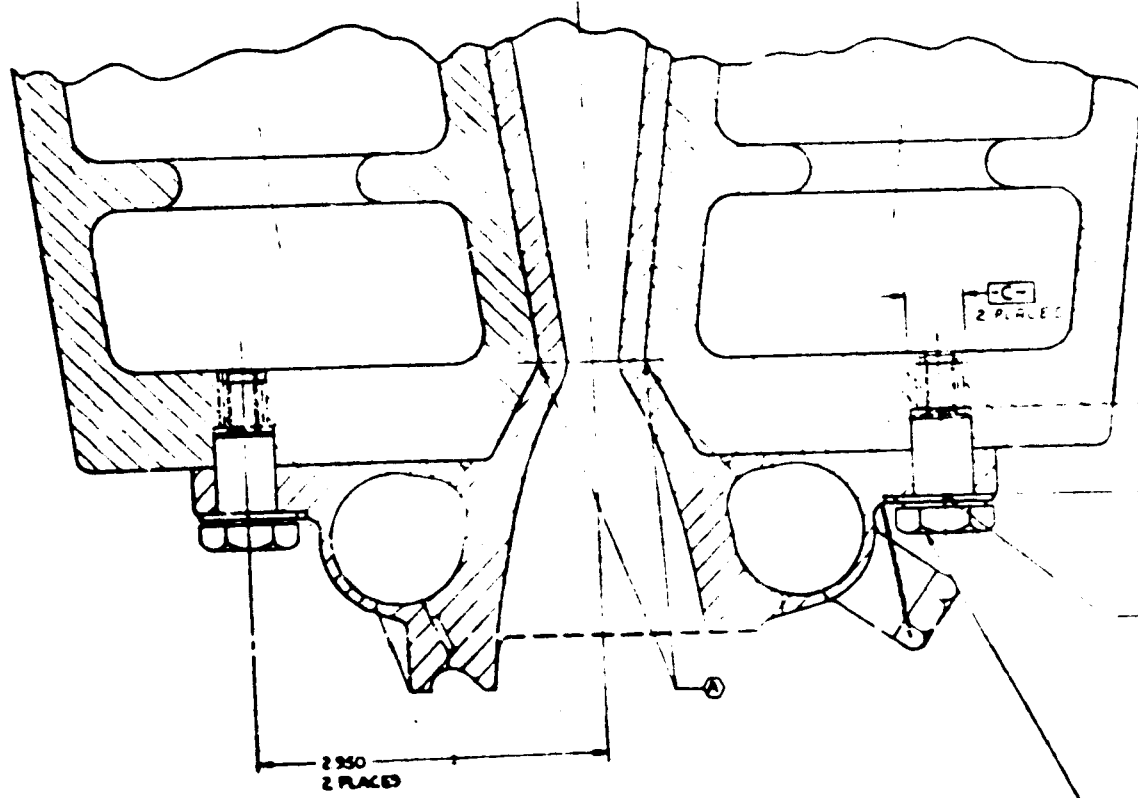
Fabrication Sequence. The basic steps involved in fabricating the breadboard combustor are listed below:

1. Clean up and repair the cast liner if required.
2. Electrical discharge machine the hot-gas wall to the required wall thickness profile.
3. Prepare the cast liner for electroform copper by welding on the injector face plate, filling the channels with Rigidax, and applying a silver powder layer over the Rigidax to initiate the deposition of copper.
4. Electroform copper.
5. Electroform nickel and intermediate machine the EFNi using a numerically controlled machine to remove excess EFNi which has been preferentially deposited. The electroform assembly was intermediately machined twice.
6. Final electroform nickel of the combustor assembly and final machine using a numerically controlled machine.
7. Electron-beam (EB) weld the manifold transition pieces to the EFNi and the manifolds to the transition pieces. TIG braze the manifold ends using Palniro 7 braze filler.
8. Water-flow calibrate the coolant circuit and adjust the discharge orifice holes if required.
9. Proof-pressure test the channel electroform bonds and the aft fuel manifolds to 2670 psi.
10. Electron-beam weld the injector assembly to the combustor assembly.
11. Proof-pressure test the combustion zone to 2250 psi using a throat plug.

FOLDOUT FRAME

FOI

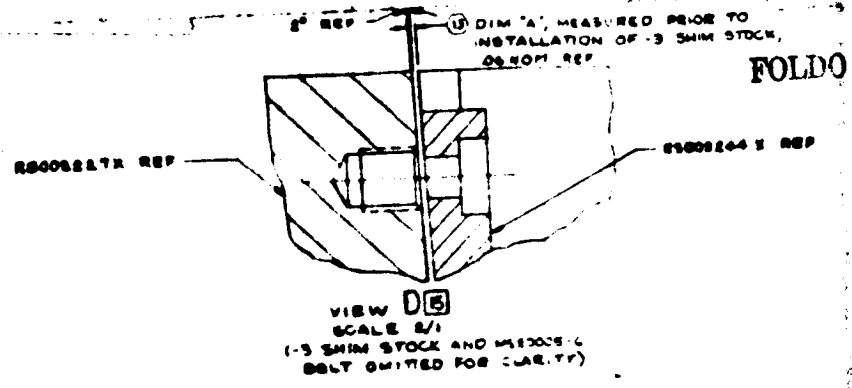
REPRODUCIBILITY OF THE ORIGINAL PAGE IS POOR.



SECTION B-B
SCALE 2/1

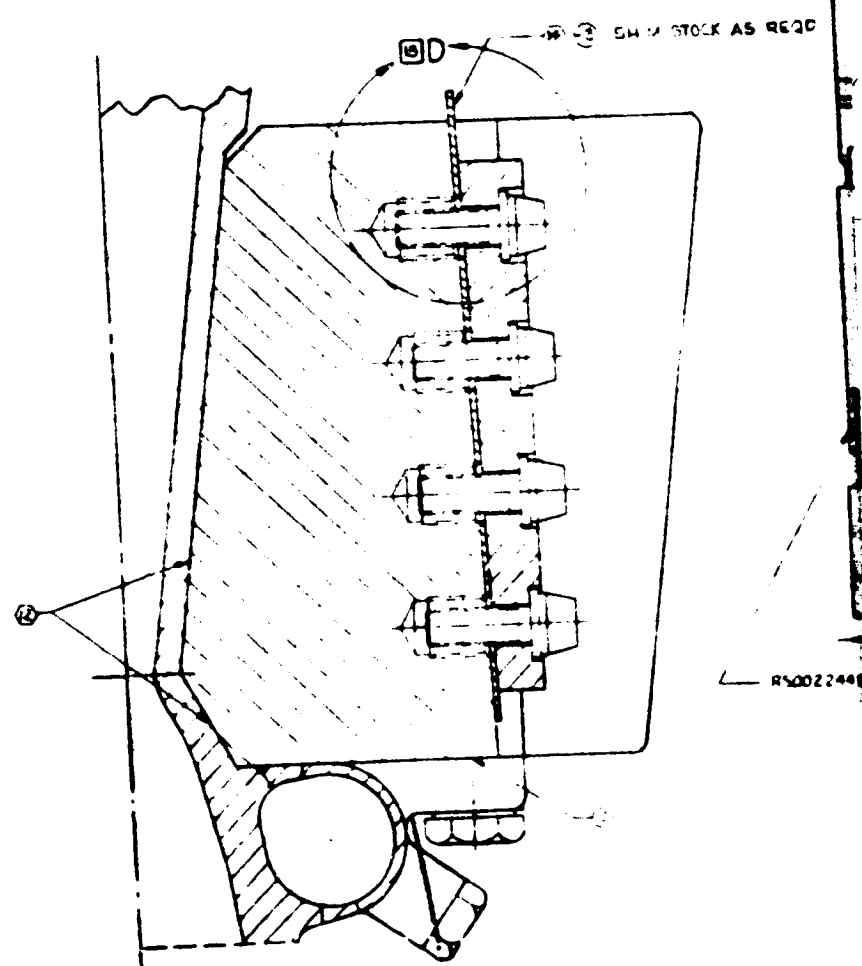
DOIT FRAME

2



FOLD O

VIEW D E
SCALE 2/1
(.3 SHIM STOCK AND MIDDLE C
BELT OMITTED FOR CLARITY)



SECTION C-C
SCALE 2/1

1 30 2 PLACES
2 30 2 PLACES

DRILL 1/4" DIA THRU 2 WALLS
SPOTFACE 1/4" DIA DEPT 1/8" MAX
SOCS - .0003 DIA DEPT 1/8" MAX AT R
CSK TO R 385.0003
TAP 1/4" - 16 UNC - 32 MAX FILL
Ø 1/4" MAX DIA
PO 3/64" - .0003 PER WALLS 1/4" R.C. TO 2 R
R5002248 REF
INSTALL .002 BELON SURFACE
PER R5001-003
2 PLACES

R5002248 REF BELT 2 REQD
R5002248 REF FASTER 2 REQD
TYPICAL TO 20.5 IN-LS

FOR TO
MINATO
GROSS
S A L
ERFOR
E PLAY
E 3 SH
AYES
BE IN
R22044
KTURE
RING A
MAGE
THE R
IDENT
BOARD
S DRAM
SEMBLY
MORING
TALL AN
TUBE VA
TALL SE
YREATE
STON IN
STRUCTURE
IN COMB
FOR 20
TALL MO
20-000
AND P
NTIFY P
CONE P

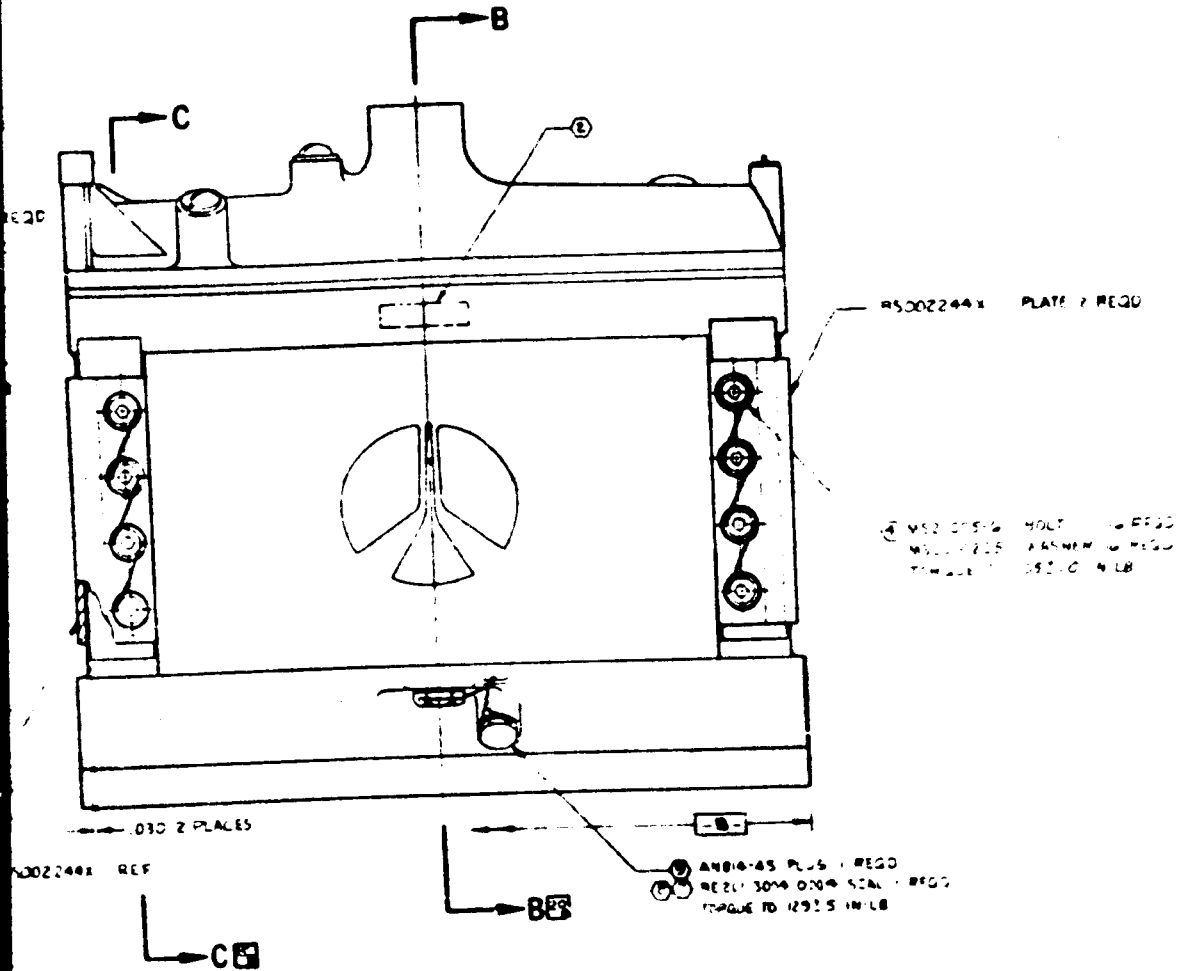
REPRODUCIBILITY OF THE ORIGINAL PAGE IS POOR.

FOLDOUT FR

FOLDOUT FRAME

3

4



3
FOLDOUT FRAME

REPRODUCIBILITY OF THE ORIGINAL PAGE IS POOR.

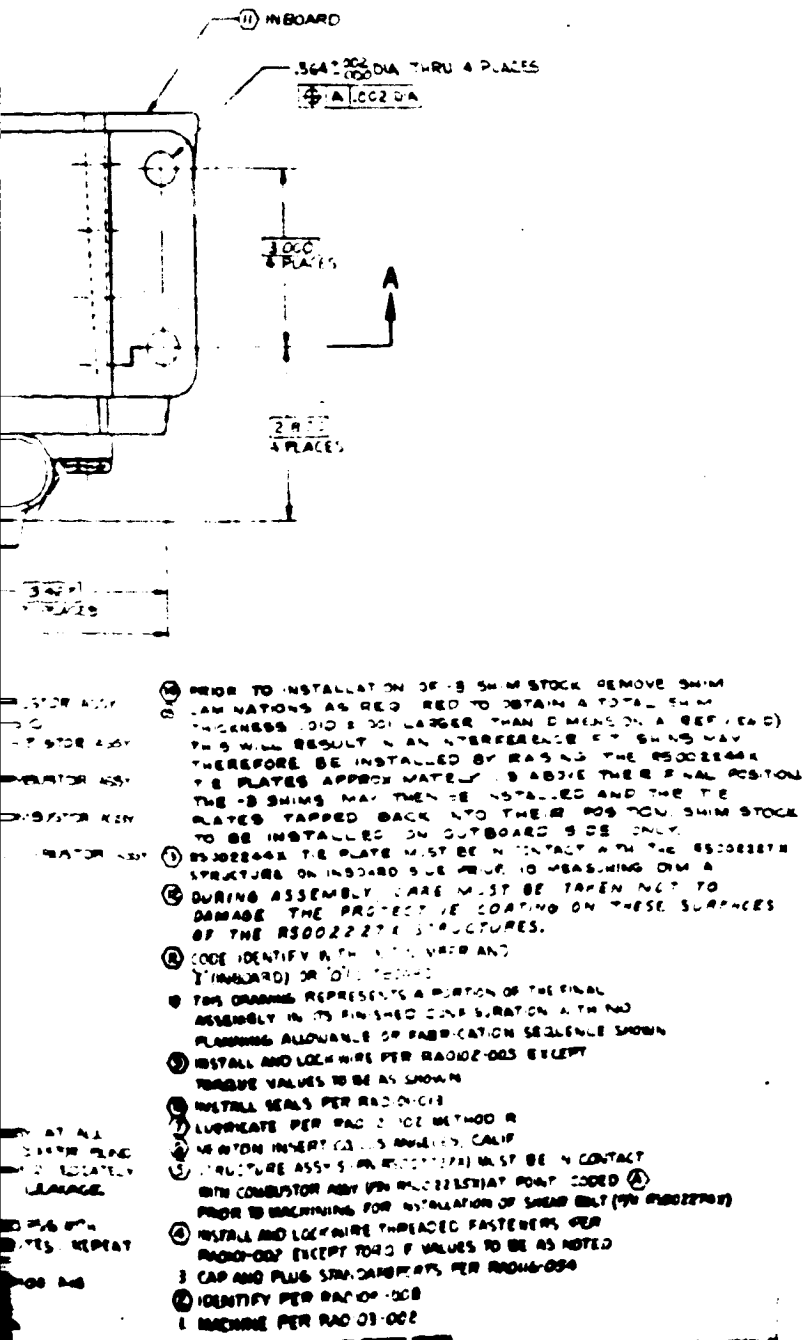


Figure 19. Final Combustor Segment Assembly

Fabrication Problem Resolution. Following is a brief description of the primary problems encountered and their resolution in the fabrication of breadboard No. 1 combustor assembly.

Cast Liner Discrepancies. Initial attempts at investment casting the combustor liner on the CSE Program were unsuccessful. Difficulty was experienced in holding the required dimensions and eliminating porosity. However, improved tooling and increased experience with the characteristics of the NARloy material resolved most of the problems.

As a result of the casting experience gained on the CSE Program, the quality of the cast liners delivered for the breadboard combustors was improved. The primary difficulties consisted of solidification shrinkage-type defects, sponginess of the thin walls, and ceramic inclusions present in the parent material. Since the discrepancies for many of the liners were relatively small, the castings were successfully reworked and then accepted.

Initial segment channel closeout copper-plating attempts presented difficulties in getting a uniform, high-quality layer in one plating cycle. The thin copper layer became porous during each plating attempt. This required interim electroform copper surface cleanup between plating cycles, and essentially resulted in several layers of plating on the first two segment assemblies (C01 and C08). Following these two units, the porosity problems were solved and single plating cycles were satisfactory.

Six segment assemblies had a weak and/or brittle bond between layers of EFNi. A metallurgical investigation was made of samples cut from trim stock on the segments and on the control panels that accompany the segments through all electroforming stages. The investigation results revealed that the cause for the weak bonds were as follows:

1. The electroform activation process allowed some deposition of silver on the EFNi surface prior to initiating the next layer of nickel. The minute quantities of silver in the bond line disturbed the EFNi bonding sufficient to cause a brittle discontinuity.

2. Electrical shorts were discovered in some of the "hot leads" used in the plating process. The lead allows the segment to complete the plating circuit as soon as the segment is introduced into the electrolyte. This prevents surface condition degradation prior to establishing current flow by the standard circuit.

An investigation using sample parts indicated that annealing the EFNi substantially reduced the brittleness of the joint and the surrounding material to give acceptable characteristics. It had previously been decided to anneal the EFNi to reduce its susceptibility to H₂ embrittlement. Therefore, the same anneal cycle was used to accomplish both objectives.

Preliminary EB weld attempts to attach the INCO 625 transition pieces to the EFNi on the segment aft fuel manifold were unsuccessful. Differences in the magnetic properties of the two materials caused the electron beam to deflect, resulting in an unsatisfactory weld joint. The beam was directed to enter the joint at the proper location, but strayed from the joint before adequate penetration was obtained. Efforts to bias the beam location, width, power, and direction to provide adequate joint depth were not successful. The transition joint attachment was then redesigned to allow thinner EB weld depth requirements. Maximum weld depth penetration requirements were decreased and EB welding of the redesigned joint configuration was successful.

INJECTOR DESIGN

The design of the injector was based on hot-fire experience with the prior CSE Program. Table 3 summarizes the cast segment injector requirements, geometry, and performance. The injector operates nominally at a mixture ratio of 5.83 and discharges to a nozzle stagnation chamber pressure of 1200 psia (1224-psia injector end chamber pressure). The injector element consists of a central oxygen core surrounded by a hydrogen annulus. Sixty-eight elements in three parallel rows were chosen, which yields a thrust per element of 182 pounds.

TABLE 3. CAST SEGMENT INJECTOR PARAMETERS

Parameter	Linear Engine		
	Element	Segment	Engine
<u>General</u>			
Thrust, klb			248
			5.83
			443
I _s (alt), seconds			1224
Injector End Chamber Pressure, psia			1200
Nozzle Stagnation Chamber Pressure, psia			182
Thrust/Element			
<u>Oxidizer*</u>			
Flow, lb/sec	0.340	23.10	462.0
Flow Area - Nozzle, in. ²	0.00385	0.262	5.24
- Post, in. ²	0.00882	0.600	12.0
Nozzle Velocity, ft/sec	179	--	--
Velocity Head, psi	245	--	--
Reynolds No.	5.8x10 ⁵	--	--
Post Velocity, ft/sec	78.2	--	--
Velocity Head, psi	46.8	--	--
Reynolds No.	3.8x10 ⁵	--	--
Pressure Loss, psi	248.5	--	--
Injection Pressure, psia	--	--	1472
Temperature, F	--	--	-288
Density, lb/ft	--	--	71
Interface Pressure, psia	--	--	TBD
Nozzle ID**, inch	0.070	--	--
Post ID/OD, inch	0.106/.134	--	--
Dome Volume, in. ³	--	TBD	TBD
Dome A _x , in. ²	--	TBD	TBD
Post Recess, inch	0.150	--	--
<u>Fuel</u>			
Flow, lb/sec	0.0566	3.85	77.0
Annulus Area***	0.0139	0.945	18.9
Velocity, ft/sec	1584	--	--
Velocity Head, psi	100	--	--
Reynolds No.	1.2x10 ⁸	--	--
Cup ID, inch	0.189	--	--
Area, in. ²	0.0281	--	--
Pressure Loss, psi	96.6	--	--
Overall Pressure Loss, psi	240.5	--	--
Injection Pressure, psia	--	--	1469
Temperature, R	--	--	640
Interface Pressure, psia	--	--	TBD
Velocity Ratio	--	--	20.3
Density, lb/ft ³			
Body	--	--	0.388
At post tip	--	--	0.370
Cup	--	--	0.357

* The four corners flow at 82 to 88 percent of listed values
 ** 0.063-inch-diameter for the four corner posts
 *** Below the support legs

Recessment of the oxidizer post tip within the fuel cup is an effective means for improving the combustion performance and stability characteristics. For a non-recessed system, the sudden expansion into the combustor results in a loss of relative velocity between the two streams which increases the mixing length and degrades the performance in a short combustor. Conversely, an excessive post tip recess increases the probability of eroding the post tip and producing high cup stagnation losses without increasing the combustion performance. Hot-fire test results during the CSE program indicated a post tip recess of 0.150 inch was satisfactory, but not necessarily optimum.

The oxidizer dome is cast in one piece, using 304-L CRES in a vacuum investment casting process. A flow deflector, located just below and in line with the inlet, also is part of the casting. The flow deflector prevents the oxidizer posts directly in line with the inlet from exhibiting greater than average flowrates due to the dynamic head. It also acts as a guide vane to turn the flow 90 degrees to each half of the dome.

Each combustor contains provisions for monitoring one chamber pressure, two fuel injection parameters (either temperature or pressure), two vertical accelerometer pads, and one oxidizer injection Photocon pressure. An active Photocon boss is at each end of the dome.

The oxidizer post hole pattern (Fig. 20) is match-drilled into the dome body. The 23 holes in each of the inner and outer rows are canted $4^{\circ}15'$ inward to the vertical centerline to present direct impingement on the chamber walls. The theoretical impingement point of these canted streams is below the throat plane. The 22 holes in the center row are on, and parallel to, the axial centerline and are drilled normal to the dome body. All holes are $0.136 + 001/-000$ inch in diameter.

The oxidizer posts shown in Fig. 21 are made of 304-L CRES and contain an integrally machined nozzle in the upstream end to maintain the flow balance and system impedance. All posts contain a 0.070-inch-diameter nozzle except the four corner posts which contain 0.063-inch-diameter nozzles. The oxidizer flow was reduced to

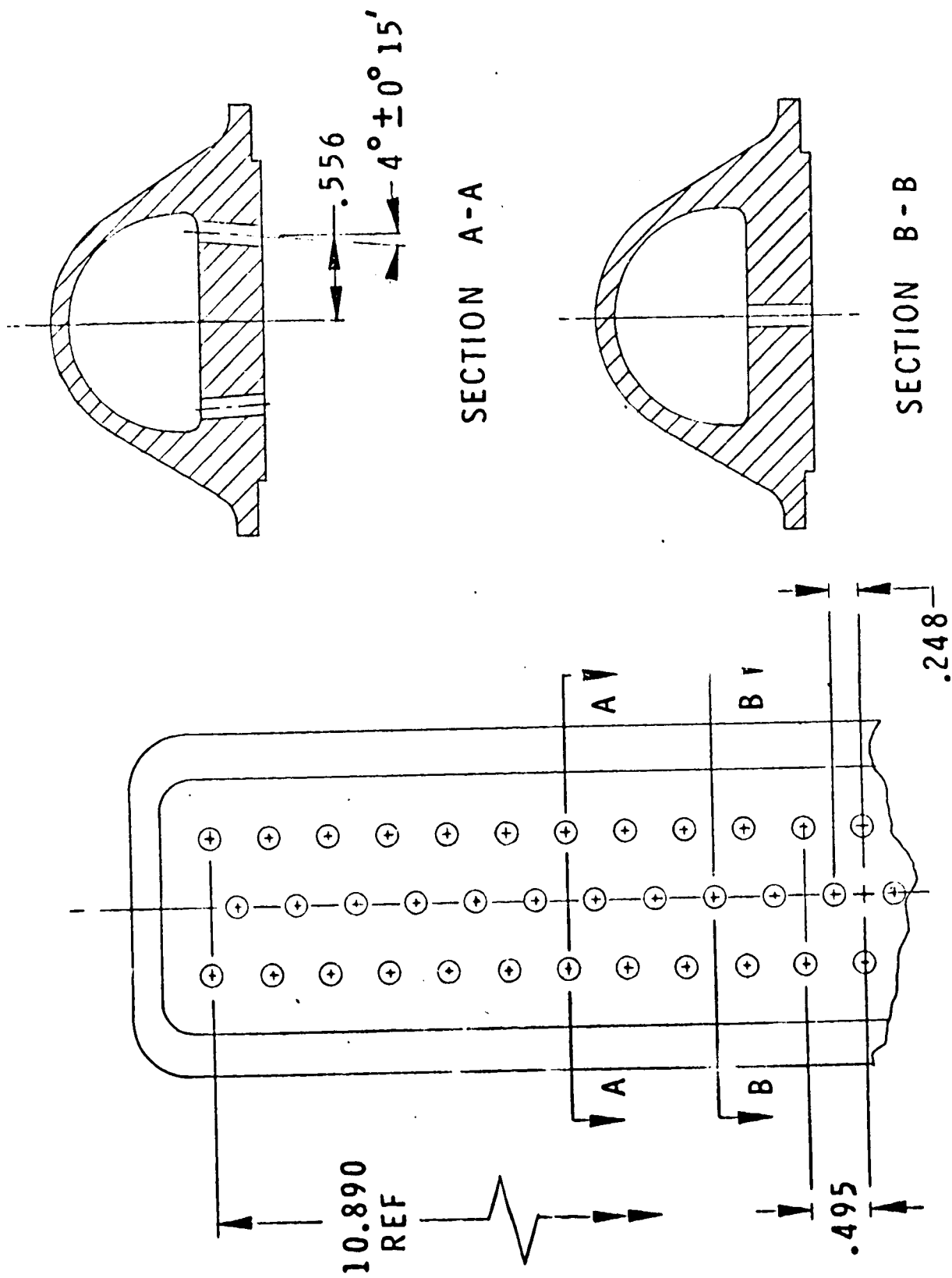
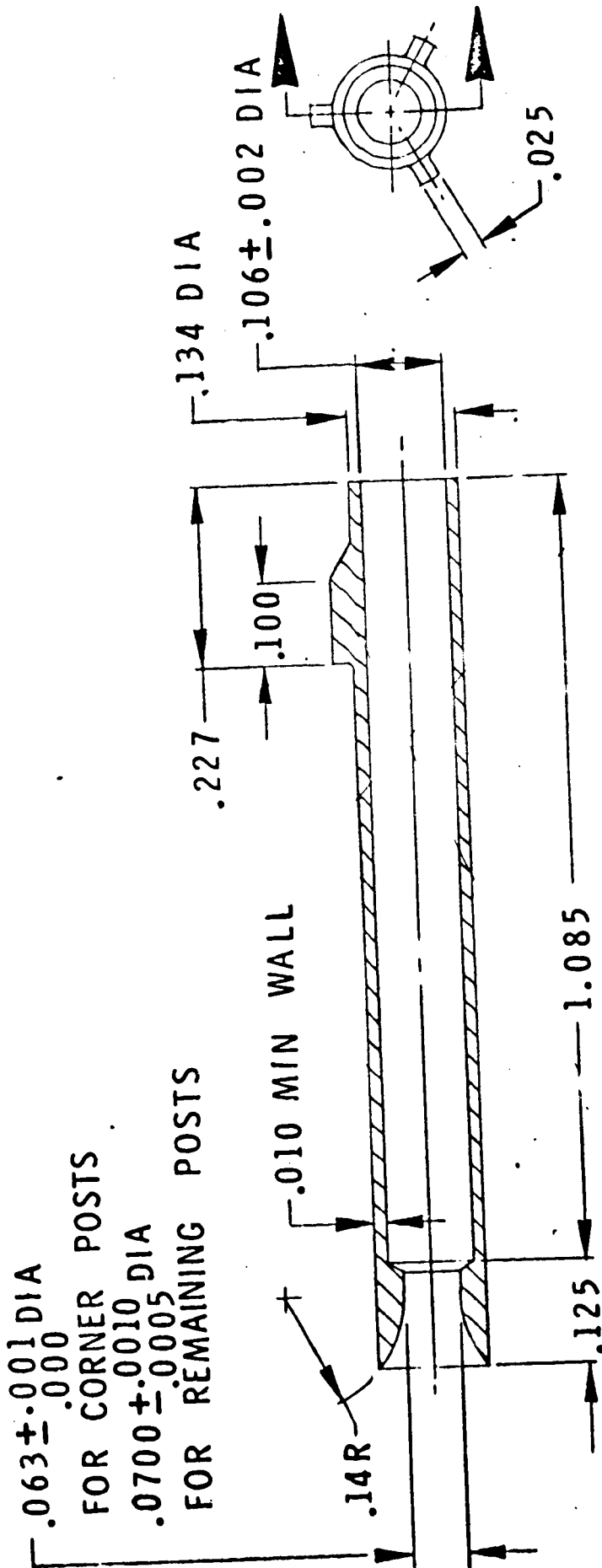


Figure 20. Oxidizer Manifold Geometry



R-9049

Figure 21. Oxidizer Post Geometry

82 to 88 percent of nominal flow in the four corners to prevent overheating in the corner. Three tabs are incorporated on the OD of the oxidizer post to position it properly in the fuel cup. The machined posts are furnace brazed into the oxidizer dome using Nioro alloy (82 percent gold-18 percent nickel).

The flow distribution for each element is obtained at a manifold flow of 100 gpm (≈ 100 psig). The water stream from each element is collected and the average flowrate per element is obtained. The nozzles of posts with flows greater than 3 percent of the average flow are peened, while the nozzles of posts flowing less than 3 percent of the average flow are reamed out. The four corner posts must flow 85 ± 3 percent of the overall average flow.

The injector faceplate containing the fuel cups is welded to the chamber. The oxidizer manifold is then welded to the chamber taking care to ensure that the LOX post recess is correct. The interaction of the oxidizer post within the fuel cup is shown in Fig.22 . Based on hot-fire tests using injectors with zero and 0.150-inch oxidizer post recess, the cup pressure loss is 96.6 psi. The total oxidizer system pressure loss is 248.5 psi and the fuel side pressure loss is 240.5 psi at rated conditions.

NOZZLE ASSEMBLY DESIGN

The brazed nozzle assembly is required to transmit the aerodynamic pressure load generated by the expanding combustion gases to the backup structure. In addition, it must be capable of withstanding the heat loads generated by these gases.

347 CRES has been the traditional material for use in hydrogen-cooled rocket nozzle skirts. This is due to the material's excellent compatibility with hydrogen, strength characteristics at cryogenic temperatures, and fabricability (being easily brazed, welded, and formed). An alternate material (Inco 625) was considered for the nozzle coolant tube. However, it was determined that 347 CRES would prove to be adequate for the application and was selected on the basis of its better fabricability.

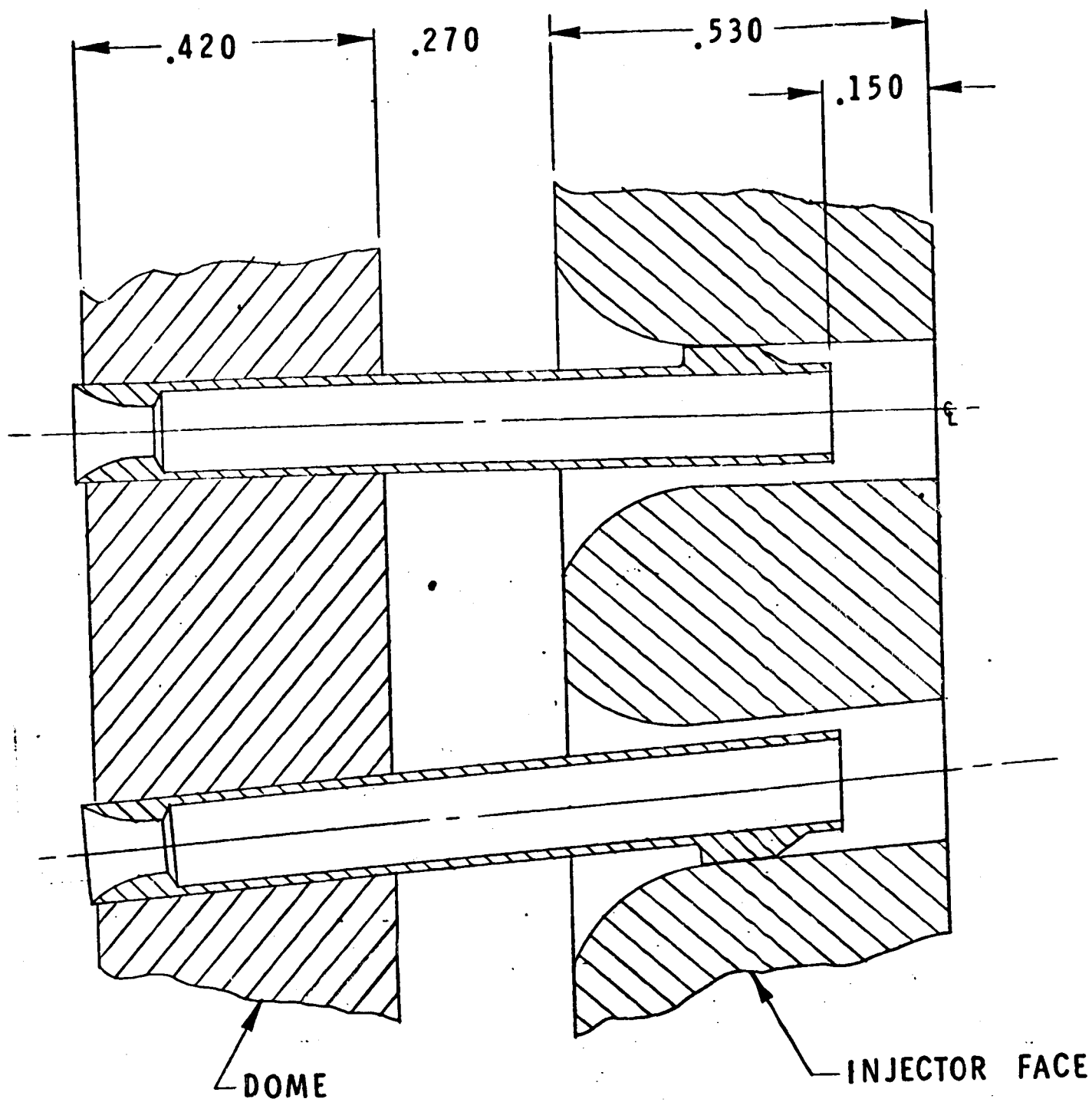


Figure 22. Oxidizer Post, Fuel Cup Interaction

The reinforcing bands or hatbands are required to transmit the aerodynamic pressure loads from the hot-gas face to the backup structure. They require attachment to the tubes and must provide for attachment to the backup structure. Tube attachment is accomplished by brazing the bands to the tube surfaces. Attachment to the backup structure is accomplished by providing mounting pads for rod end bearings which, in turn, transmit the loads to the backup structure.

The expected aerodynamic loading is shown in Fig. 23 for the values of chamber pressure expected during engine start and mainstage operation. It is of interest to note that the nozzle wall will experience a local pressure load of approximately 34 psia at virtually every point along its length during engine start. This behavior results in the equal spacing of the hatbands. The flanged (three corner box) shape of the hatbands was selected because of its simple fabricability and high structural efficiency. The longitudinal slots, placed at 12.40-inch intervals along the length of the hatbands, allows the bands to accommodate differential thermal growth.

The basic requirements for the fuel inlet manifold are equal distribution and low pressure drop. The minimum cost method is to manufacture a large-volume, untapered tube. Since weight was less important than cost, a 3.50-inch OD by 0.300 inch wall pipe was used to distribute the fuel. The thick wall section results from the pressure requirements and the loss of material at the point where the pipe joins the coolant tubes. Pressure drop through this manifold was estimated to be 19.50 psid, while good fuel distribution was assured by the low cross velocity head of 4.28 psid.

The primary function of the forward manifold joint is to provide attachment of the nozzle coolant tubes to the combustor and to survive the relatively high heat transfer rates predicted for this location on the nozzle. The forward bar, made of OFHC copper and machined to provide a close fit over the tube crowns, operates at a temperature of 900 F.

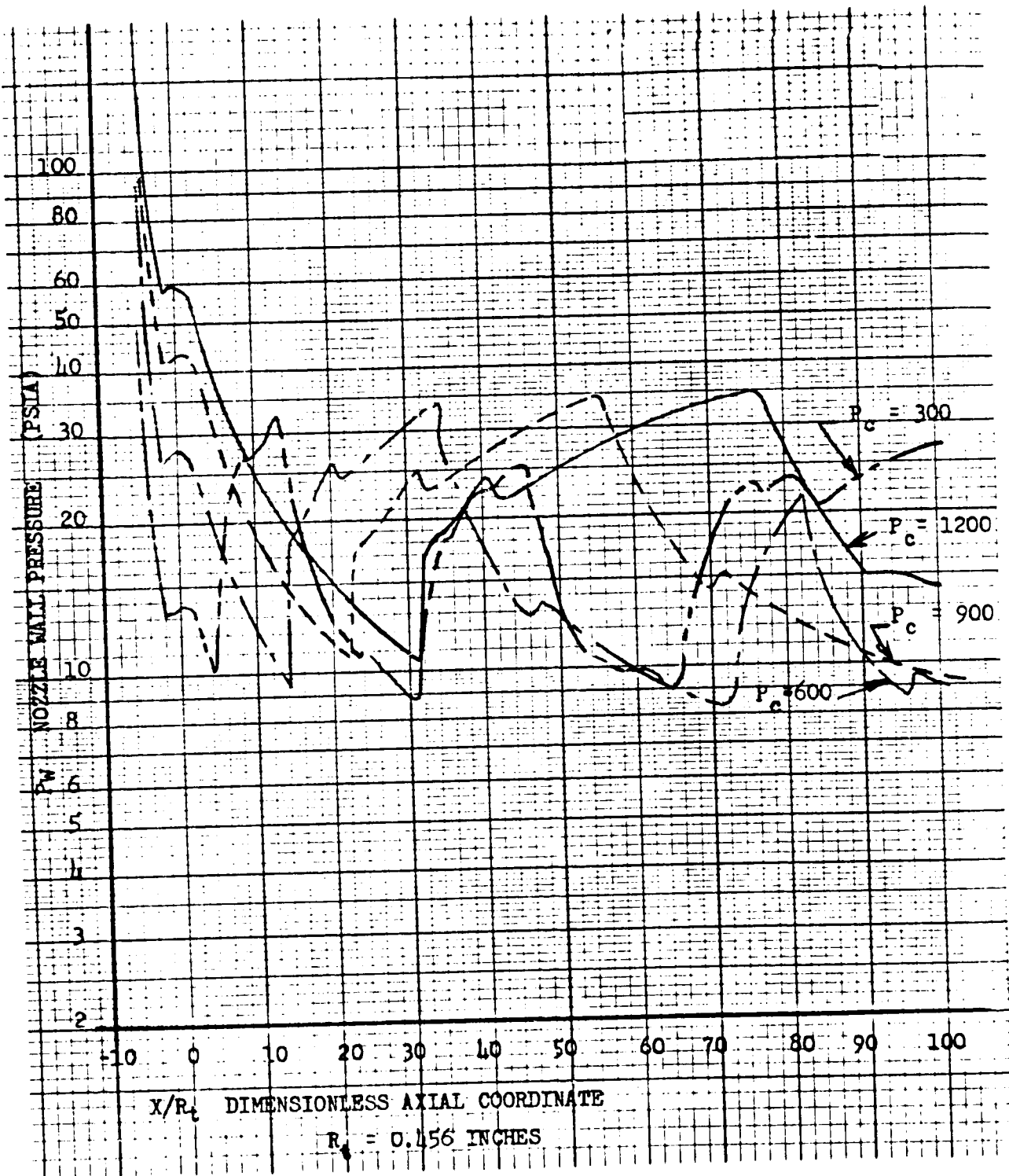


Figure 23. Nozzle Wall Pressure Profiles

COOLANT TUBE DESIGN

The test bed required a nozzle structure that was light in weight and capable of tolerating high heat transfer rates over approximately 100 sq ft of surface area. The primary material candidates for this application were 347 CRES and Inconel 625. Nickel and other high-conductivity materials for the coolant tube were rejected due to the high weight factor.

Figure 24 illustrates the constraints placed on the tube size by stress and wall temperature conditions. Also shown is the upper limit line for the ratio of the tube OD to tube-wall thickness for 347 CRES and Inconel 625 tubes stressed by an internal pressure of 2160 psia. It is apparent that Inconel 625 offers the potential of a design with much thinner tubes and, consequently, less pressure drop and weight than would a 347 CRES design.

Fabrication experience with Inconel 625 is limited. Brazeability has been demonstrated, but only for nickel-plated Inconel 625 to 347 CRES; however, there was some uncertainty as to its brazeability in a hydrogen atmosphere. 347 CRES has been used extensively for brazed tube assemblies with excellent results. Since 347 CRES would be adequate from the heat transfer and stress stand points, it was decided not to risk the potential fabrication difficulties of Inconel 625 and to use 347 CRES for the linear engine nozzle coolant tube.

A single uppass cooling circuit was selected for the nozzle which offers the advantage of minimum pressure loss while permitting a reasonable tube size.

The gas-side heat transfer coefficients were calculated for the nozzle contour specified. The technique used is similar to the Bartz boundary layer analysis. The coolant-side heat transfer film coefficients were calculated according to the McCarty¹ correlation. The point of maximum heat transfer coefficient is where the combustor and tube bundle are joined. Using the above heat transfer coefficients, the tube size was determined to be 0.200 inch for the diameter and 0.015 inch wall thickness.

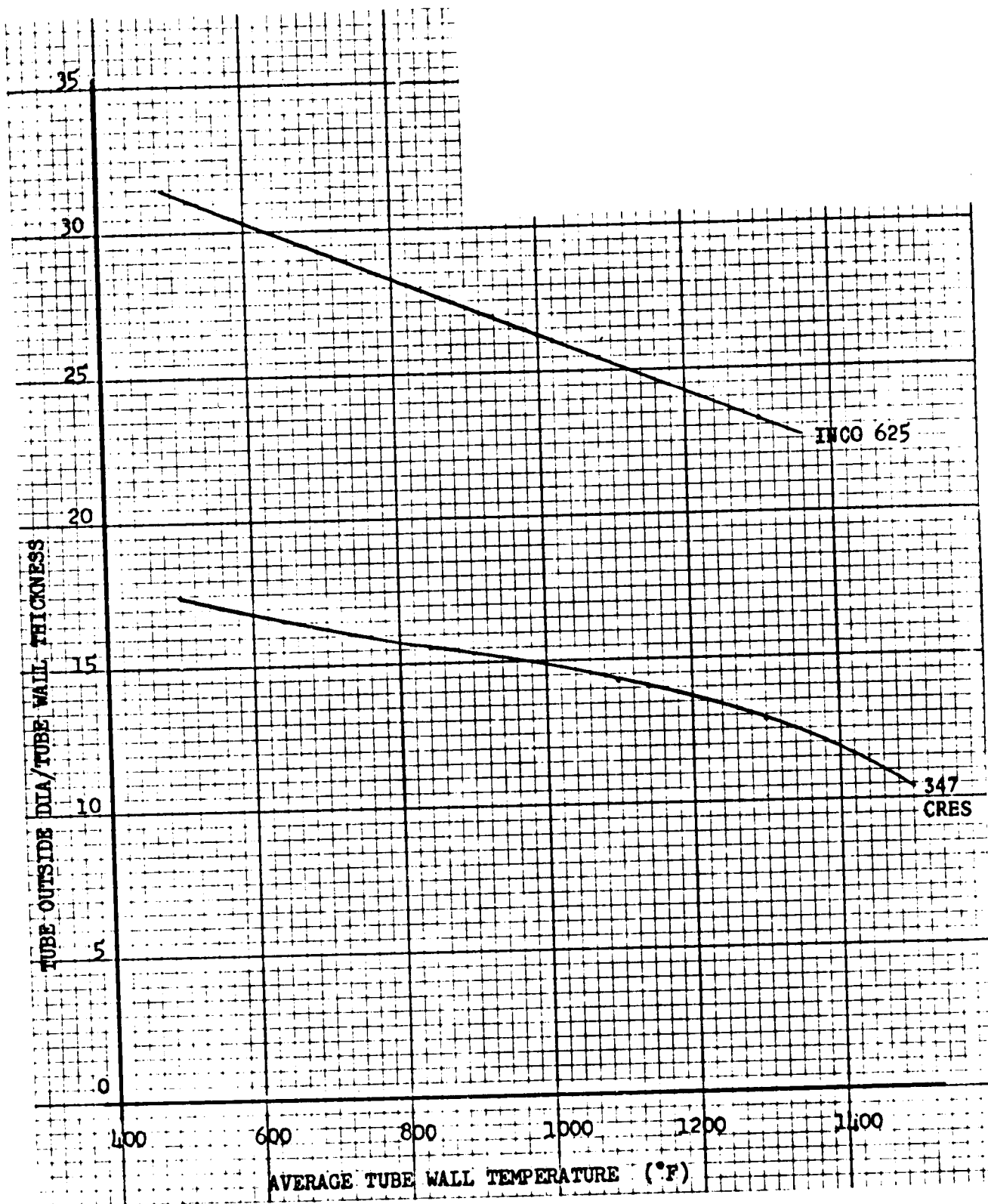


Figure 24. Lines of Maximum OD/T_w for 347 CRES and INCO 625 With 2160-psia Internal Pressure

Thermal cycles to failure for the 0.200 x 0.015 wall 347 CRES tube were calculated to be 62. The analysis used assumed that the tube was rigidly supported and, therefore, would yield a value of effective plastic strain somewhat higher than would be seen in practice. The analysis is therefore conservative and the tube should easily meet life-cycle requirements.

External Dimensions (Nozzle Contour)

The nozzle wall contour was initially determined to be an ideal spike designed for an expansion ratio of 112.94 and truncated to an $X/R_T = 100$ (R_T is the nozzle throat gap of 0.456 inch). This corresponds to 24 percent of the length of a 15 degree half angle plane flow conical nozzle of equal area ratio. A relatively severe sea level recompression pressure (with accompanying high heat transfer rates) just downstream of the combustor exit was alleviated by means of a minor contour change that reduced the effective flow divergence just downstream of the combustor exit.

THRUST CHAMBER FABRICATION AND ASSEMBLY

The first 10-foot rail, comprised of 10 combustor assemblies and 2 5-foot nozzle sections together with corresponding fuel and oxidizer manifolding and support structure, was completed in July 1971. The second rail, which includes the turbine exhaust manifold and additional support structure, was completed in August providing a complete thrust chamber assembly. The thrust chamber assembly process was relatively trouble free.

Each 10-foot rail was assembled separately in a fabrication jig which accurately positioned each of the component parts. The two 5-foot nozzle sections were first joined by hand brazing along the mating line formed by the end tube of each section.

Furnace brazing of the nozzle sections resulted in transverse distortion (bowing) of the tube bundles and mislocations of the brazed-on support bands, resulting in a mating line that was not perfect. The bowed nozzle tube bundles were aligned on assembly through the use of external clamps and holding fixtures. The strains

imposed by this procedure resulted in a few cracks in the two tubes at the joint, which were braze repaired. The cracks and resultant leaks, however, increased during hot-fire, apparently due to the residual strains imposed here. Adapter plates were used to compensate for the mislocated hat bands (up to 1/2 inch) at each end of the nozzle bank thereby permitting attachment of the end fences. None of these assembly difficulties resulted in a significant delay in the assembly schedule.

Welding the fuel manifold to the aft nozzle band end bars was accompanied by some minor distortion of the aft end of the nozzle. Cracks also developed in the manifold attachment welds at the center of the nozzle. The thermal distortion initially experienced was later minimized by controlling heat input into the weld joint and nearly eliminated by selectively torch heating the manifold. The cracking in the region of the braze joint was eliminated by stopping the weld short of the brazed region, and closing out the joints with tungsten inert gas (TIG) braze.

Attachment of the combustor assemblies to the nozzle forward end bars was accomplished by first welding all 10 combustors together. This was followed by welding on the 10-foot nozzle. The attachment of the segments to each other by welding around the segment fuel manifolds caused the end cap closing braze joints of several of the segment fuel manifolds to develop small leaks. No attempt was made to seal the leaks, and vent holes were drilled in the end cavities to discharge the hydrogen leakage into the exhaust gas stream. In those segments not completed at the time the problem was discovered, the closeout braze was replaced with weld, which eliminated the problem. The TIG brazing of the NARloy segment to the copper end bar on the nozzle also resulted in some joint leakage. Repairs sealed those leak paths.

The thrust chamber assembly was completed by mounting each 10-foot bank assembly onto the support structure. Dimensional tolerances accumulating between the chamber support ribs and the nozzle tubes required custom shimming of the rib mounting pads to keep the nozzle flat when attached to the cross structure.

The configuration of the base closure seal had previously been proved by laboratory testing of simulation samples, which permitted the seal fabrication and installation to proceed smoothly. Interference of turbine exhaust manifold instrumentation ports with the seal was remedied by relocating the instrumentation ports.

COMBUSTOR FLOW DISTRIBUTION AND CALIBRATION

The combustor assemblies were subjected to a flow distribution and calibration test prior to installation into the test bed. The flow distribution was determined for each combustor to ensure the proper inner, outer contour wall and side plate flow distribution. Flow calibration data were utilized to determine the engine combustor orificing requirements.

Flow distribution in the parallel circuits is controlled by drilled orifice holes at the coolant exit end of the inner contour wall. The discharge orifices are drilled oversize with the capability of being peened to reduce inner contour wall flow. The analytically determined flow resistance for the parallel system is shown in Fig. 25.

In accordance with the heat transfer analysis, the combustor cooling circuits were designed to provide 46 percent of the total flow to each contour wall and 4 percent to each side plate.

The fluid analysis is based on operating conditions with hydrogen and, as such, utilizes a diminishing density value. The combustor flow distribution evaluation was accomplished using water ($\rho = C$). The water flow required to yield the proper hydrogen distribution under hot-fire conditions was determined by utilizing the resistance values shown in Fig. 25 assuming no resistance shift from hydrogen to water. The required water flow distribution is:

Inner contour wall 47.2 percent
Outer contour wall 45.5 percent
Side plates 3.65 percent

Pc 1224 psi

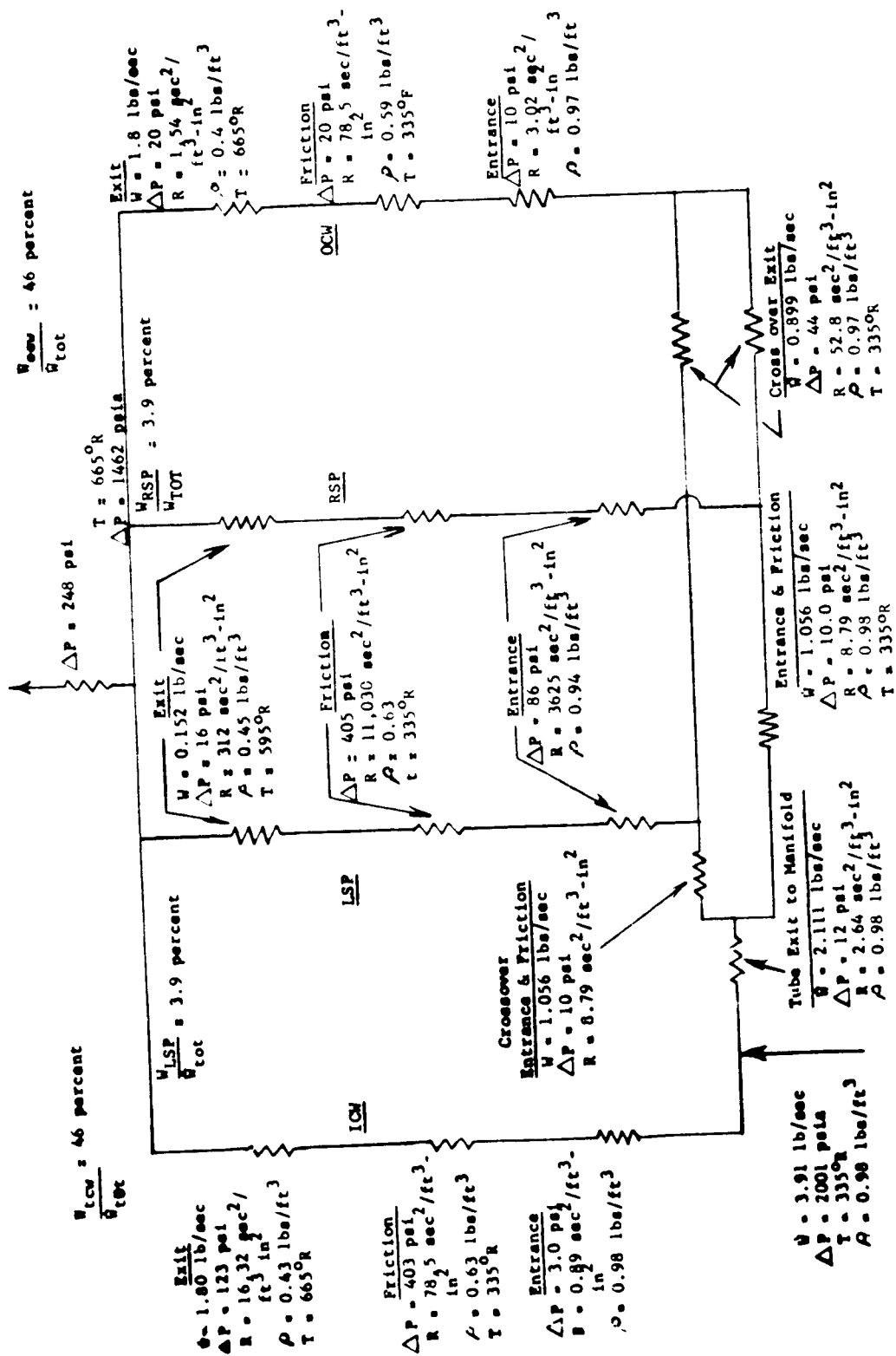


Figure 25. Flow Resistance for the Parallel System

In accordance with the analytically determined cooling capacity requirements, a tolerance on the flow distribution was established;

Inner contour wall 46.9 to 49.0 percent

Outer contour wall 44.0 to 46.0 percent

Side plates 4.0 to 4.8 percent

Flow distribution for all 21 combustors was established in the medium flow laboratory. The inlet and outlet ends of the combustor were fitted with a fixture so that the flow could be supplied to the inner contour wall inlet and the individual outlet, flow from each of the four walls could be collected and measured.

The test procedure consisted of flowing water at inlet pressures from 100 to 250 psig at uniform discharge pressures controlled by the four discharge valves. Back-pressure was employed to preclude cavitation. The flowrates from the four walls of the combustor were measured and utilized to calculate the flow split. The flow distribution of all 20 combustors was found to be reasonably consistent and within the specified tolerance limits.

Following the flow tests, the distribution of fuel and oxidizer flow to the individual combustors was defined by analysis using a digital multielement flow analysis.

The procedure was initiated by using fuel injection pressure and temperature and chamber pressure measurements in conjunction with fuel injector body resistances defined by analysis and fuel cup resistance defined from the studies of cup pressure drop.

Individual combustor fuel flows were computed and summed to compare to total measured combustor fuel flow. The sum in most cases agreed with the measured within 1 percent or less.

The injector cup pressure drop defined from the fuel-side analysis, the injector body resistance from the calibration data, and calculated oxidizer system feed system resistances were used to compute the oxidizer flow to each combustor. The

sum of the individual flows were compared to total measured flow. Individual combustor c^* efficiencies were computed from the calculated flows. They varied by approximately ± 5 percent. The sum of oxidizer flows, in general, did not agree with measured values. An iteration procedure was established on individual combustor feed system resistances until the c^* efficiencies approached the average value. The sum of the oxidizer flows then generally agreed with measured values within less than 1/2 percent.

Table 4 shows the results of the computations including pressure drops combustor heat load, combustor ΔT , average temperatures, pressure drops, flows, and mixture ratios for run 012 (1971). The distribution of flow to the individual combustors remains essentially the same for all test firings. The mixture ratio distribution shown in the table is typical. The percentage variation of any individual combustor from the mean value remains essentially the same for all runs. The summation error indicated on fuel and oxidizer flow is in lb/sec.

Flow distribution testing of the complete engine assembly (both fuel and oxidizer sides), to verify the analysis and establish more definitive values for the oxidizer feed system resistance, would permit more precise definition of the flow distribution. Flowrates from each combustor as a percentage of total flow would be measured.

BASE SEAL

The base seal is a sheet metal member welded to the outer edge of the turbine exhaust manifold and the fuel manifold. The seal provides a positive means of preventing gas flow between the turbine exhaust base and the engine compartment during firing. Figure 26 illustrates the configuration of the base seal installed on the engine.

Thermal expansion of the turbine exhaust manifold and thermal contraction of the nozzle fuel inlet manifold results in shear deformation of the seal. The maximum shear deformation occurs in the corners of the seal. Figure 27 illustrates the thermal movement of the turbine exhaust manifold and the hydrogen line at this point. Point A on the turbine exhaust manifold translates to A^1 , and point B

TABLE 4. COMBUSTOR FLOW ANALYSIS

SEGMENT FLOW BREAKDOWN BASED ON FL RES
 SUMMATION ERROR, FUEL FLOW= 0.698

OX FLOW= -.921

POSN	PCIE	SFG MR	C* EFF	W FL	W OX	Q
1	1113.8	5.621	98.946	4.014	22.561	8298.5
2	1112.9	5.277	98.969	4.018	21.203	9617.1
3	1167.8	5.237	99.044	4.229	22.144	8447.0
4	1089.3	5.197	98.865	4.145	21.544	8424.4
5	1119.0	5.402	98.978	4.205	22.715	7951.3
6	1117.7	6.194	99.298	3.753	23.217	7853.5
7	1128.5	5.328	98.983	3.921	20.889	8092.1
8	1180.8	5.539	99.179	4.049	22.425	8205.8
9	1162.0	5.108	99.050	4.147	21.184	7379.7
10	1167.3	5.252	99.029	4.171	21.908	7659.9
11	1125.3	5.345	98.969	3.958	21.157	7141.1
12	1107.7	5.044	98.885	4.041	20.383	8177.1
13	1135.5	5.653	98.992	3.873	21.894	9441.3
14	1058.1	5.141	98.858	3.963	20.371	8213.1
15	1112.4	4.969	98.805	4.152	20.635	7998.4
16	1109.4	4.890	98.865	4.055	19.828	7837.5
17	1075.5	4.887	98.829	4.048	19.783	7726.6
18	1120.8	5.631	99.020	3.872	21.804	8020.1
19	1100.4	4.983	98.874	4.026	20.061	7619.2
20	1110.6	5.186	98.833	3.961	20.545	8548.2

POSN	CUP R-FL	CUP R-FL	INJ R-FL	SEG R-OX	CUP R-OX	INJ P
1	84.2	2.060	5.361	15.328	11.696	1339.2
2	71.8	2.040	5.341	14.165	11.298	1319.3
3	65.7	1.846	5.147	14.416	9.477	1378.0
4	99.4	2.532	5.833	14.294	15.153	1329.5
5	93.6	2.344	5.645	14.877	12.831	1364.8
6	73.7	2.120	5.421	16.484	9.650	1357.1
7	69.3	2.060	5.361	15.935	11.227	1325.0
8	68.6	2.060	5.361	15.536	9.646	1399.8
9	59.5	1.865	5.166	15.889	9.379	1353.3
10	76.0	2.160	5.461	14.987	11.195	1376.7
11	72.2	2.080	5.381	17.839	11.419	1332.9
12	68.2	1.981	5.283	16.800	11.613	1302.0
13	77.1	2.060	5.361	14.963	11.375	1345.1
14	73.4	2.080	5.381	17.239	12.517	1249.9
15	71.8	1.904	5.205	15.117	11.931	1311.8
16	61.5	1.865	5.166	17.044	11.061	1291.2
17	75.3	2.221	5.522	17.033	13.611	1253.3
18	73.7	2.040	5.341	16.105	10.960	1343.1
19	73.1	2.180	5.481	16.990	12.856	1297.4
20	83.6	2.282	5.583	15.798	14.014	1325.2

TABLE 4. (Concluded)

POSN	AV INJ T	ICW T	DELT T	WALL T	AV W T=1028.1
1	607.4	629.2	323.4	1092.5	
2	700.3	674.0	416.3	1526.6	
3	587.9	578.1	303.9	994.0	
4	597.4	627.5	313.4	1102.6	
5	558.4	580.2	274.4	896.0	
6	614.5	674.7	330.5	1059.0	
7	606.4	632.0	322.4	1052.0	
8	595.9	582.8	311.9	980.6	
9	527.5	554.3	243.5	703.2	
10	543.2	569.5	259.2	775.2	
11	534.2	561.3	250.3	739.2	
12	595.0	574.8	311.0	1048.7	
13	712.9	682.2	428.9	1499.7	
14	608.9	599.9	324.9	1150.5	
15	568.2	596.9	284.2	940.8	
16	570.0	564.3	286.0	929.8	
17	563.3	573.1	279.3	930.9	
18	608.5	646.0	324.5	1054.9	
19	558.8	573.2	274.8	884.5	
20	633.1	627.0	349.1	1201.3	

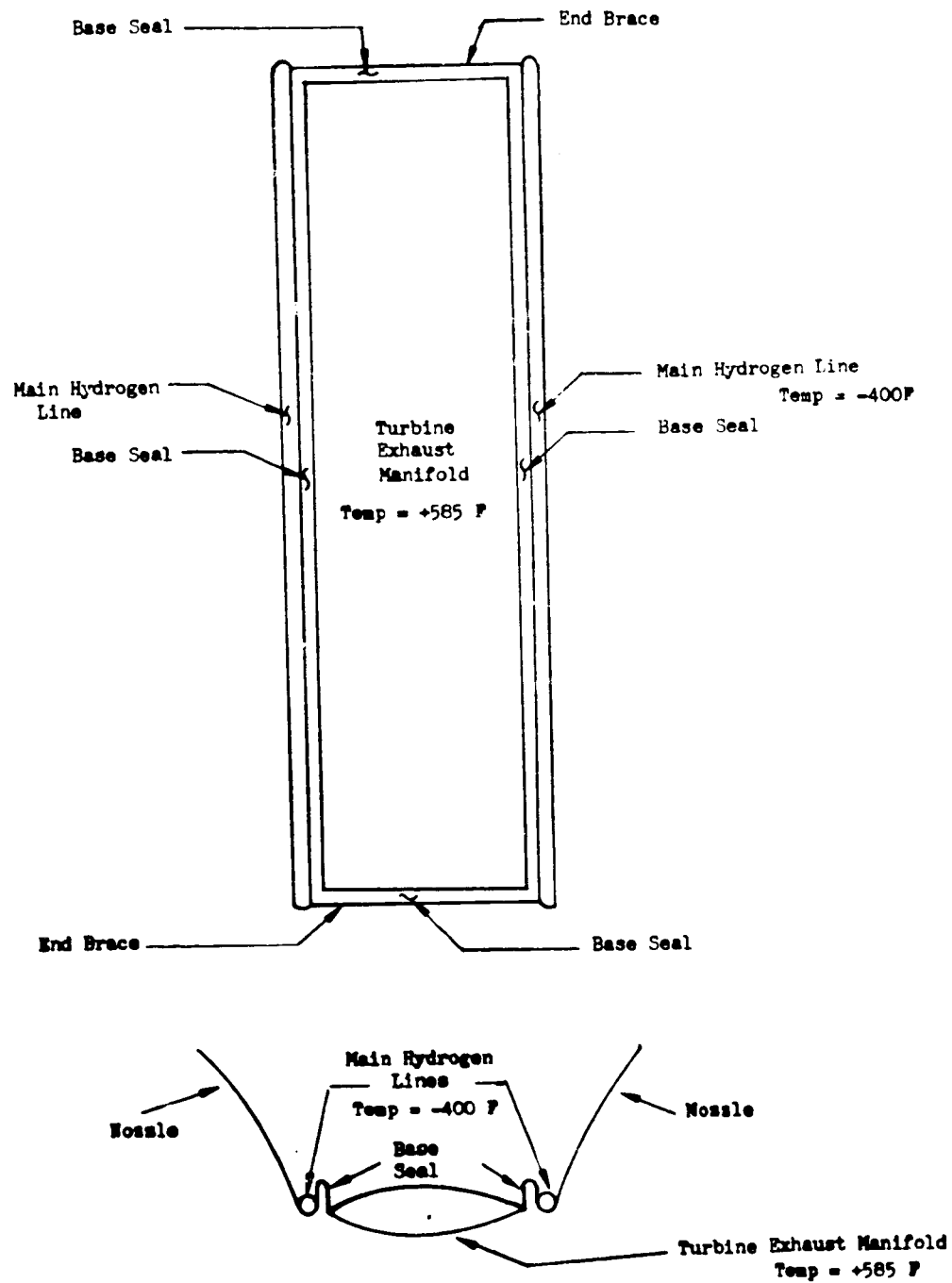


Figure 26. Base Seal Engine Installation

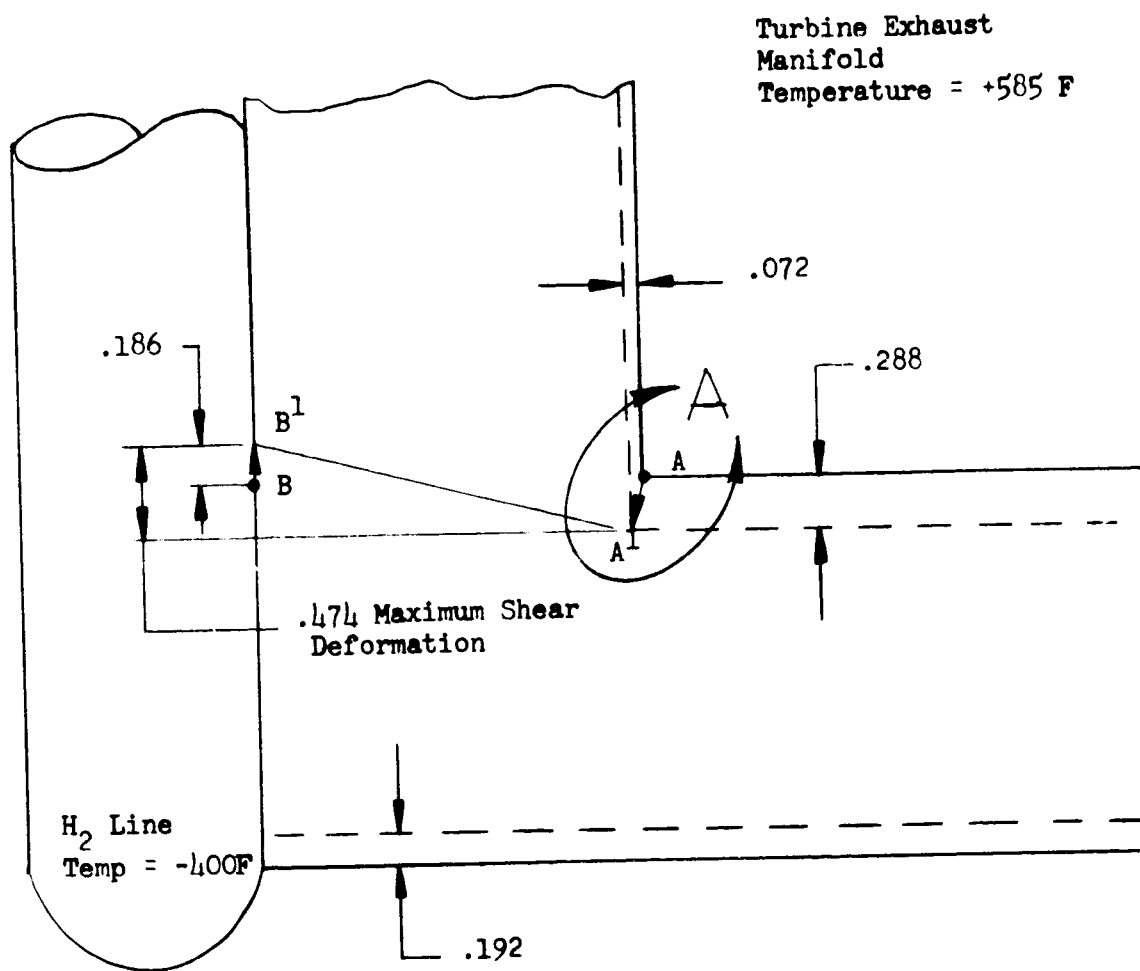


Figure 27. Maximum Base Seal Shear Deformation

on the fuel manifold translates to point B¹ as a function of the thermal expansion and contraction, thereby producing considerable shear deformation (0.476 inch) in the seal. The amount of shear deformation gradually decreases from the maximum value shown to zero at the midsection of the seal.

Several designs were subjected to simulated engine shear deformation tests. The test setup consisted of 1-inch-diameter CRES tubing to which the seal was welded. Rigid mounting was provided so that the total thermal movement of the seal was simulated. Liquid nitrogen was employed to chill the cold side. Hot nitrogen gas was supplied from a furnace-mounted coil to heat the hot side. The hot-side temperature was overdriven to 800 F (585 F nominal engine operating temperature) to compensate for the higher-than-normal temperature of the cold side (-200 F versus -400 F during engine operation). The differential temperature of 1000 F was simulated producing the same relative thermal movement of the seal as would be seen during actual engine operation.

As a result of the laboratory temperature-cycling tests, it was concluded that a seal was needed offering considerable flexibility and, consequently, resistance to damage as a result of shear deformation.

The first waffle pattern design was evolved to provide a maximum of flexibility. A 5-inch by 5-inch square sample (to determine the feasibility of fabrication) was fabricated of 0.016-inch 302 stainless steel.

The sample was fully annealed and installed in a test setup in which two parallel sides of the test sample were welded to stainless-steel bars. One bar was rigidly held, while the other bar was held with a pin slot mechanism. A hydraulic actuator was used to offset the latter bar, thereby placing the test part in shear deformation. A dial indicator was used to measure the amount of offset. A total of 330 mechanical cycles (shear deformation) were performed at displacements ranging from 0.1 inch to 0.5 inch. A total of 330 cycles were performed with 110 of the cycles made at 0.5-inch deformation. During cycling at all displacements, the part exhibited excellent flexibility. No tendency to buckle or crack was noted except adjacent to those cracks that were in the part before testing.

Following completion of mechanical cycling, the flat sample was formed around a 2-inch-diameter mandrel, thereby simulating the part as it will be installed on the engine. The part formed readily exhibiting no cracking, buckling, or deformation tendencies during the forming operation (Fig. 28).

The engine configuration employs a base seal 8 inches wide formed in a U shape with a 1-inch-diameter radius. The part tested was only 5 inches wide and was able to comply with the deflection requirements.

A 7.5- by 7.5-inch mitered corner sample was fabricated using the waffle pattern. The sample was installed in the mechanical cycling test setup as shown in Fig. 29 . The setup consisted of welding the outer periphery of the seal to a rigid metal bracket with the inner periphery of the seal welded to a steel plate, which could be displaced with a hydraulic actuator along a line parallel to the resultant displacement of the interior corner.

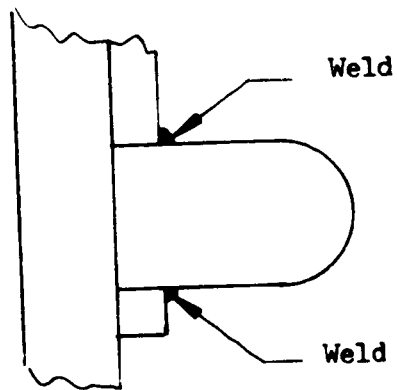
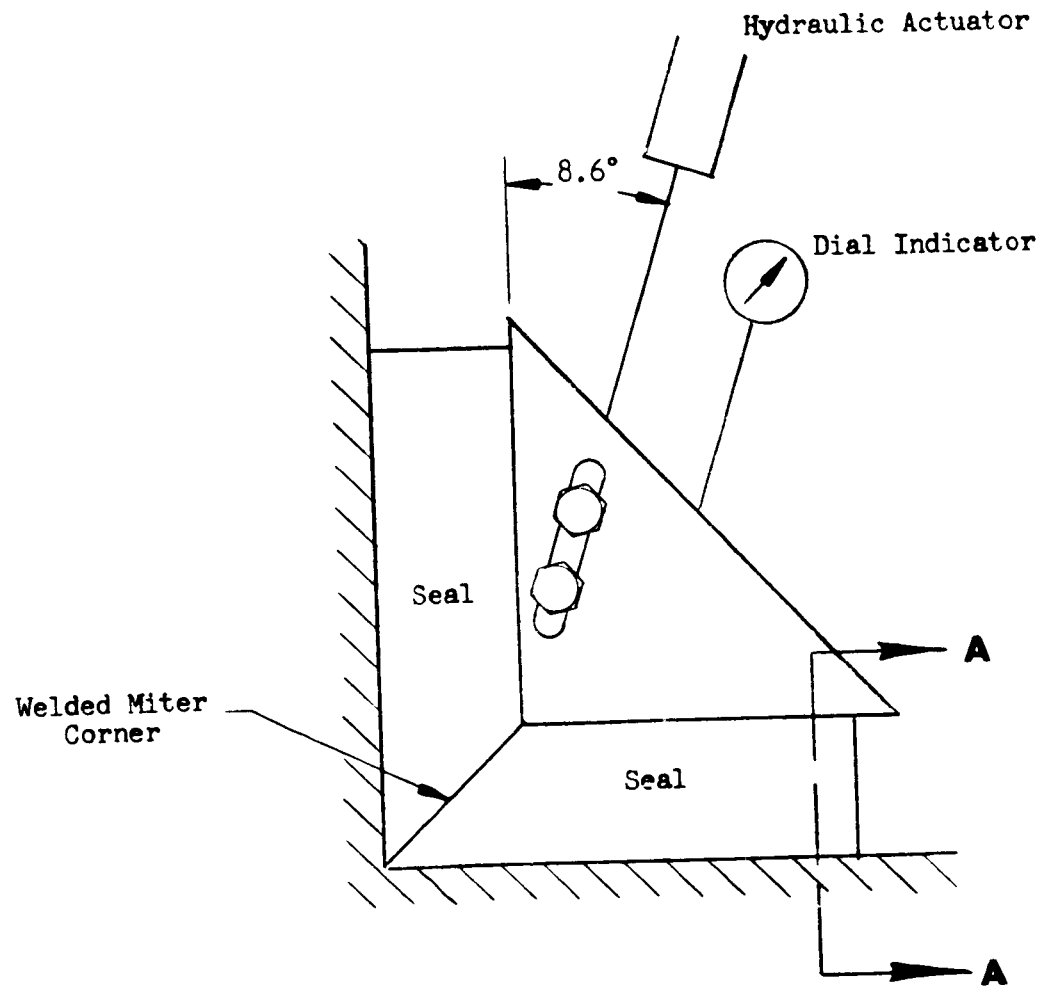
The corner was subjected to 113 mechanical cycles at a displacement of 0.482 inch. A double-exposed photograph of the test sample during mechanical cycling is shown in Fig. 30 . A small crack developed in the mitered weld after 87 cycles. Analysis of the crack indicated that the weld was thin at the point of failure due to an improper fit prior to welding. The test indicated the waffle pattern miter corner design to have adequate flexibility and cycle life for the application.



1XZ65-6/8/71-CIA

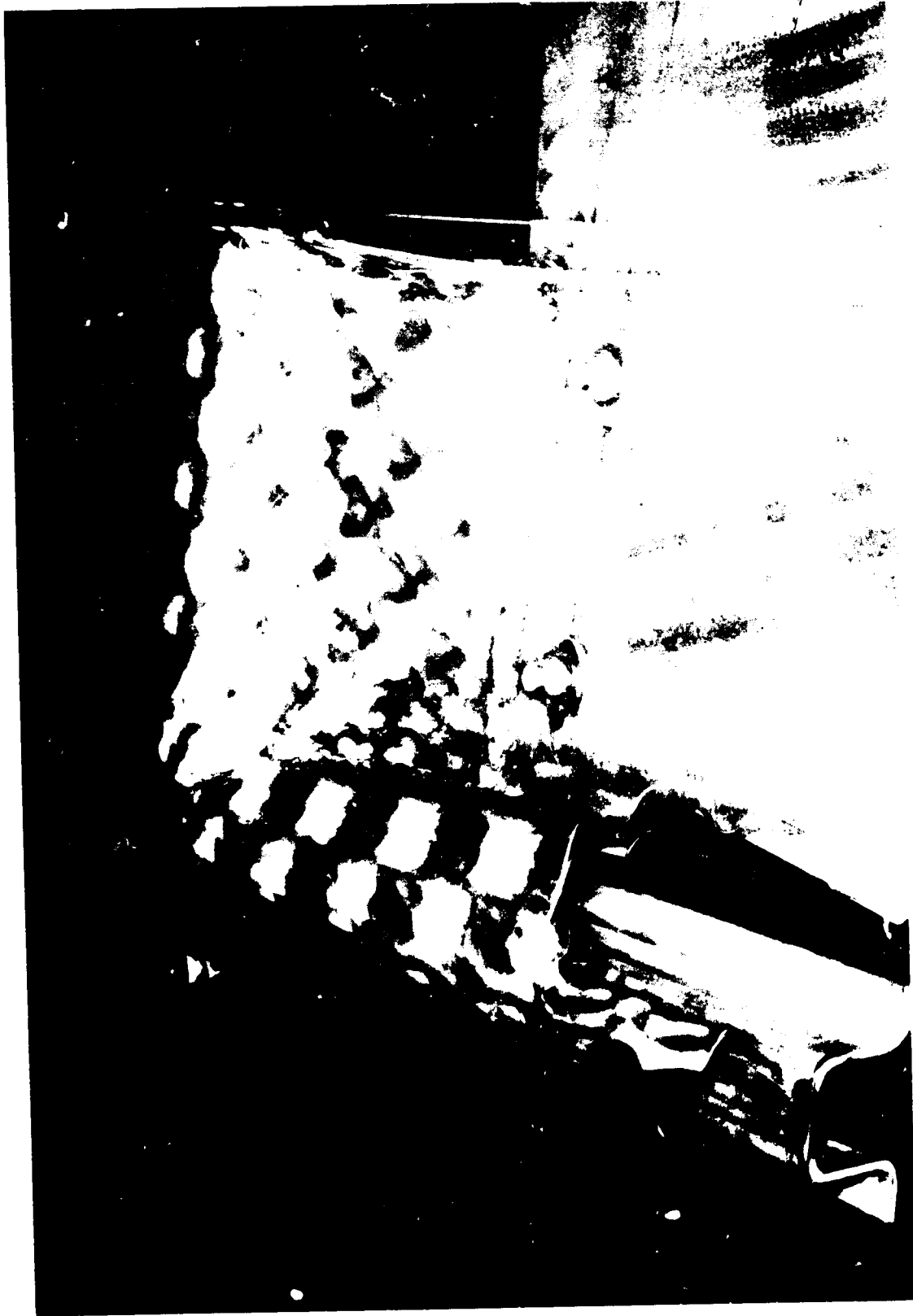
Figure 28. Waffle Pattern Seal Sample After Forming to Simulate Engine Seal Configuration

R-9049



View **A-A**

Figure 29. Base Seal Corner Segment Mechanical Cycling Test Setup



1XZ66-8/11/71-CIF

Figure 30. Double Exposure of Corner Section of Base Seal
During Mechanical Cycling

R-9049

69/70

SYSTEM OPERATION AND PERFORMANCE

TEST SUMMARY

Forty-four tests were conducted on test bed No. 1 at test stand Delta-2B. Fourteen tests were ignition/transition tests and 30 tests were mainstage tests. Eight of the ignition/transition tests were in conjunction with the fluorine ignition system, and six were associated with the combustion wave ignition system. Twenty-one of the mainstage tests achieved mainstage for a total mainstage duration of 3112.9 seconds. Three of the mainstage tests exceeded 500 seconds duration (tests 624-022, 023, and 028). Major test objectives, conditions, and results are shown in Table .a.

START AND CUTOFF

Engine Start

Two engine start techniques were developed on this program to be compatible with the two ignition systems evaluated. Prior to the first engine tests with each ignition system, the start sequences were selected with the aid of a digital start model written for this program. Ignition system dependent engine start constraints were investigated during a multisegment component program which is discussed elsewhere in this report.

Fluorine Ignition Start

The start sequence developed for the fluorine ignition system is presented in Figure 31. When an engine start signal is received, the helium control solenoid is opened to supply control pressure to the valves, and an engine start timer is started to allow sufficient time for charging the engine helium accumulator. Upon expiration of the engine start timer, the engine start solenoid, mainstage start solenoid, igniter fluorine, and igniter LOX valves are opened and an ignition stage timer is started. The main propellant valves are sequenced to provide a gaseous oxygen lead, a necessity discovered during the multisegment program. During the

TABLE 4. LINEAR TEST BED PROGRAM, TEST SUMMARY

Test No.	Date	Major Objective	Fuel Pump Inlet Pressure, psig	Oxidizer Pump Inlet Pressure, psig	Chamber Pressure, psia	Mixture Ratio, O/F	Duration, seconds	Comments
001	9-16-71	Ignition	35.7	29.6	--	--	--	MOV first position angle was set at 15 degrees. The oxidizer bleed valve was open during chilldown. No ignition detection was achieved. Circuit was not turned on. All segments lighted. Approximately 200 nozzle tube crowns eroded downstream of segment exit.
002	10-1-71	Ignition	45.9	30.8	--	--	--	MOV first position angle was reset to 12 degrees. The oxidizer bleed valve was closed during chilldown 3 inches of ceramic coating was sprayed to nozzle-to-segment interface. No ignition detected. Circuit was not armed. Segments No. 4 and 9 would not have triggered circuit.
003	11-1-71	Ignition plus fuel spin	46	31	--	--	--	MOV first position angle was reset to 13.5 degrees. Ceramic coating was extended 15 inch. Ignition was satisfactorily detected. Fuel spin did not occur.

TABLE 4a. (Continued)

Test No.	Date	Major Objective	Fuel Pump Inlet Pressure, psi	Oxidizer Pump Inlet Pressure, psi	Chamber Pressure, psia	Mixture Ratio, O/F	Duration, seconds	Comments
004	11-2-71	Ignition plus fuel spin	46	31	--	--	--	No ignition detection was achieved. Segments No. 13 and 16 did not attain sufficient fuel injection temperature to trigger circuit. Minor buckling of fences occurred.
005	11-8-71	Ignition plus LOX dome prime	40.9	30.1	--	--	--	No ignition detection was achieved. Segment No. 12 did not attain sufficient fuel injection temperature rise to trigger circuit. No system spin occurred.
006	11-9-71	Repeat of test 005	41.9	35.9	--	--	--	Extended ignition timer 270 msec. Satisfactory ignition. LOX dome prime did not occur. Propellant utilization valve in minimum position.
007	11-10-71	Ignition plus LOX dome prime	41.3	36.0	--	--	--	LOX dome prime was achieved. Propellant utilization valve was set at nominal position. Extended spin timer 400 msec. Utilized facility oxidizer bleed system to precondition system.

TABLE 4a. (Continued)

Test No.	Date	Major Objective	Fuel Pump Inlet Pressure, psig	Oxidizer Pump Inlet Pressure, psig	Chamber Pressure, psia	Mixture Ratio, o/f	Duration, seconds	Comments
008	11-18-71	Transition - MOV ramp to 50 percent open	40.7	36.0	--	--	--	Satisfactory transition characteristics. MOV ramp rate was 1.0 second. Cutoff was initiated 600 msec after control signal.
009	11-19-71	5.0 second mainstage	41.5	35.6	805	3.39	5.1	Successful mainstage operation. A fuel purge line was installed to the four ends of the fuel inlet manifold to augment cutoff purge effectivity.
010	11-29-71	15 second mainstage-- increased power level operation	41.2	36.3	997	4.08	15.1	Successful mainstage test. Ignition stage timer was decreased to 1050 msec to reduce ignition stage duration. OTBO orifice size was changed to increase power level operation. A 4000 cu in. helium bottle was installed to increase fuel side purge capacity.
011	12-2-71	30 second mainstage-- initial 20 seconds with PU valve in null position. Final 10 seconds in maximum position	41.2	35.2	1012-1127	4.51-4.95	30.1	Successful mainstage test. A smaller diameter OTBO orifice was installed. The GG oxidizer and fuel orifices were changed. The propellant utilization valve program was satisfactory.

TABLE 4a. (Continued)

Test No.	Date	Major Objective	Fuel Pump Inlet Pressure, psia	Oxidizer Pump Inlet Pressure, psia	Chamber Pressure, psia	Mixture Ratio, o/r	Duration, seconds	Comments
012	12-8-71	100 second mainstage-- during initial 20 seconds PU valve null. Between 20 -85 seconds PU valve at maximum. 85 second to cutoff PU valve at null	40.6	353	1011-1130	4.50-4.98	100.1	Successful mainstage test. The PU valve excursion program operated satisfactorily and all test objectives were achieved.
013	12-21-71	30 second mainstage-- evaluate low power level operation PU valve program consisted of 20 seconds at null and 10 seconds at maximum position	40.6	35.7	810-907	3.61-4.00	30.1	Successful test. Test system compartment purge system was augmented to minimize potential fire hazard. System was partially successful but will require additional modification.

R-9049

TABLE 4a. (Continued)

Test No.	Date	Major Objective	Fuel Pump Inlet Pressure, psig	Oxidizer Pump Inlet Pressure, psig	Chamber Pressure, psia	Mixture Ratio, o/f	Duration, seconds	Comments
001	1-5-72	70 seconds main-stage over the PU range	41.4	35.6	--	--	--	Premature cutoff. No ignition OK. No ignition detect on segment 9.
002	1-5-72	Repeat of test 001	41.6	35.5	--	--	--	Premature cutoff. Spin system electrical problem.
003	1-13-72	Repeat of test 001	39.0	36.1	680-923	3.17-3.99	70.1	Programmed duration
004	1-19-72	200 seconds main-stage over the PU range at higher Pc and mixture ratio levels	39.9	36.1	--	--	--	Premature cutoff. No ignition OK. No ignition detect on segment 18 until 100 m/sec after cutoff
005	1-19-72	Repeat of test 004	39.9	36.1	984-1164	4.75-5.60	78.9	Premature cutoff (observer) upon Pc decay of segment 5. Throat erosions in most segments.
006	2-4-72	Ignition - combustion wave evaluation	34.9	31.0	--	--	--	No ignition OK. No ignition. No premixer fuel. 12° MDV angle.
007	2-9-72	Repeat of test 006	34.5	30.9	--	--	--	Satisfactory ignition. Open air explosion occurred at ignition. Base hot gas seal damaged.

TABLE 4a. (Continued)

Test No.	Date	Major Objective	Fuel Pump Inlet Pressure, psia	Oxidizer Pump Inlet Pressure, psia	Chamber Pressure, psia	Mixture Ratio, o/f	Duration, seconds	Comments
008	2-15-72	Preignition evaluation	35.3	30.2	--	--	--	Hot gas seal damaged. Same sequence to spark signal except exit igniters on pre-engine start. Cutoff initiated at spark signal (no combustion wave). 7 segments ignited by exit igniters. No open air explosion.
009	2-21-72	Ignition plus LOX dome prime	35.3	30.8	--	--	--	No ignition OK. No ignition detected on segments 14, 16, 17 and 18. Segments 12 and 19 detected after cutoff. Engine LOX bleed at -20 minutes.
010	2-22-72	Ignition plus LOX dome prime	34.9	36.1	--	--	--	No ignition OK. No ignition detect on segment 18 until after cutoff. 1 minute engine LOX bleed at -20 minutes.
011	2-22-72	Ignition plus LOX dome prime	29.8	36.1	--	--	--	Satisfactory test.
012	2-23-72	10 seconds main stage with 5 seconds at maximum P.U.	30.1	35.8	724-900	3.34-3.98	10.1	Programmed duration.

R-9049

TABLE 4a. (Continued)

Test No.	Date	Major Objective	Fuel Pump Inlet Pressure, psig	Oxidizer Pump Inlet Pressure, psig	Chamber Pressure, psia	Mixture Ratio, o/f	Duration, seconds	Comments
013	2-24-72	30 seconds mainstage with 25 seconds at maximum P.U.	29.9	35.8	916	4.03	30.1	Programmed duration
014	2-28-72	100 seconds mainstage with 95 seconds at maximum P.U.	29.9	36.0	916	4.04	81.3	Premature cutoff (observer) upon indication of engine compartment fire. Dome to combustor leak on segment 13. Aluminum backup structure on segment 13 and instrumentation on segment 15 damaged. Fuel inj. temp redlines initiated.
015	3-8-72	500 seconds mainstage with 495 seconds at maximum P.U.	29.9	36.4	--	--	--	Premature cutoff. No M/S OK press. sv. pickup due to propellant quality and extended spin. Hardware OK.
016	3-10-72	Repeat of test 015	30.2	35.6	918	4.07	219.6	Programmed cutoff when the fuel inj. temp of segment 6 exceeded the redline value. 5 minor erosions on throat outer contour wall of segment 8.
017	3-16-72	Same as test 015	29.6	35.5	861-958	3.88-4.21	227.4	Programmed cutoff when the fuel inj. temp. of segments 6 and 18 continued to increase at null P.U. Segment 8 erosions increased in depth. Base split at weld joint.

TABLE 4a. (Continued)

Test No.	Date	Major Objective	Fuel Pump Inlet Pressure, psia	Oxidizer Pump Inlet Pressure, psia	Chamber Pressure, psia	Mixture Ratio, o/f	Duration, seconds	Comments
018	3-21-72	Same as test 015	30.2	35.8	--	--	--	Premature cutoff. No ignition OK. No ignition detect on segment 16.
019	3-21-72	Same as test 015	30.1	37.9	--	--	--	Premature cutoff. GG link break electrical continuity reestablished.
020	3-22-72	Same as test 015	30.1	38.2	910	4.05	280.4	Premature cutoff. Short in power supply unit. Base hot gas seal cracked.
021	3-27-72	500 seconds mainstage over the P.U. range	26.3	32.3	--	--	2.5	Premature cutoff - fuel inlet pressure lowered, fuel inlet pressure redline not lowered.
022	3-30-72	Same as test 021	31.5	40.4	657-898	3.17-4.02	500.1	Programmed duration.
023	4-3-72	Same as test 021	31.8	39.6	662-904	3.18-4.05	500.1	Programmed duration. Base split at weld joint.
024	4-11-72	500 seconds mainstage over the P.U. range at higher Pc and mixture ratio	31.7	38.7	814-1024	4.05-4.92	272.0	Premature cutoff. Fuel turbine inlet temp. T/C failed, spiked upscale, and exceeded the redline. Base split, and water fence leaked.

TABLE 4a. (Concluded)

Test No.	Date	Major Objective	Fuel Pump Inlet Pressure, psig	Oxidizer Pump Inlet Pressure, psig	Chamber Pressure, psia	Mixture Ratio, o/f	Duration, seconds	Comments
025	4-17-72	Same as test 024	36.4	39.2	--	--	--	Premature cutoff. No ignition OK. High fuel inlet press. (DIGR zero shift).
026	4-17-72	Same as test 024	36.0	39.8	--	--	--	Premature cutoff. No ignition OK. High fuel inlet press. (DIGR zero shift).
027	4-17-72	Same as test 024	35.8	39.8	--	--	--	Premature cutoff. No ignition OK. No combustion wave spark.
028	4-19-72	Stand duration	29.3	39.1	826-1035	4.10-4.98	592.5	Programmed duration. Base split.
029	4-24-72	15 seconds main-stage with 10 seconds at maximum P.U. at higher Pc and mixture ratio	29.7	40.2	1125-1248	4.08-5.52	15.1	Programmed duration. Few minor erosions (34 total) on OCW of segments 2, 3, 4, 7, 8, 11, 19 and 20.
030	5-23-72	Stand duration at lower Pc and mixture ratio	29.6	40.9	--	--	2.6	Premature cutoff. Erroneous high fuel inlet temp.
031	5-23-72	Repeat of test 030	29.7	40.9	754-915	3.47-4.10	49.6	Premature cutoff. Press sv. cutoff upon Pc decay. G.G. power loss. High G.G. LOX system resistance.

TOTAL TESTS - 44
 TOTAL MAINSTAGE TESTS - 30
 TOTAL MAINSTAGE DURATION - 3112.9 SECONDS

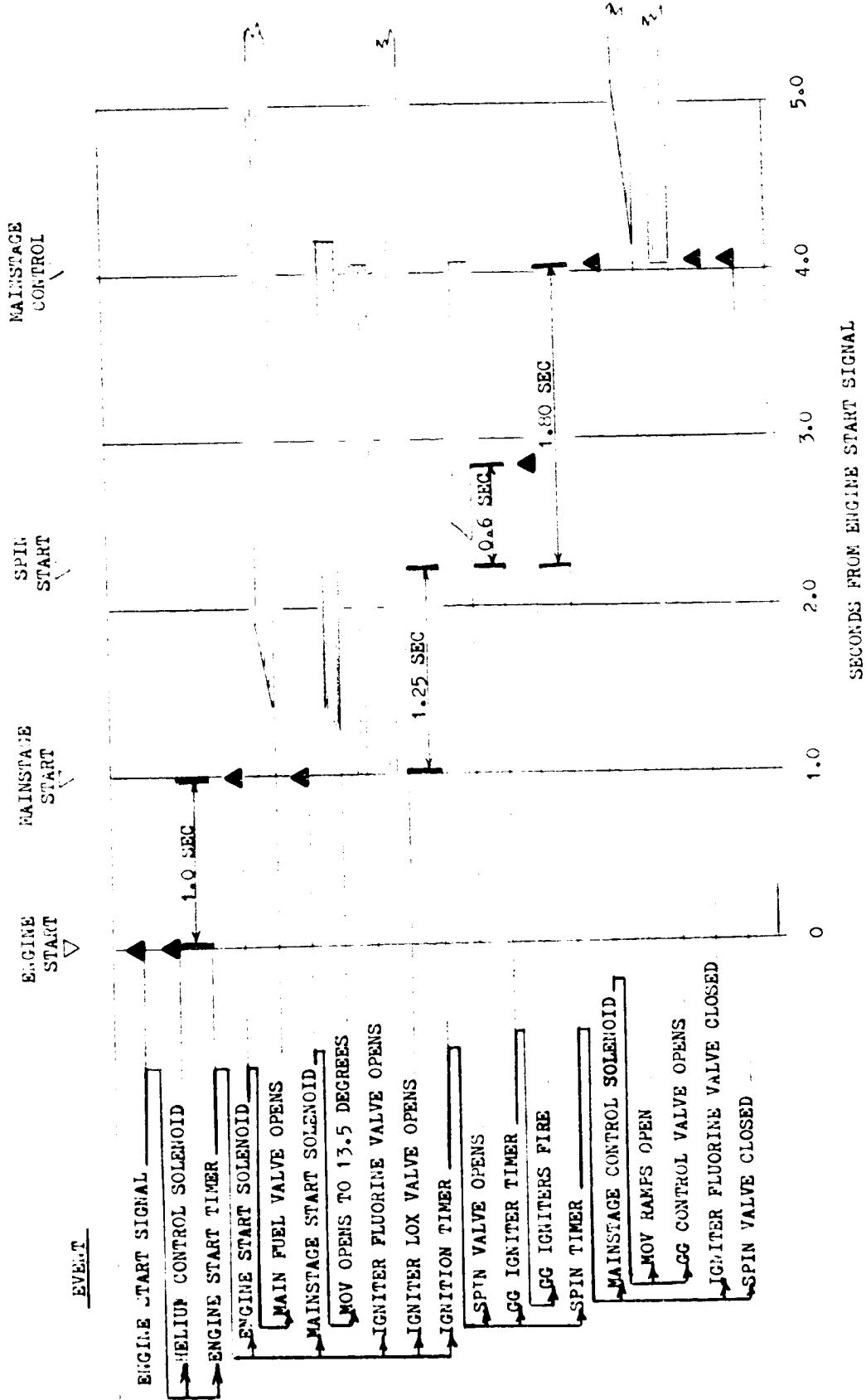


Figure 31. Test Bed No. 1 Start Sequence (Fluorine Ignition)

ignition stage, main oxidizer, main fuel, and igniter fluorine are supplied in a gaseous state to the thrust chamber combustors. When ignition has been detected and the ignition timer has expired, the gaseous hydrogen spin valve is opened to power the turbomachinery, a gas generator igniter timer is started, and the spin duration timer is activated. The turbopumps are powered with the main oxidizer valve at a first-stage position of 13.5 degrees until the oxidizer dome has primed and the engine is operating at a throttled position under spin gas power. The gas generator igniters are fired during the spinup period, and at the expiration of the spin timer, the gas generator control valve is opened, the igniter fluorine and spin valves are closed, and the main oxidizer valve is ramped to full open as the engine bootstraps into mainstage.

Combustion Wave Ignition Start

The engine start logic for the combustion wave igniter (Fig. 32) required a substantial modification to the start sequence prior to the spin start signal. The sequence was modified to provide a gaseous hydrogen lead, and an ignition delay timer to allow the combustion wave manifold to prime with gaseous propellant. At engine start, the engine start solenoid and main fuel valve are opened, and a mainstage start timer is started. When the mainstage start timer has expired, the mainstage start solenoid is actuated opening the main oxidizer valve to 12 degrees, the ignition system propellant valves are opened, and the ignition delay timer is activated. Upon expiration of the ignition delay timer, the spark unit is fired sending a combustion wave to the combustors, and the igniter oxidizer valve is closed to prevent afterfire in the premixer unit. An ignition-detect timer is started to allow time for the detection of 20 injection temperature rise rates. When ignition has been detected and the timer has expired, the spin valve is opened and the start sequence from this point is identical with the fluorine sequence. Typical start transients are presented in Fig. 33 through 38

Engine Cutoff

Approximately 70 pounds of liquid oxygen are stored downstream of the main oxidizer valve on test bed No. 1. Cutoff model studies showed that an oxidizer-side purge at cutoff would result in a sustained oxidizer-rich condition that

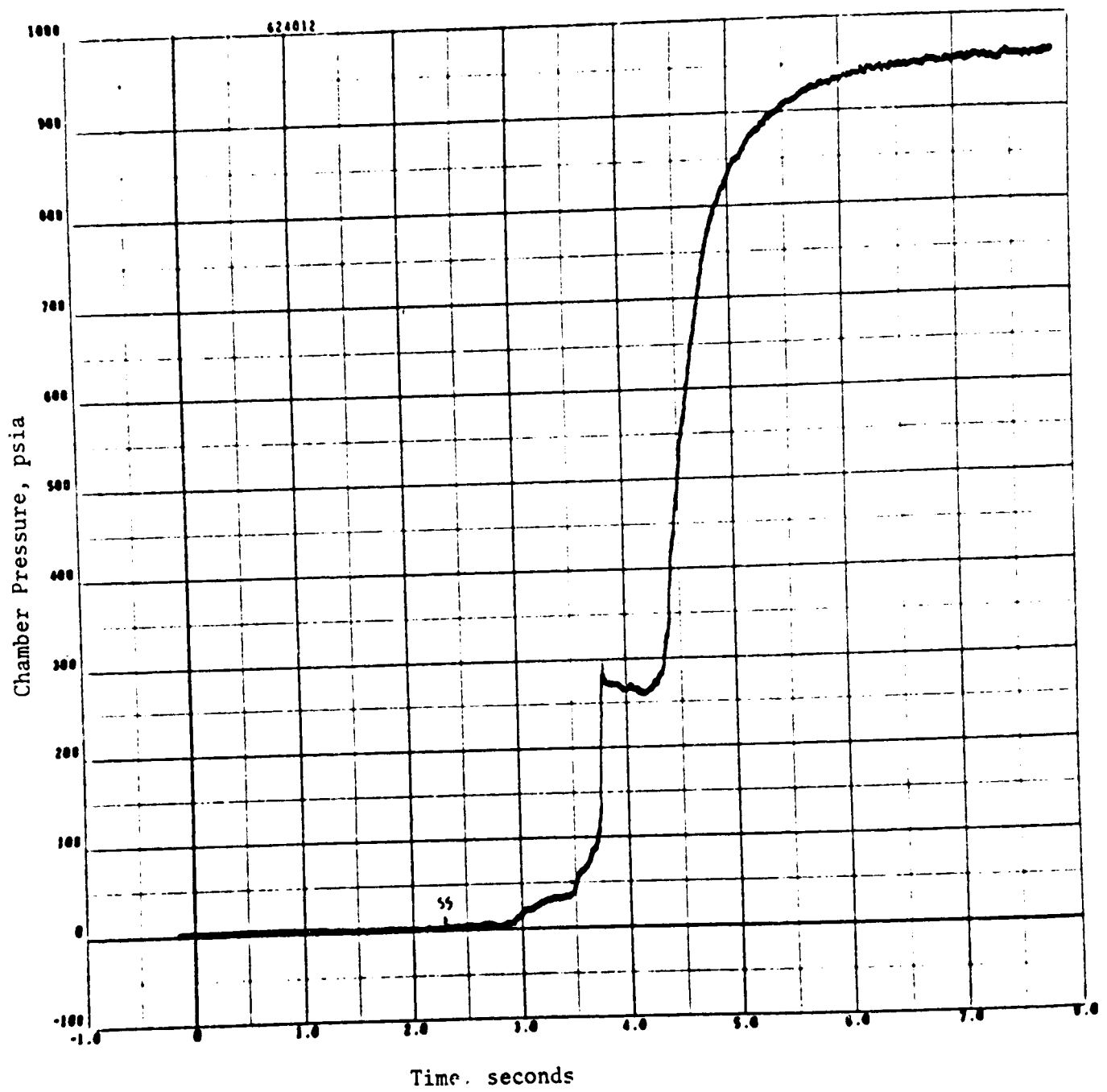


Figure 33. Linear Test Bed Program Chamber Pressure vs Time, Test 012

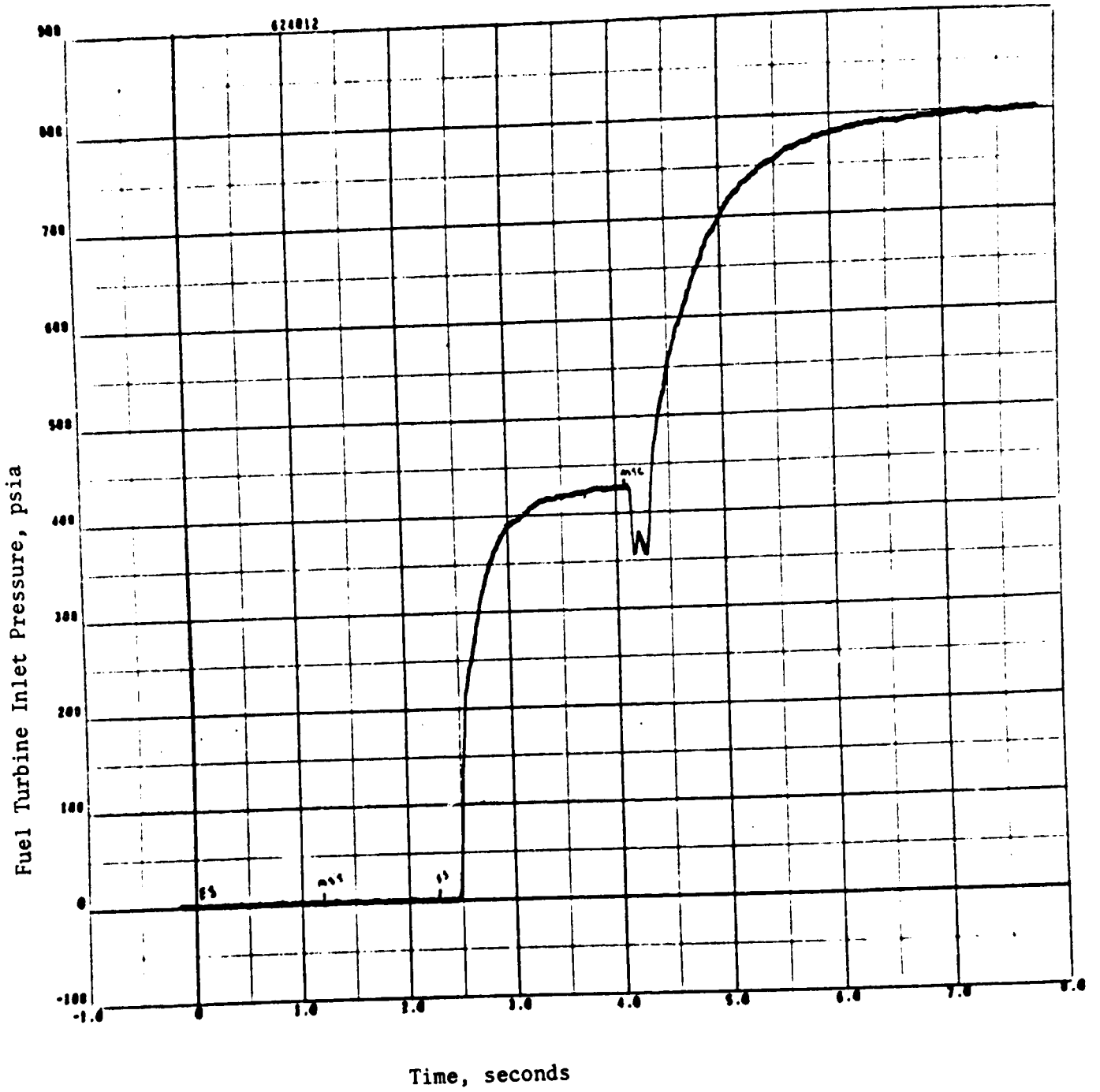


Figure 34. Linear Test Bed Program Fuel Turbine Inlet Pressure, Test 012

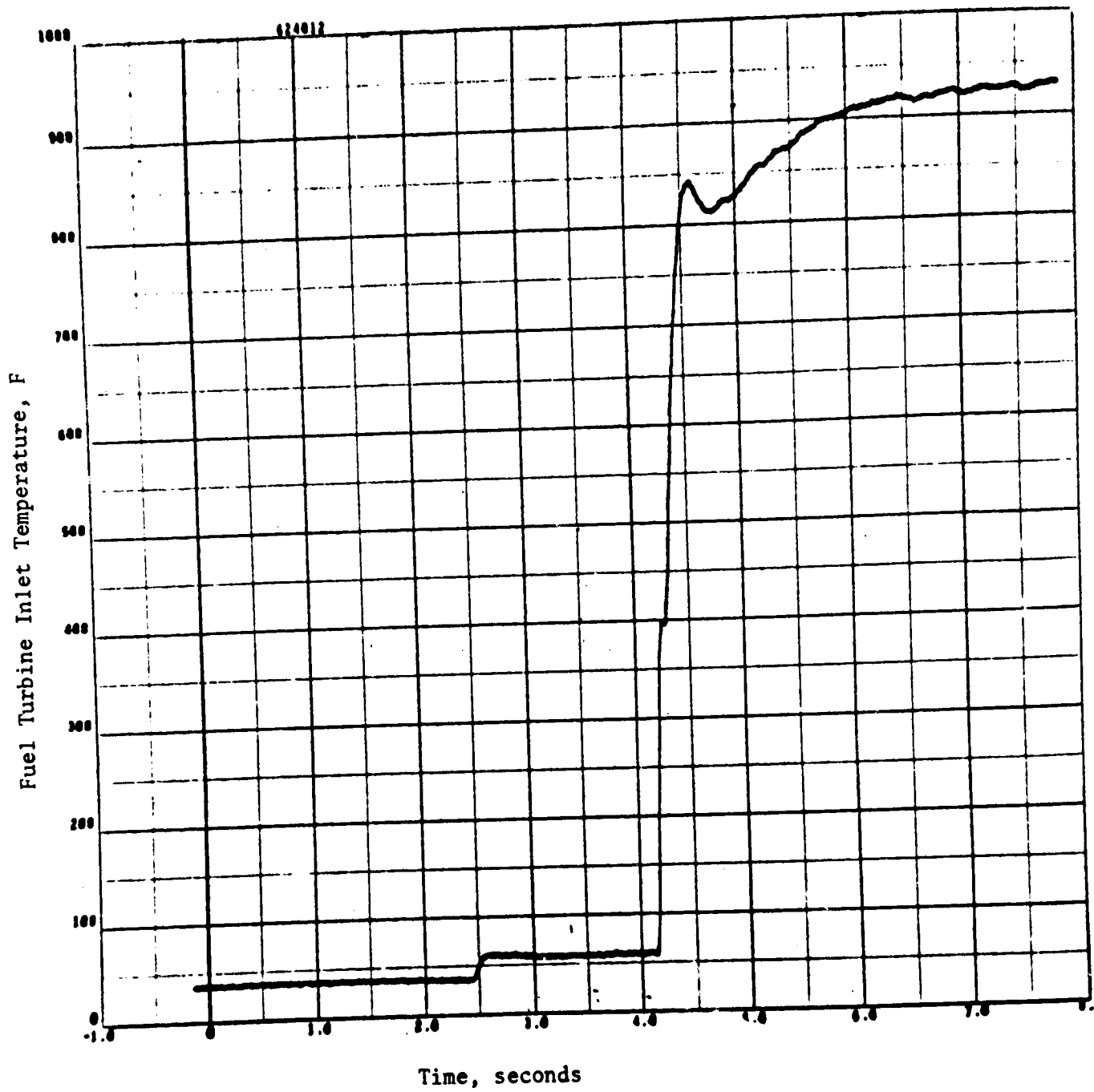


Figure 35. Linear Test Bed Program Fuel Turbine Inlet Temperature, Test 012

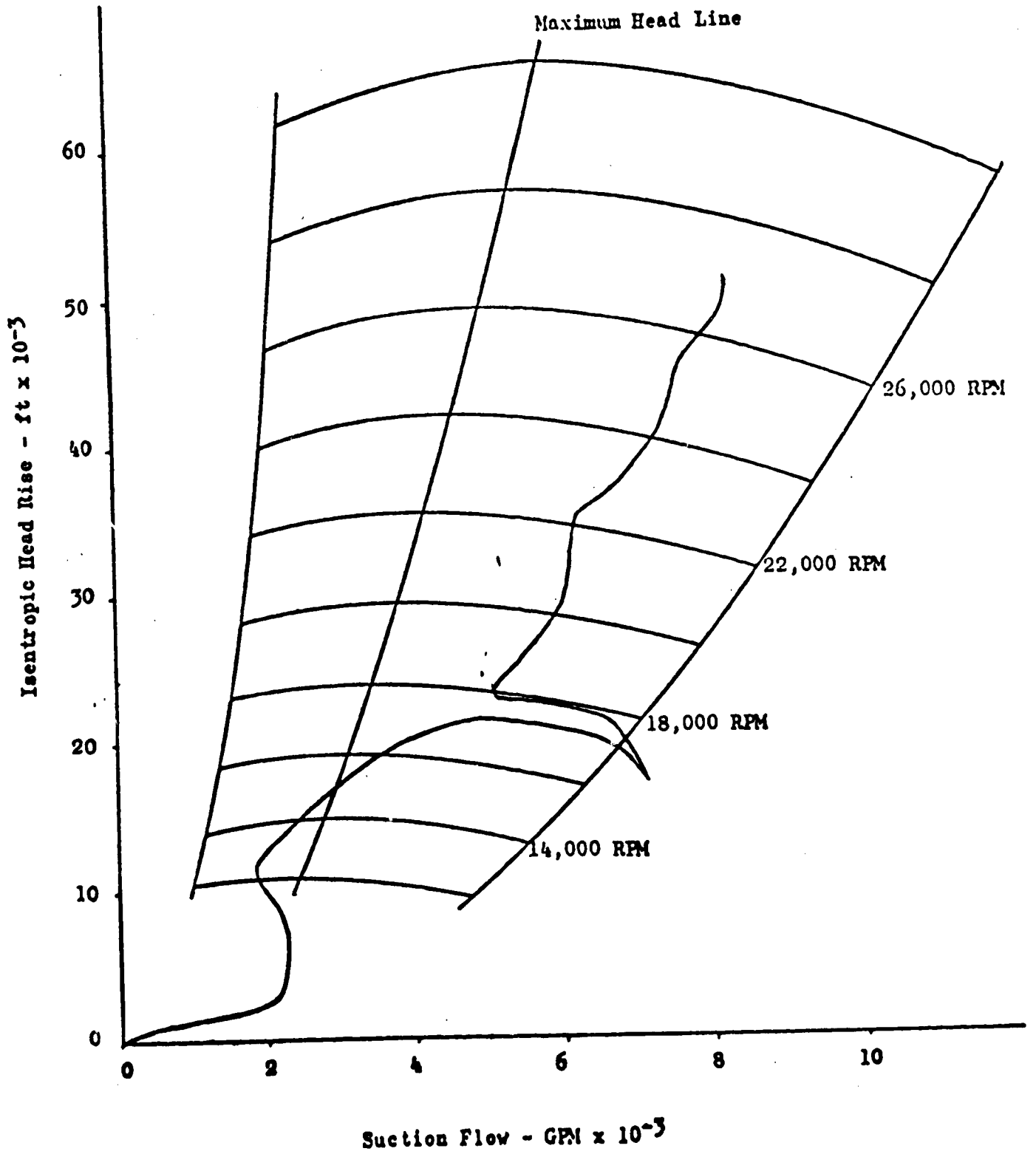


Figure 36. Linear Test Bed Program, Mark 29 Fuel Pump Start Transient Head vs Flow, Test 012

R-9049

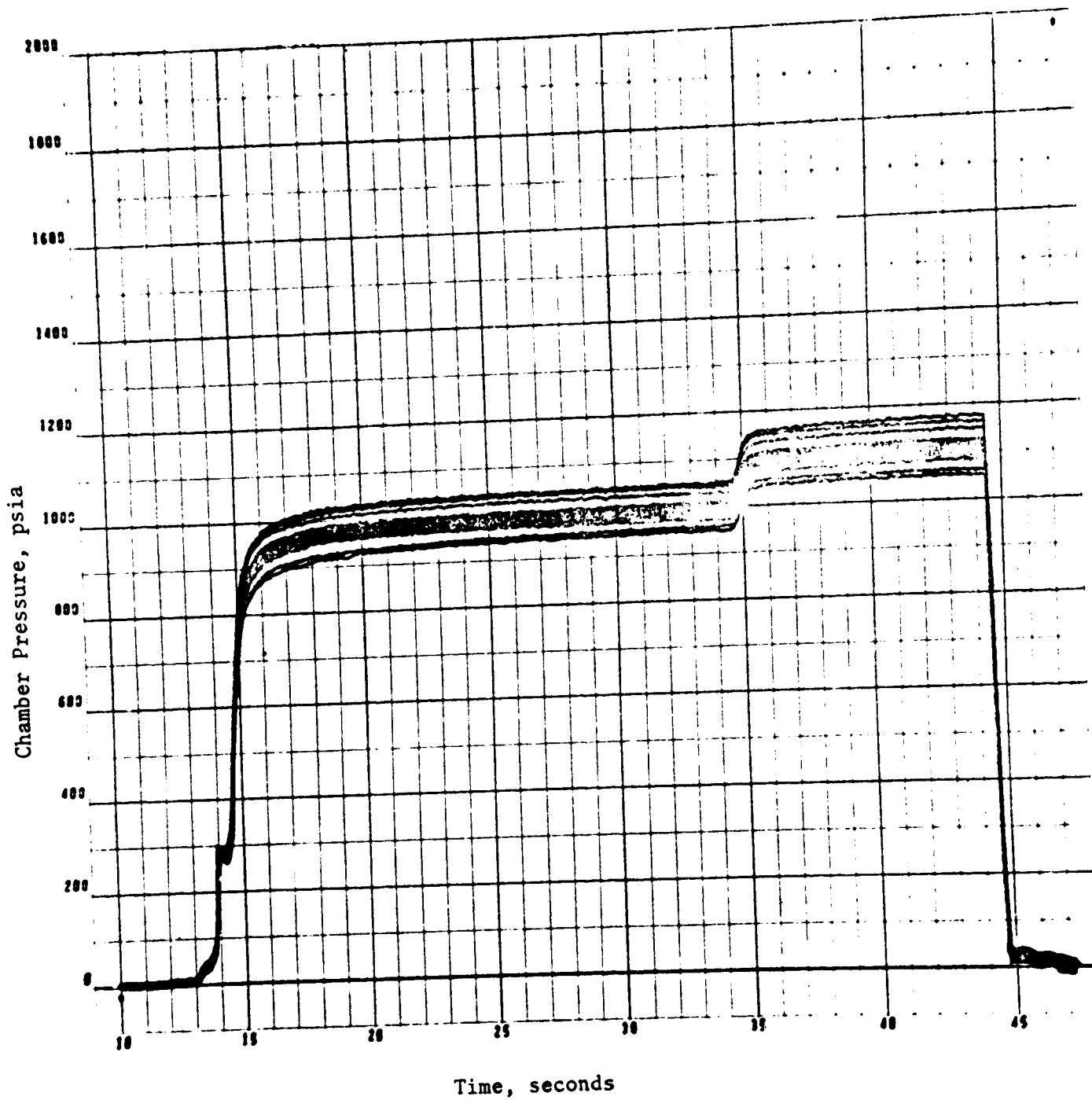


Figure 37. Linear Test Bed Program, Composite of 19 Chamber Pressures, Test 011

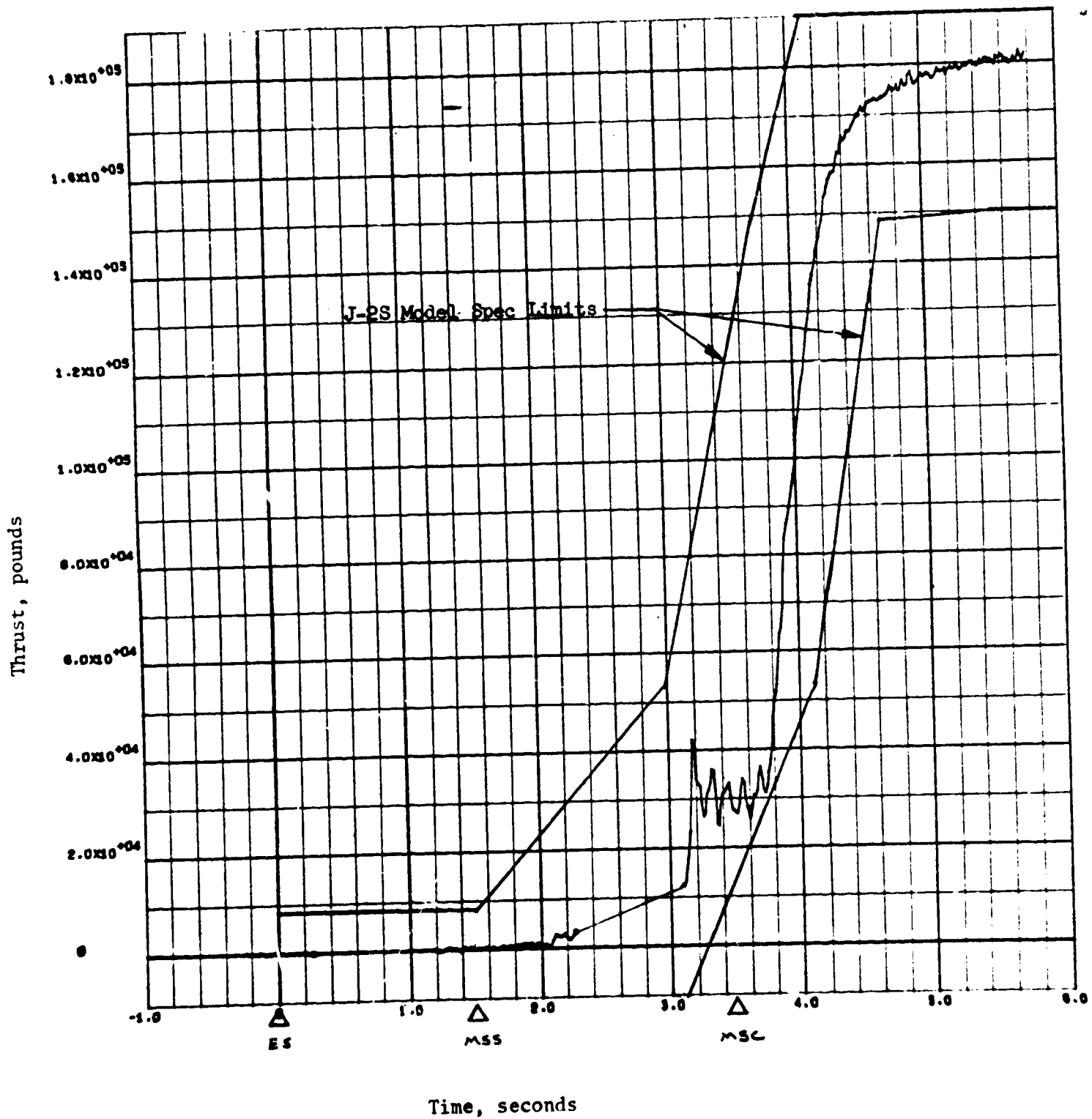


Figure 38. Test Bed No. 1 Start Transient Main Thrust, Test 024-027

would undoubtedly be damaging to the combustors. No oxidizer purge at all would result in chugging at cutoff as the oxidizer drained from the manifold and result in an uncontrolled and unrepeatable cutoff transient. A massive fuel system purge was selected as a method of extinguishing the combustors as quickly as possible. Heat transfer analysis showed that a fuel purge was feasible if the combustors were driven through stoichiometric mixture ratio and flameout quickly enough. A 5-lb/sec helium fuel-side purge actuated by a comparator circuit on the main fuel valve position indicator was selected as the cutoff method. The cutoff sequence is shown in Fig. 39.

At engine cutoff signal, the igniter valve closes (igniter LOX valve in the fluorine sequence and igniter fuel valve in the combustion wave sequence), the mainstage start and mainstage control solenoids are de-energized, and the main oxidizer and gas generator control valves are closed. The engine start solenoid is de-energized and the main fuel valve is sequenced closed. When the main fuel valve reaches 20 percent open, the fuel purge valve is opened and the combustors inerted.

A typical cutoff transient is presented in Fig. 40.

IGNITION SYSTEM OPERATION

Of the 44 tests conducted on test bed, No. 1, 19 tests were run using the gaseous fluorine ignition system, and 24 tests were started with the combustion wave igniter. A description of the operation of these system follows.

Fluorine Ignition System

Fluorine ignition was accomplished with a gaseous oxygen and gaseous fluorine leak to the thrust chamber combustors, followed by the introduction of gaseous hydrogen after main fuel valve actuation. The 20 fluorine igniter elements, which were concentric with an oxidizer post in each injector, were allowed to pass through the stoichiometric hydrogen/fluorine mixture ratio and produced a period of maximum heat release while the injector was passing through the stoichiometric

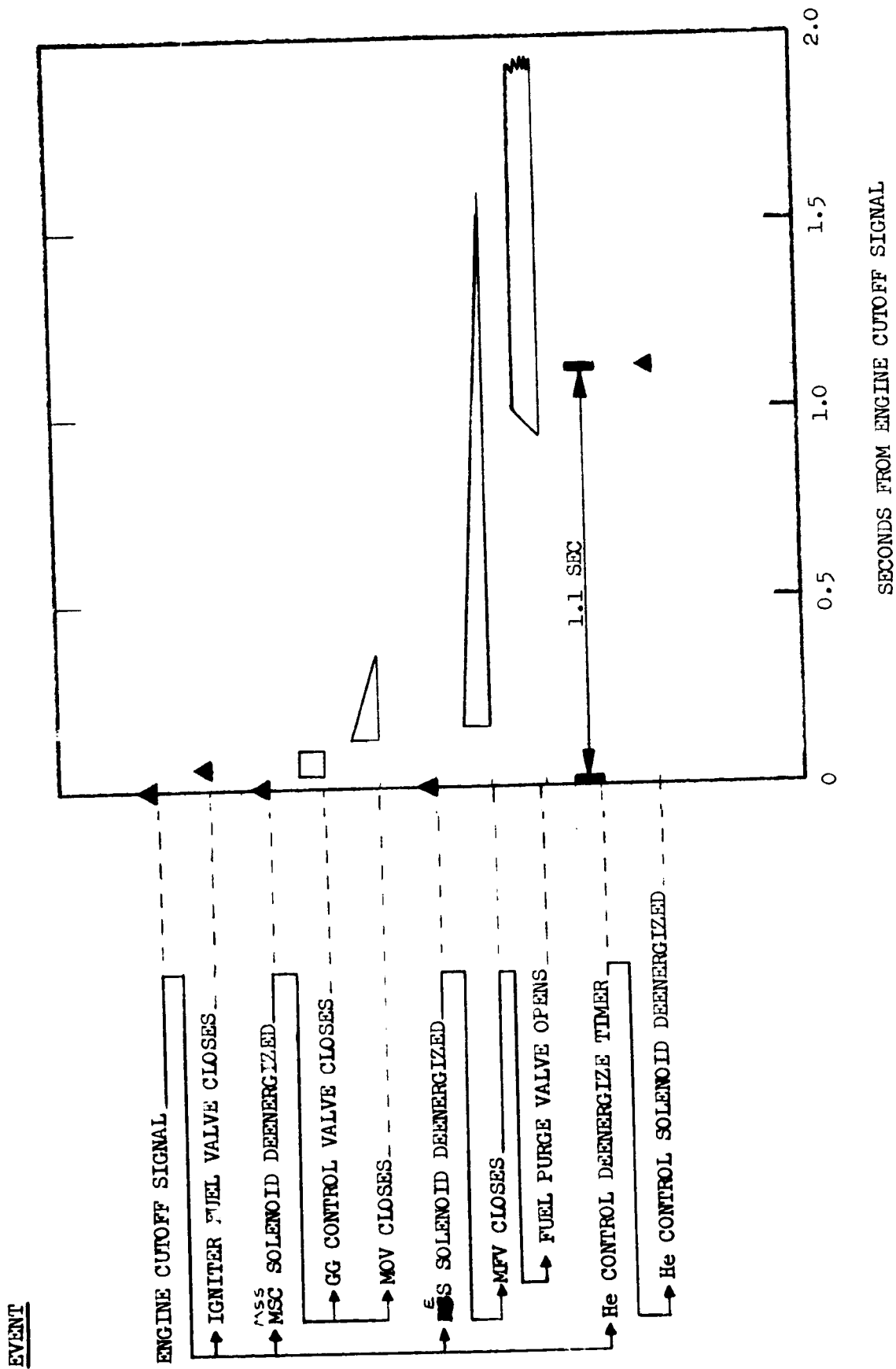


Figure 39. Linear Test Bed Program, Test Bed No. 1 Cutoff Sequence

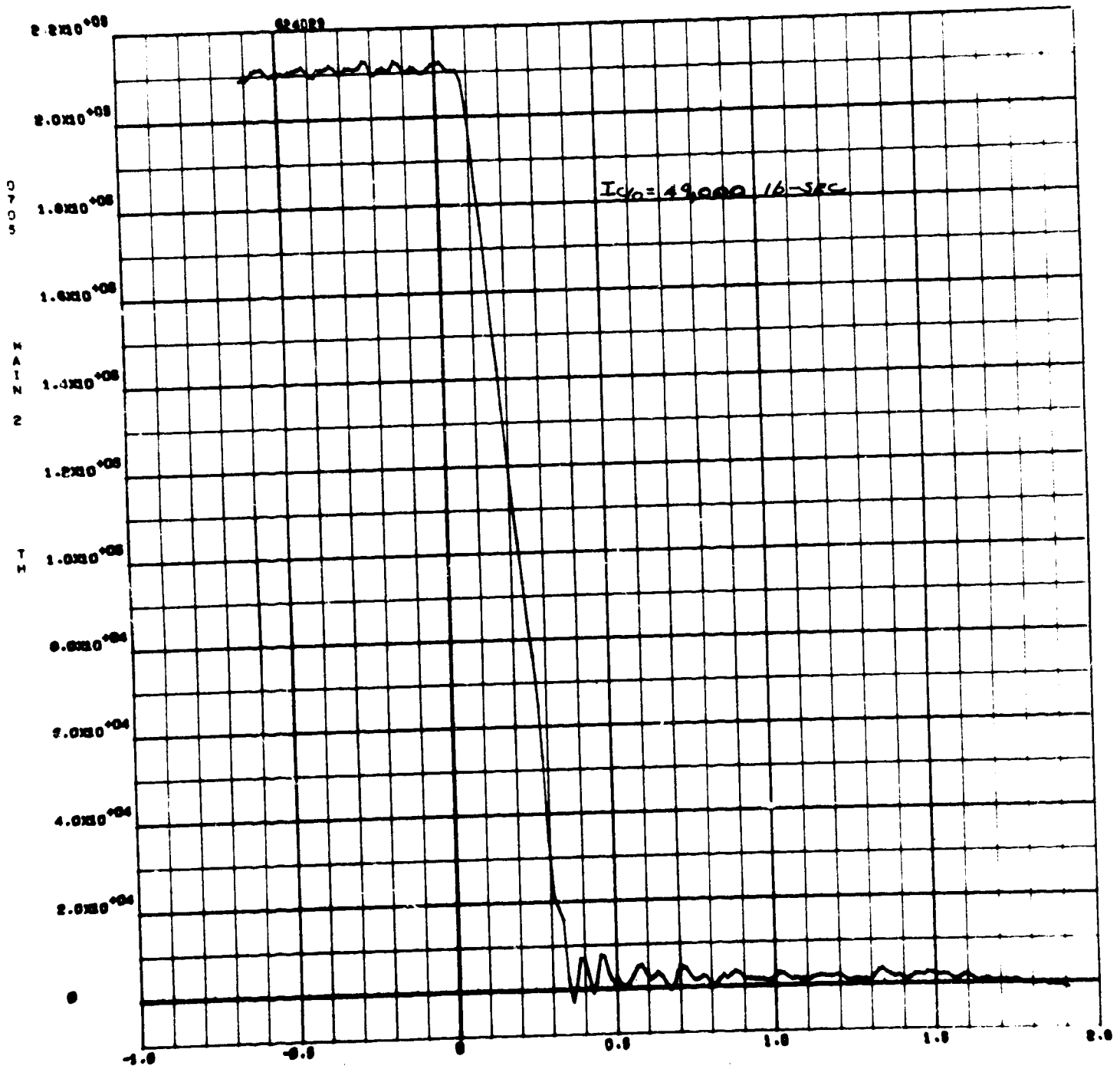


Figure 40. Test Bed No. 1 Cutoff Transients, Main Thrust

hydrogen/oxygen mixture ratio. This ignition sequencing resulted in 19 successful ignitions. The ignition-detection method used on all test bed No. 1 tests was developed during the fluorine ignition component test series. The inner contour wall discharge temperature (fuel injection temperature) was monitored on all 20 combustors; a temperature rise rate in excess of 40 degrees/sec was required on all combustors to signal ignition detected. Operationally, ignition is detected by amplifying the output of 20 fuel injection thermocouples and electronically determining the slope of each signal during the ignition-detection period. If all 20 signals exhibit a slope exceeding 40 degrees/sec before the ignition-detection timer expires, an ignition-detected signal is locked in and turbine spinup is allowed to proceed. The minimum rise rate of 40 degrees/sec was dictated by the minimum signal-to-noise ratio of the detection circuitry. Multi-segment testing showed positive ignitions at fuel injection temperature rates as low as 15 degrees/sec.

No ignition system malfunctions or hardware damage were sustained with the fluorine ignition system. Ignition occurred on every test, although several tests were required to adjust the injector mixture ratio so that a detectable fuel injection temperature slope rate could be obtained.

Combustion Wave Ignition System

The combustion wave ignition system was first operated on test 624-007 in 1971 and resulted in a successful, detected ignition on all combustors. Because of the nature of the start sequence required for the test bed No. 1 combustion wave igniter concept, an open-air detonation occurred at ignition, necessitating the use of thrust chamber exit igniters on subsequent tests. In the combustion wave ignition sequence, the main fuel valve is opened at engine start to provide a gaseous fuel lead to the combustors. When the main fuel valve reaches fully open, the igniter propellant valves are opened to allow priming of the combustion wave manifold with gaseous, premixed propellants under tank-head pressure. The main oxidizer valve is opened to the 12-degree position and sufficient time is allowed to prime the oxidizer feed system and injector manifolds with gaseous oxygen. When the igniter and main propellant manifolds have been filled with

gaseous propellants, a spark plug is fired in the premixer and a combustion wave is generated through the premixed propellants flowing through the combustion wave manifold. As the combustion wave propagates through the manifold, a shock front soon develops and propagates into a detonation wave with a recovery temperature in excess of 5000 F. The detonation wave exits into the combustors through 20 igniter elements similar in design to the fluorine elements, igniting the triaxial igniter elements which propagate combustion across the injector face. The igniter oxidizer valve is closed within 50 milliseconds after the spark signal to prevent sustained combustion in the premixer. The igniter fuel valve remains open during spinup and mainstage and provides a positive purge of the combustion wave manifold to prevent cross-flow communication between combustors. A schematic description of the combustion wave ignition process is shown in Fig. 41 .

All 24 tests conducted with the combustion wave ignition system resulted in successful ignition in 20 segments. Because of the fuel lead start and the reduced first-stage main oxidizer valve angle investigated during this test series, pump inlet conditions were varied on several tests until an acceptable ignition mixture ratio for ignition detection was achieved.

IGNITION SYSTEMS PROBLEM RESOLUTION

Most ignition system problem areas were resolved during the component development program conducted at the Los Angeles Division Thermodynamics Laboratory, the Rocketdyne Propulsion Research Area, and CTL-3 multisegment test stand. A summary of problems solved during components testing is presented below; a detailed discussion of the ignition systems component development program is discussed elsewhere in this report.

1. Injector Ignition Limits--injector mixture ratios exceeding 1.25 were found necessary for oxygen-hydrogen ignition with either gaseous fluorine or combustion wave ignition
2. Ignition Detection--externally mounted thermocouples were proved inadequate for monitoring ignition detection. The inner contour wall discharge temperature thermocouples were monitored through a slope detection circuit to successfully detect main propellant ignition.

R-9049

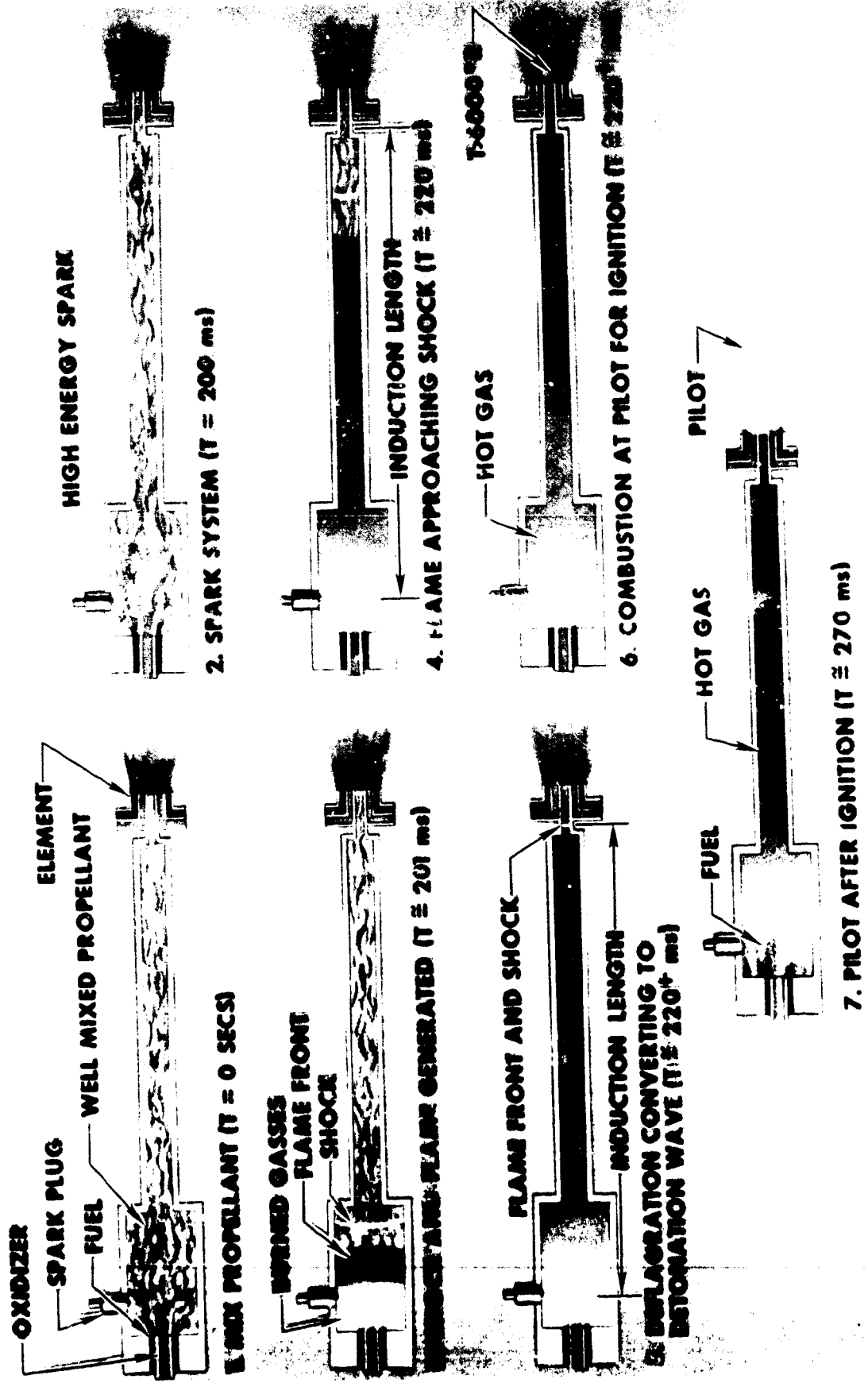


Figure 41. Combustion Wave Ignition Sequence

3. Fuel-lead Start--The proposed fuel-lead start sequence for test bed No. 1 with the fluorine ignition was proved inadequate for ignition-detection purposes during multisegment testing. A successful oxygen-lead sequence was developed during multisegment testing and was used during test bed No. 1 evaluation.
4. Fluorine-Hydrogen Hypergolicity--Two instances of fluorine-hydrogen ignition failure were encountered on the multisegment with the fuel-lead start sequence. The problem could not be duplicated in an extensive test series conducted with identical test setup conditions. The problem was considered a statistical result of marginal operating conditions with the fuel lead caused by poor element mixing and high combustion zone velocity. The oxygen-lead sequence, which allowed both the igniter element and main injector to pass through stoichiometric mixture ratio, resulted in no ignition failures.
5. Premixer Combustion--The premixer design for test bed No. 1 did not allow cyclic combustion wave generation. An unidentified heat source in the premixer, either a hot surface or low-level combustion in the premixer element, resulted in sustained combustion on attempts to reprime the premixer with oxygen and hydrogen. The premixer can be redesigned to eliminate hot spots and to purge the oxidizer manifold prior to recycling the combustion wave process.

During engine testing, ignition-detection problems were encountered with the slope detection system. The signal-to-noise ratio of the amplification circuitry did not allow slope detection rates of less than 40 degrees per second to be monitored. The ignition mixture ratio was increased by adjusting pump inlet conditions, and successful ignition detection was achieved. An open-air detonation problem with the combustion wave sequence was discovered on the first engine test with this system. Exit igniters were provided on each side of the thrust chamber to eliminate the problem. An additional test was conducted without exit igniters using approximately one-half the propellant priming time used on the first test. An open-air detonation still occurred at ignition, and the exit igniters were re-installed for the remaining tests on the engine.

MAINSTAGE PERFORMANCE

Performance data on all tests which achieved mainstage are shown in Table 5 . Detailed data for test 624-029 are shown in Table 6 , which also reflects the "rated performance" based on test 624-029. "Rated performance" is at sea level with nominal engine inlet pressures, design chamber pressure, engine mixture ratio, and fuel turbine inlet temperature.

The site engine specific impulse relative to average P_c and mixture ratio is shown in Fig. 42. The correlation with P_c is exceptionally good.

Performance-time trends are shown in Fig. 43 through 45 . Compared to the J-2S engine, test bed No. 1 stabilizes rapidly. The thrust change from 30 to 120 seconds mainstage duration is 2.2 percent for J-2S and 0.73 percent for test bed No. 1.

Figures 46 through 50 show the engine performance variations resulting from propellant utilization valve operation on test 624-028. The average ΔMR obtained with the PU valve from closed to open was 0.82 mixture ratio units. ΔMR can readily be increased by increasing the PU valve inlet orifice diameter (test bed No. 1 utilized the J-2S valve configuration).

The gain factors applicable to test bed No. 1 were determined empirically from test data to be as follows:

Oxidizer Turbine Bypass Orifice Area (in.²)

$$\frac{\Delta MRE}{\Delta A} = -0.29, \frac{\Delta P_c}{\Delta A} = -66, \frac{\Delta T_{ft\ in}}{\Delta A} = -77$$

$$\left(R = \frac{\rho \Delta P}{W^2} = \frac{\text{sec}^2}{\text{ft}^3 \text{-in}^2} \right)$$

GG LOX System Resistance

$$\frac{\Delta MRE}{\Delta R} = 0, \quad \frac{\Delta P_c}{\Delta R} = -0.22, \quad \frac{\Delta T_{ft \text{ in}}}{\Delta R} = -0.53$$
$$(R = \frac{\rho \Delta P}{W^2} = \frac{\text{sec}^2}{\text{ft}^3 \text{ in}^2})$$

GG Fuel System Resistance

$$\frac{\Delta MR}{\Delta R} = 0, \quad \frac{\Delta P_c}{\Delta R} = 0, \quad \frac{\Delta T_{ft \text{ in}}}{\Delta R} = +5.8$$

THRUST VECTOR MEASUREMENTS

The thrust measuring system for test bed No. 1 is shown in Fig. 51 . Although the system is redundant, the additional attach points were considered necessary to properly restrain the assembly during transient operating periods or in the event of a test bed malfunction. Careful attention to hardware and facility alignments while operating the test bed permitted accurate resolution of the true thrust vector. Comparison of thrust vectors, with and without the additional restraints, showed insignificant thrust vector changes.

Test bed No. 1 thrust vector readings are recorded in Table 7 . Note that thrust was not measured in the X-plane during tests 624-009 through 624-011.

As an aid to analysis, system and thrust chamber values of site mixture ratio and average chamber pressure and system thrust also are given in Table 7 .

At present, no differences are shown between engine and thrust chamber values of thrust. Thrust contributions by the turbine exhaust gases with the present end fence configuration are not measured separately and are assigned as part of thrust chamber thrust.

TABLE 5. LINEAR TEST BED PROGRAM, MAINSTAGE TEST SUMMARY

Item	TEST NO.					
	624-009	624-010	624-011	624-011	624-012	624-013
Duration, seconds from mainstage control	5.1	15.1	30.1	30.1	100.1	30.1
Test slice time, seconds from mainstage control	4.9	13.5	17.1	27.1	84.1	26.0
P.U. valve position	½ open	½ open	½ open	closed	½ open	closed
Thrust, pounds x 10 ⁻³	117.1	153.0	158.1	181.6	181.2	135.8
System mixture ratio, O/F	3.39	4.08	4.51	4.95	4.98	3.97
Specific impulse, seconds	328.3	342.0	340.8	348.4	347.2	333.7
Chamber pressure, psia	808	991	1015	1130	1130	907
Total LOX flow, lb/sec	275.5	359.3	379.7	433.7	434.7	326.6
Total fuel flow, lb/sec	81.2	88.0	84.2	87.6	87.3	81.6
GG LOX flow, lb/sec	3.93	4.79	4.54	5.07	5.11	3.98
GG fuel flow, lb/sec	4.67	5.26	5.91	6.09	6.00	5.75
GG LOX orifice diameter, inches	.394	.394	.325	.325	.325	.325
GG fuel orifice diameter, inches	.474	.474	.518	.518	.518	.518
OREO diameter, inches	3.159	2.650	2.300	2.300	2.300	3.050

TABLE 5. (Continued)

Item	TEST NO.							
	624-016	624-051	624-017	624-020	624-022	624-023	624-023	
Duration, seconds from mainstage control	219.6	227.4	227.4	280.4	500.1	500.1	500.1	500.1
Test slice time, seconds from mainstage control	218.9	170.0	200.0	273.7	20.1	135.0	20.8	135.0
P.U. valve position	closed	closed	$\frac{1}{2}$ open	closed	open	closed	open	closed
Thrust, pounds $\times 10^{-3}$	141.4	150.0	128.9	137.8	97.4	136.0	98.0	140.8
System mixture ratio, O/F	4.07	4.21	3.84	4.05	3.17	4.00	3.18	4.05
Specific impulse, seconds	333.2	337.2	327.7	326.5	321.3	328.3	v321.5	334.4
Chamber pressure, psia	917	958	860	884	657	898	662	904
Total LOX flow, lb/sec	339.9	357.0	312.3	338.5	230.3	331.5	231.9	337.6
Total fuel flow, lb/sec	83.5	84.8	81.3	83.6	72.7	82.8	73.0	83.4
CG LOX flow, lb/sec	4.26	4.45	3.99	4.24	3.05	4.15	3.07	4.22
CG fuel flow, lb/sec	4.34	4.99	4.84	4.92	4.47	4.88	4.47	4.89
CG LOX orifice diameter, inches	.325	.325	.325	.325	.325	.325	.325	.325
CG fuel orifice diameter, inches	.474	.474	.474	.474	.474	.474	.474	.474
OTBO diameter, inches	3.050	3.050	3.050	3.050	3.050	3.050	3.050	3.050

TABLE 5. (Concluded)

Item	TEST NO.			
	624-024	624-024	624-028	624-028
Duration, seconds from mainstage control	272.0	272.0	592.5	592.5
Test slice time, seconds from mainstage control	19.8	250.0	182.4	400.0
P.U. valve position	closed	open	closed	open
Thrust, pounds x 10 ⁻³	164.4	212.1	166.1	123.5
System mixture ratio, O/F	4.92	4.05	4.97	4.10
Specific impulse, seconds	339.3	320.6	339.8	322.3
Chamber pressure, psia	1024	914	1035	826
Total LOX flow, lb/sec	402.7	303.1	406.9	308.1
Total fuel flow, lb/sec	81.8	74.8	81.8	75.1
GG LOX flow, lb/sec	4.55	3.63	4.58	3.69
GG fuel flow, lb/sec	5.01	4.71	5.05	4.74
GG LOX orifice diameter, inches	.295	.295	.295	.295
GG fuel orifice diameter, inches	.474	.474	.474	.474
OTSO diameter, inches	2.300	2.300	2.300	2.300
			624-029	624-029
			15.1	15.1
			5.0	14.4
			$\frac{1}{2}$ open	closed
			184.7	206.5
			5.08	5.52
			342.6	340.8
			1124	1248
			450.4	513.0
			88.6	92.9
			5.20	5.81
			6.63	6.80
			.334	.334
			.625	.625
			2.190	1.790
			2.300	2.300
			624-031	624-031
			49.6	49.6
			5.0	5.0
			$\frac{1}{2}$ open	closed
			110.6	141.7
			3.47	4.10
			320.9	331.1
			754	915
			267.6	344.0
			77.1	84.0
			3.48	4.23
			4.62	4.88
			.325	.325
			.474	.474
			3.050	3.050

TABLE 6. TEST BED NO. 1 MAINSTAGE PERFORMANCE
TEST 624-029 AND RATED

	Test 624-029 (Site)	Rated* (Sea Level)
1. System Performance (Site)		
Thrust, pounds	206520	5.5000
Mixture Ratio	5.5237	
Specific Impulse, seconds	340.87	
Oxidizer Weight Flow, lb/sec	512.99	501.30
Fuel Weight Flow, lb/sec	92.87	91.15
Total Weight Flow, lb/sec	605.85	592.45
Ambient Pressure	13.81	14.70
2. Thrust Chamber Performance--Average		
Mixture Ratio	5.8926	5.8285
Pressure Injector, psia (Static)	1248.4	1224.0
c* Injector	7541.64	7555.35
c* Efficiency Nozzle	0.9709	0.9709
Oxidizer Weight Flow (Total), lb/sec	507.17	495.55
Fuel Weight Flow (Total), lb/sec	86.07	85.02
Total Weight Flow, lb/sec	593.24	580.57
Throat Area Correction (Total), in. ²	111.38	111.38
Expansion Ratio (Estimated)	115.82	115.82
3. Fuel Pump Performance		
Inlet Pressure, psia (Total)	43.03	30.00
Outlet Pressure, psia (Total)	2148.66	2119.43
Inlet Density, lb/cu ft	4.409	4.401
Outlet Density, lb/cu ft	4.615	4.606
Pump Speed, rpm	30986	30851
Head, feet	64620.6	64227.3
Volume Flow, gpm	9454.96	9295.9
Weight Flow, lb/sec	92.87	91.15
Efficiency, percent	0.7227	0.7219
Required Horsepower	15098.8	14744.6
4. Oxidizer Pump Performance		
Inlet Pressure, psia (Total)	50.77	39.00
Outlet Pressure, psia (Total)	1797.79	1749.11
Inlet Density, lb/cu ft	70.89	70.89
Outlet Density, lb/cu ft	71.0	70.88
Pump Speed, rpm	10960	10837
Head, feet	3543.2	3474.2
Volume Flow, gpm	3248.1	3178.4
Weight Flow, lb/sec	512.99	501.30
Efficiency, percent	0.7258	0.7242
Required Horsepower	4672.1	4488.3

TABLE 6. (Concluded)

	Test 624-029 (Site)	Rated* (Sea Level)
5. Gas Generator Performance		
Oxidizer Weight Flow, lb/sec	5.815	5.75
Oxidizer Density, lb/cu ft	70.78	70.79
Fuel Weight Flow, lb/sec	6.801	6.125
Fuel Density, lb/cu ft	4.39	4.38
Total Weight Flow, lb/sec	12.616	11.877
Mixture Ratio	0.855	0.939
Pressure Injector Calculated, psia	1116.00	1076.91
6. Fuel Turbine Performance		
Total Weight Flow, lb/sec	12.616	11.877
Inlet Pressure, psia (Total)	1060.83	1023.84
Exit Pressure, psia (Static)	118.71	112.97
Pressure Ratio	8.936	9.063
Inlet Pressure, psia (Static)	1045.81	1009.39
Inlet Temperature, R	1516.4	1660.3
Exit Temperature, R	1030.18	1138.25
Developed Horsepower	15098.7	14744.6
Efficiency, percent	0.6353	0.6247
7. Oxidizer Turbine Performance		
Total Weight Flow, lb/sec	10.983	10.168
Inlet Pressure, psia (Total)	117.15	111.60
Exit Pressure, psia (Static)	40.46	38.93
Pressure Ratio	2.896	2.867
Inlet Pressure, psia (Static)	114.36	108.95
Inlet Temperature, R	1030.18	1138.25
Exit Temperature, R	886.36	983.07
Developed Horsepower	4672.1	4488.3
Efficiency, percent	0.5936	0.5870

*Rated P_c , MR, and T

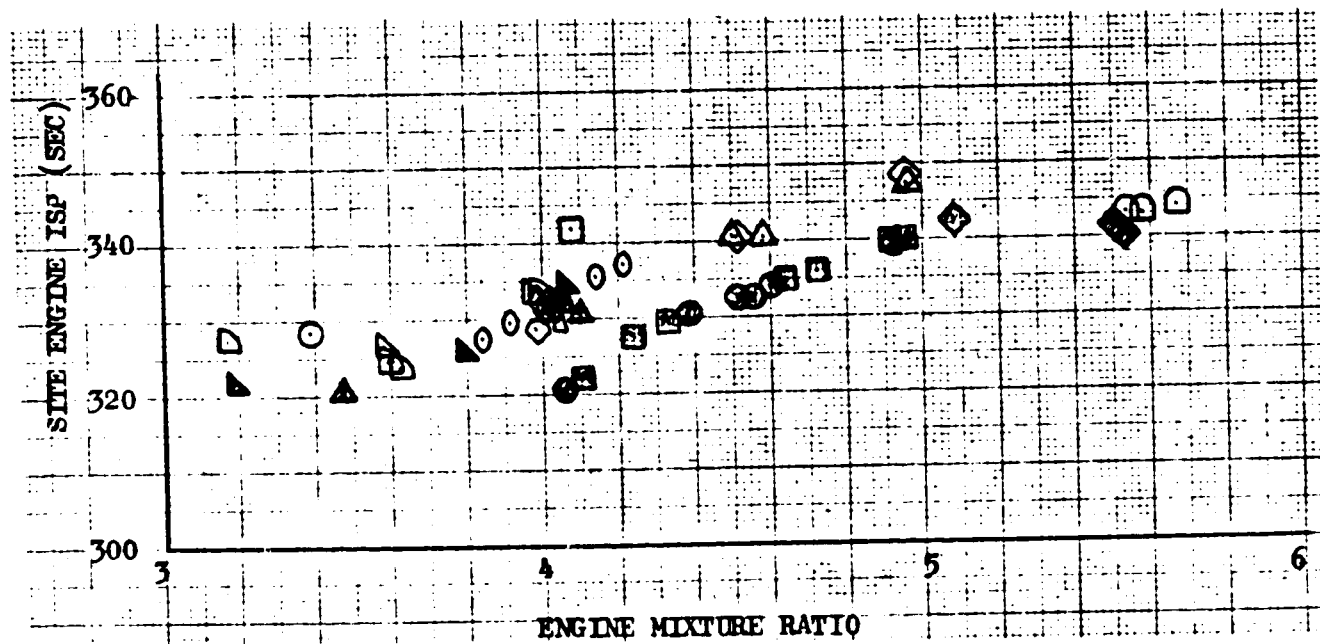
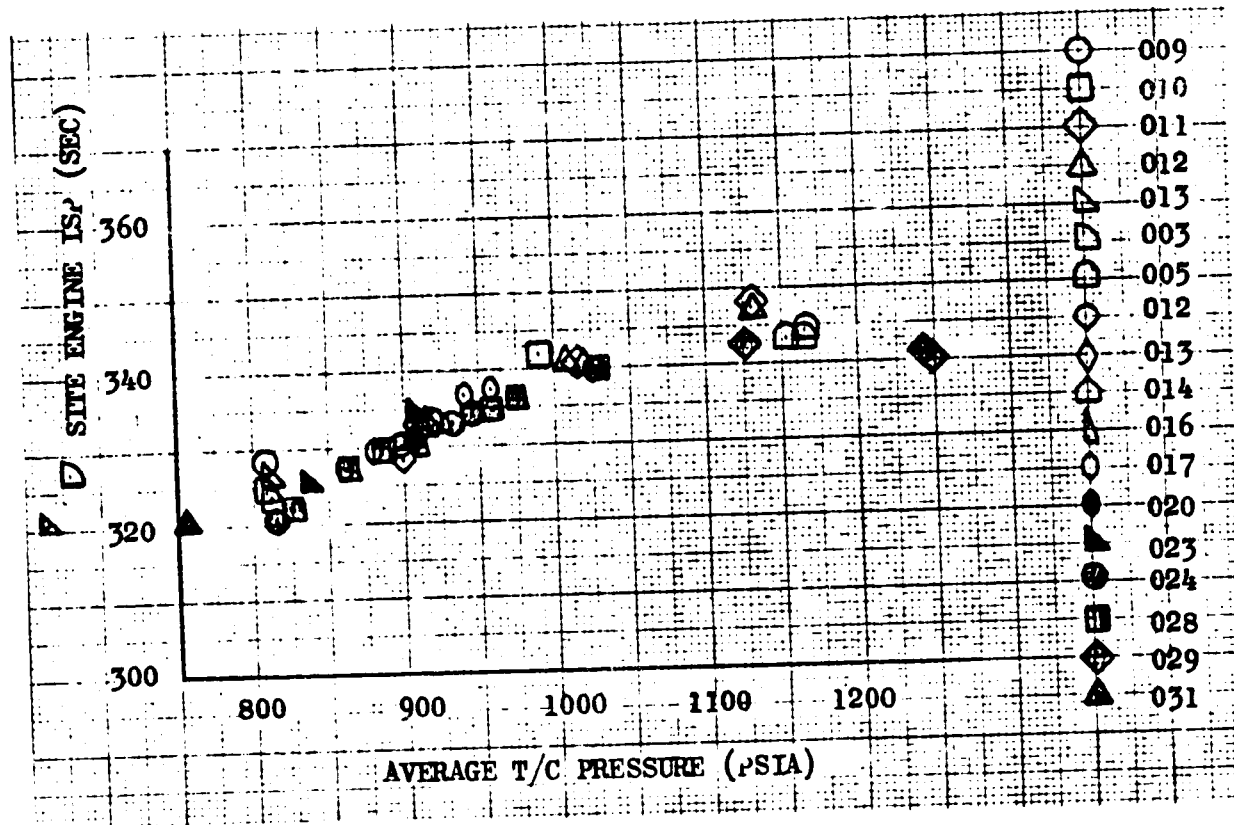


Figure 42. Linear Test Bed Program, Site Engine Specific Impulse vs Chamber Pressure and Mixture Ratio

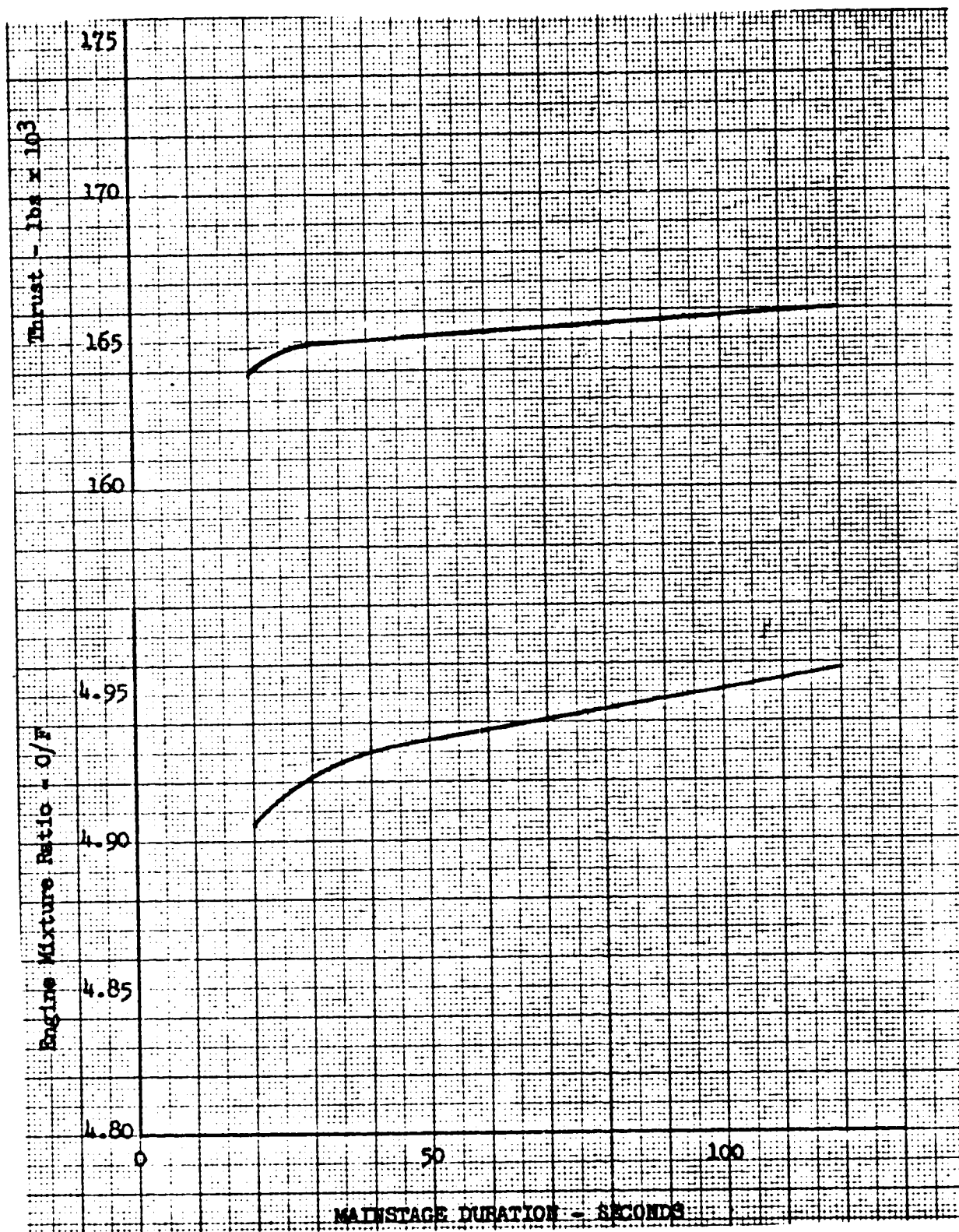


Figure 43. Linear Test Bed Program, Test Bed No. 1 Performance Trends, Test 624-028

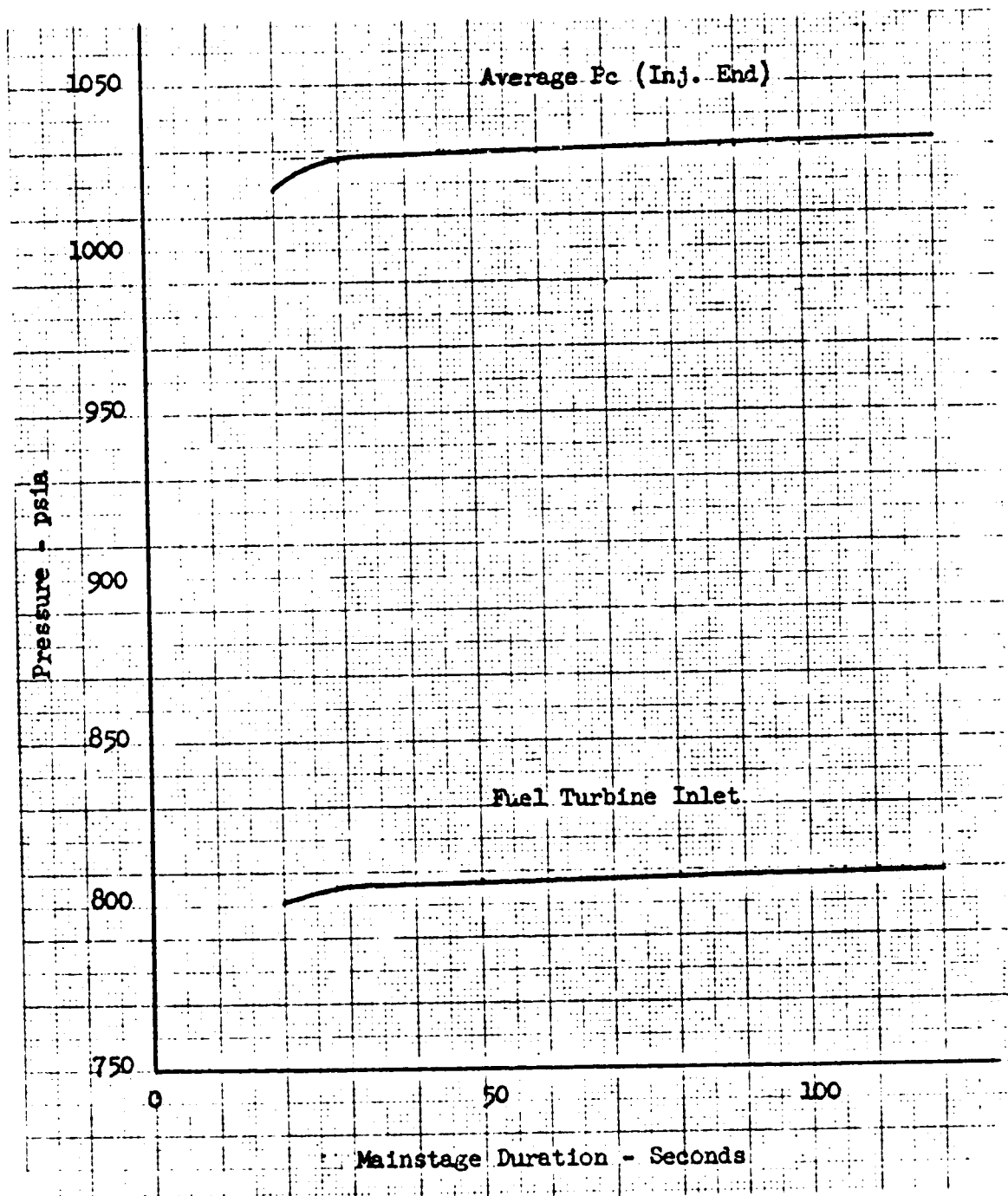


Figure 44. Linear Test Bed Program, Test Bed No. 1 Performance Trends, Test 624-028

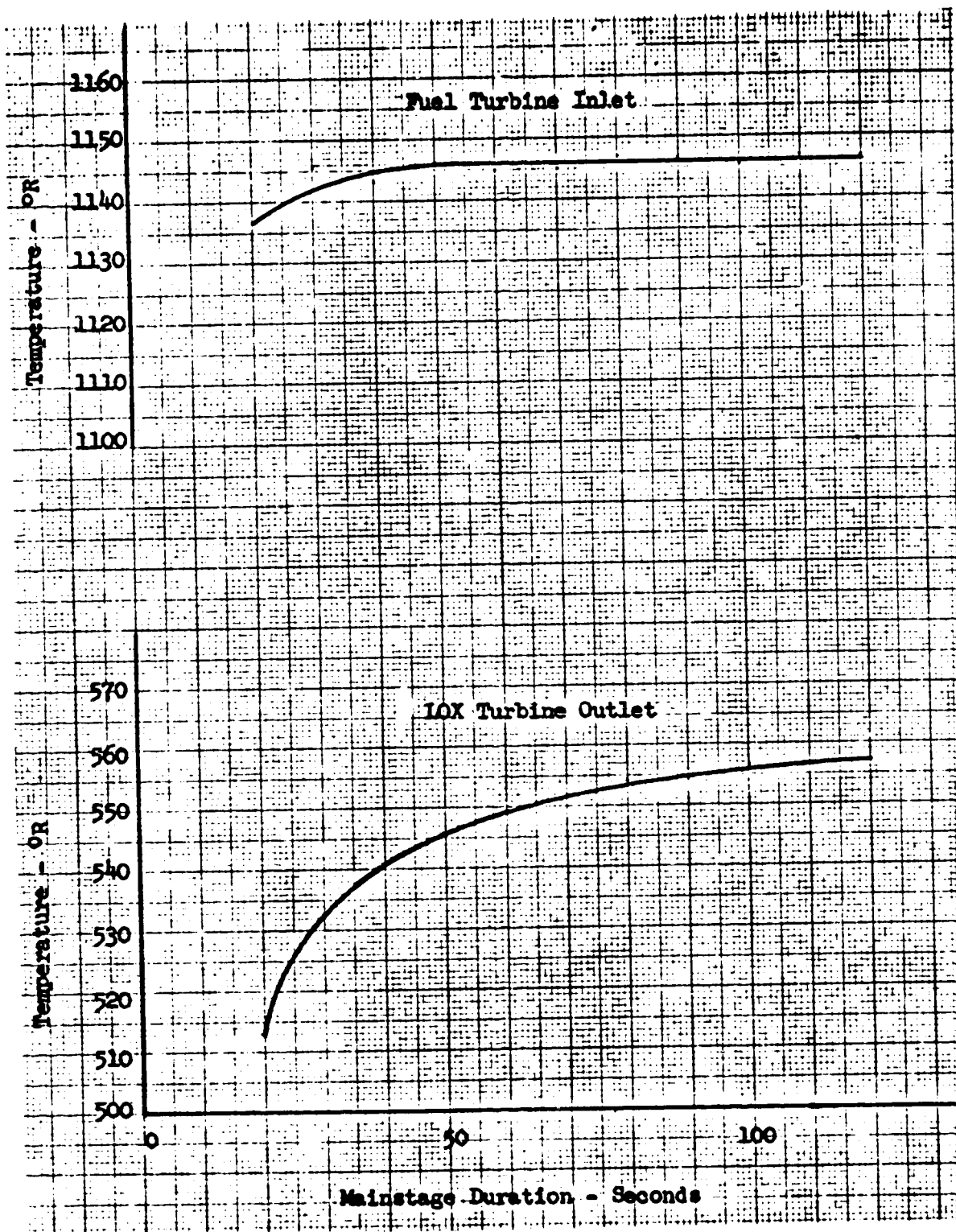


Figure 45. Linear Test Bed Program, Test Bed No. 1 Performance Trends, Test 624-028

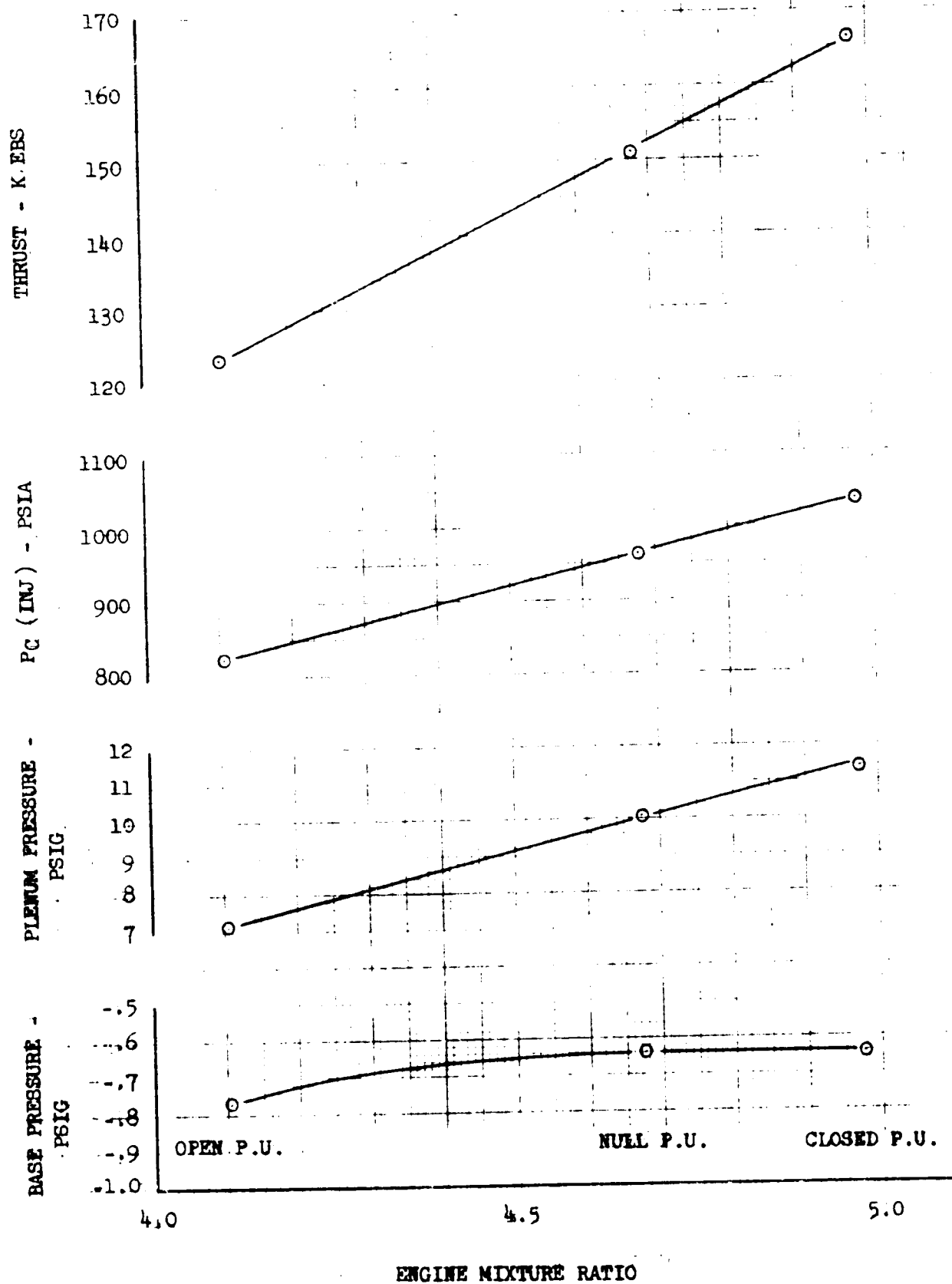


Figure 46. Linear Test Bed Program, Test Bed No. 1 Performance vs Mixture Ratio, Test 624-028

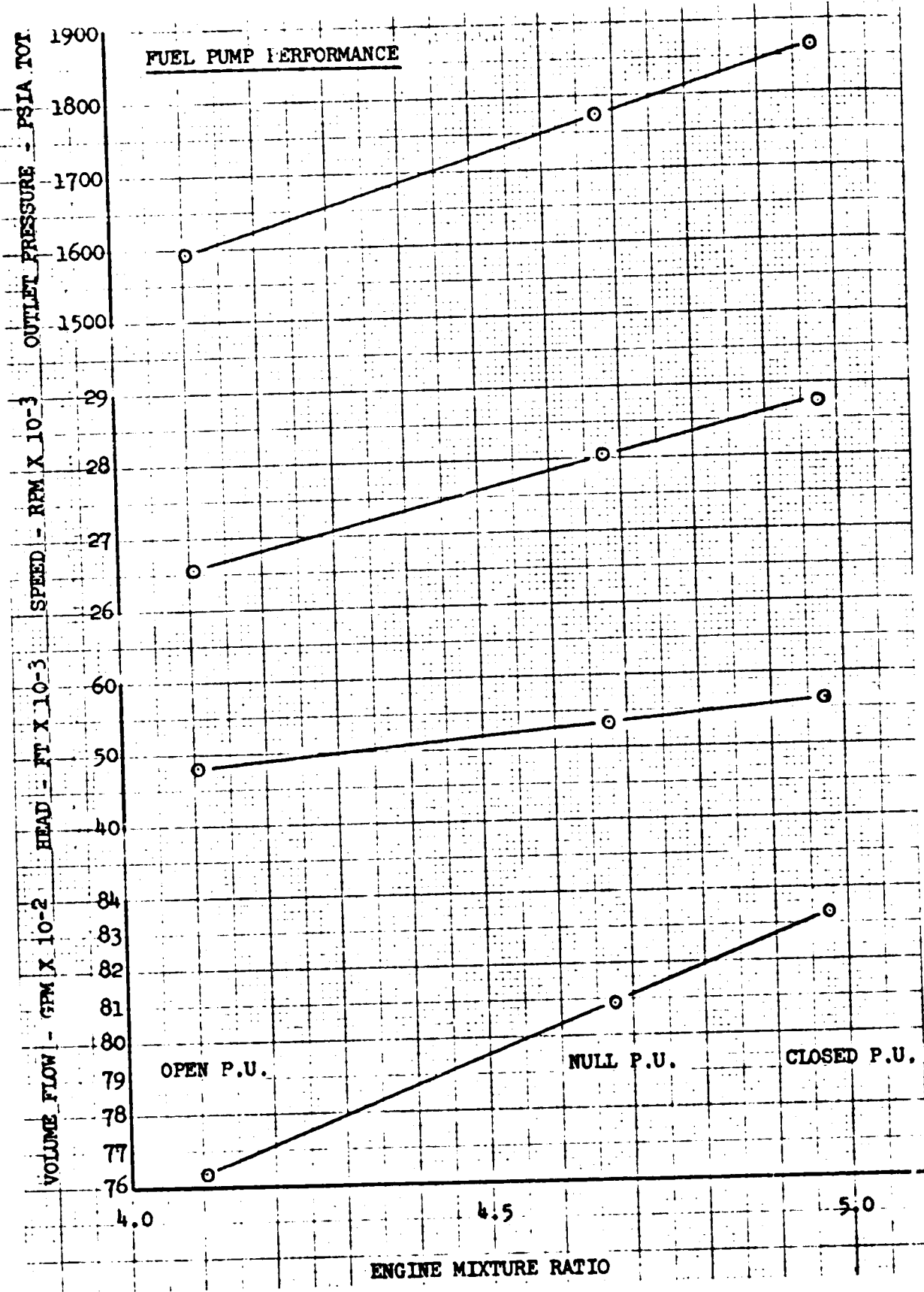


Figure 47. Linear Test Bed Program, Test Bed No. 1 Performance vs Mixture Ratio, Test 624-028

R-9049

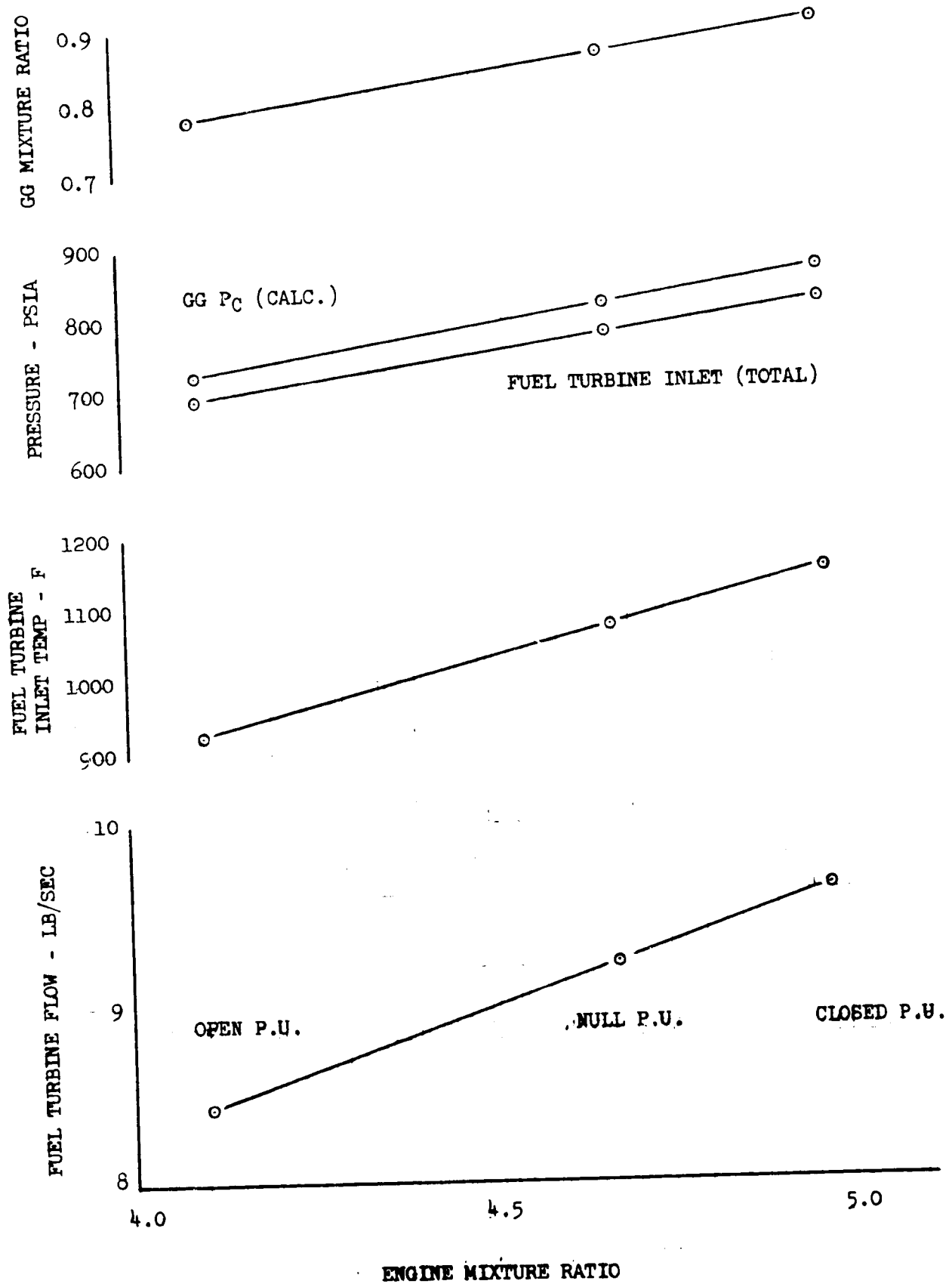


Figure 48. Linear Test Bed Program, Test Bed No. 1 Performance vs Mixture Ratio, Test 624-028

R-9049

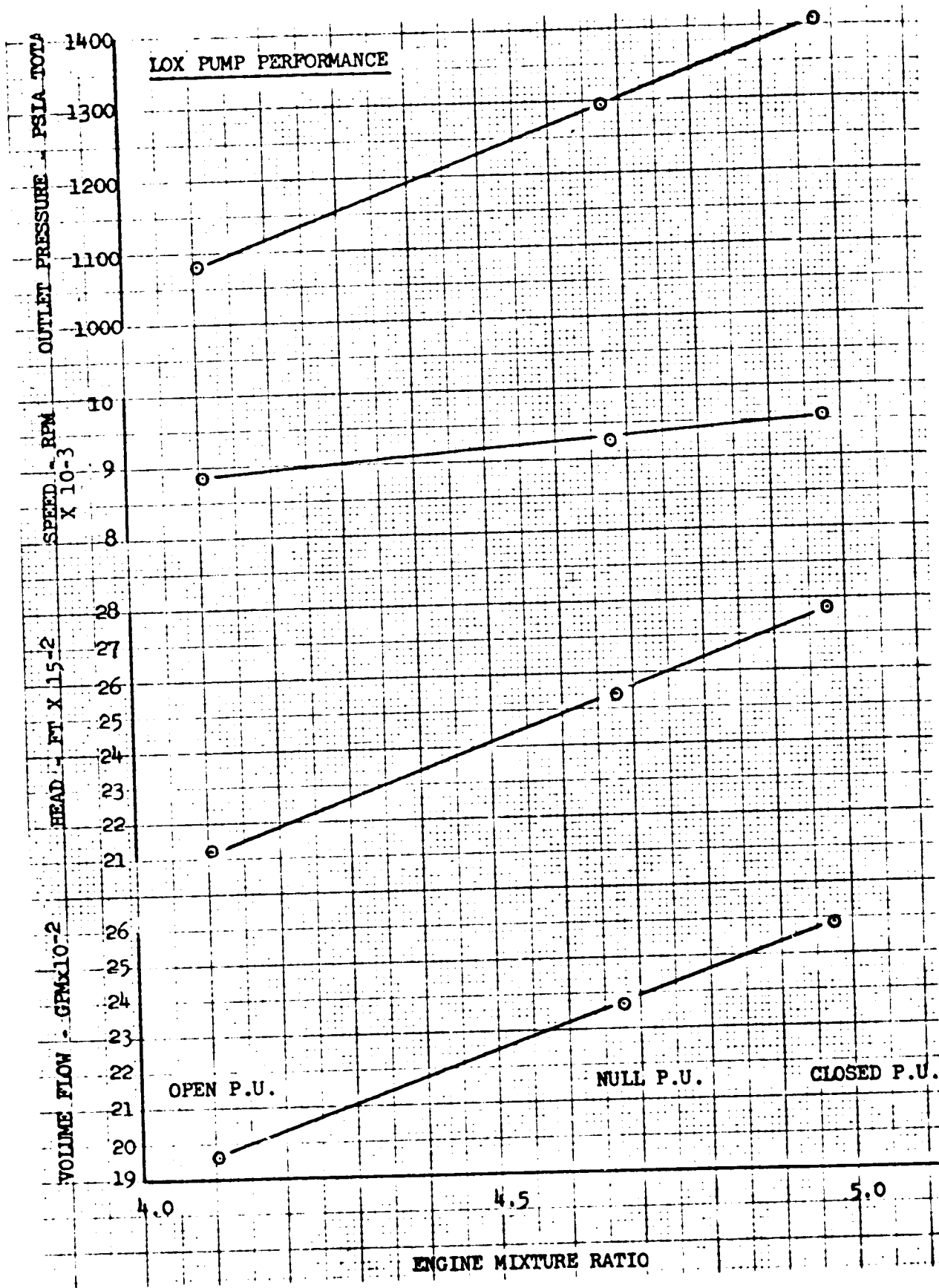


Figure 49. Linear Test Bed Program, Test Bed No. 1 Performance vs Mixture Ratio, Test 624-028

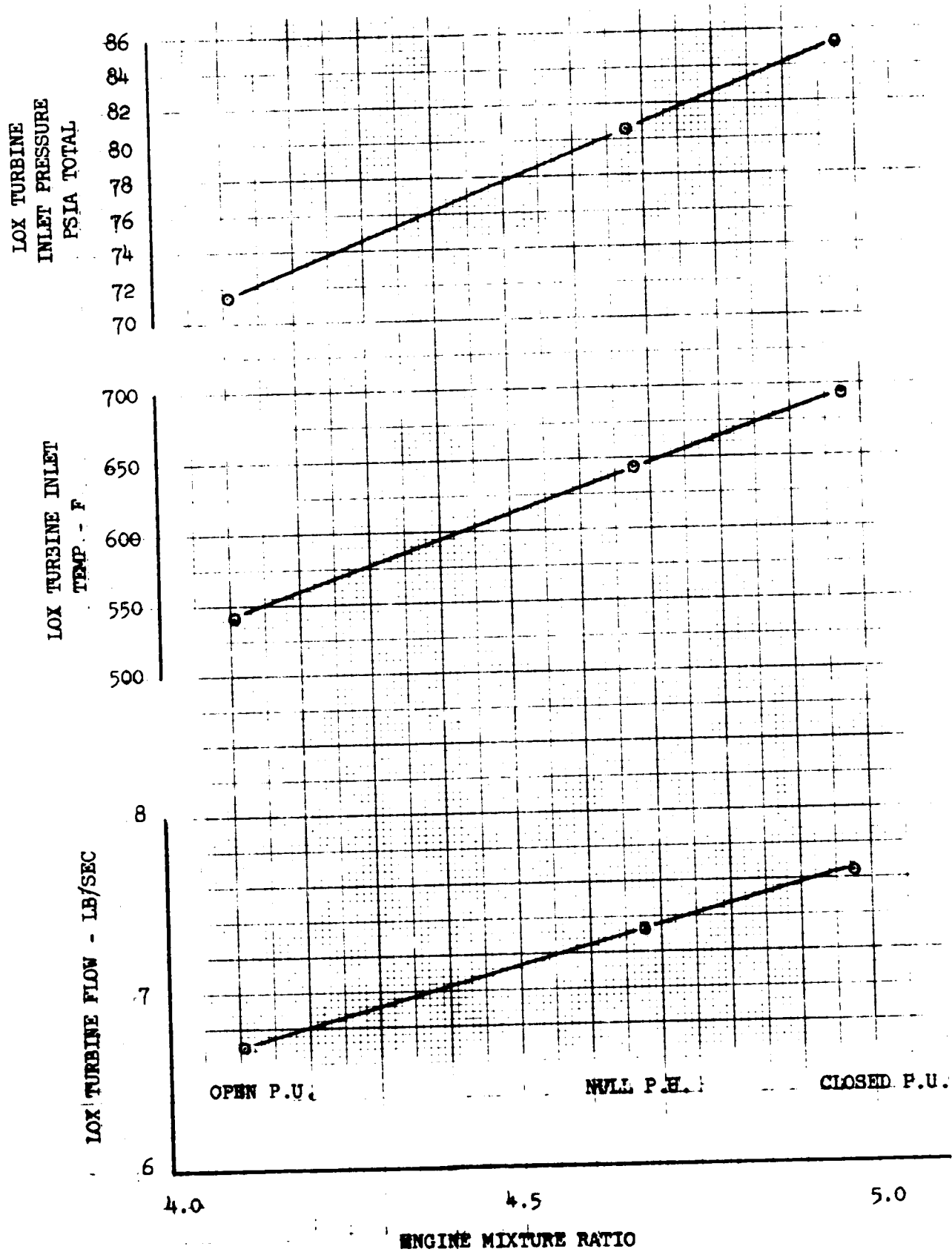


Figure 50. Linear Test Bed Program, Test Bed No. 1 Performance vs Mixture Ratio, Test 624-028

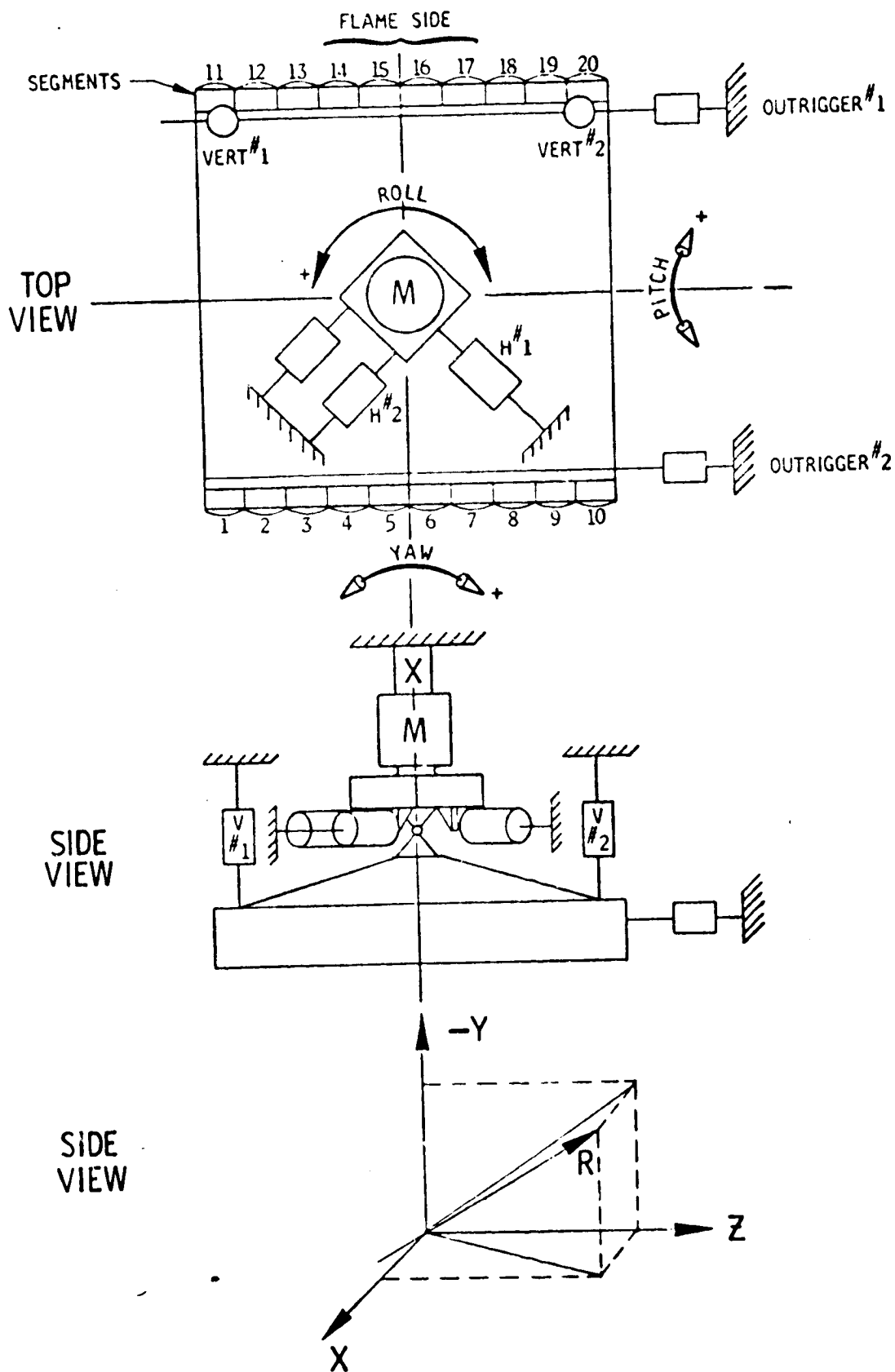


Figure 51. Load Cell Locations and Axis Definitions

TABLE 7. LINEAR TEST BED PROGRAM TEST BED NO. 1, THRUST VECTOR DATA

ITEM	TEST NO. 624 -									
	009	010	011	011	012	012	013	013	003	003
Slice time (sec)	7.8	16.4	21.0	31.0	22.5	87.0	23.6	28.6	48.0	68.0
Engine mixture ratio (O/F)	3.39	4.08	4.51	4.95	4.50	4.98	3.58	3.97	3.99	3.17
Ave. T/C mixture ratio (O/F)	3.56	4.29	4.81	5.28	4.80	5.30	3.80	4.21	4.19	3.34
Ave. T/C pressure (psia)	808	991	1015	1130	1011	1130	810	907	923	580
Engine thrust (K lbs)	117.07	152.99	158.99	158.09	181.59	157.60	181.24	135.75	138.34	99.76
X axis thrust (K lbs)	0*	0*	0*	0*	-0.31	-0.25	0.29	-0.23	-0.13	0.41
-Y axis thrust (K lbs)	117.07	162.99	158.09	181.59	157.59	181.24	117.94	135.75	138.34	99.76
Z axis thrust (K lbs)	1.08	0.35	0.15	0.05	1.33	1.34	1.64	1.13	0.58	0.48
Displacement in X-Z plane (din)	1.066	0.280	0.367	0.355	0.324	0.302	0.667	0.382	0.399	0.853
dz (in)	0.325	-0.244	-0.321	-0.302	-0.260	-0.255	-0.099	-0.336	-0.369	-0.120
dx (in)	-1.016	-0.138	-0.176	-0.186	-0.193	-0.162	-0.660	-0.182	-0.154	-0.844
Pitch (K in-lb)	118.8	21.12	27.87	33.82	30.39	29.28	77.82	24.70	21.27	84.22
Yaw (K in-lb)	-15.34	44.67	53.92	55.77	57.00	62.05	33.03	56.44	54.84	18.18
Roll (K in-lb)	63.45	-19.91	-18.90	-18.80	2.97	8.72	63.76	-4.38	-5.04	14.72
Angular deviation from -Y axis	0.528	0.131	0.053	0.014	0.496	0.429	0.808	0.486	0.248	0.364

* Thrust not measured in this axis

TABLE 7. (Continued)

ITEM	TEST NO. 624 -									
	005	012	013	014	016	017	017	020	023	023
Slice time (sec)	82.5	9.8	29.3	79.8	218.9	170.0	200.0	200.0	20.8	135.0
Engine mixture ratio (O/F)	5.67	3.98	4.03	4.04	4.07	4.21	3.84	4.05	3.18	4.05
Ave. T/C mixture ratio (O/F)	5.99	4.20	4.23	4.24	4.27	4.42	4.04	4.24	3.34	4.24
Ave. T/C pressure (psia)	1164	899	916	916	917	958	860	908	662	904
Engine thrust (K lbs)	187.14	135.59	140.27	140.17	141.07	148.97	128.94	138.83	98.04	140.80
X axis thrust (K lbs)	-0.39	0.01	-0.23	-0.55	-0.33	-0.31	-0.06	-0.61	-0.22	-0.75
-Y axis thrust (- lbs)	187.14	135.59	140.27	140.17	141.07	148.97	128.94	138.83	98.04	140.79
Z axis thrust (K lbs)	0.38	0.72	0.81	0.35	0.11	-0.71	-0.82	0.20	1.26	1.09
Displacement in X-Z plane (din)	0.274	0.660	0.506	-0.582	0.679	0.640	0.726	0.701	0.712	0.705
dz (in)	-0.237	-0.519	-0.486	-0.580	-0.517	-0.435	-0.489	-0.557	-0.094	-0.476
dx (in)	-0.137	-0.409	-0.142	-0.054	-0.440	-0.469	-0.537	-0.425	-0.706	-0.520
Pitch (K in-lb)	25.70	55.39	19.96	-7.51	62.04	69.85	69.25	59.07	69.17	73.24
Yaw (K in-lb)	43.87	72.53	72.22	79.80	74.25	61.00	53.86	80.11	31.13	74.15
Roll (K in-lb)	2.17	-5.54	-4.84	-0.40	10.74	-4.28	8.82	18.30	10.53	-1.56
Angular deviation from -Y axis	0.166	0.304	0.342	0.266	0.140	0.297	0.365	0.265	0.750	0.540

TABLE 7. (Concluded)

ITEM	TEST NO. 624 -							
	024	024	028	028	029	031		
Slice time (sec)	19.8	250.0	182.4	400.0	5.0	14.4	5.0	33.8
Engine mixture ratio (O/F)	4.92	4.05	4.97	4.10	5.08	5.52	3.47	4.10
Ave. T/C mixture ratio (O/F)	5.18	4.28	5.24	4.33	5.43	5.89	3.65	4.30
Ave. T/C pressure (psia)	1024	814	1035	826	1124	1248	754	915
Engine thrust (K lbs)	164.42	121.12	166.06	123.50	184.69	206.49	110.62	141.72
X axis thrust (K lbs)	-0.65	-0.41	0.14	0.13	-0.36	0.21	-0.003	-0.50
-Y axis thrust (k lbs)	164.42	121.12	166.06	123.50	184.69	206.49	110.61	141.72
Z axis thrust (K lbs)	1.25	0.10	-0.96	-1.09	0.66	0.49	1.07	1.05
Displacement in X-Z plane (din)	0.449	0.662	0.438	0.523	0.392	0.930	1.119	0.590
dz (in)	-0.297	-0.350	-0.314	-0.259	-0.217	-0.058	0.012	-0.340
dx (in)	-0.337	-0.562	-0.304	-0.455	-0.327	-0.929	-1.119	-0.482
Pitch (K in-lb)	55.34	58.04	50.55	56.15	60.33	191.72	123.75	68.30
Yaw (K in-lb)	61.50	35.99	35.06	11.83	46.40	26.62	21.17	59.81
Roll (K in-lb)	-10.74	23.49	-8.47	17.49	-9.32	22.23	51.14	-11.69
Angular deviation from -Y axis	0.492	0.198	0.335	0.511	0.233	0.147	0.554	0.469

Corrections were applied to the resultant thrust vector to correct for LOX and fuel inlet duct forces. The dumped water flowrate through the end fences of approximately 40 lb/sec contributed about 295 pounds of force; however, pretest thrust measurement zeros were taken with the water flowing and test values did not require correction.

Test-to-test consistency on the thrust vector measurement is shown in Fig. 52, which indicates the thrust vector pierce point displacements from the gimbal center in the X-Z plane. This value is unaffected by the missing load measurements along the X axis.

THRUST CHAMBER PERFORMANCE

The relationship of chamber pressure and mixture ratio for the mainstage tests performed on breadboard No. 1 engine are displayed in Fig. 53. A fairly uniform relationship exists, as the figure indicates. Performance data are displayed as a function of chamber pressure only because, for this engine, knowing a chamber pressure implies a corresponding mixture ratio.

Figure 54 displays the results of mainstage tests of site engine specific impulse as an average value of 346 seconds indicated at a chamber pressure of 1200 psia.

Site specific impulse was computed using measured thrust as being the result of the summation of the vertical load cell measurements. Measured flowrates from the facility flowmeter was used for the engine flow rate.

Figure 54 displays c^* efficiency as a function of chamber pressure for the mainstage tests. The darkened symbols reflect c^* computed using an estimated throat area change of approximately 2 percent posttest 005 caused by the chamber erosions.

The latter tests in the series indicated a depressed c^* efficiency as compared to the earlier testing. This was brought about by an accumulation of hydrogen leaks in the combustors due to wall erosions and leakages from the nozzle.

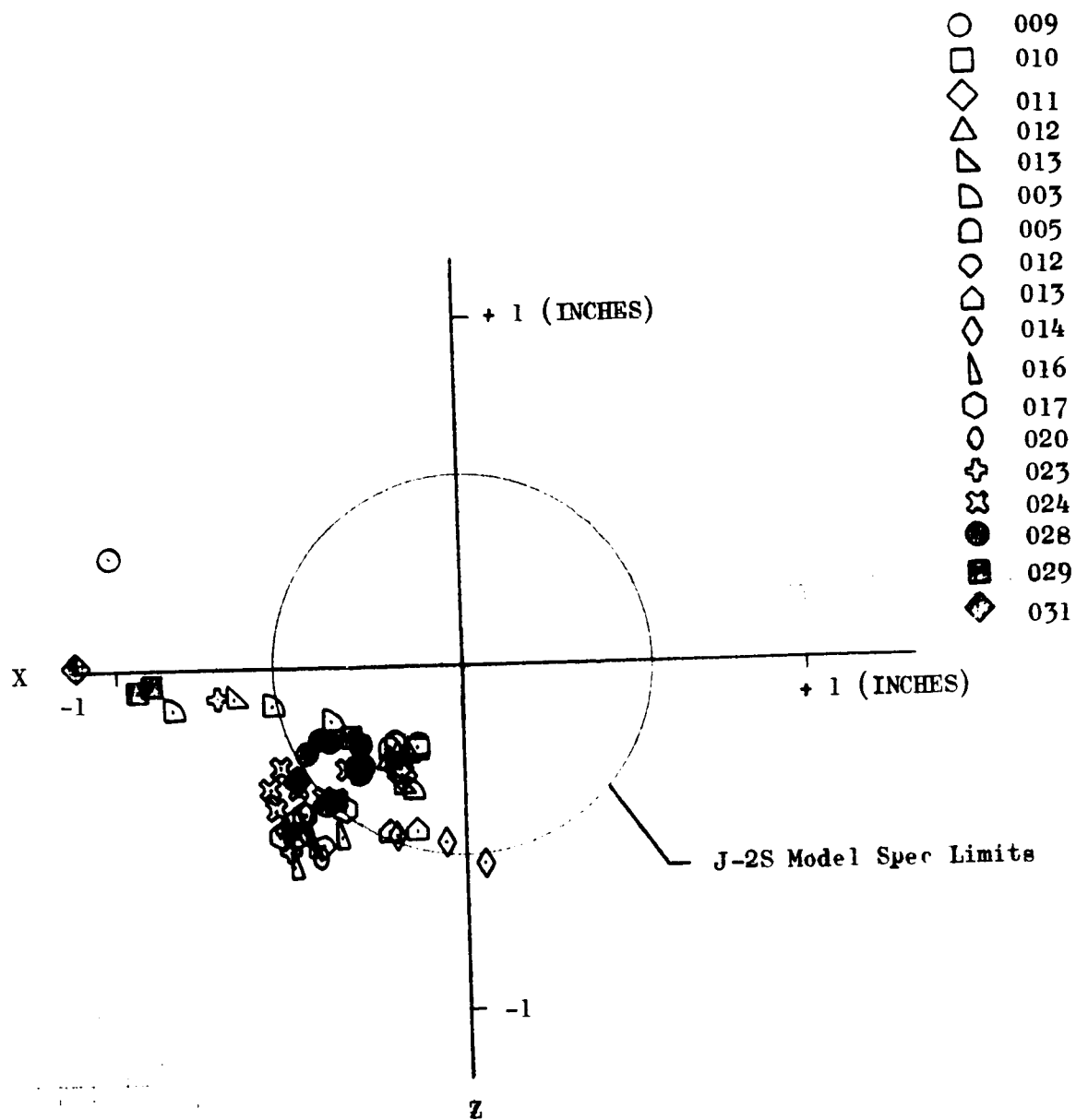


Figure 52. Linear Test Bed Program Thrust Vector Analysis;
Pierce Point Displacement in the X-Z Plane

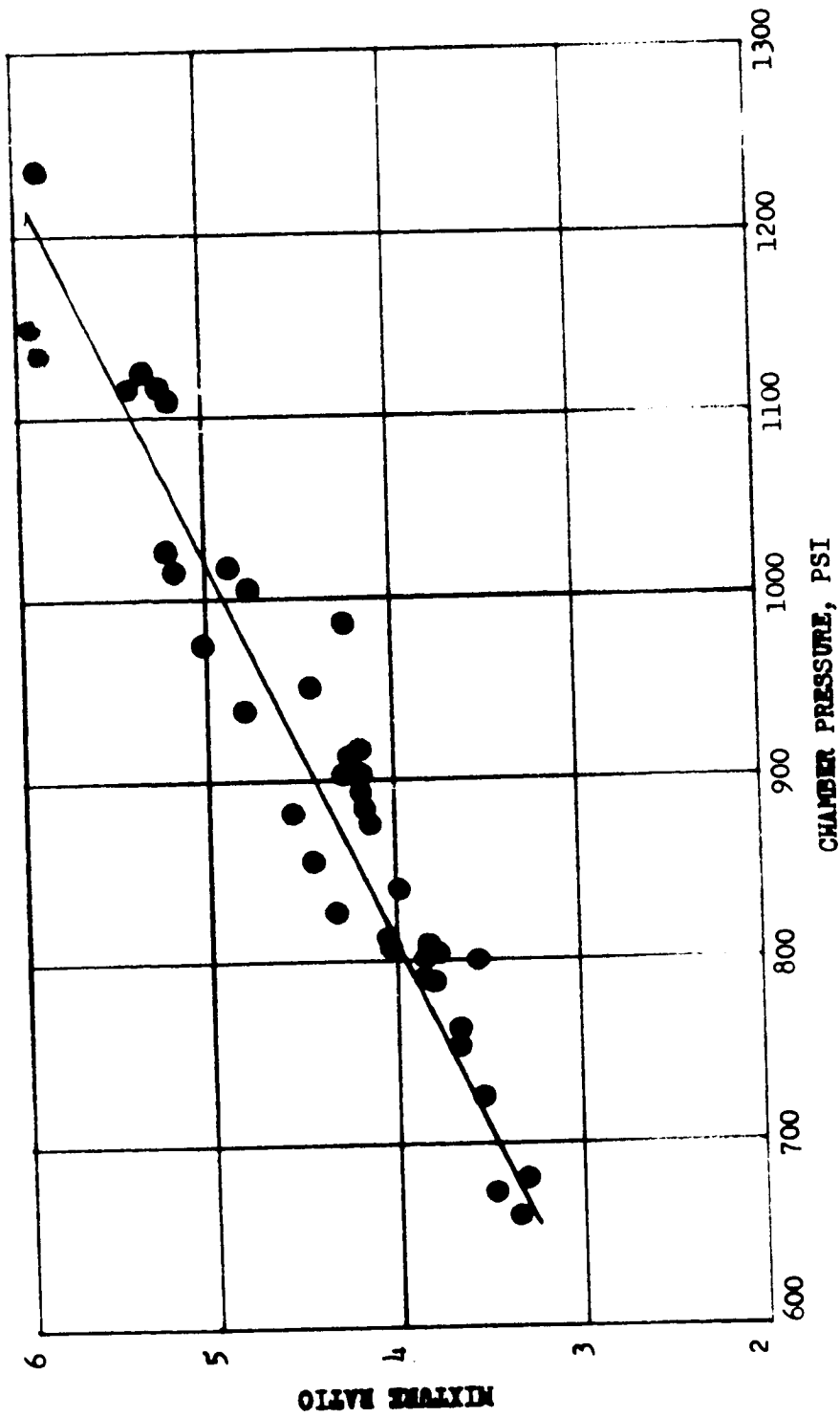


Figure 53. Breadboard No. 1 Engine Mixture Ratio vs Chamber Pressure

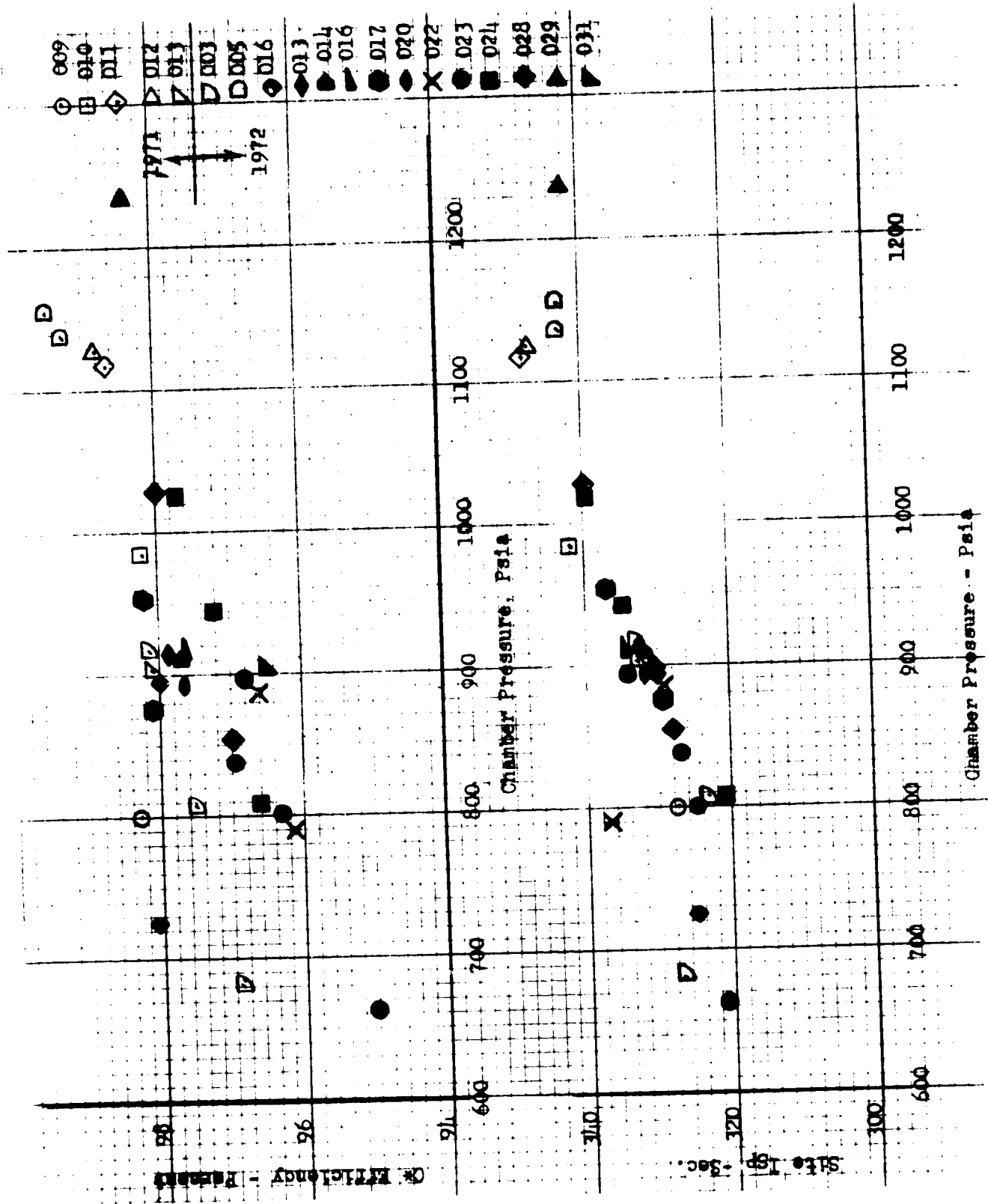


Figure 54. Engine Performance vs Chamber Pressure

Characteristic velocity was computed from:

$$c^* = \frac{P_{NS} A_t g}{\dot{W}_{\text{primary}}}$$

Where

$$P_{NS} = P_c \text{ Avg} \left(\frac{\text{Momentum correction}}{\text{Rayleigh Loss}} \right)$$

$$\text{Momentum Correction} = \left[\frac{144}{1 + A_{\text{inj}} P_c \text{ avg} \dot{W}} \right] \left[\frac{\dot{W}_f^2}{\rho_f A_f} + \frac{\dot{W}_o^2}{\rho_o A_o} \right]$$

where A_o , A_f is the oxidizer and fuel injection area, respectively. Rayleigh loss was a curve fit of the Rayleigh loss as a function of contraction ratio. Average contraction ratio was used. The value of the Rayleigh loss was approximately 1.022. The throat area was taken as:

$$A_t = C_D \left[\sum_1^{20} L \times G_{\text{avg}} \right] \left[20 \times 0.000269 (P_c \text{ avg}^{-100}) \right]$$

or, the sum of individual throat areas corrected for pressure effects on the throat area (approximately 3.2 percent). The discharge coefficient was used as a product of the potential flow discharge coefficient and boundary layer viscous effects ($C_D \approx 0.99$).

The primary flowrate was computed by subtracting the estimated gas generator flows from measured engine flows; c^* efficiency was computed from:

$$\eta_{c^*} = \frac{c^*}{c^*_{\text{theor}}} \times 100$$

The site data recorded for the breadboard engine corrects to an altitude specific performance value of 455 seconds utilizing existing wind tunnel data to correct the nozzle thrust coefficient from the test pressure ratio to vacuum. Vacuum I_s was computed as follows:

$$\text{Vacuum } I_s = \frac{c^*}{g} \left(C_{T \text{ measured}} \times \frac{C_{F \text{ optimum}}}{C_{T \text{ ratio}}} \times \frac{\epsilon \text{ overall}}{PR_{\text{des}}} \right)$$

$$\text{where } C_{T \text{ measured}} = \frac{C_{F \text{ measured}}}{C_{F \text{ optimum}}}$$

$C_{T \text{ ratio}}$ = wind tunnel data
best fit for linear nozzle (Fig. 55)

$\epsilon \text{ overall}$ = overall expansion area ratio

PR_{des} = design pressure ratio

Measured Nozzle Pressure Profiles

Figures 56 through 58 display measured nozzle wall pressures as compared to the predicted pressure profiles at chamber pressures of 600, 900, and 1200 psia. Ripples developed in the nozzle wall near the upstream pressure tap. Attempts were made to correct the measured values for this effect, as indicated in the figures. The measured values, in general, agree quite well with the theoretical predicted values particularly at chamber pressures of 900 psi or greater.

Nozzle Heat Load

Figure 59 indicates the measured nozzle heat load of Btu/sec as a function of the operating pressure ratio of the engine for all mainstage tests. The anticipated relationship is indicated in the figure. The data indicate good agreement with expected values near 1200-psi chamber pressure. The nozzle heat load was below expected values at lower chamber pressures.

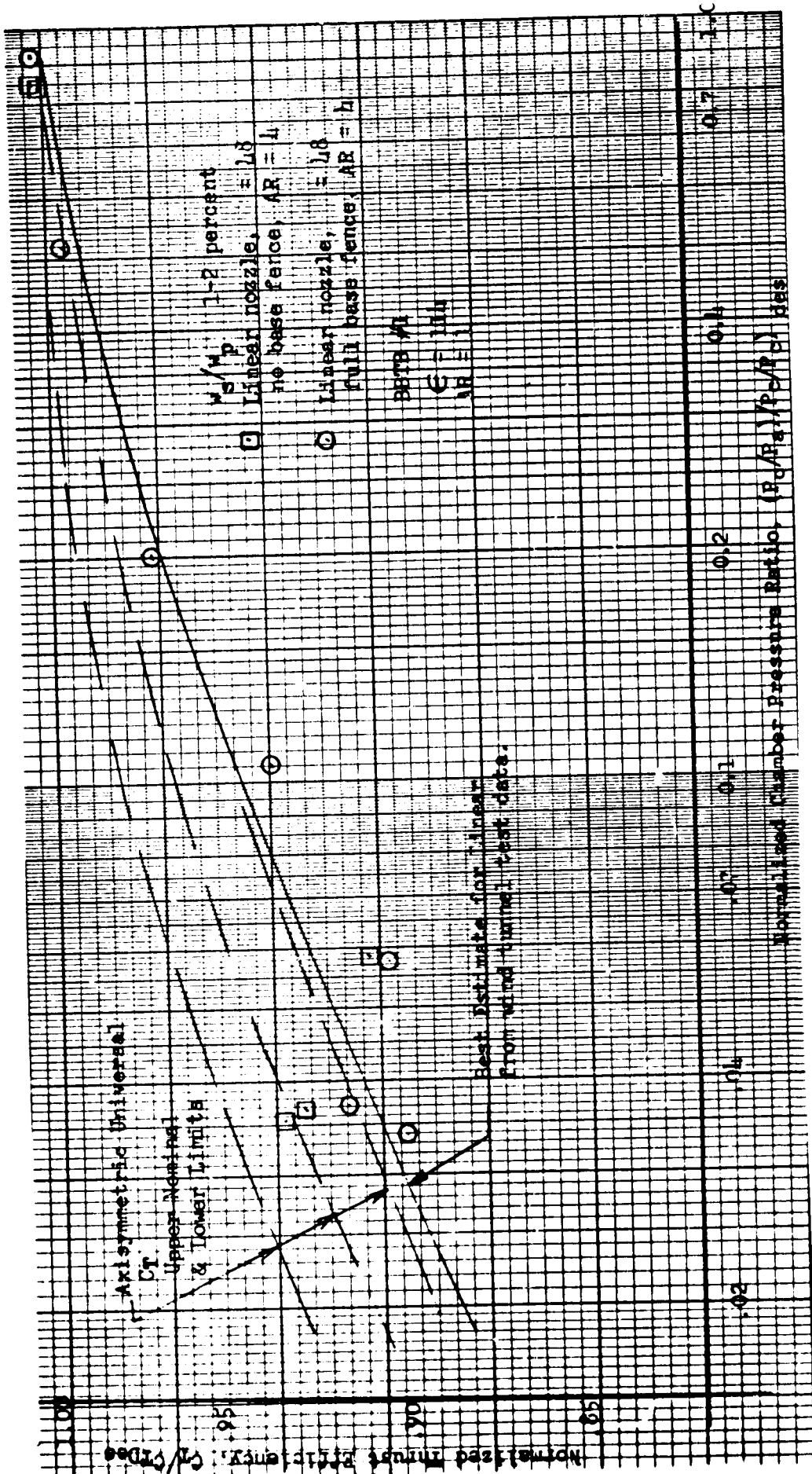


Figure 55. Wind Tunnel Test Data

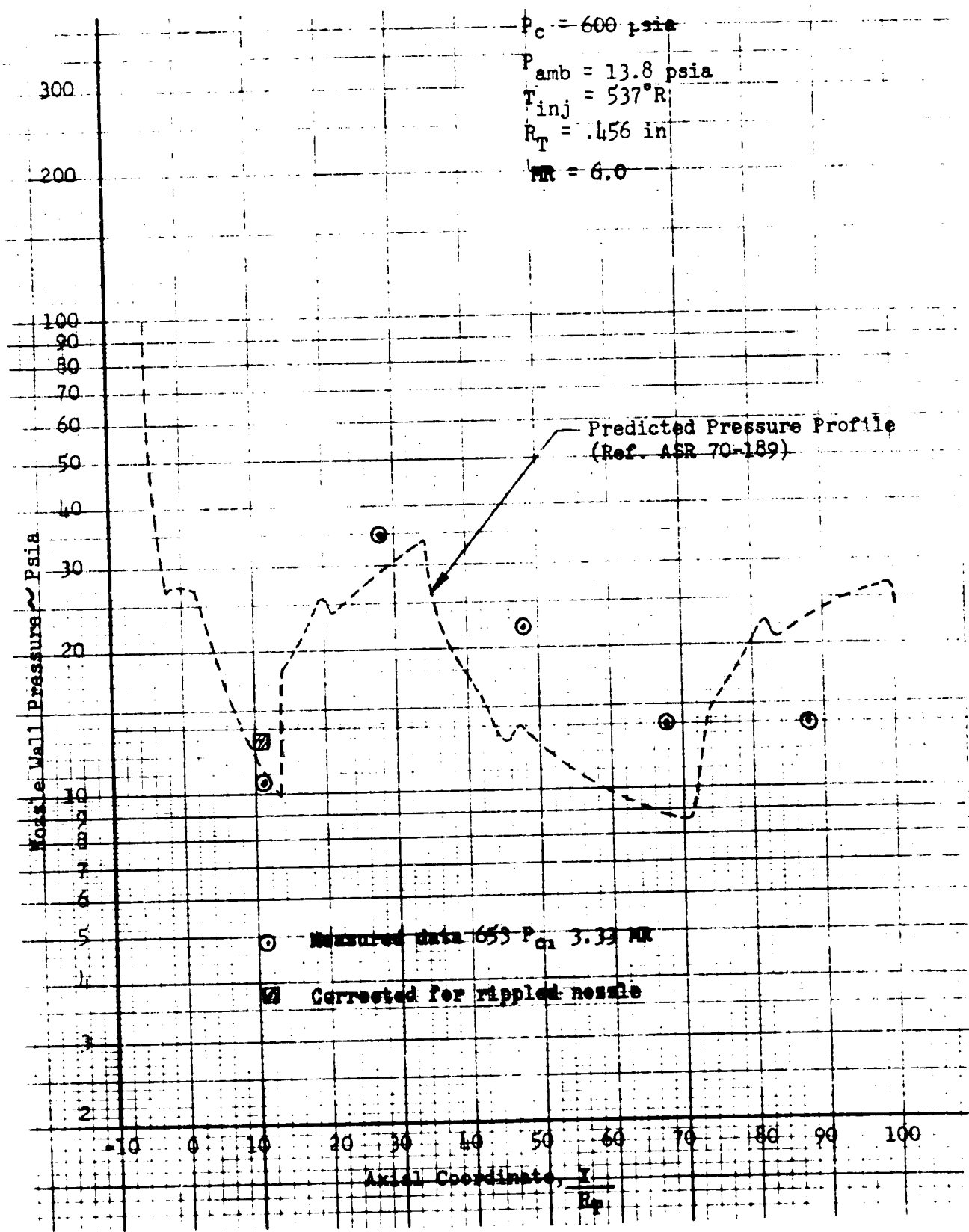


Figure 56. Breadboard Engine No. 1 Nozzle Pressure Profile

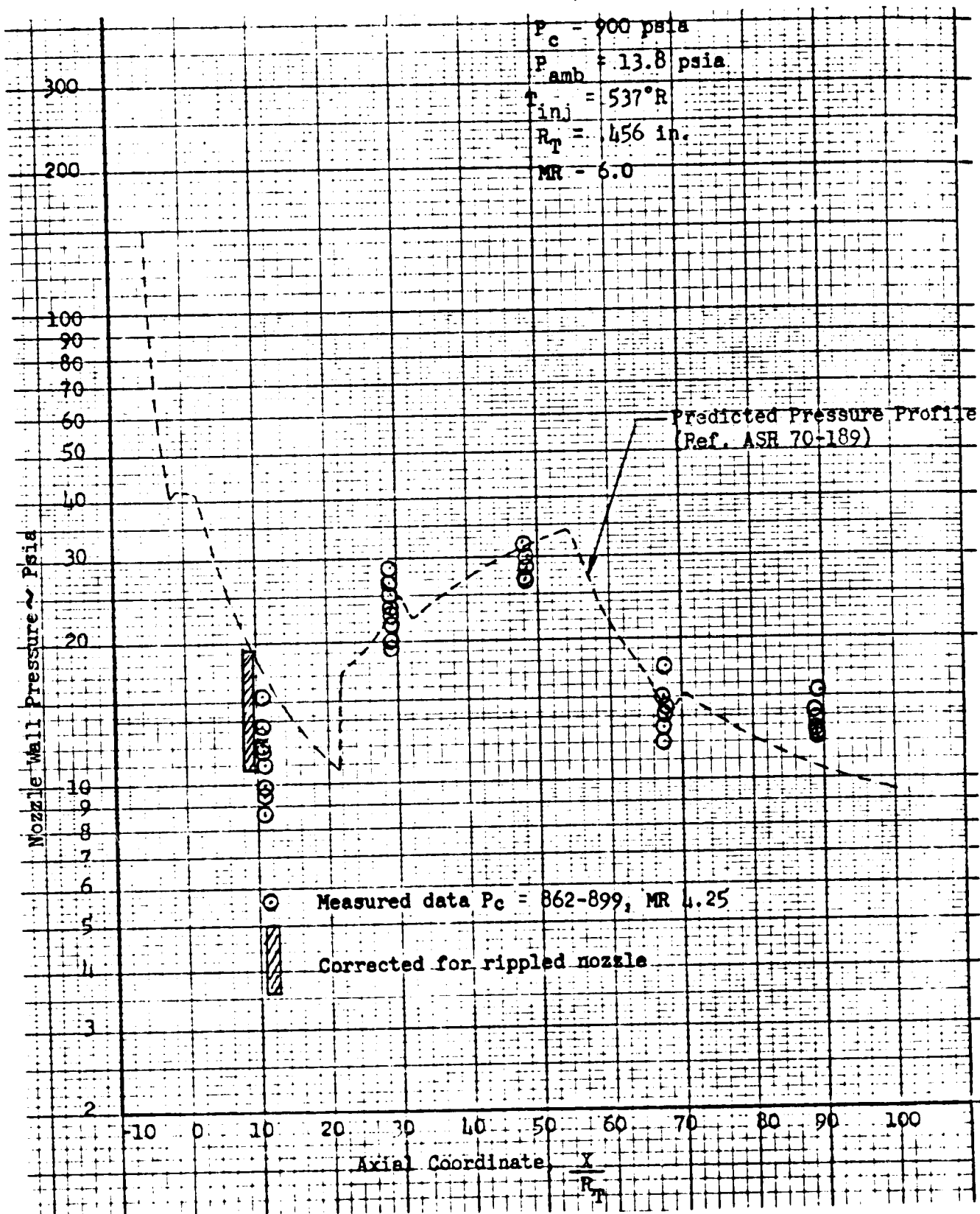


Figure 57. Breadboard Engine No. 1 Nozzle Pressure Profile

$P_c = 1200 \text{ psia}$
 $P_{amb} = 13.8 \text{ psia}$
 $T_{inj} = 537^\circ R$
 $R_T = .456 \text{ in.}$
 $MR = 610$

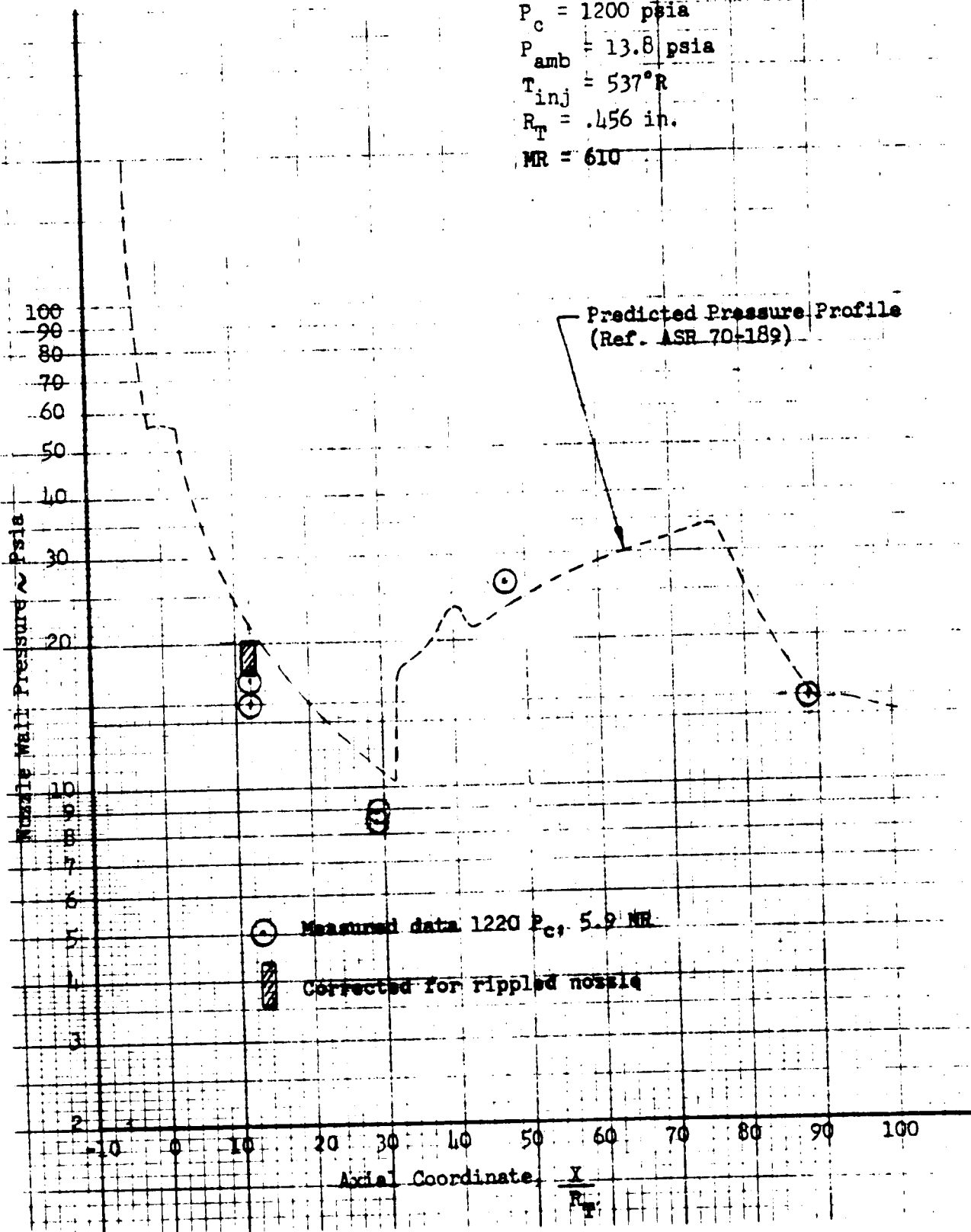


Figure 58. Breadboard Engine No. 1 Nozzle Pressure Profile

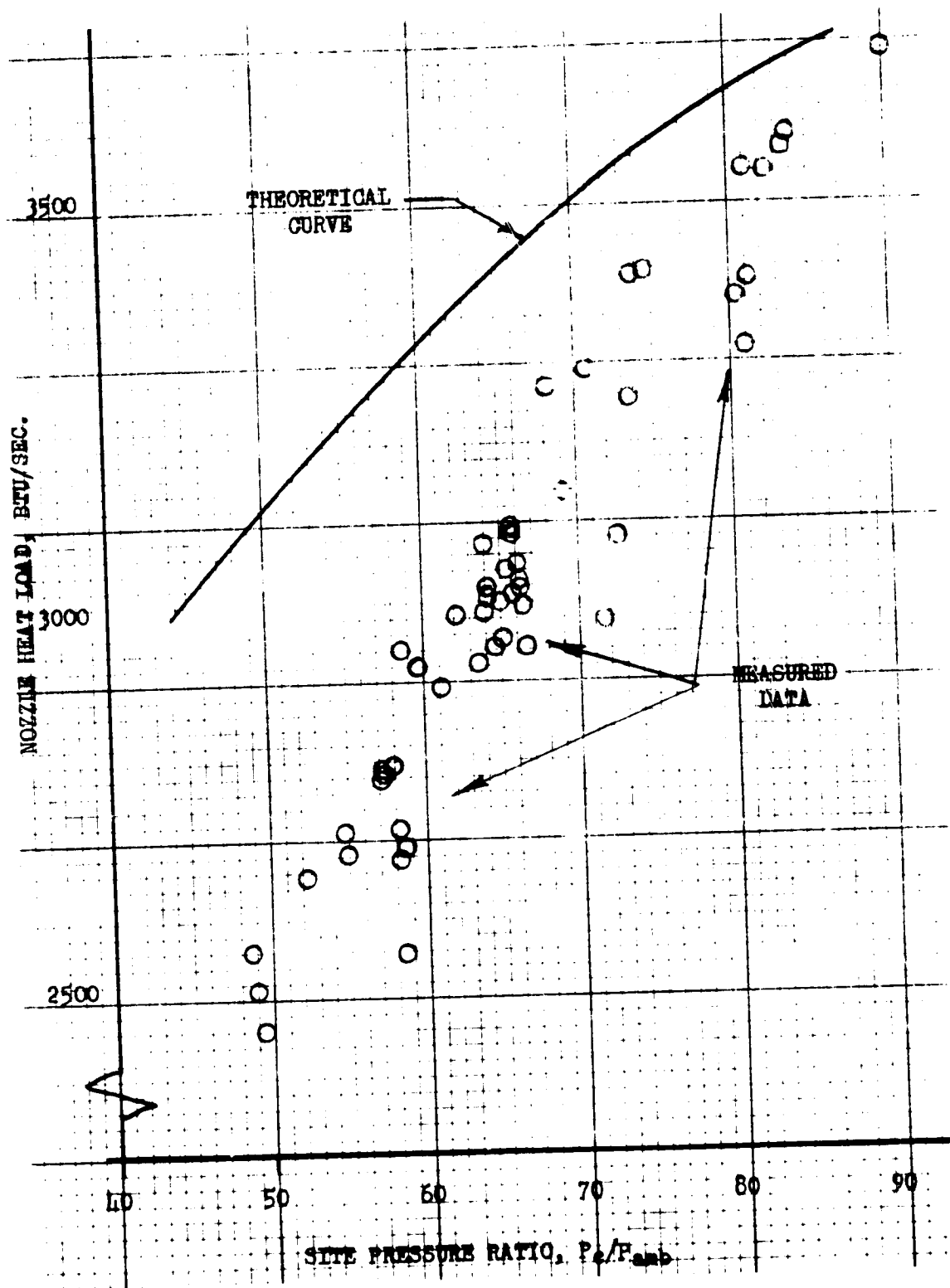


Figure 59. Nozzle Heat Load vs Pressure Ratio

Base Pressure Measurements

Figure 60 shows the average values of the base pressure measurements taken for the mainstage tests as a function of engine operating pressure ratio. The base pressure was nearly constant at 96 percent of the ambient pressure. Figure 61 indicates the distribution of pressure longitudinally and in the transverse direction across the base. Base pressure tended to be lower near the edges and peaked near the center portion of the base.

Measured Fuel Injection Temperatures

Figures 62 and 63 display the outer contour wall and inner contour wall fuel injection temperatures for each combustor recorded during mainstage testing. Specific data points are not shown in the interest of clarity. Lines drawn on the figures for each combustor represent the average of the data obtained for that combustor. The data were quite consistent permitting the outer contour wall temperature to be defined in terms of inner contour wall temperature. Combustor 6 (Fig. 62) indicated the largest differential between inner and outer wall contour temperature varying from a differential of approximately 100 to 150 F. The inner contour wall temperature was higher than the outer contour wall.

The data were used in this form to obtain an average injection temperature in performance and flow distribution studies. The limitation of the number of channels available for recording temperature would not permit simultaneous recording of all 40 injection temperature values.

Comparison of Design and Test Operating Conditions

Table 8 compares selected engine and combustor segment operating parameters for test 029 to the values anticipated in the original design.

The system flow resistance and pressure drop was less than anticipated. The combustor average throat area was larger than design. The throat areas of the combustors will be sized during fabrication to maintain desired values in future use.

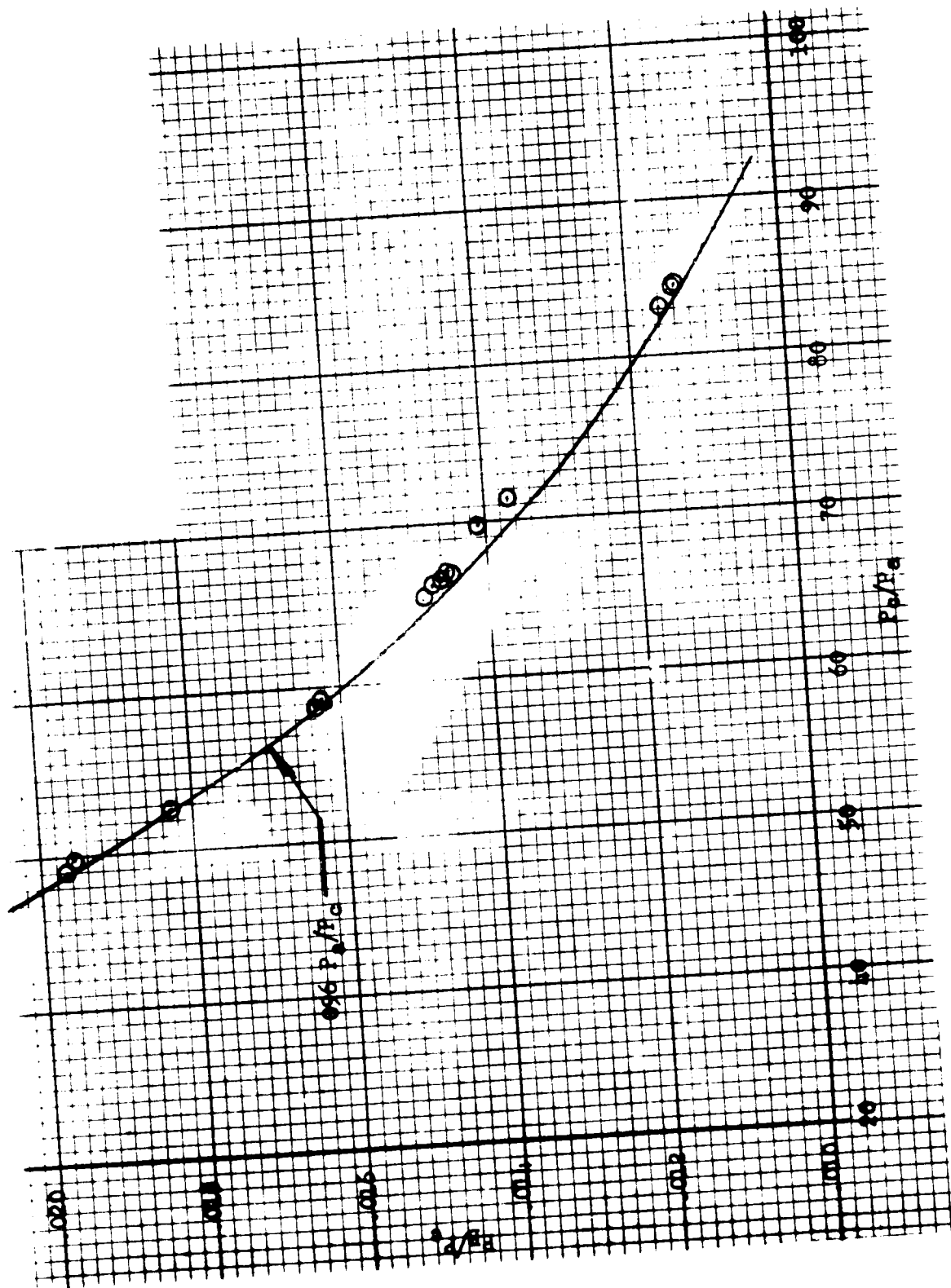


Figure 60. Average Base Pressure vs Nozzle Pressure Ratio

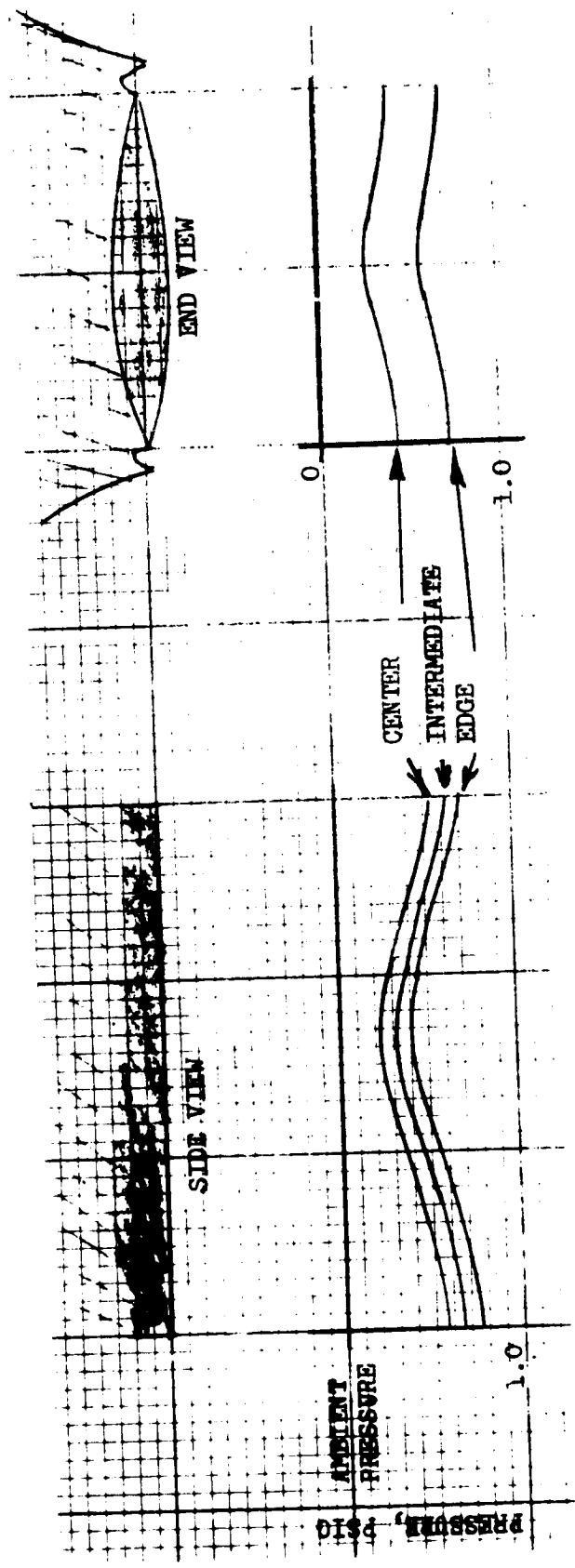


Figure 61. Estimated Base Pressure Profiles

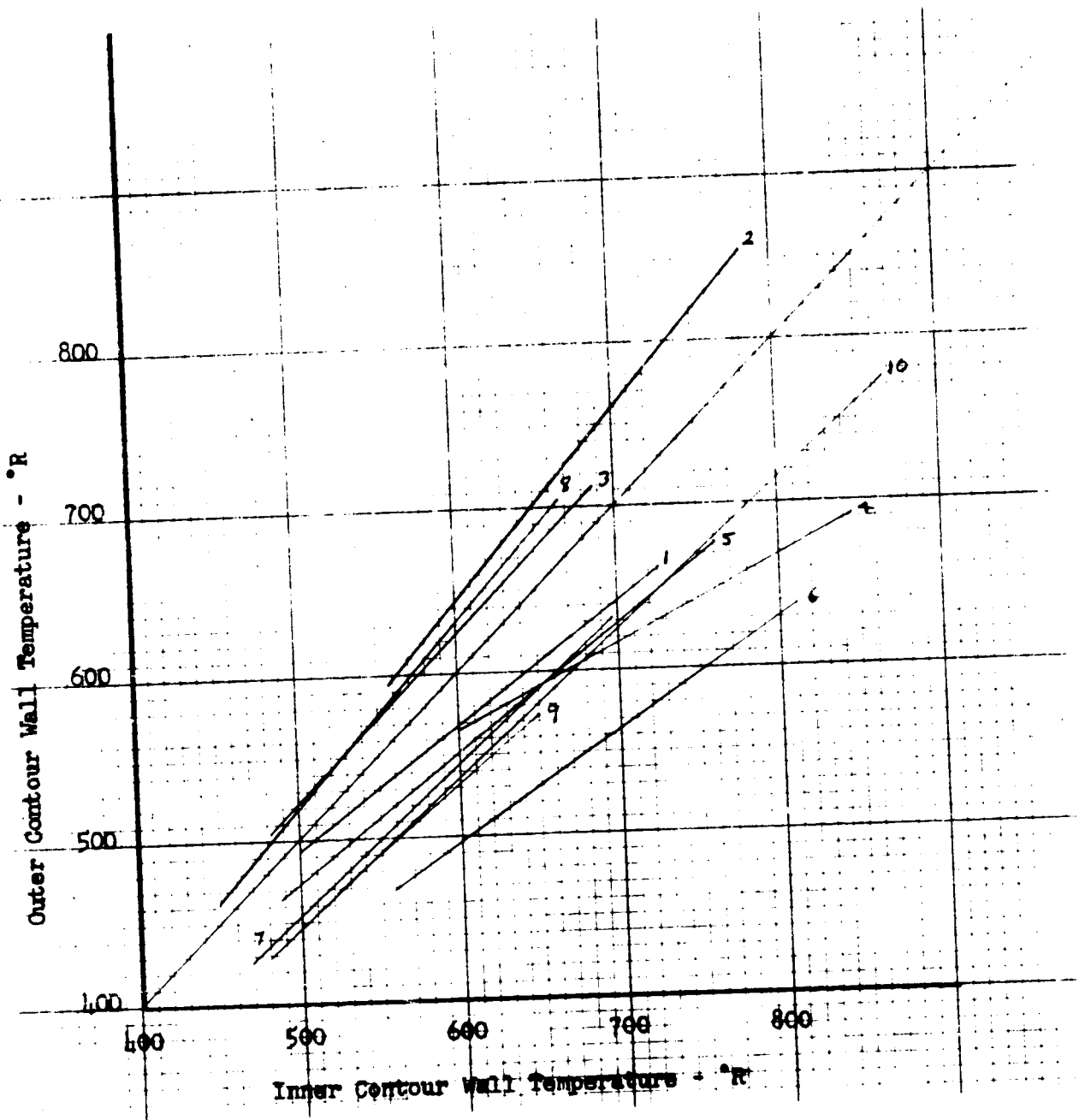


Figure 62. Linear Breadboard No. 1 Combustor Flow Balance Studies, Inner Temperature vs Outer Contour Wall Temperature (Test 016-029)

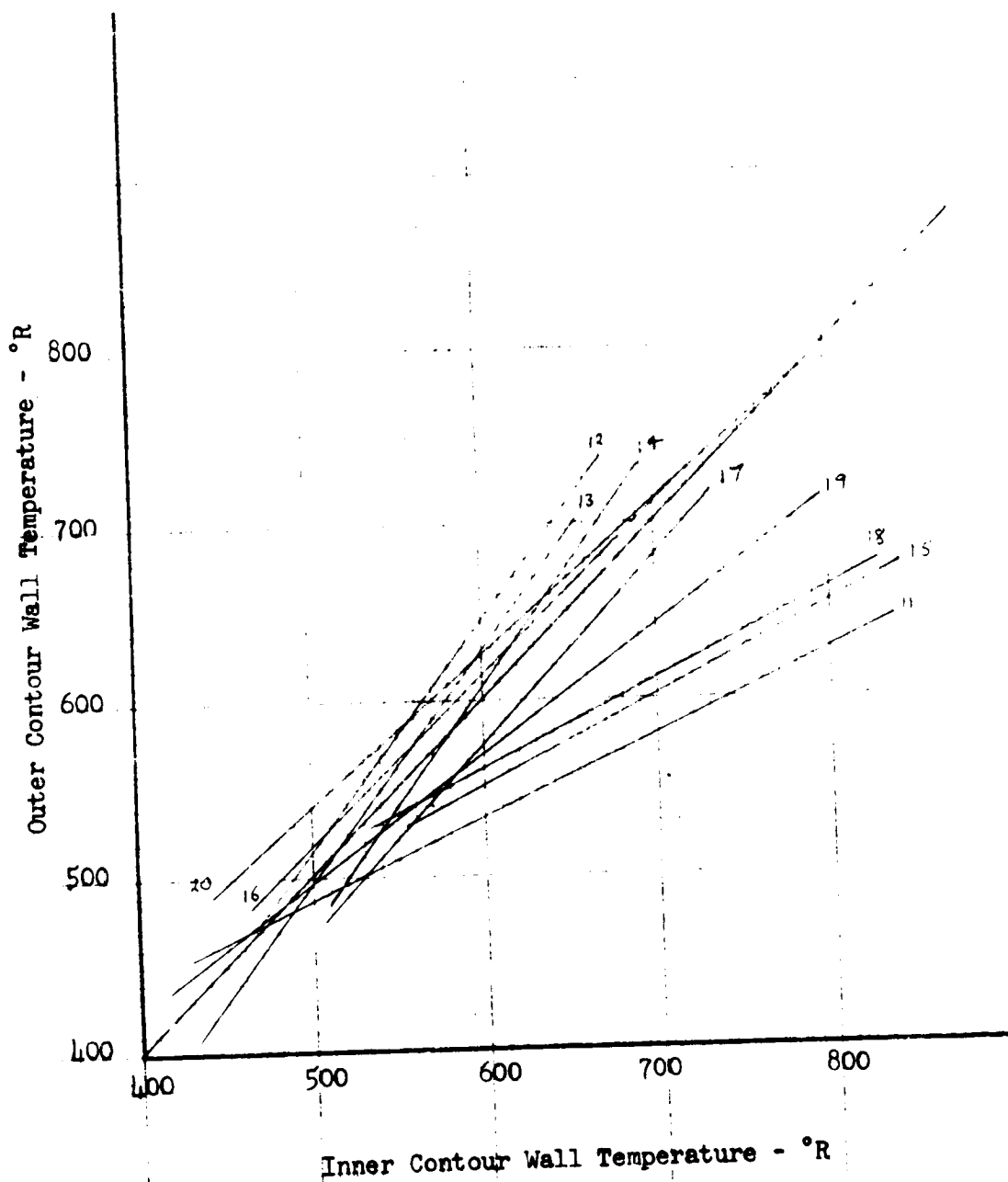


Figure 63. Linear Breadboard No. 1 Combustor Flow Balance Studies, Inner Temperature vs Outer Contour Wall Temperature (Test 016-029)

TABLE 8. COMPARISON OF DESIGN AND TEST OPERATING CONDITIONS

	DESIGN		TEST 029	
	FUEL	OXIDIZER	FUEL	OXIDIZER
PUMP OUT PRESSURE - PSIA	2195	1766	2120	1740
SEGMENT FLOW RATE - LB/SEC.	3.91	23.0	4.3	25.4
FUEL INJECTION TEMPERATURE - °R	633	-	644	-
INJECTION PRESSURE PSIA	1378	1434	1470	1531
SYSTEM ΔP - PSI	971	558	882	502
SYSTEM RESISTANCE (2) - SEC ² /FT ³ -IN ²	24.0	72.4	19.4	54.9
INJECTOR RESISTANCE (2) - SEC ² /FT ³ -IN ²	3.61	28.1	4.85	32.0
CHAMBER PRESSURE - PSIA		1224		1238
SEGMENT MIXTURE RATIO		5.88		5.89
SEGMENT THROAT AREA - IN ²		5.13		(5.57-5.68) ⁽¹⁾
w/A _t - LB/SEC-IN ²		5.25		5.23 ⁽¹⁾

(1) ESTIMATED VALUE AFTER EROSIONS

(2) SINGLE SEGMENT VALUES $\frac{\rho \cdot P}{w^2}$ (INJECTION DENSITY)

HARDWARE DURABILITY

A total of 44 tests was performed on breadboard engine No. 1. Included in this total were 23 mainstage tests, achieving an accumulated mainstage duration of 3113 seconds. Table 9 presents the hardware condition associated with each test.

The initial tests demonstrated the operational and structural integrity of the test bed hardware. Ignition, start, mainstage, and cutoff operations were verified with no serious hardware discrepancies noted. The combustors, injectors, injection elements, igniter elements, turbine exhaust, turbine exhaust base seal, and all structural members exhibited excellent durability. The only hardware discrepancies were associated with the tube wall nozzles, end fences, and the combustor walls. These abnormalities did not preclude achieving the overall test objectives, and are of the type normally encountered during initial testing of a new concept.

The following sections present descriptions of the problem areas with explanation as to cause and the proposed method of correction on future designs.

NOZZLE TUBE DURABILITY

Tube erosion was observed after the initial ignition test (624-001) and was experienced only with the nozzle tubes. Tube erosion was observed on the nozzle tubes adjacent to combustors 1, 2, 3, 8, 9, and 10 on the road side, and combustors 12, 13, 15, 18, 19, and 20 on the flame side. The location of the segments which exhibited eroded nozzle tubes is shown in Fig. 64.

The erosions began 0.25 inch below the tube-to-copper transition interface, and were 0.1 to 0.4 inch in length. Typical tube erosion is shown in Fig. 65. A total of 198 tubes was eroded. Figure 66 indicates the number and location of the eroded tubes with respect to each combustor.

FOLDOUT FRAME

Condition			Comments
Nozzles	End Fences	Turbine Exhaust and Base Seal	
<ul style="list-style-type: none"> Tube crown erosions combustors 1, 2, 3, 8, 10, 13, 15, 18, 19, 20 Tile tubes OK. Slight indication of tube hot spots downstream of zirconium oxide coating. 	No discrepancies	No discrepancies	<p>Tube erosions probably caused by high MR during ignition and cut-off transients. Satisfactory ignition all combustors.</p> <p>Satisfactory ignition all segments.</p>
<ul style="list-style-type: none"> discrepancies 	No discrepancies	No discrepancies	<p>Spin shutoff valve failed to actuate. Spin not achieved. All segments ignited.</p>
<ul style="list-style-type: none"> Slight waves in both nozzles between 1 and 2, 2 and 3, and 4 hat bands 	Two buckles in each end fence	Dents on exit of turbine exhaust	Spin successfully achieved.
<ul style="list-style-type: none"> Waves in nozzle remain unchanged 	Buckles remain unchanged	Dents remain unchanged	Fuel and oxidizer spin not achieved. Test cut due to late ignition detect on combustor No. 12.
<ul style="list-style-type: none"> Dark streak noted on nozzle full length below each witer element. Waves remain unchanged 	Buckles remain unchanged	Dents remain unchanged	Oxidizer and fuel spin achieved. Spin duration not sufficient to achieve combustor oxidizer manifold prime.
<ul style="list-style-type: none"> Wave pattern change. Road side: 2 waves between hat band 1 and 2, 2 between 2 and 3, 1 between gusset 3 and 4. Flame side: 2 waves between hat band 1 and 2, 1 between 2 and 3, 1 between 3 and 4. Slight chipping of zirconium oxide at 3- and 15-inch wide interface 	Buckles same as 006	Dents remain unchanged	Successful ignition and LOX dome prime test.
<ul style="list-style-type: none"> Waves in nozzle same as test 007. Zirconium oxide continues to chip off at 3- to 4-inch interface 	Three buckles in each end fence	Turbine exhaust dents partially straightened out	MOV ramp rate 1.0- second cutoff initiated 600 ms after ECS. Satisfactory bootstrap transition.
<ul style="list-style-type: none"> Same as 008. Zirconium oxide surface chipping noted on 3-inch wide band of casing. 4 combustors on flame side of engine 	Same as 007.	Turbine exhaust dents 90 percent straightened out, base seal die pin inspected; excellent condition	Successful mainstage operation. Mainstage duration 5.1 seconds.
<ul style="list-style-type: none"> Same as 008 	Same as 007	Same as 007	Successful mainstage operation. Mainstage duration 15.1 seconds.
<ul style="list-style-type: none"> Zirconium oxide continues to chip off as described for test 009 	No change	No change	Successful mainstage operation. Mainstage duration 30.1 seconds.
<ul style="list-style-type: none"> Zirconium oxide continues to chip off. New coating on combustors 18, 19, and 20. Extensive chipping. No tube erosion noted on exposed tubes. Posttest nozzle leak check - 13 leaks on flame side, 4 on road side old side of nozzle 	Buckles remain same. Support gussers heat affected; 10 total	No change	Fire in engine compartment. Satisfactory mainstage operation. Mainstage duration 100.1 seconds.
<ul style="list-style-type: none"> Zirconium oxide continues to chip off. No evidence of tube erosion 	Same as 012	No change	Evidence of fire. Posttest nozzle leak check indicated sizeable leak at midsection of flame-side nozzle, 3 hat bands down, mainstage duration 30.1 seconds.
<ul style="list-style-type: none">	Test cut during ignition transient. Failure to detect ignition. Ignition detection system malfunction.
<ul style="list-style-type: none">	Test cut during spin transient. Spin system electrical problem.
<ul style="list-style-type: none"> Zirconium oxide continues to chip off 	No change	External base pressure probes failed. Seven bolt heads popped off on base heat shield	Successful 70.1-seconds of mainstage test.
<ul style="list-style-type: none">	Test cut during ignition phase due to late ignition detection on combustor No. 18.

TABLE 9. BREADBOARD ENGINE NO. 1
POSTTEST HARDWARE
CONDITIONS

FOLDOUT FRAME

Test No.	Test Date	Accumulated		Test Objectives	Test Conditions	Thrust Chamber Average Pressure, psia	Average MR	Ignition Elements	Injector Elements	Combusor Wall Erosions
		Tests	Time							
624-005	1-19-72	18	329.5	Target 200 seconds mainstage test	Same as 012; 5 seconds null 74 seconds maximum Ignition detection circuit on combustors 11, 17, 18, and 19 blocked	983 116?	5.09 5.97	Same as test 003	No discrepancies	All combustors except No. 14 indicate ICW and OCW erosions. Magnitude of erosions range from surface roughness to >0.010-inch deep, 79 percent of erosions on ICW. Erosion more extensive on road side of engine
006	2-4-72	19	329.5	Evaluate ignition characteristics using combustion wave ignition system	12-degree MOV; oxidizer inlet 31 psig fuel inlet 36 psig; 1200 ms LOX lead exit burners inactive	--	--	--	--	--
007	2-9-72	20	329.5	Same as test 006	Same as test 006	--	--	No discrepancies	No discrepancies	No discrepancies
008	2-15-72	21	329.5	Determine if detonation can be prevented by using exit burners and 500-ms fuel lead. Base seal leaks repaired.	12-degree MOV; oxidizer inlet 31 psig, 500-ms fuel lead test cut at sparks on signal.	--	--	No discrepancies	No discrepancies	No discrepancies
009	2-21-72	22	329.5	Evaluate start transient through turbine spin employing combustion wave ignition	12-degree MOV; oxidizer inlet 31 psig; fuel inlet 36 psig; fuel lead 380 ms, exit burners active. Test cut at mainstage control signal	--	--	No discrepancies	No discrepancies	--
010	2-22-72	23	329.5	Same as test 009	Same as 009 except oxidizer and fuel inlet pressure 36 psia	--	--	--	--	--
011	2-22-72	24	329.5	Same as test 009. LOX inlet pressure increased to provide higher ignition phase MR	Same as test 009 except fuel inlet 31 psi, oxidizer inlet 36 psig	180	--	No discrepancies	No discrepancies	No discrepancies
012	2-23-72	25	339.6	Evaluate mainstage operation with combustor wave ignition (10 seconds) following rework of combustor wall erosions. Erosions occurred during test 624-005.	Same as test 011; 5-seconds 700 P _c , 3.5 MR 5-seconds 900 P _c , 4.0 MR	724 899	3.5 4.2	No discrepancies	No discrepancies	Minute surface roughness on all combustors; one minor erosion combustor 12-OCW erosion filed smooth. Thermal cracks in bottom of deep erosions: 1 on combustor 7, 1 on combustor 5, 1 on combustor 6, 3 on combustor 7, 1 on combustor 11; H ₂ bleed through cracks.
013	2-24-72	26	368.7	Same as 012; duration 30 seconds erosion on combustor No. 12 smoothed down	Same as test 012; 5 seconds 700 P _c , 3.5 MR 25 seconds 900 P _c , 4.0 MR	673 916	3.5 4.2	No discrepancies	No discrepancies	One minor ICW erosion combustor 12. General minute surface roughness; no significant change from test 012. Thermal cracks in bottom of deep erosions: 2 on combustor 1, 1 on combustor 5, 2 on combustor 6, 3 on combustor 7, 2 on combustor 11, 1 on combustor 13; H ₂ bleed through cracks
014	2-28-72	27	451.0	Same as 013; target 100-seconds duration. Small leak oxidizer inlet weld repaired. Erosion on combustor 12 smoothed down. Base seal leaks repaired	Same as test 012; 5 seconds null, 700 P _c , 3.5 MR 76 seconds maximum, 900 P _c , 4.0 MR	914	4.3	No discrepancies	No discrepancies	No significant change as a result of test. Minute general surface roughness about the same. No new erosions or thermal cracks.
015	3-8-71	28	451.9	Same as 014; target 500 seconds. Nozzle leaks repaired. Engine compartment deflectors sealed with metal tape. Combustor walls polished	Same as test 012; 5 seconds null, 700 P _c , 3.5 MR 495 seconds, maximum, 900 P _c			No discrepancies	No discrepancies	No change
016	3-10-72	29	671.5	Same as 015	Same as 015 Fuel inlet temperature redline combustors: Combustor 6 160 F 7 90 F 11 60 F 13 70 F 5 seconds, null 5 seconds, 219.6 maximum	917	4.27	No discrepancies	No discrepancies	No new erosions on ICW. Very minute roughness on all combustor walls very minor new erosions: 2 on combustor 1, 1 on combustor 3, 1 on combustor 7, 6 on combustor 8, 1 on combustor 12, 4 on combustor 17, 1 on combustor 18. All erosions very minor and extend through throat except OCW erosions on combustor 7, 17, and 18; no erosion on combustor 6
017	3-16-72	30	898.8	Same as test 016. Combustor walls polished pretest. All oxidizer elements in alignment with new OCW erosions peened. Test facility and fences installed	Same as 016; target-500 seconds; fuel inlet temperature on combustors 2, 6, 17, and 18 redlined at 30 degrees above last data since test 016: Combustor 7 176 F 6 193 F 17 117 F 18 135 F Null 0.3 seconds Maximum 60 seconds Null 154.3 seconds	950 880	4.4 4.1	No discrepancies	No discrepancies	Inner contour walls in about same condition as pretest. Minute wall erosion; OCW erosions noted during 016 slightly deeper on combustor 8; 4 new OCW erosions combustor 1; 1 new OCW erosion combustor 20

FOLDOUT

FOLDOUT FRAME

Test No.	Test Date	Accumulated		Test Objectives	Test Conditions	Thrust Chamber Average Pressure, psia	Average MR	Hardware Condition			
		Tests	Time					Ignition Elements	Injector Elements	Combustor Walls	Nozzle
624-018	3-21-72	31	898.8	Same as 016; target-500 seconds; combustor walls polished; turbine exhaust repaired; base seal repaired; mid-section of flame size nozzle leak repaired; static nozzle transducers installed; base pressure probes repaired	Same as 016; if redline values are achieved, test to be switched to null PU and a new redline established 30 degrees above stabilized null PU; fuel injector temperature noted during test 017	--	--	No discrepancies	No discrepancies	No discrepancies	No discrepancies
019	3-21-72	32	899.05	Same as 018	Same as 018 except oxidizer inlet - 38 psig; fuel inlet - 31 psig	--	--	No discrepancies	No discrepancies	No discrepancies	No discrepancies
020	3-22-72	33	1179.0	Same as 019	Same as 019; null - 5 seconds maximum - 175.5 seconds	755.8 902.6	3.68 4.23	No discrepancies	Dark discoloration around injector fuel cups, random all combustors. No burning or erosion	Slight roughness of OCV and ICW. No new erosions	Large leak at flame side nozzle hot-gas low combustor 1, 2, 9, 10, 11, 19, and 20
021	3-24-72	34	1182.05	Same as 019 evaluation of lower fuel inlet pressure on ignition transient. No exit burners. Nozzle leaks repaired, seal cracks repaired, combustor walls polished	Same as 020 except fuel inlet 27 psig, oxidizer inlet 33 psig. Fuel inlet redline temperatures: combustor 2 190 F 6 205 F 17 125 F 18 150 F	--	--	No discrepancies	No discrepancies	ICW and OCV roughness. No new erosions	Small cracks in tubes 0.5 inch piece below combustor 14, 15, 14, 19
022	3-30-72	35	1682.15	Same as 019. Turbine exhaust and base seal repaired. Combustor walls polished; leak at mid-section of flame side nozzle repaired	Same as 020 except fuel inlet 31 psig, oxidizer inlet 38 psig: 10-second null PU 10- to 20-second minimum PU 20- to 321-second maximum PU 371- to 500-second null PU	888 793	4.2 3.84	No discrepancies	No discrepancies	General ICW OCV roughness. No new erosions	Nozzle leak on gas side of flame side nozzle. Shielding block change in nozzle on hot-gas side
023	4-3-72	36	2182.25	Same as 019	Same as 022: 10-second null PU 10- to 20-second minimum PU 20- to 175-second maximum PU 175 to 500.1 null PU	761 897 841	3.67 4.2 3.8	No discrepancies	No discrepancies	General ICW OCV roughness; slight increase in erosion depth of existing erosions.	No discrepancy pressure probe increase in nozzle tube crack
024	4-11-72	37	2454.25	Evaluate performance and durability at 1050-psi P _c , 5.0 MR; combustor walls polished; turbine exhaust weld repaired	Same as test 023: 0- to 10-second null PU 10- to 20-second maximum PU 20 seconds + 225 null PU 225 to 272 minimum PU	1024 945 812	5.18 4.8 4.2	No discrepancies	No discrepancies	Leak in fuel EB weld combustor 13. Combustor wall roughness more severe at higher P _c and MR. No new erosions	Two nozzle probe hat band 2, 4, 10 failed; crack on nozzle between 5, and 6. No below combustor and 20 slight
025	4-17-72	38	2454.25	Same as 024; combustor walls polished; nozzle pressure probes repaired; end fence cracks brazed; pressure transducer installed on seal near combustor 10	Same as 024, except oxidizer inlet 39 psig, fuel inlet 36.4 psig	--	--	--	--	--	--
026	4-17-72	39	2454.25	Same as 025	Same as test 025	--	--	--	--	--	--
027	4-17-72	40	2454.25	Same as 025	Same as test 025	--	--	--	--	--	--
028	4-19-72	41	3046.75	Same as 025; combustor walls polished	Same as 024: maximum PU nominal PU	1055 884	5.24 4.57	No discrepancies	No discrepancies	Surface roughness ICW and OCV	Leak on cold flame-side bands 3 and crease in combustors 18, 19, and
029	4-24-72	42	3061.85	Determine performance and hardware durability at 1250-psi P _c , 5.5 MR combustor walls polished, 1/3 of base plate replaced; two flush-mounted base pressure transducers installed, end fence gussets repaired	Same as 024 except oxidizer inlet 40 psig, fuel inlet 30 psig: 5-second null 10.1-second maximum	1124 1248	5.4 5.9	No discrepancies	No discrepancies	New minor erosions noted on OCV: combustor 2 7 erosions 3 3 4 1 7 1 8 5 11 7 16 2 19 2 20 12	No discrepancy
030	5-23-72	43	3064.45	Test stand duration test at 900-psi P _c and 4.0 MR. Combustor walls polished pretest. Temperature sensitive paint installed on turbine exhaust base and base seal	Same as 029; oxidizer inlet-40.9 psig, fuel inlet-29.6 psig; combustor fuel inlet temperature redlines combustor 2 180 F 6 205 F 17 125 F 18 178 F	--	--	No discrepancies	No discrepancies	Slight increase in surface roughness. No new erosions noted	No discrepancy
031	5-23	44	3114.1	Same as 030; combustion walls not polished post-test 030	Same as test 029: maximum PU	907	4.3	No discrepancies	No discrepancies	Surface of combustor walls rough; no new erosions noted	Numerous low combustor 12, 13, 14 and 20. progressive test 624-

FOET 2 NAME

TABLE 9. (Concluded)

Hardware Condition				Comments
Combustor Walls	Nozzles	End Fences	Turbine Exhaust and Base Seal	
Cracks	No discrepancies	No discrepancies	No discrepancies	Test terminated during ignition phase. Combustor 14 indicated late ignition.
Cracks	No discrepancies	No discrepancies	No discrepancies	Test termination at mainstage control signal + 0.250 second due to re-establishment of gas generator igniter break links continuity.
Thickness of OCW and Erosions	Large leak at mid-section of flame side nozzle cold side. Nozzle hot-gas side leaks below combustor exit. Combustors 1, 2, 9, 10, 12, 13, 14, 18, 19, and 20	Small leaks at fence nozzle interface combustor 10-3, combustor 20-2	Numerous seal cracks, 17 total, miter corner, crack combustor 11	Test terminated at 280.5 seconds due to drop in flame bucket coolant pressure caused by burned through instrumentation lines. Lines burned by fire in engine compartment on flame side.
Roughness. No	Small cracks noted in nozzle tubes 0.5 inch from transition piece below combustor 12, 13, 14, 15, 18, 19, and 20	No change	Explosion in base turbine exhaust; orifice plate pulled away from end plate on AS side. Numerous cracks in orifice plate and base seal. Seal deformed base; pressure probe No. 2 damaged	Test termination at 2.5 seconds due to fuel inlet redline pressure. Redline not set at proper level compatible with 27-psig fuel inlet pressure. Explosion in base area due to fuel accumulation. No exit igniters.
OCW roughness. Erosions	Nozzle leak mid-section cold-gas side of flame-side nozzle. Shielding blown away. No change in nozzle tube cracks on hot-gas side	No change	Dents and tears in base orifice plate. Base seal had numerous leaks at miter corner on combustor 1 and 10	500.1-second duration. Ran at null PU from 371 to 500 seconds to conserve fuel supply.
OCW roughness; Increase in erosion; Existing erosions.	No discrepancies. One nozzle pressure probe failed. Slight increase in magnitude of nozzle tube cracks below combustor	No change	All base pressure probes except No. 6 failed. Turbine exhaust plate pulled away from structure on flame side.	500.1-second duration. Combustor No. 18 exceeded redline fuel injector temperature; at 175 seconds PU changed to null. No evidence of fire in engine compartment.
EB weld comb. Combustor wall more severe at and NR. No new	Two nozzle pressure probes on hat band 2, and 12 on hat band 10 failed; copper flame sprayed on nozzle below combustor 1, 5, and 6. Nozzle tube cracks below combustor 14, 18, 19, and 20 slightly increased	Tube splits noted in fence tubes adjacent to nozzle at combustor 1, 10, and 20. Cracks in end fence gussets	Numerous small leaks. No cracks	Test terminated at 272 seconds by erroneous automatic fuel turbine inlet overtemperature. No evidence of engine compartment fire. At 225 seconds, combustor 18 fuel injector temperature redline exceeded switch to minimum PU
	--	--	--	Test terminated during start transient; no spin; combustors 12, 14, 16, 17, 18, late ignition detect.
	--	--	--	Terminated prior to spin; combustor 18 late ignition detect.
	--	--	--	Terminated prior to spin; spark system did not work
Roughness ICW and OCW	Leak on cold-gas side of flame-side nozzle at top hat bands 3 and 5. Slight increase in tube splits below combustors 12, 13, 14, 15, 18, 19, and 20	End fence gusset cracked	Turbine exhaust base orifice plate had extensive cracking midsection	Test terminated at 592.5 seconds test stand duration; fire in engine compartment flame side of engine; combustor 18 exceeded redline switch to PU - 180 seconds minimum PU - 760 seconds
Erosions noted on	No discrepancies	Tube splits in end fences at nozzle interface	No discrepancies	Program test - 15.1 seconds mainstage termination.
or 2 7 erosions 3 3 4 1 7 1 8 5 11 3 16 2 19 2 20 12				
Increase in surface No new erosions	No discrepancies	No discrepancies	No discrepancies	Test terminated at 2.6 seconds by erroneous automatic fuel inlet temperature redline
of combustor walls No new erosions noted	Numerous cracks in nozzle below combustor 1, 2, 9, 10, 12, 13, 14, 15, 17, 18, 19, and 20. Cracks have become progressively larger since test 624-021	No discrepancies	No discrepancies. Temperature-sensitive paint indicates turbine exhaust orifice plate - 600 F	Test terminated at 49.6 seconds due to turbopump power decay. Last test on engine. Total number of tests - 44 Total mainstage tests - 23 Total mainstage accumulated duration - 3114.1 seconds

R-9049
138

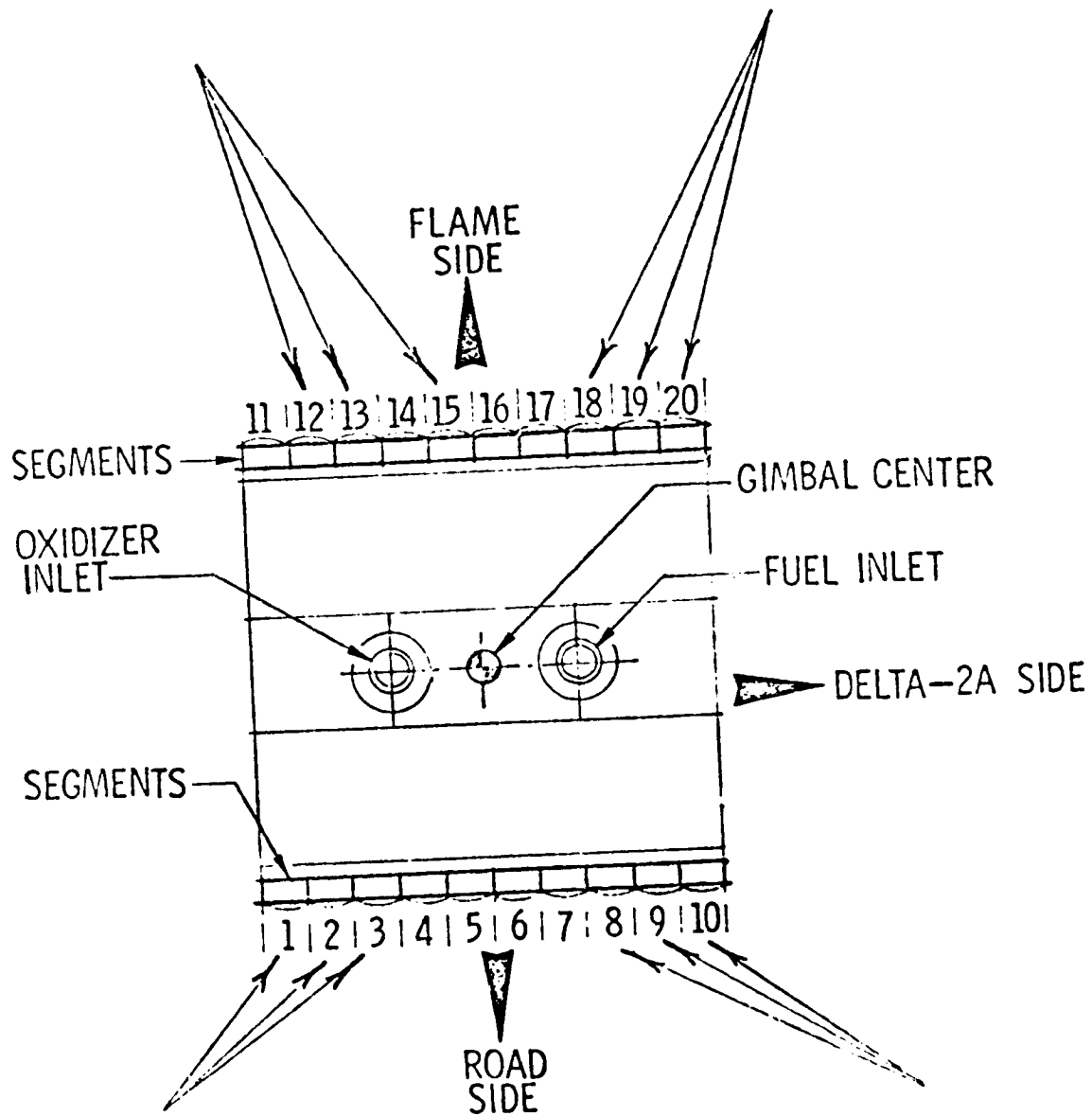
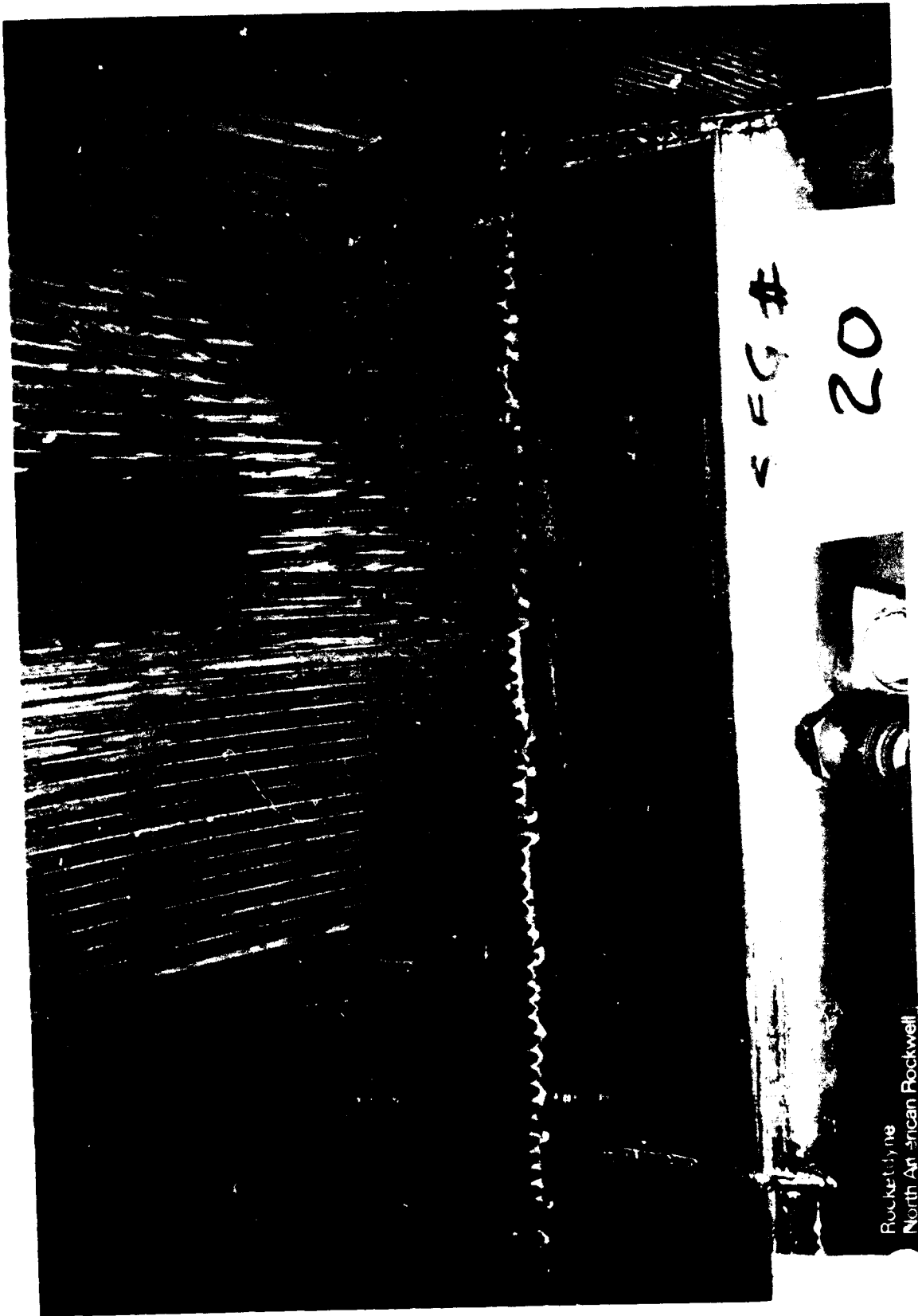
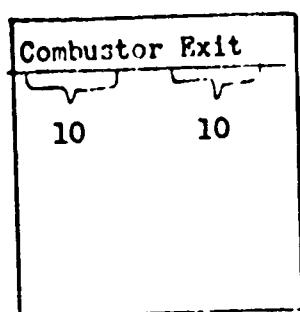


Figure 64. Location of Segments Which Exhibited Eroded Nozzle Tubes

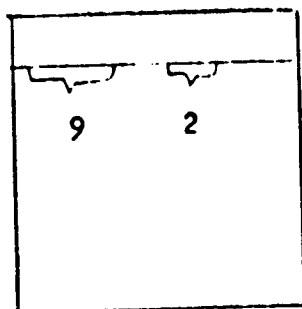


1XZ35-9/17/71-SIJ*

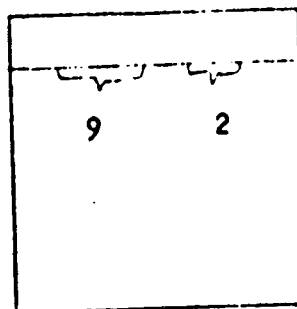
Figure 65. Typical Tube Erosion (Posttest 623-001)



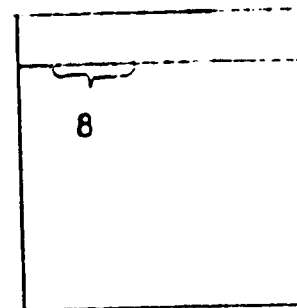
Segment No.1



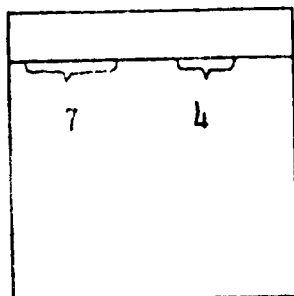
Segment No.2



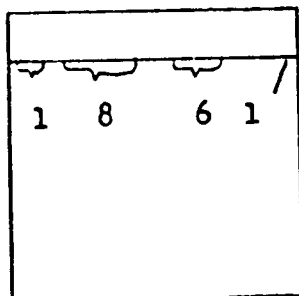
Segment No.3



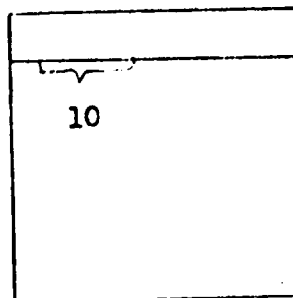
Segment No.8



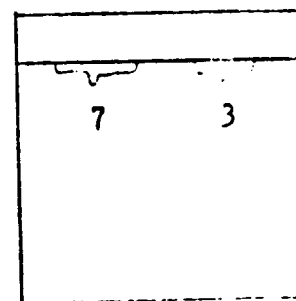
Segment No.9



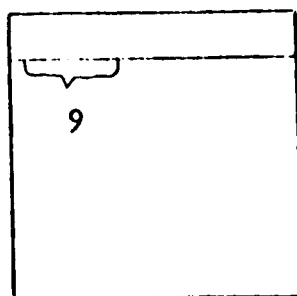
Segment No.10



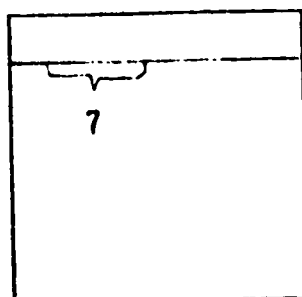
Segment No.12



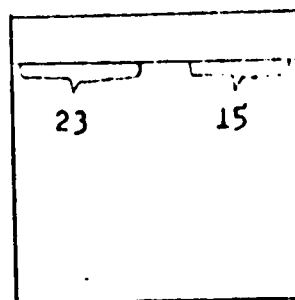
Segment No.13



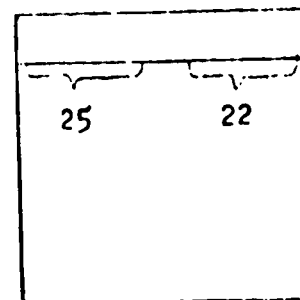
Segment No.15



Segment No.18



Segment No.19



Segment No.20

Figure 66. Number and Location of Eroded Tubes

The tubes in the center of each combustor (four to six tubes) were not eroded, with the exception of combustor 12. The highest concentration and greatest magnitude of erosion were associated with combustors 18, 19, and 20. A large percentage of the tubes which were not eroded exhibited discoloration. Downstream of the erosion, the nozzle was in excellent condition.

Following test 001, all eroded tubes were weld repaired and the nozzles coated with zirconium oxide 0.015-inch thick from the weld of the combustor transition piece to a line 3 inches aft (Fig. 67). The coating was added to provide protection while safe start and cutoff transients were being developed.

During the second ignition test, an extended fuel cutoff and a lower mixture ratio start transient was employed to eliminate nozzle erosion. No tube erosion was noted on subsequent tests.

The nozzle tubes immediately downstream of the zirconium oxide coating, and in alignment with the dark streak on combustor No. 2, exhibited slight overheating. The combustors on the flame side did not exhibit streaking. A slight amount of surface chipping was noted on the leading edge of zirconium oxide on both sides. The degree of chipping was not considered significant. Following test 624-002, the zirconium oxide coating was extended to a point 18 inches below the transition piece weld.

During subsequent tests (624-003 through 624-013), chipping and flaking of the zirconium oxide was progressive. Figure 68 illustrates typical coating surface chipping. In numerous locations, the coating was completely chipped off exposing the nozzle tubes. No evidence of tube wall erosion was noted, indicating the start and cutoff sequence modifications incorporated were successful in preventing tube damage.

Following test 624-012 (a 100-second mainstage test), a helium leak check indicated several leaks on the cold side of the nozzle, principally on the flame side. Approximately 30 percent of the leaks were in the region of the braze joint between the



IXZ35-9/29/71-SIA*

Figure 67. Initial 3-Inch-Wide Zirconium Oxide Coating Prior to Test (625-002)



IXZ25-11/23/71-SIF*
Figure 68. Typical Nozzle Zirconium Oxide Coating Chipping

two sections of the nozzle. The remaining leaks were adjacent to the fences, where the cracks in the end tubes were circumferential. Numerous attempts to repair the leaks at the center braze joint were not successful due to difficulty in determining the exact location of the leaks.

A fire was noted in the engine compartment during six of the mainstage tests. They were attributed to hydrogen leakage on the cold-gas side of the flame side nozzle.

The cracks are attributed in part to stresses imposed during assembly. The joints at the center and ends did not fit properly, requiring clamping and hand fitting. The joint clearances were excessive and stresses were induced in the joints by the straightening of the distortions from the furnace brazing. Further stresses are introduced by the thermal gradients during test, particularly at the water-cooled end fence attachment to the hydrogen-cooled nozzle where a large thermal gradient is present.

Improvements in the straightening and fitting of the nozzle sections at the center and end joints should eliminate the stresses and prevent the leakage encountered. Reinforcements are planned for test bed No. 2 on the end tubes at the hat band joint.

Following test 624-017 (16 March 1972), numerous small leaks were noted on nozzle tubes below combustors 10, 11, 12, 13, 17, 18, 19, and 20. The small leaks, detected by pressurization of the nozzle tubes with helium, were located approximately 0.25 inch below the copper transition piece.

This is the same location where the tubes were weld repaired following the initial ignition test. No evidence of tube cracks could be seen. The zirconium oxide remained intact over the leakage areas. As the test program progressed, the tube leakage became increasingly widespread and more severe. Following test 624-021, visible cracks were noted in the zirconium oxide exposing the tube circumference and longitudinal cracks.

END FENCE DURABILITY

Buckling of the end fence was first noted after test 624-004. Each fence was buckled approximately 20 inches below the combustor exits. Figure 69 shows a typical fence illustrating the buckling.

Following test 624-005, the fences were straightened and the gussets slotted to provide increased flexibility and, therefore, increased ability to accommodate thermal strain. The buckling reappeared and remained essentially unchanged during the subsequent tests with no operational or functional problems noted.

The water-cooled fences on test bed No. 1 do not represent a finalized design of a hydrogen-cooled fence of the type that would be used on an operational engine. Since the fence in the buckled condition performs its function, no further work to preclude the buckling was performed.

Following test 624-020 small cracks in the end fence tubes interfacing with the nozzle were noted on the fences below combustor 10 and 20. The cracks were weld repaired. Cracks were noted again following tests 624-024 and 624-029. The cracks are thought to be caused by thermal fatigue associated with the large temperature difference between the tube wall nozzle and the end fences.

INJECTORS AND IGNITER ELEMENTS DURABILITY

No abnormalities were noted with respect to the injector faces or injection elements. Following the initial mainstage test, the tips of igniter elements in combustors No. 2 and 8 exhibited slight tip erosion. The condition did not appear to increase as a result of the subsequent mainstage tests, and does not appear to warrant corrective action.



IXZ25-11/19/71-S1E

Figure 69. End Fence Buckling

R-9049

147

NOZZLE ASSEMBLY DURABILITY

Test 624-004 was the first test during which the tube-wall nozzle was exposed to an extended chill. Fuel pump spinup was accomplished on this test. Ripples in the nozzle were observed posttest. Three distinct ripples were noted in both nozzles, located between the first four hat bands below the combustor exits. Following test 624-007 (the first LOX dome prime test), the ripples increased slightly. The condition did not change significantly during the remainder of the program. Figure 70 illustrates the nature of the nozzle ripples.

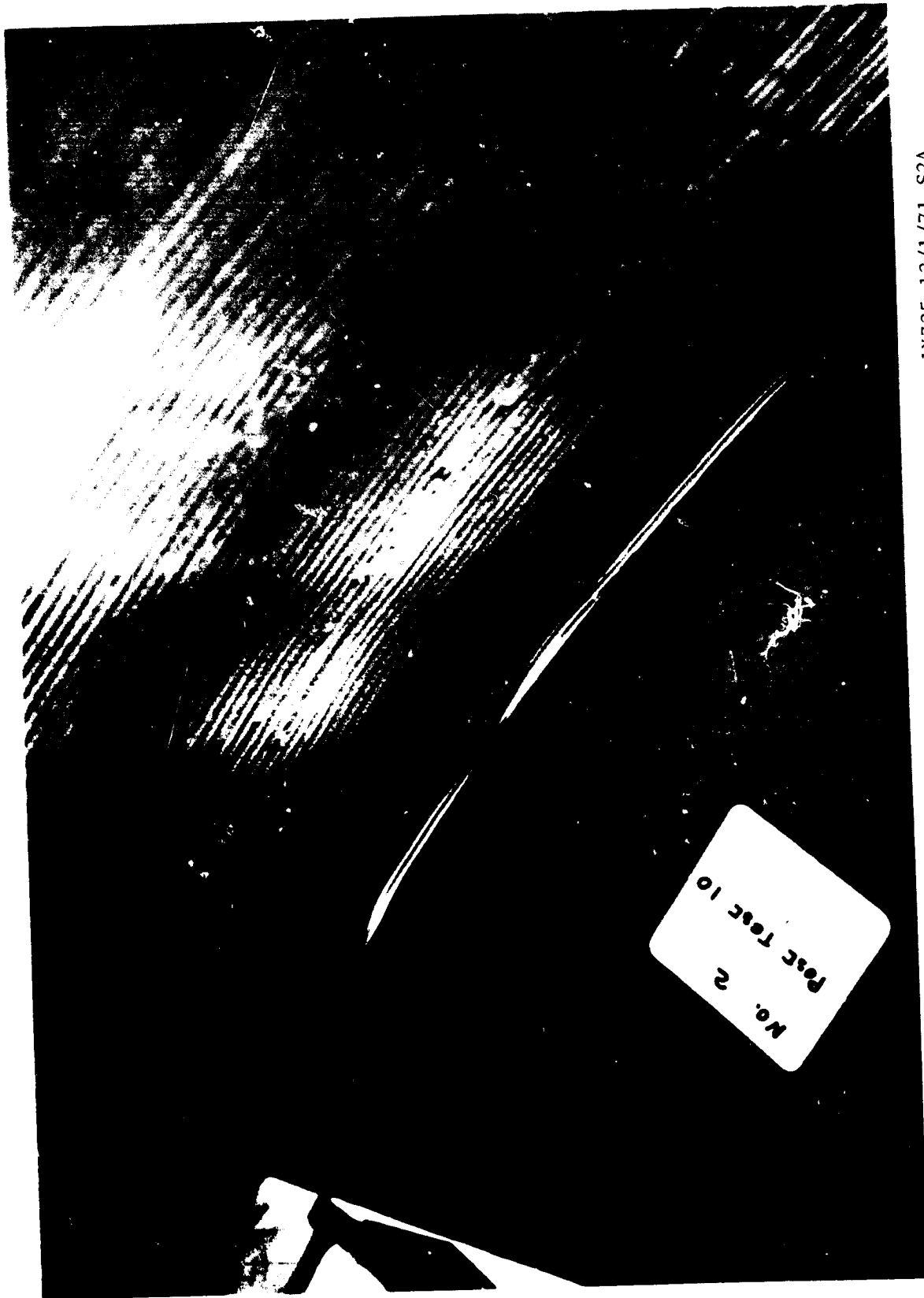
The thermal gradients in the tube from the hot to cold side induce stresses beyond the yield point. The residual stresses produced caused the tube to bow in the manner observed.

An increase in the tube cross section to provide an increased area moment of inertia of the tube is believed necessary in future nozzles to prevent the ripples. The tubes did not bow immediately adjacent to the combustor where the thermal gradient is most severe. This section of the tube is dimpled on the back side to increase coolant velocity. A wire is brazed in the dimple, thus providing a significant increase in the cold side resistance to bending.

TURBINE EXHAUSTS AND BASE SEAL DURABILITY

The turbine exhaust and the base seal have performed their intended function, exhibiting no serious abnormalities. The turbine exhaust orifice plate has exhibited dents and subsequent cracking as a result of thermal cycling. The dents did not present a problem relative to operation.

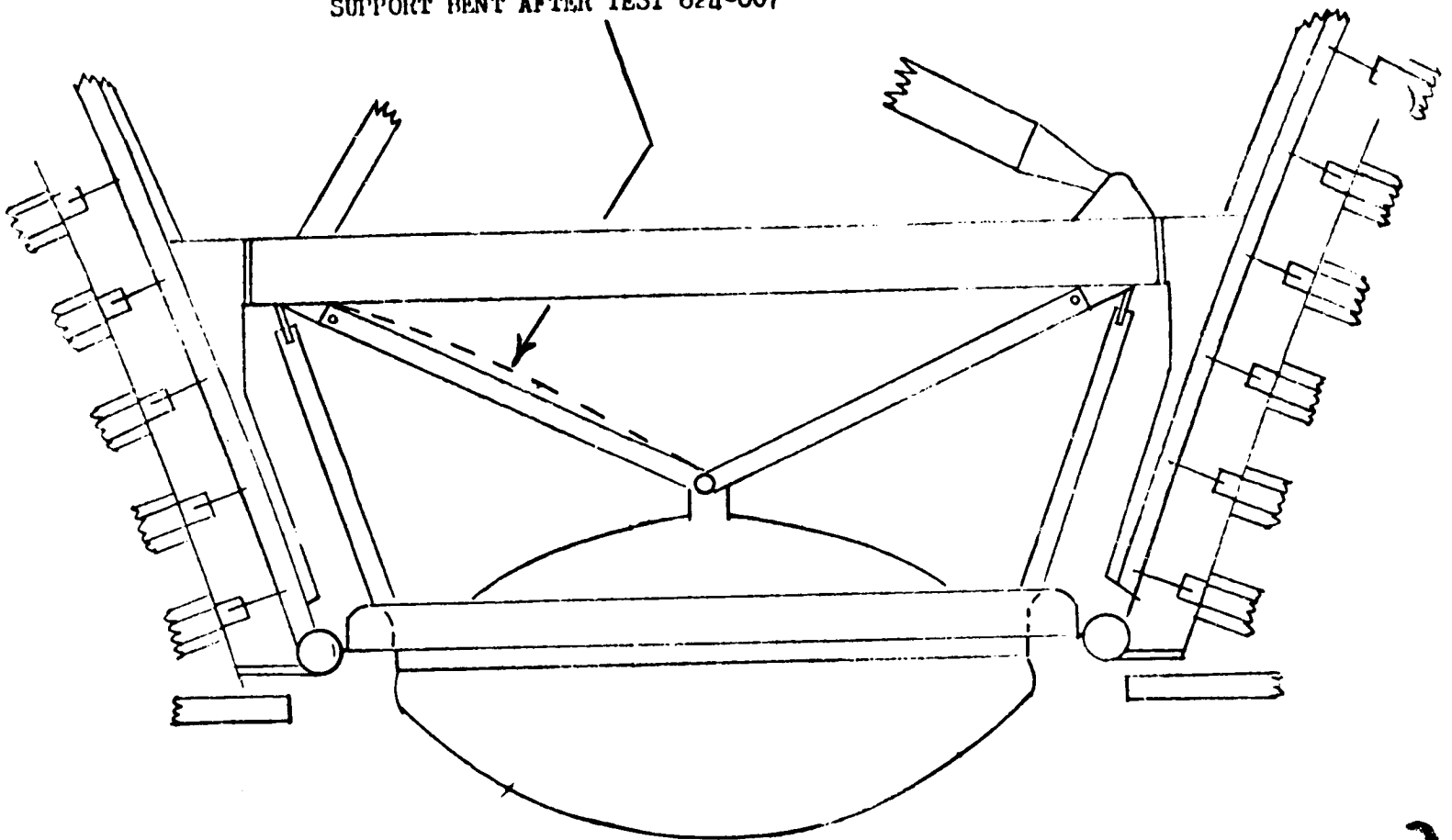
During an experimental ignition-only test (test 624-007), an open-air explosion occurred below the engine, producing deformation of both the turbine exhaust orifice plate and the base seal. The turbine exhaust orifice plate exhibited large dents with sharp radii. The base seal was deformed due to overpressure causing numerous cracks. The explosion also moved the complete turbine exhaust upward approximately 0.5 inch, bending the support members. Figure 71 illustrates the damage noted.



IXZ25-12/1/71-S2A

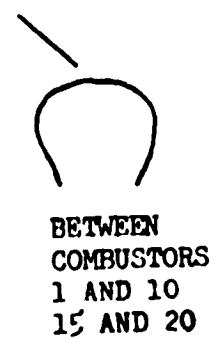
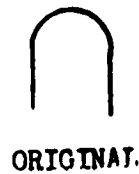
Figure 70. Nozzle Tube Wall Ripples (Posttest 624-010)

TURBINE EXHAUST MANIFOLD
SUPPORT BENT AFTER TEST 624-007



CRACKS AND TEARS DEVELOPED IN BASE CLOSURE SHEET
AFTER TEST 007 REQUIRING REPAIR AFTER MOST
SUBSEQUENT TESTS. TEST 028 LARGE SECTION WAS
RIPPED. NEW BASE CLOSURE SHEET WELDED IN PLACE.

AFTER TEST
624-007



BASE SEAL CROSS SECTION

Figure 71. Turbine Exhaust and Base Seal Damage Following
Test 624-007

The base seal cracks were weld repaired. No effort was made to remove the turbine exhaust dents or to straighten the support members. As a result of subsequent tests, numerous cracks were noted in both the seal and the exhaust orifice plate. These were weld repaired. Another explosion occurred in the base area during test 624-021, another experimental start sequence test. The magnitude and extent of the seal and turbine exhaust damage increased. As the test program progressed, cracking in the orifice plate and seal progressed. Following each test, the cracks were weld repaired. After test 624-029, the cracks in the turbine exhaust orifice plate were not repairable. Approximately 30 percent of the plate was replaced. No further orifice plate problems were encountered during the remaining two mainstage tests.

COMBUSTOR EROSION

Test 624-005 was conducted on January 19 for a duration of 78 seconds at an average chamber pressure of 1170 psi at a 5.6 engine mixture ratio. During this test, significant erosions occurred on all but 1 of the 20 combustors. The erosions required approximately 2 weeks of hand smoothing (polishing) repairs. The experience of test 005 and its background is discussed to delineate the underlying causes and significance of the damage experienced. The effects on subsequent testing and their results are summarized.

In an attempt to delineate the cause for the combustor erosions, the most enlightening description comes from observations of differences from the multisegment testing to the breadboard testing. Table 10 is a summary of the major differences believed to contribute to the onset of erosions, a discussion of which follows. The start transient of the test bed lasts 4 to 5 seconds and transits from a low mixture ratio during ignition to a high mixture ratio in mainstage. The fuel injection velocity of the test bed was about 20 percent higher than the multisegment due to higher injection temperatures and a lower mixture ratio. The heat flux and wall temperature of the multisegment closely follow expected values. The heat flux and wall temperature parameters on the test bed increase with the number of tests and test duration if the wall surface finish is not maintained by a smoothing

TABLE 10. DIFFERENCES OBSERVED IN THE BREADBOARD ENGINE VERSUS COMPONENT TESTING

	Component and Multisegment	Breadboard No. 1
Start Transient	Very Rapid Pressure Stand	4 to 5 second pump fed; low to high MR
Material	$O_2 = 40$ to 80 ppm	$O_2 = 50$ to 650 ppm
Erosion	1 Coolant Channel Width	Injection element alignment - 3 to 4 coolant channels
Heat Flux Parameter	Unchanging	Increases if wall condition not maintained
Fuel Velocity	1250 ft/sec	1650 ft/sec
Element Mixing Tests - Transient	Not Applicable	Percent mass in outer zone above injected MR = 8.0
Measured η_{c*}	$\eta_{c*} = 96.5$	$\eta_{c*} = 98.5$

operation. Cold-flow element mixing tests indicate the injector elements produce a high mixture ratio combustion zone next to the combustor walls during the thrust buildup from LOX dome prime to mainstage. Evidence from the movie coverage indicates some form of copper oxidation during the start transient. The NARloy material oxygen content was significantly higher than that of the multisegment hardware. The erosions on the test bed combustors were approximately 0.3 inch in width compared to the multisegment erosions which were approximately 0.100-inch wide.

Data studied and evidence in the form of hardware condition and types of erosions would indicate the injector to be the primary cause of the combustor erosions. The most probable mechanism is chemical reduction of the combustor interior surface material by the hydrogen-rich environment during ignition followed by oxidation during the LOX dome prime and transition to mainstage.

The oxidation is caused by the injector element mixing characteristics described above. The surface produced by this type of reaction would be porous, the surface roughness gradually increasing depending on the amount of reaction that has taken place. This surface layer would exhibit a low thermal conductivity, thus tending to increase the wall surface temperatures. This surface roughness condition, once produced, would tend to be aggravated by the mainstage operating conditions. Local hot spots would appear and deterioration would be progressive with time. The single-element mixing test indicate that significantly higher mixture ratios would be present near the combustor walls at the mainstage steady-state injection conditions of the engine compared to the multisegment operating conditions at chamber pressures near 900 psia. This condition would further aggravate the progressive roughening of the combustor wall in mainstage.

The combustor material oxygen content could contribute to accelerating the oxidation reduction of the combustor walls by providing a source of oxygen within the material.

Description and Characteristics of Combustor Erosions

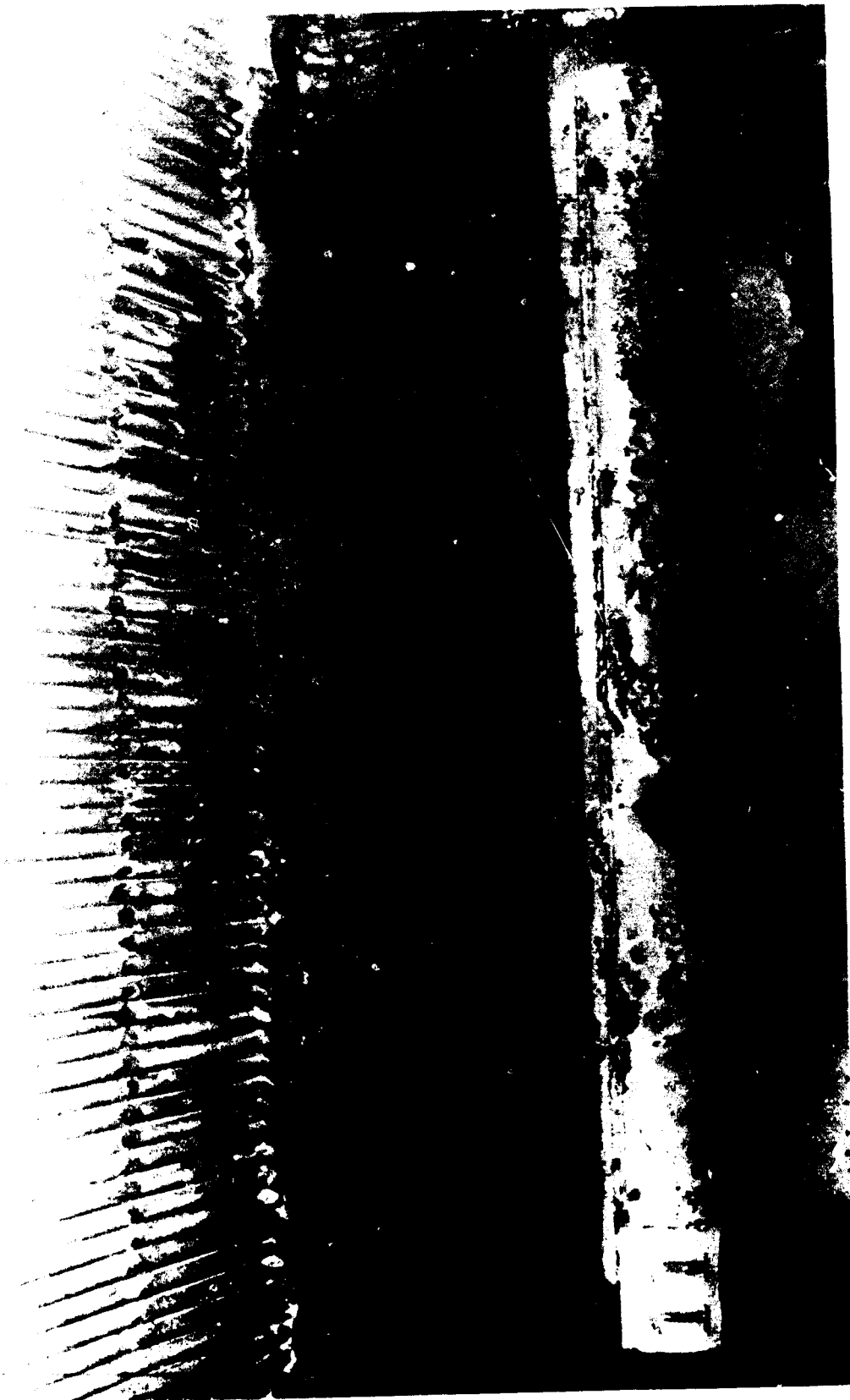
Approximately 80 percent of all major erosions were on the inner contour walls. All erosions noted on the outer contour were minor, in many instances surface roughness only. A photograph of the combustor exhibiting the most excessive erosion is shown in Fig. 72.

Repairs performed on the combustor erosions consisted of removal of roughness with flat files and emery cloth. Figure 73 indicates the cross section of a typical erosion before and after repair. The raised section on each side of the erosions was removed and the roughness in the bottom of each erosion was smoothed out. Care was taken to remove as little material as possible. The effort to remove the roughness in the bottom of the deep erosions in combustor No. 13 resulted in exposure of the internal flow channels in two places.

A test by test description of the erosions observed and repairs performed are summarized in Table 11. Tables 12 and 13 summarize the general nature, number, and magnitude of erosions present posttest 005 and 031 following the completion of testing.

A significant difference exists in the erosion characteristics observed in the breadboard combustors as compared to those observed on component and multisegment testing. Figure 74 shows the general nature of the breadboard combustor erosions progressing from a typical surface roughness in line with the injector element to a minor erosion starting approximately 2-1/2 inches upstream of the throat but not extending through the throat plane. A large erosion will extend through the throat for a distance of approximately 1/2 inch. The erosion will be approximately 0.3 inch in width which encompasses 3 to 4 combustor coolant channels.

Figure 75 displays schematically a comparison of a typical breadboard erosion with a typical erosion observed in the multisegment. Erosions in the breadboard and multisegment were in alignment with injector elements. The multisegment erosion was approximately 0.100 inch in width, implying an association with the coolant channels with a spacing of 0.100 inch.

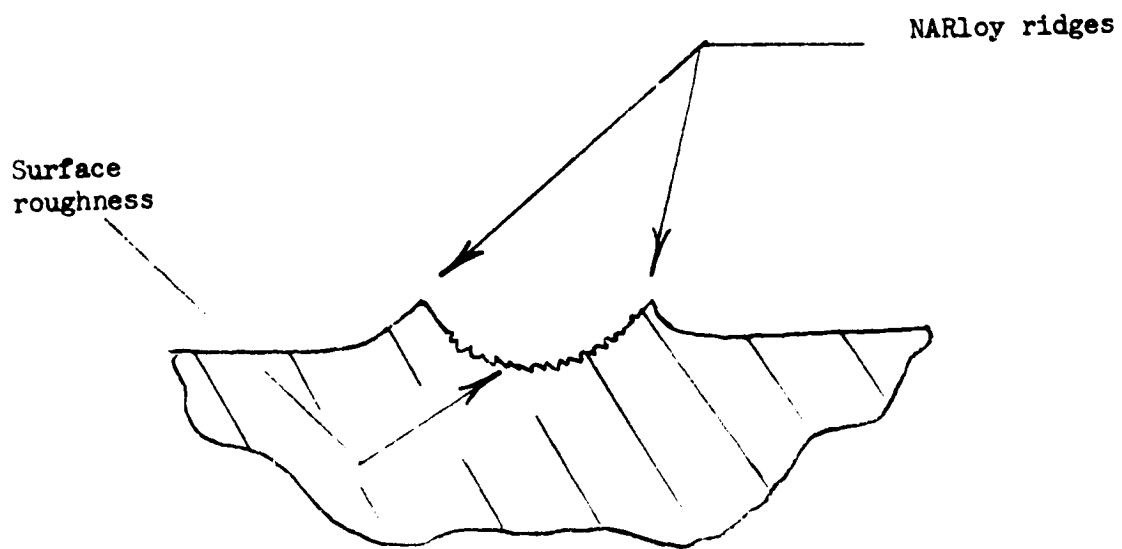


1XZ35-1/26/72-S1A

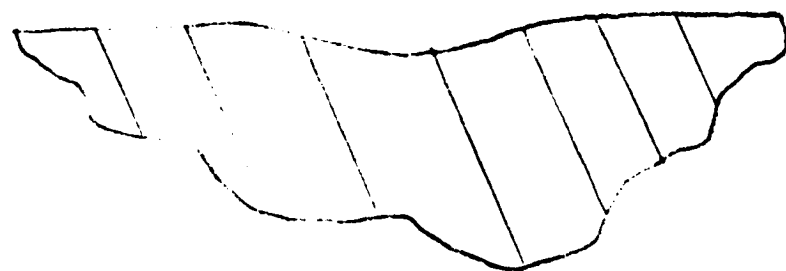
Figure 72. Combustor Erosion

R-9049

155



Cross Section Typical Erosion Prior to Rework



Cross Section Typical Erosion Following Rework

Figure 73. Combustion Erosion Rework

TABLE 11. BREADBOARD ENGINE NO. 1 MAINSTAGE TEST COMBUSTOR EROSION SUMMARY

Mainstage Test No.	Test Date	Duration, seconds		Average Combustion		MR	Combustor Wall Condition
		Test	Cum.	Time, seconds	Pc, psia		
624-009	11-19-71	5	5	5	808	3.39	Very slight surface roughness located downstream of oxidizer elements on all combustor walls
624-010	11-29-71	15	20	10	991	4.08	Very slight increase in condition noted on test 009
624-011	12-2-71	30	50	20 10	1014 1127	4.51 4.95	Very slight increase in condition noted after test 009 and 010
624-012	12-8-71	100	150	10 65 15	1021 1130 1020	4.58 4.98 4.58	Three small erosions noted ICW Combustor 6; 1 small erosion ICW combustor 11. All erosions in alignment with outer row oxidizer elements. Erosions smoothed out. Oxidizer elements peened to reduce oxidizer flow. Very slight increase in general wall roughness noted.
624-013	12-21-71	30	180	20 10	810 907	3.61 4.00	No change in erosions combustors 6 and 11. One small erosion combustor 17. Outer contour wall condition slightly rougher.
624-003	1-13-72	70	250	20 20 20 10	809 923 681 812	3.59 3.99 3.17 3.61	Very slight increase in magnitude of erosions on combustors 6, 11, and 17. One small erosion combustor 20. Slight increase in general surface roughness
624-005	1-19-72	79	329	5 74	983 1163	5.09 5.97	All combustors except No. 14 indicate ICW and OCW erosions. Magnitude of erosions range from surface roughness to 0.010-inch deep. 79 percent of erosions on ICW; erosions most severe on combustors 1, 5, 6, 7, 8, 11, 12, 13, and 20. All erosions smoothed out with file and emery cloth.
624-012	2-27-72	10	339	5 5	724 899	3.50 4.20	One minor erosion combustor 12 OCW. General minute surface roughness all combustors. Cracks bottom deep erosions: 1 on combustor 1, 1 on combustor 5, 1 on combustor 6, 3 on combustor 7, and 1 on combustor 11.

TABLE 11. (CONTINUED)

Mainstage Test No.	Test Date	Duration, seconds		Average Combustion		MR	Combustor Wall Condition
		Test	Cum.	Time, seconds	P _c , psia		
624-013	2-24-72	30	369.0	5	673	3.50	One minor ICW erosion combustor 12. General minute surface roughness all combustors. No significant change from test 012. New thermal cracks, bottom deep erosions: 2 on combustor 1; 1 on combustor 5, 2 on combustor 6, 3 on combustor 7, 2 on combustor 11, 1 on combustor 13
				25	916	4.20	
624-014	2-28-72	81	450.0	5	915	4.29	No significant change as a result of test. Combustor walls polished posttest
				76			
624-015	3-8-72	0.9	450.9	219.6	917	4.30	No new erosions; minute surface roughness
624-016	3-10-72	219.6	670.5				
624-017	3-16-72	227.3	897.8	5	755.8	3.68	Combustor walls smoothed pretest. Erosions noted during 624-016 slightly deeper. New OCW erosions: 4 on combustor 1, 1 on combustor 20.
				175.5			
624-020	3-22-72	280.5	1178.3	10	760	3.70	Two transition tests, 018 and 019, run prior to 020. Combustor walls smoothed prior to 018; not smoothed prior to 020. One very minor OCW erosion on combustor 14.
				229			
624-021	3-24-72	500.1	1680.9	10	888	4.20	Combustor walls smoothed pretest; no new erosions; slight surface roughness.
				301			
624-022	3-30-72						Combustor walls smoothed pretest; no new erosions

TABLE 11. (CONCLUDED)

Mainstage Test No.	Test Date	Duration, seconds		Average Combustion		MR	Combustor Wall Condition
		Test	Cum.	Time, seconds	P _c , psia		
624-023	4-3-72	500.1	2181.0	10	761	3.67	Combustor walls smoothed pretest; no new erosions
				335	841	3.80	
				155	897	4.20	
				47	812	4.20	
624-024	4-11-72	272.0	2453.0	215	945	4.80	Combustor walls smoothed pretest; no new erosions
				10	1024	5.18	
				232	1035	5.25	
624-028	4-19-72	592.5	3045.5	360	884	4.57	Combustor walls smoothed pretest; no new erosions
				5	1124	5.40	
624-029	4-24-72	15.1	3060.6	10.1	1248	5.90	Combustor walls smoothed pretest; new OCW erosions
624-030	5-23-72	2.6	3063.2	5	810	4.00	Old erosions, slight increase in magnitude. Combustor walls smoothed pretest; no new erosions
				44.6	903	4.30	
624-031	5-23-72	49.6	3112.8				Combustor walls not smoothed pretest; no new erosions noted

TABLE 12. COMBUSTOR EROSION SUMMARY, BREADBOARD ENGINE NO. 1 POSTTEST 624-005

Combustor No.	Unit No.	Inner Contour Wall				Outer Contour Wall				Comments
		Erosion Amplitude Estimate, inches				Erosion Amplitude Estimate, inches				
		Slight Roughness	<0.005	0.005 to 0.010	>0.010	Slight Roughness	<0.005	0.005 to 0.010	>0.010	
1	C-13	10	4			2			ICW* nozzles 0.125 inch diameter	
2	C-24	7	2	1		2				
3	C-27	General Roughness	13	1		General				
4	C-06	General Roughness	2			1				
5	C-17		10			General			heavy wall	
6	C-14			8	4	General				
7	C-22	1	6	12		3				
8	C-37	6	4	8						
9	C-38		4	2		2				
10	C-36		3	1		1			Heavy wall	
11	C-16		3	6		2			Heavy wall	
12	C-15	General Roughness	3	10	5	General Roughness	3			
13	C-12			15		3				
14	C-05	Very Slight				Very Slight				
15	C-09		6			General	1			
16	C-02	General				General				
17	C-03	3				1				
18	C-11	7	2			General	2		Heavy wall	
19	C-19	General	2			General			Heavy wall	
20	C-20			12	1			1		
Total Erosions			51	54	40		38	2		189

*All other units peened to 0.109-inch diameter.

TABLE 13. BREADBOARD TEST BED NO. 1 EROSION SUMMARY POSTTEST 624-031

Combustor No.	Unit No.	Inner Contour Wall				Outer Contour Wall				Total Erosions											
		Erosion Amplitude Estimate, inches				Erosion Amplitude Estimate, inches															
		Roughness	0.005	0.005 to 0.010	0.01	0.01	0.01	0.005	0.005 to 0.01		0.01										
1	C-13	Smooth			5							Smooth			5						10
2	C-14	Smooth			16							Smooth			7						23
3	C-27	Rough		8		1						Smooth			1						10
4	C-06	Rough	3					2				Rough			1						4
5	C-17	Rough						5				Rough			1						2
6	C-14	Rough										Slight Roughness			1						6
7	C-22	Rough		11		3						Rough			2						16
8	C-37	Rough		9								Rough									19
9	C-38	Smooth										Smooth									0
10	C-36	Rough	4		8							Smooth									4
11	C-16	Rough							5			Smooth			1						14
12	C-15	Rough				6						Smooth									11
13	C-12	Smooth	7						1			Smooth									8
14	C-05	Smooth										Smooth			1						1
15	C-09	Smooth										Smooth			2						2
16	C-02	Smooth										Smooth			1						1
17	C-03	Smooth										Smooth									1
18	C-11	Smooth							1			Smooth									2
19	C-19	Slight Roughness	1									Slight Roughness			2						3
20	C-20	Slight		5								Slight Roughness									13
Total Erosions			15	41	27	18								11	34					4	150

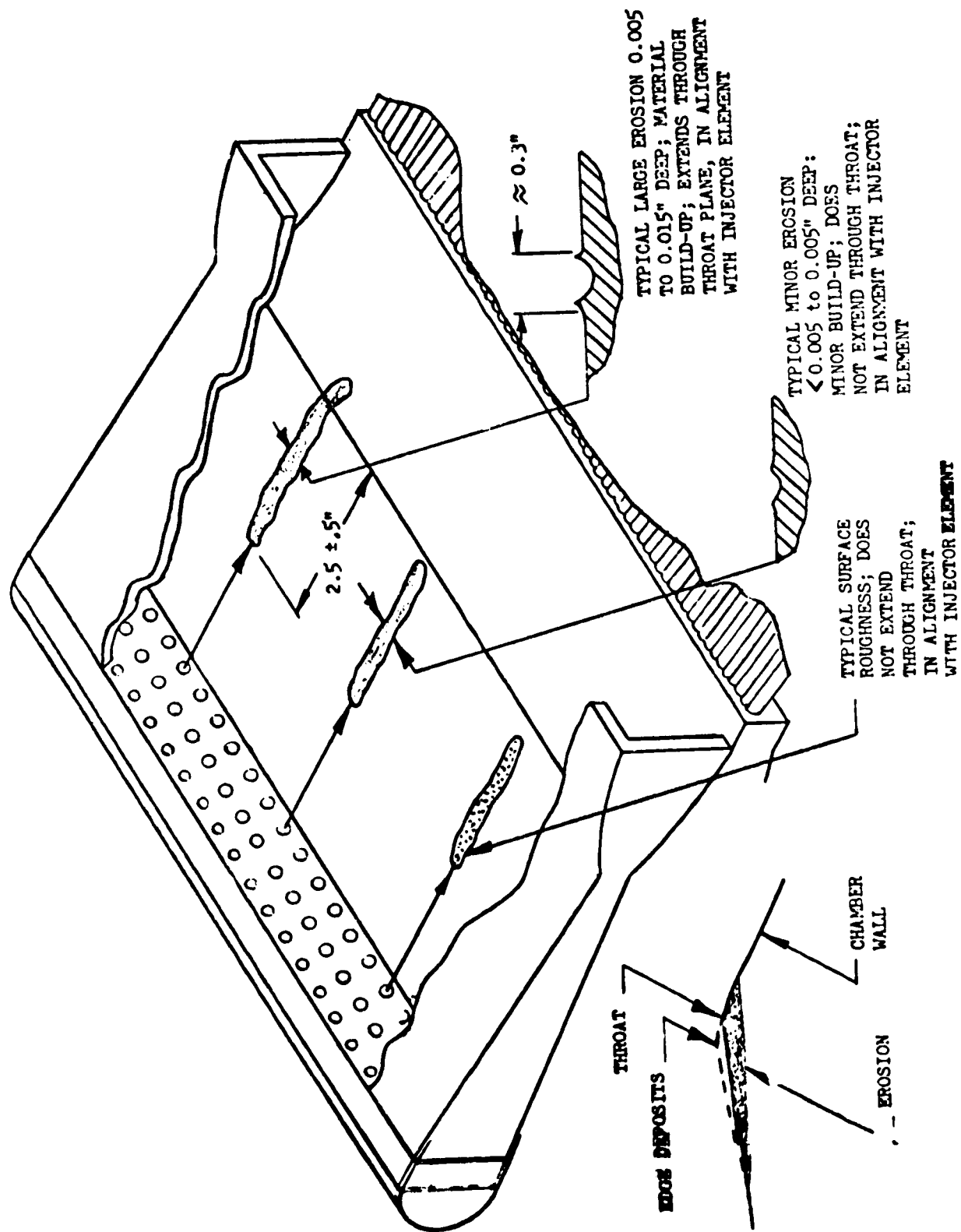
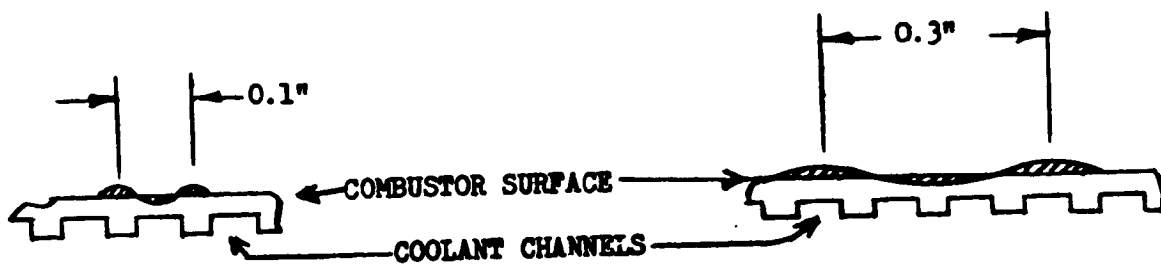


Figure 74. Combustor Wall Erosions, Breadboard No. 1



TYPICAL
MULTISEGMENT
EROSION

TYPICAL
BREADBOARD NO.1
EROSION

COOLANT CHANNEL
ORIENTED

INJECTOR ELEMENT
ORIENTED

INJECTOR ELEMENT
ALIGNMENT

Figure 75. Comparison of Combustor Erosion Characteristics

Measured Combustor Heat Load and Analysis

The integrated heat input of the combustors was established using the measured combustor fuel inlet and fuel injector manifold temperatures, the measured fuel flow-rates and injector manifold pressures.

The parameter used to compare results is:

$$\left(\frac{\dot{Q}}{\dot{W}_T}\right) (D) (P_C^{-0.2})$$

where

- \dot{Q} = combustion zone heat load, Btu/sec ($Q_T \times 0.74$)
- \dot{W}_T = total propellant flow, lb/sec
- D = throat gap, inches
- P_C = chamber pressure, psia

Displaying the results in this fashion permits comparison of a common basis of tests at varying conditions of P_C , mixture ratio, etc. The engine mainstage testing began (test 009) with a normalized heat load of approximately 266. This is nearly the same level as exhibited by the multisegment of 256 to 271, and approximately 6.5 percent greater than the design base prediction. Figure 76 displays the results of the breadboard testing in comparison to the multisegment (C06) fired as a single segment and the design base (the tapoff segment). Combustor C06 (now linear combustion No. 4 on the breadboard hardware) realized the highest normalized integrated heat load of the linear combustors tested to date. Results from tests up to and including test 005 are indicated by darkened circuits.

The heat load increased approximately 22.5 percent during the testing until the chamber erosions occurred during test 005. The first increase of significance in

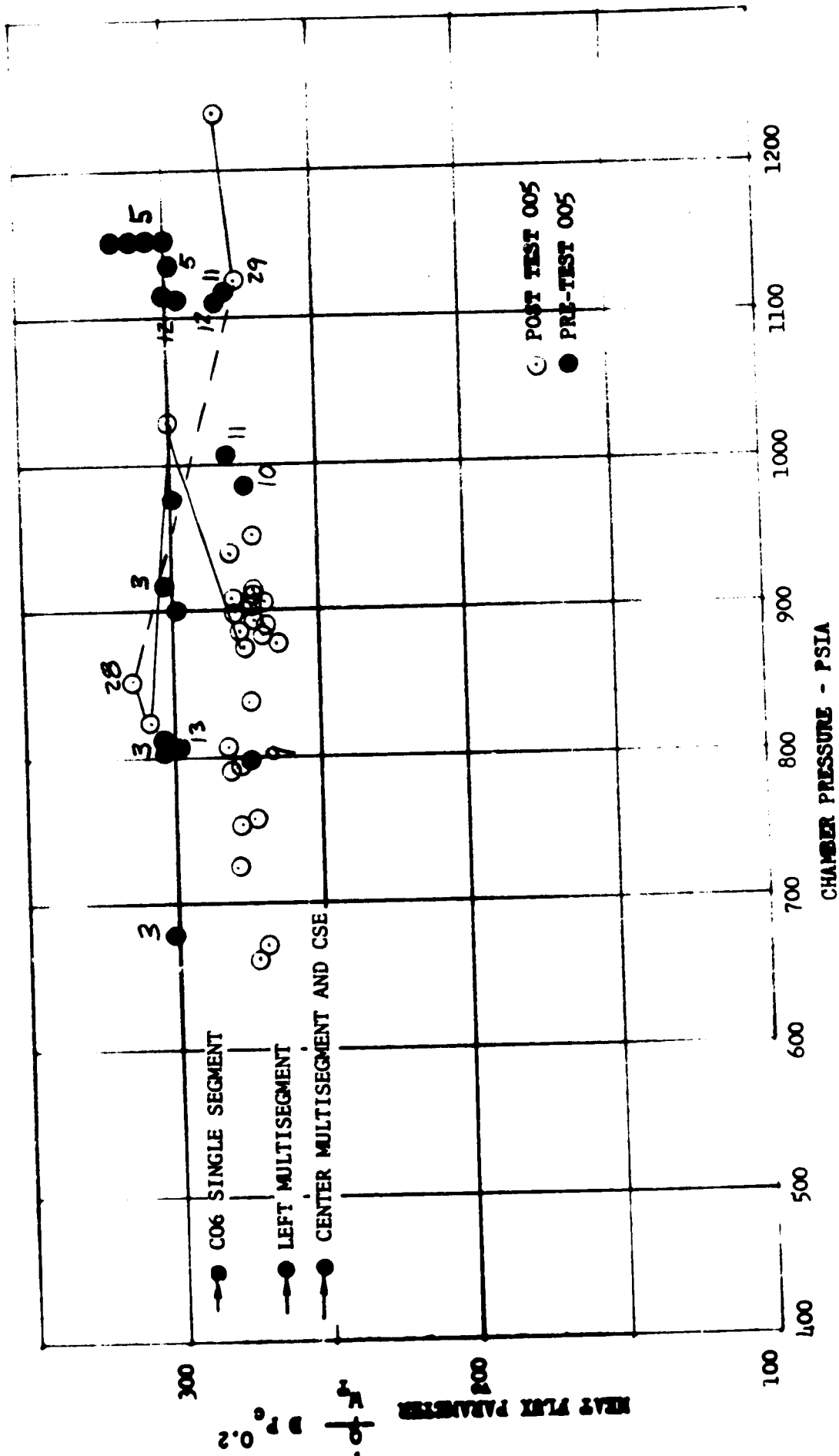


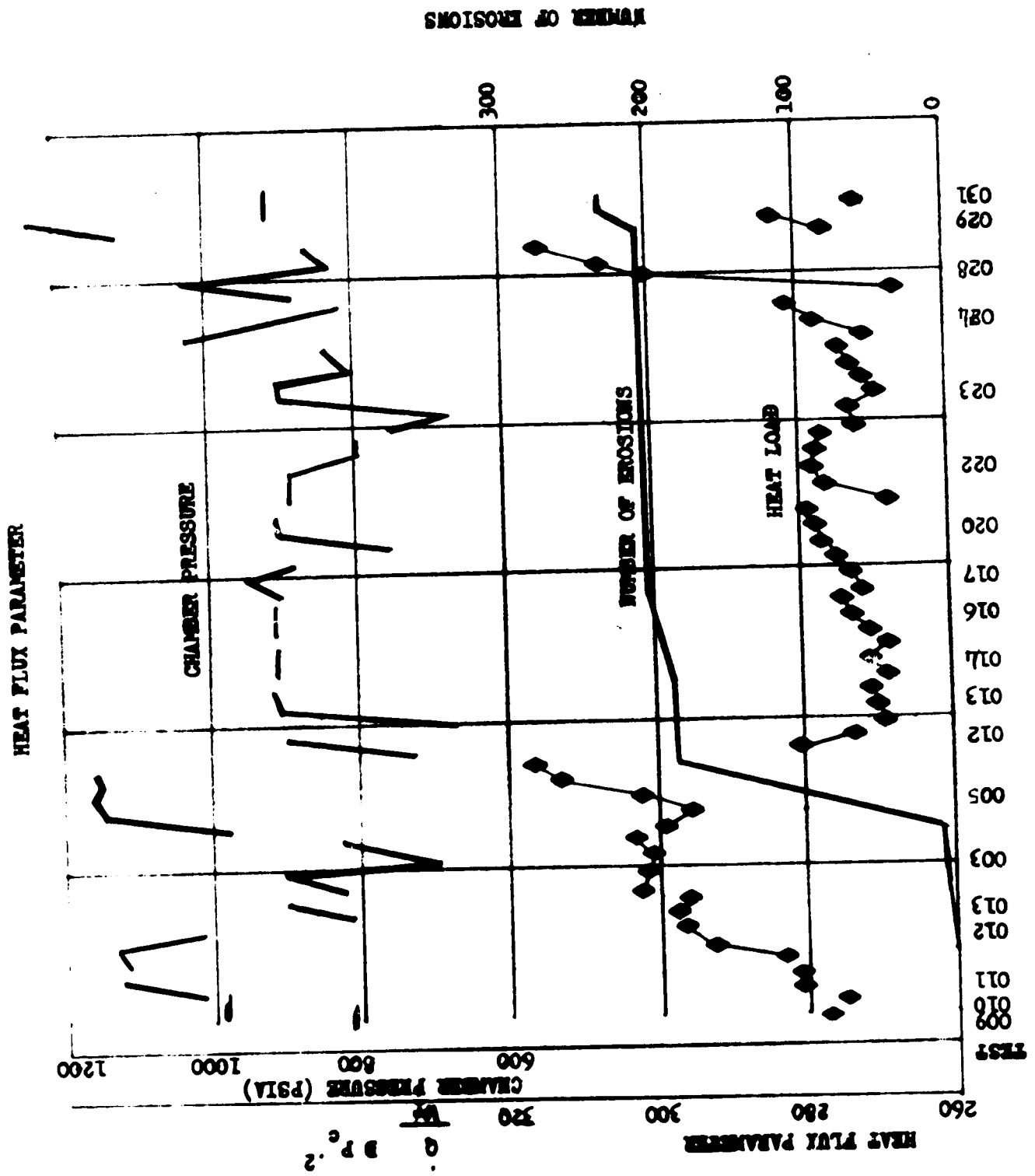
Figure 76. Linear Breadboard No. 1 Combustor Heat Flux Parameter

the heat flux parameter occurred during test 12, with the parameter increasing approximately 275 to 300. This test produced the first evidence of erosions in the combustors. Subsequent tests 013 and 003 were performed at low chamber pressures. The heat flux parameter did not rise during these tests. During test 005, the heat load increased approximately 7 percent. Following test 005, there was a total of 189 erosions of various degrees of severity on the combustor walls. Polishing and smoothing the combustors resulted in the normalized heat loads returning on test 012 to nearly the same level obtained on the first mainstage test (009) in 1971. Figure 77 displays the heat flux parameter, the chamber pressure, and the number of erosions for each mainstage test. The effects of the smoothing operation performed between each mainstage test and after test 005 are evident in the figure. For example, the heat load parameter was reduced from approximately 280 to 265 due to the smoothing operation between test 020 and test 022. All tests exhibited a rise in the heat flux parameter during a mainstage test. The smoothing operation prevented any significant amount of erosions through the remainder of the program. There is a relationship between the heat flux parameter and the chamber pressure in producing the onset of erosions. During test 028, for example, the heat flux parameter rose to values identical with those found in test 005 but erosions did not occur. Test 028 was performed with a chamber pressure approximately 900 psi, while test 005 performed at approximately 1150 psi. Test 029, which produced erosion in the combustor was performed at 1200 psi, however, the heat flux parameter was at nearly normal levels.

Wall Temperature Analysis

A convenient comparison of the test severity experienced during testing of the No. 1 breadboard engine can be made by calculating an estimated wall temperature with the following equation.

$$T_1 = 950 + 137.5 (4.0 - \dot{W}_{H_2}) + 1350 \left[\frac{\dot{W}_{H_2} \Delta T}{4.28 P_c^{0.8}} - 1 \right] \\ + 1000 (t_w - 0.035) + 0.38 (T_{in} - 320)$$



NUMBER OF EROSIONS

Figure 77. Heat Flux Parameter vs Test Number

where:

- T_1 = wall temperature parameter
- W_{H_2} = combustor fuel flowrate, lb/sec
- ΔT = combustor fuel temperature rise, R
- P_c = injector end chamber pressure, psia
- t_w = combustor wall thickness at the throat, inches
- T_{in} = combustor fuel inlet temperature, R

The equation represents a linearization of the effect of the various quantities on the predicted wall temperature and can be considered an estimate of the actual wall temperature if measured test parameters are used. The distribution of h_g values must maintain the same percentage of maximum values along the chamber length for this comparison to be valid.

Engine Tests. The wall temperature parameter was computed for each test and each combustor (on breadboard No. 1) from test 009 to test 013. The numerical average of the wall temperature parameter from all combustors is presented in Fig. 77. Several trends are evident. The most significant changes are noted for the high chamber pressure and mixture ratio tests (011, 012, and 005), indicating that a progressive change in the heat transfer rate was taking place. The points that are from the low chamber pressure and mixture ratio tests (009, 010, 013, and 003) yield a positive but decreased slope. A second significant trend is that each of the high power level tests appear to start at a slightly higher wall temperature than does the previous test. This would indicate that there could be some adverse influence attributable to either the effects during start or transition to main-stage operation.

The wall temperature parameter is also compared to the theoretical wall temperature determined from design values of h_g and flowrates at the chamber pressure and mixture ratio conditions of the test (Fig. 78). Six test data points were input

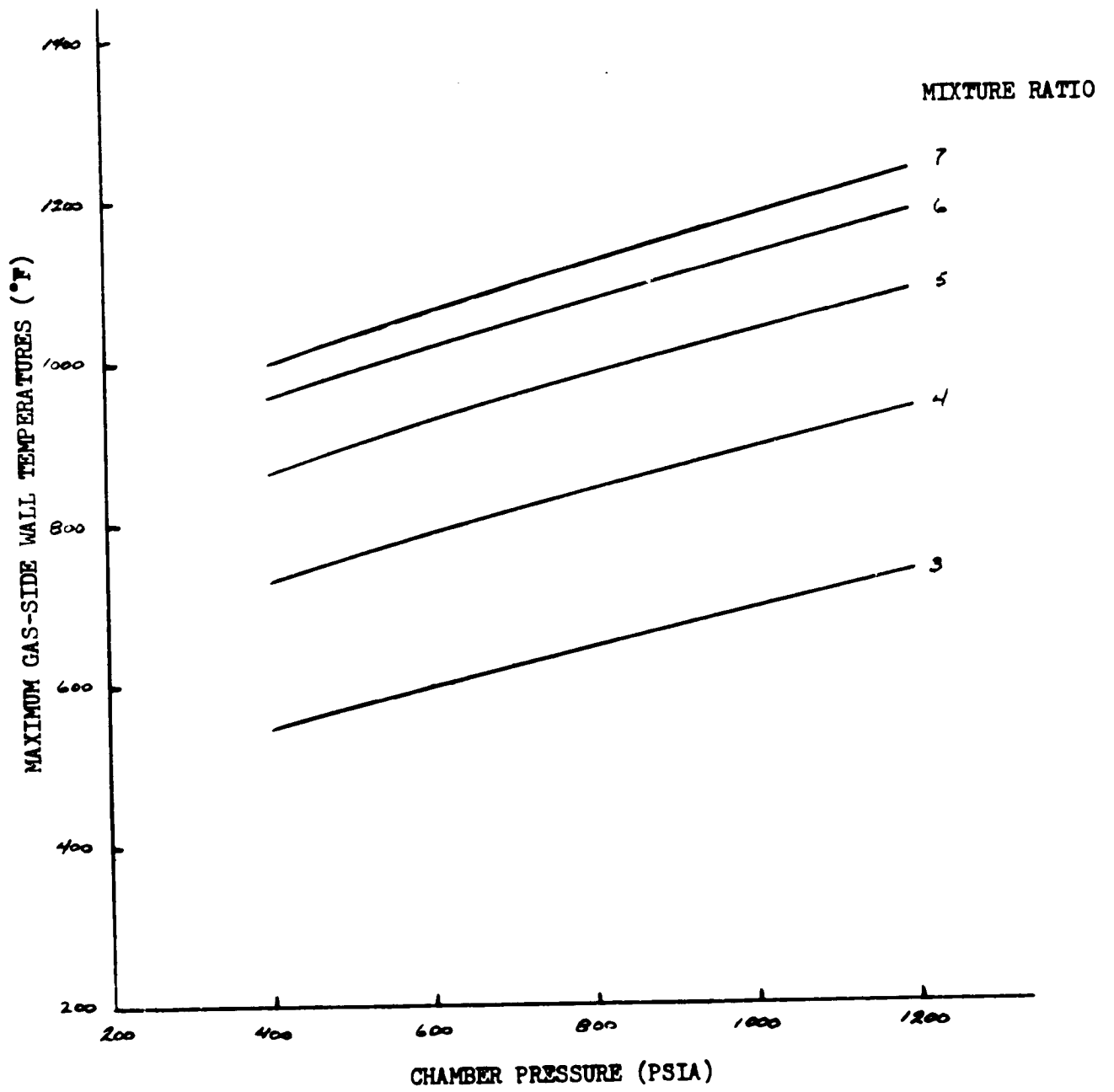


Figure 78. Theoretical Wall Temperature

into a two-dimensional heat transfer model so that these data could be compared to the linear approximation temperature parameter. In summary, the data presented in Fig. 79 suggests that the computed test gas-side wall temperatures were in reasonable agreement except where major combustor surface erosions had taken place (test 005).

The wall temperature parameter is computed for all mainstage tests and the results are displayed in Fig. 80. It can be seen in the figure that reasonable agreement between theoretical wall temperature and experimental wall temperature was obtained with initial testing of the breadboard engine. There is, however, posttest 005 a disparity of approximately 100 to 200 degrees between theoretical and experimental values. This would indicate that the posttest 005 smoothing operation did not restore the combustor wall surface to the original condition.

Component Testing. Wall temperature parameter results for the multisegment assembly tests are presented in Fig. 81. They are compared to the design theoretical wall temperature for each test. Significant data anomalies cannot be detected from the temperature history plots. The wall temperature parameter appears to follow the predicted theoretical wall temperature value. The wall temperature rises through several of the tests after test 015 because the hydrogen inlet temperature was increased during the test, thereby decreasing the hydrogen mass flow rate, increasing mixture ratio, and increasing the gas-side wall temperature.

Conclusions. The computed average wall temperature from engine tests agree with the design predictions for the first mainstage test. The computed test wall temperature gradually deviates from and exceeds the design predictions as test time was accumulated. The computed wall temperature at the end of test 005, where severe erosions were present posttest, exceeds the design prediction (1170 F) by approximately 200 F.

The computed wall temperature from the multisegment and component tests follows the design predictions reasonably well.

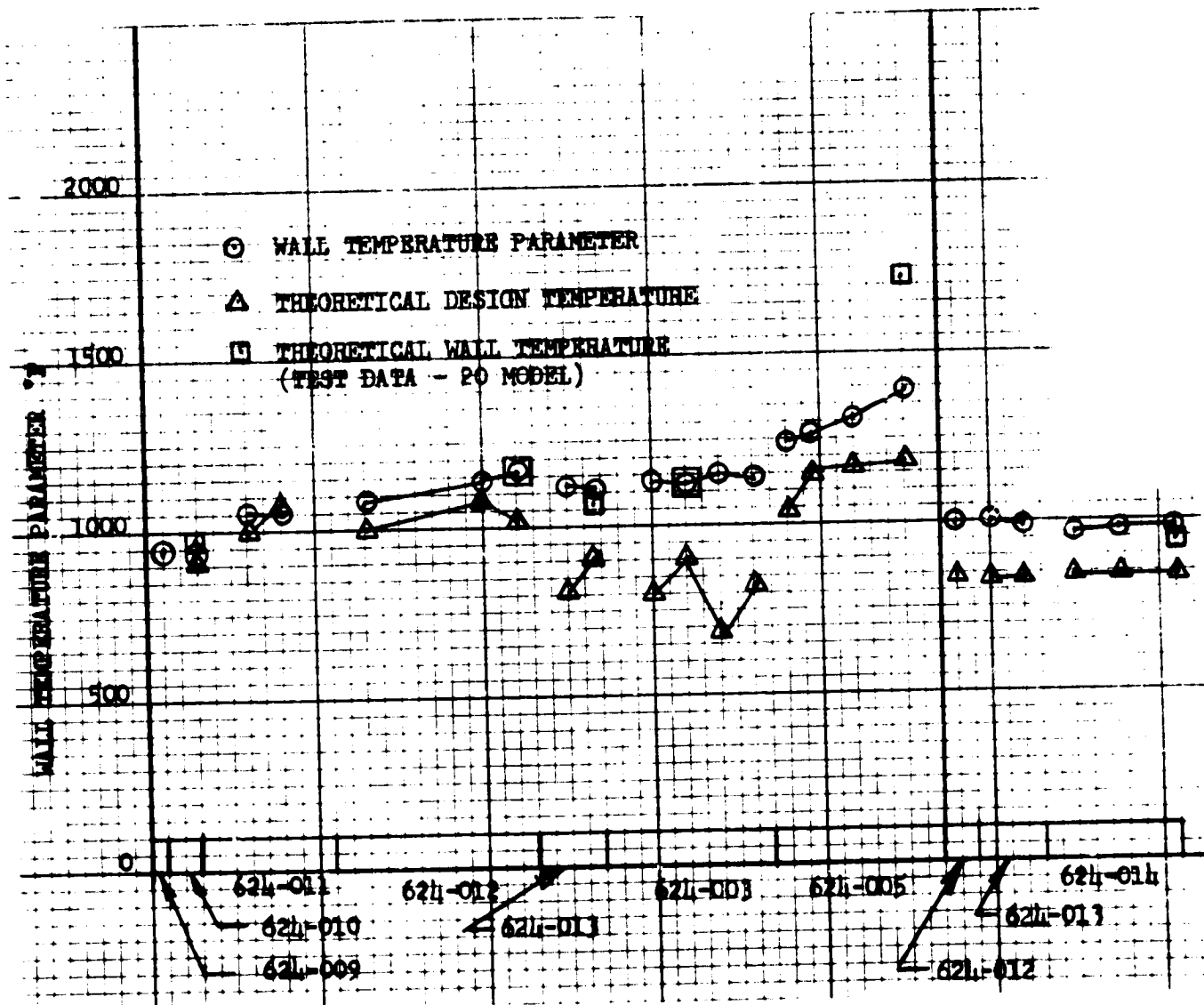


Figure 79. Average Wall Temperature Parameter History Breadboard No. 1

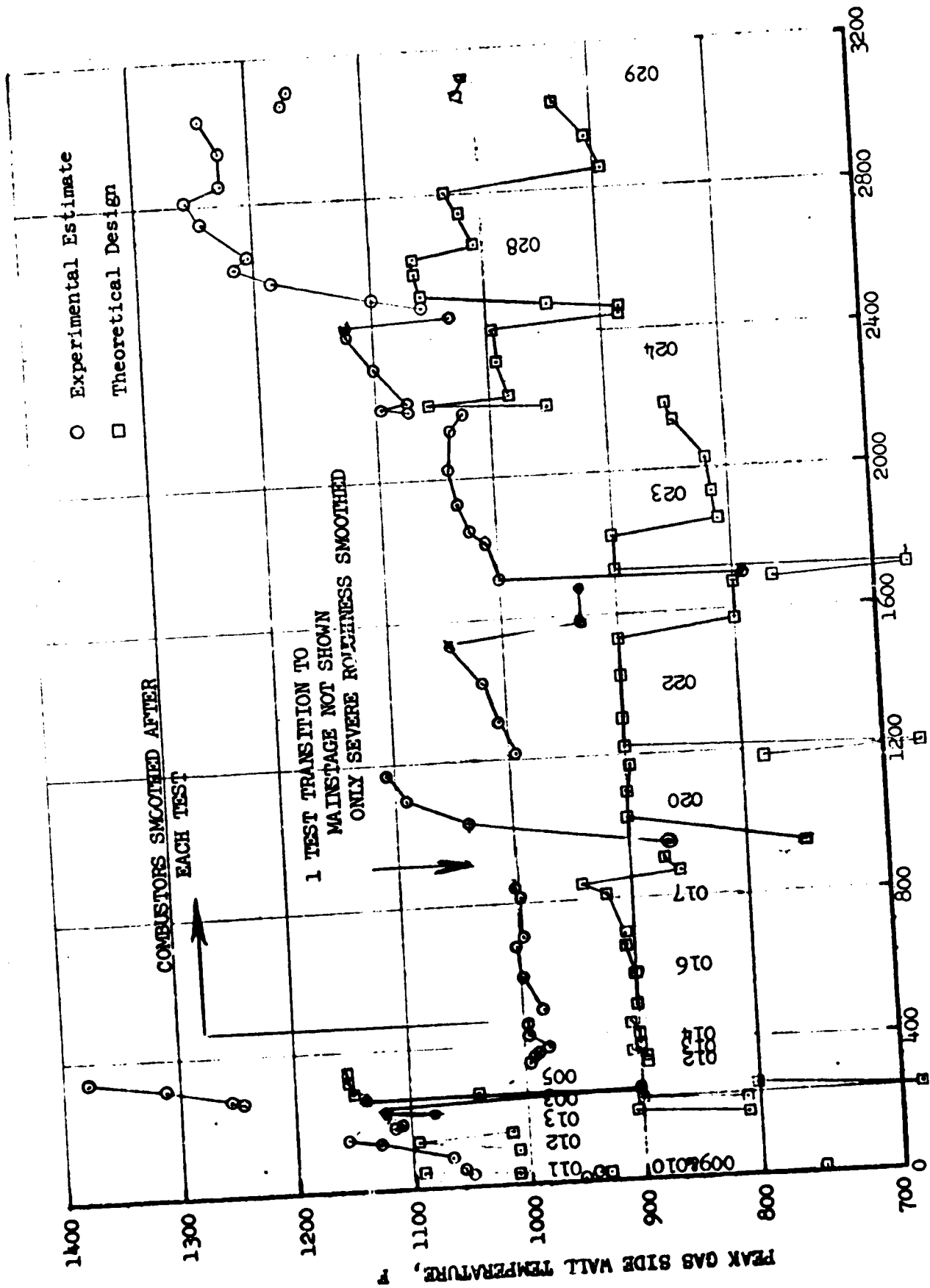


Figure 80. Maximum Gas Side-Wall Temperature Breadboard Engine No. 1

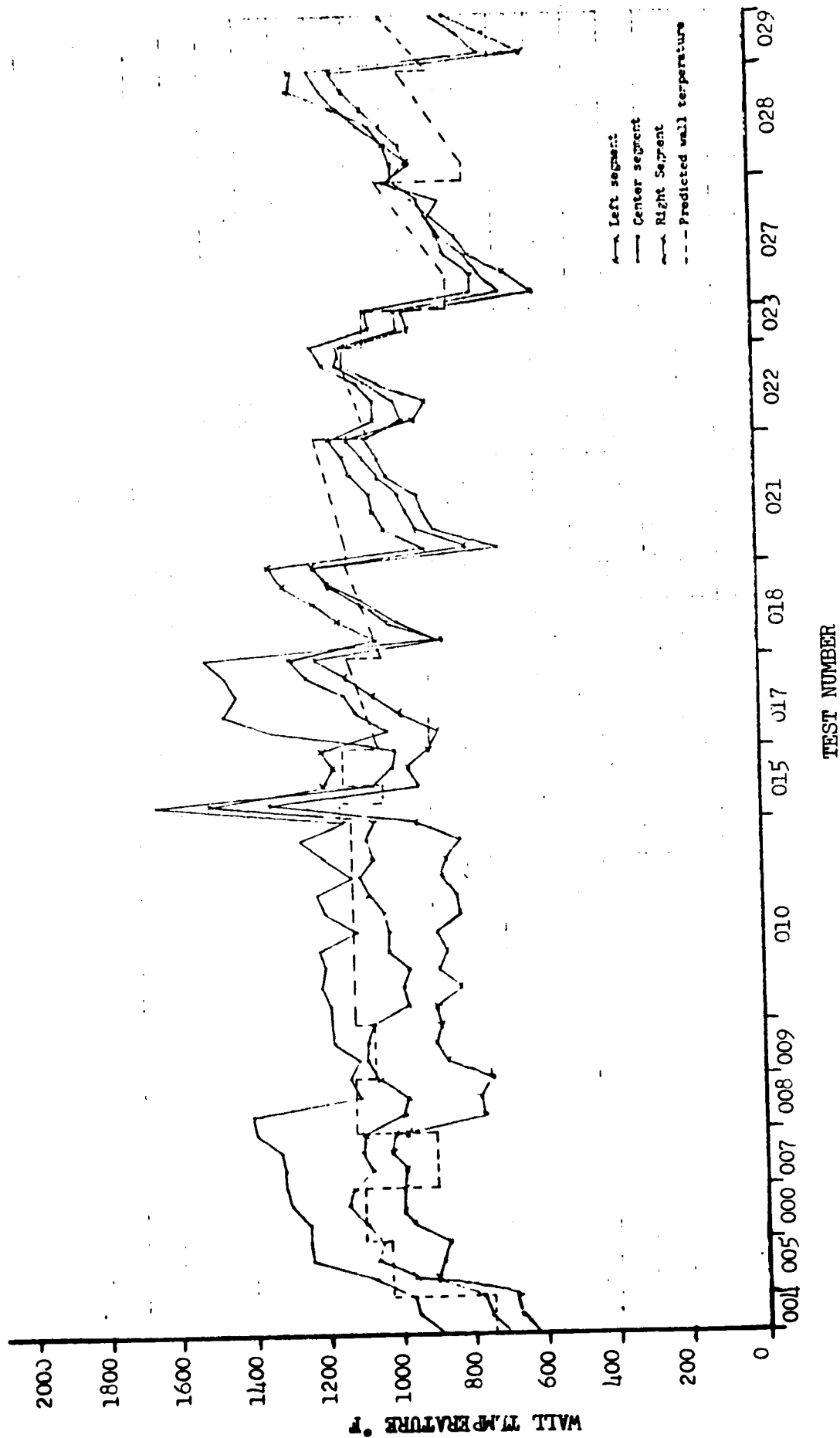


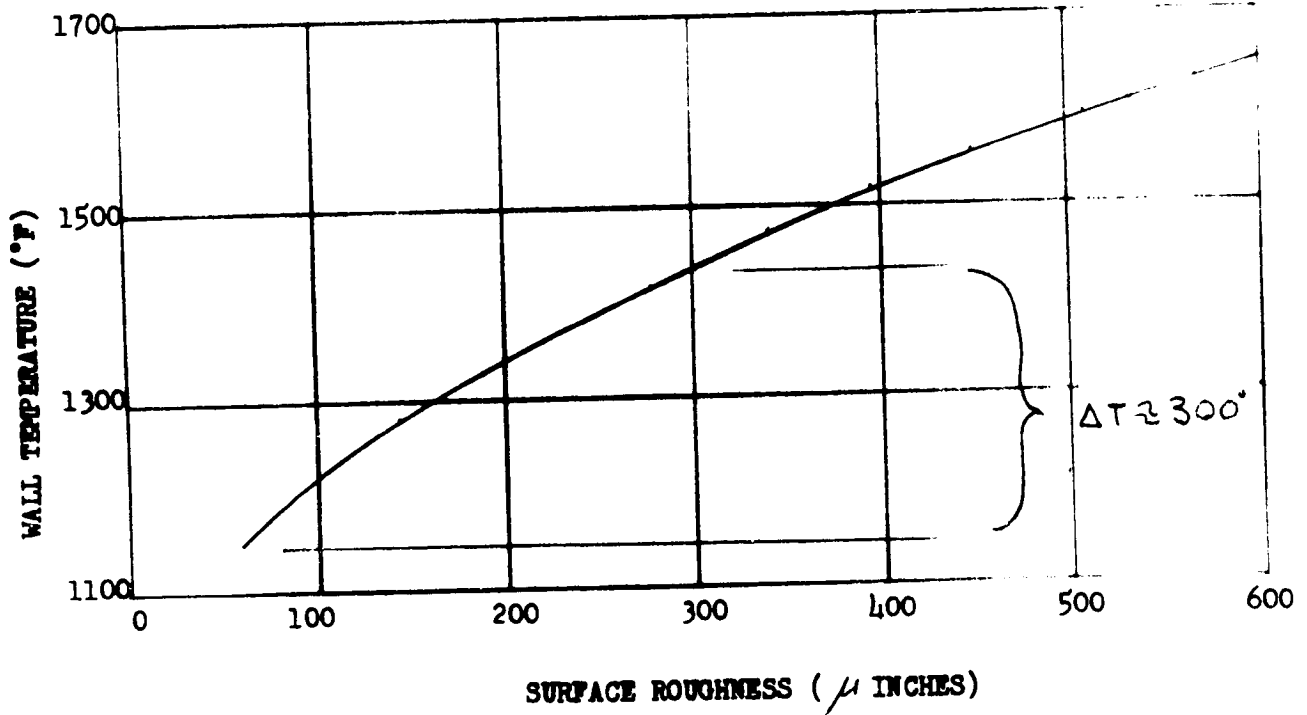
Figure 81. Wall Temperature History Three Segment Testing

Surface Roughness Effects. An analysis was performed to determine the variation of the gas-side film coefficient with surface roughness and to compute the resultant rise in wall temperature. Measurements on new combustors indicated a wall surface finish of approximately 60 microinches. On-site observations produced an estimate of 200 to 300 microinches for the wall surface finish prior to the onset of erosions. Figure 82 indicates the results of the analysis of the variation of the film coefficient and wall temperature as a function of combustor surface roughness. A wall temperature increase of approximately 300 degrees was indicated with the surface finish increase from 60 to 300 microinches.

Correlation of Data. An attempt to define significant influences on the incidence of erosion was made. Several parameters were chosen and plotted versus the severity of erosion and number of erosions that occurred in each combustor.

Chamber pressure, fuel injection temperature, combustor resistance, throat wall thickness, and wall thickness 2.5 inches upstream of the throat were studied. No correlations were evident from this study with the exception of a slight indication that the erosion may be less severe when the combustor resistance is high. A combination of chamber pressure and mixture ratio indicates a stronger tendency for damage when both are high.

MAXIMUM GAS SIDE WALL TEMPERATURE
SURFACE ROUGHNESS EFFECT



VARIATION OF h_g WITH SURFACE ROUGHNESS

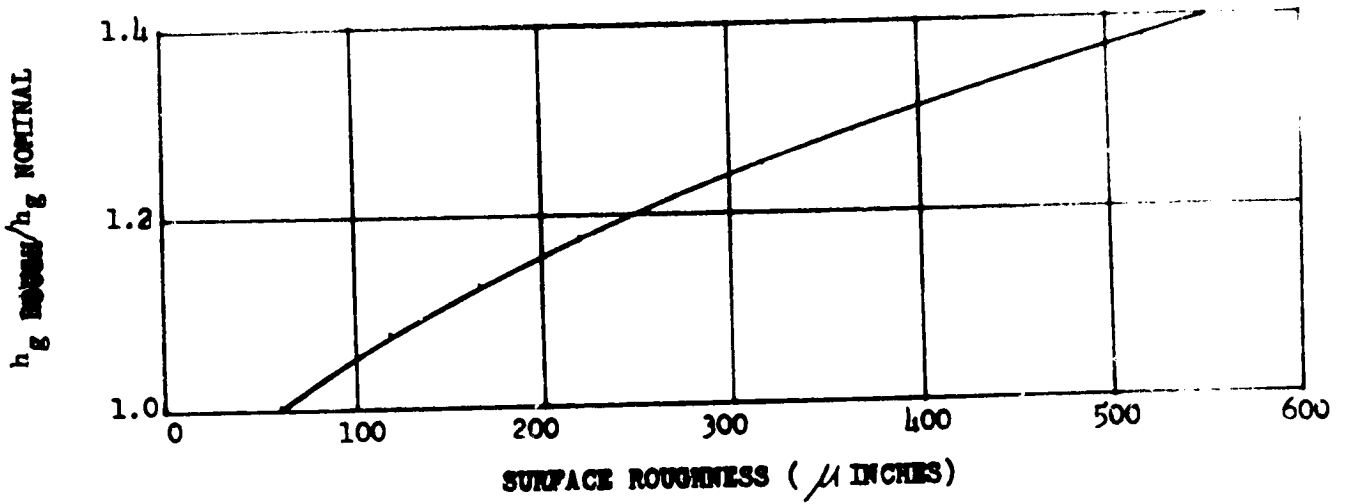


Figure 82. Combustor Surface Roughness Analysis

COMPONENT DEVELOPMENT PROGRAM

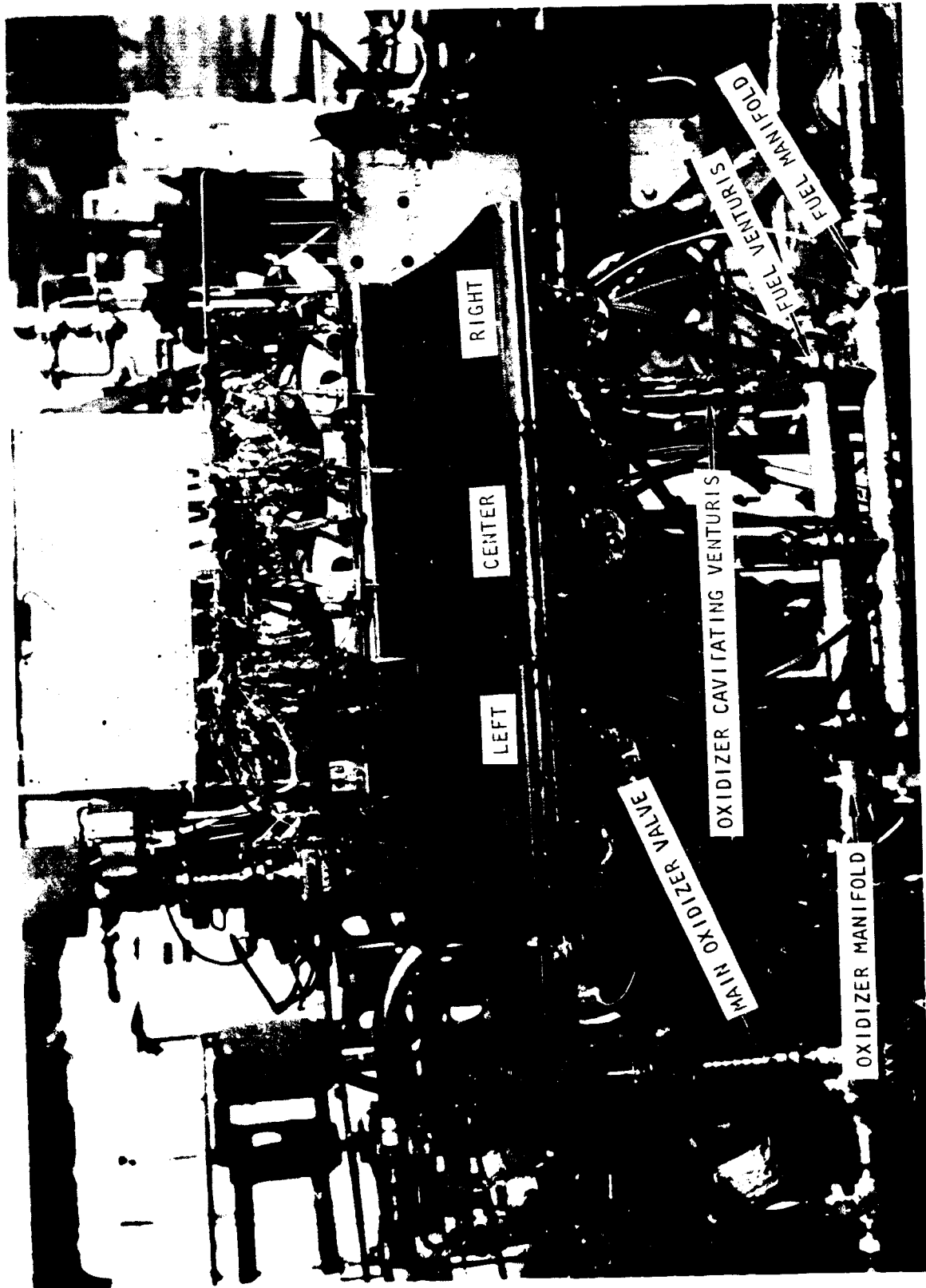
IGNITION SYSTEMS

A comprehensive component test program was conducted to verify the operational feasibility of the fluorine and combustion wave ignition systems at simulated engine start conditions. As a result of the component testing, the fluorine ignition sequence for test bed No. 1 was changed from a fuel lead to an oxidizer lead, a reliable ignition-detection method for multicombustor thrust chambers was developed, the main propellant flammability limits were defined, and a new ignition concept, the combustion wave system, was successfully demonstrated. A summary of the component development program for each ignition system used on test bed No. 1 is presented.

Fluorine Ignition System

Gaseous fluorine ignition had been used extensively during segment component testing on pressure-fed test facilities. However, main propellant ignition using a fluorine-hydrogen element at engine tank-head conditions had not been demonstrated. The initial evaluations of tank-head fluorine ignition were conducted on a multi-segment assembly (Fig. 83), comprised of three combustors with a 20-inch-long tubular expansion nozzle. The combustor injectors were identical to the test bed No. 1 configuration, i.e., 67 coaxial injection elements and 1 triaxial igniter element. The igniter element geometry is shown in Fig. 84. The proposed engine start sequence, a gaseous fuel-lead, was simulated during the initial tests and the ignition characteristics were evaluated. The simulated engine sequence is compared with the component sequence (successfully used for hundreds of component tests) in Fig. 85. Thirty-two tests were conducted to evaluate the proposed ignition sequence for test bed No. 1. Propellant flowrates and injection pressures were controlled to duplicate the engine start model results which predicted nominal propellant flows per segment of:

<u>Hydrogen</u>	<u>Oxygen</u>	<u>Fluorine</u>
0.11 lb/sec	0.154 lb/sec	0.0175 lb/sec



1XZ23-1/15/71-SIE

Figure 83. Multisegment Test Stand Cell 18A, CTL-3 Santa Susana Field Laboratory (Front View)

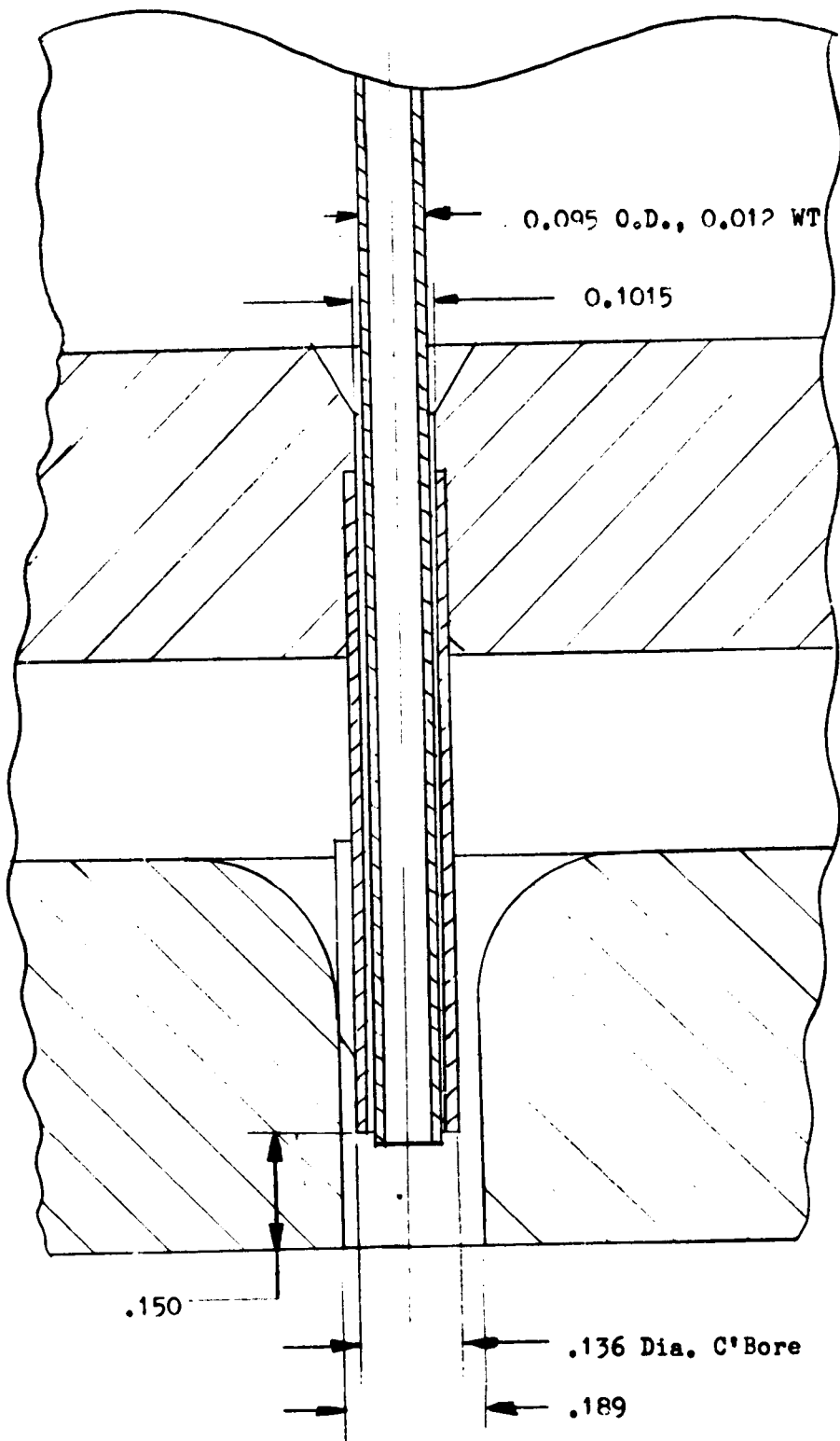


Figure 84. Igniter Element

R-9049

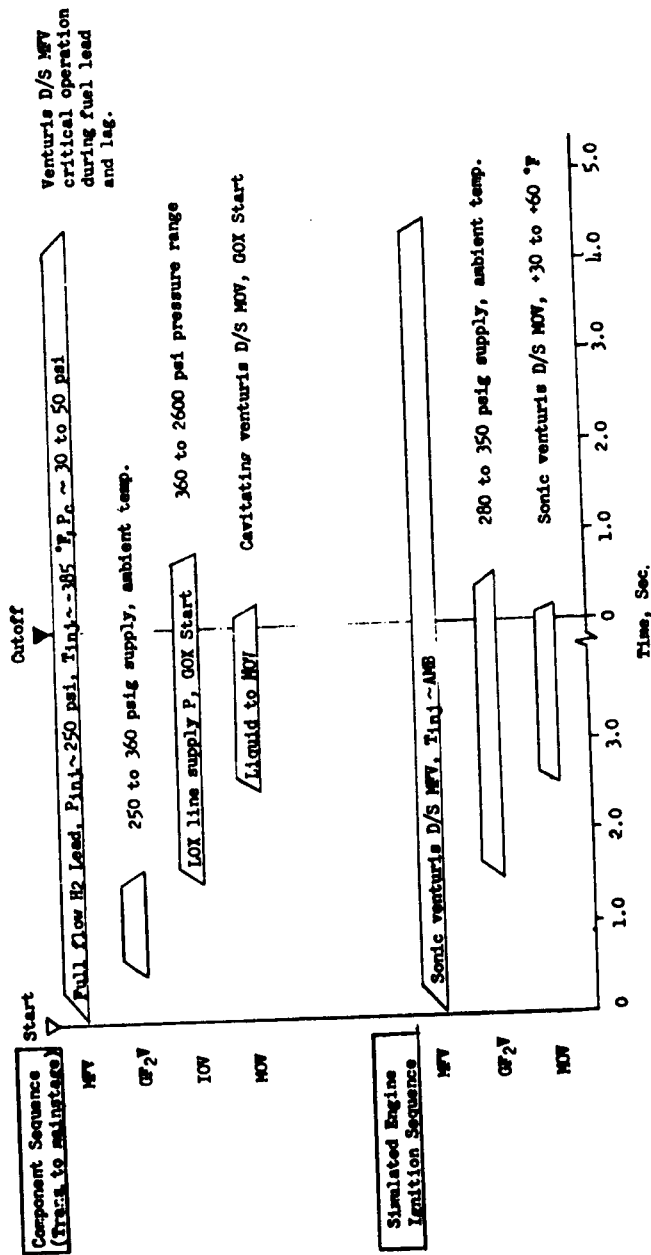


Figure 85. Ignition Sequence Comparison Component and Simulated Engine Start Sequence

Propellants were supplied at ambient temperature, as predicted by the start model, and the injector mixture ratio was varied to explore the flammability limits of the main propellants with the linear injector configuration.

The results of the fuel-lead test series were as follows:

1. Main propellant ignition can be achieved with a tank-head fuel-lead start if the injector mixture ratio exceeds the oxygen-hydrogen flammability limit. The lower mixture ratio limit for ignition with this injector configuration proved to be 1.25 for ambient temperature (70 F) propellants.
2. A reliable method of ignition detection was developed. The injection temperature thermocouples were used in conjunction with a slope detection integrator. An injection temperature rise-rate of 25 degrees/sec was determined to be a positive indication of main propellant ignition. Detection times with the fuel lead were found to be unacceptably long.
3. Cross-ignition of unignited combustors from adjacent ignited combustors was not demonstrated on any test with the fuel lead. Cross-ignition capability was a firm requirement for test bed No. 1.

A comparison of the multisegment ignition limits with established laboratory ignition results is presented in Fig. 86. The difference between the segment limit and the laboratory limit for well-mixed, static gas is attributed to incomplete mixing in the outer zones of the segment injector elements. Five additional tests were conducted to evaluate the effect of a gaseous oxidizer-lead start in improving the initial heat transfer rate to the ignition-detect thermocouples, in providing a more energetic ignition transient, in eliminating the open air detonations sometimes associated with the fuel-lead start, and in establishing a cross-ignition capability for unignited segments. The oxidizer-lead ignition sequence was successful in accomplishing all the desired ignition goals and was selected as the fluorine ignition sequence for test bed No. 1. The oxidizer lead resulted in instant main propellant ignition when fuel reached the main injector, and the ignition-detection thermocouples responded rapidly at an increased rate. Cross-ignition was accomplished at mixture ratios exceeding 1.25, and no open-air detonations were experienced. No hardware damage or overheating resulted from the sequence.

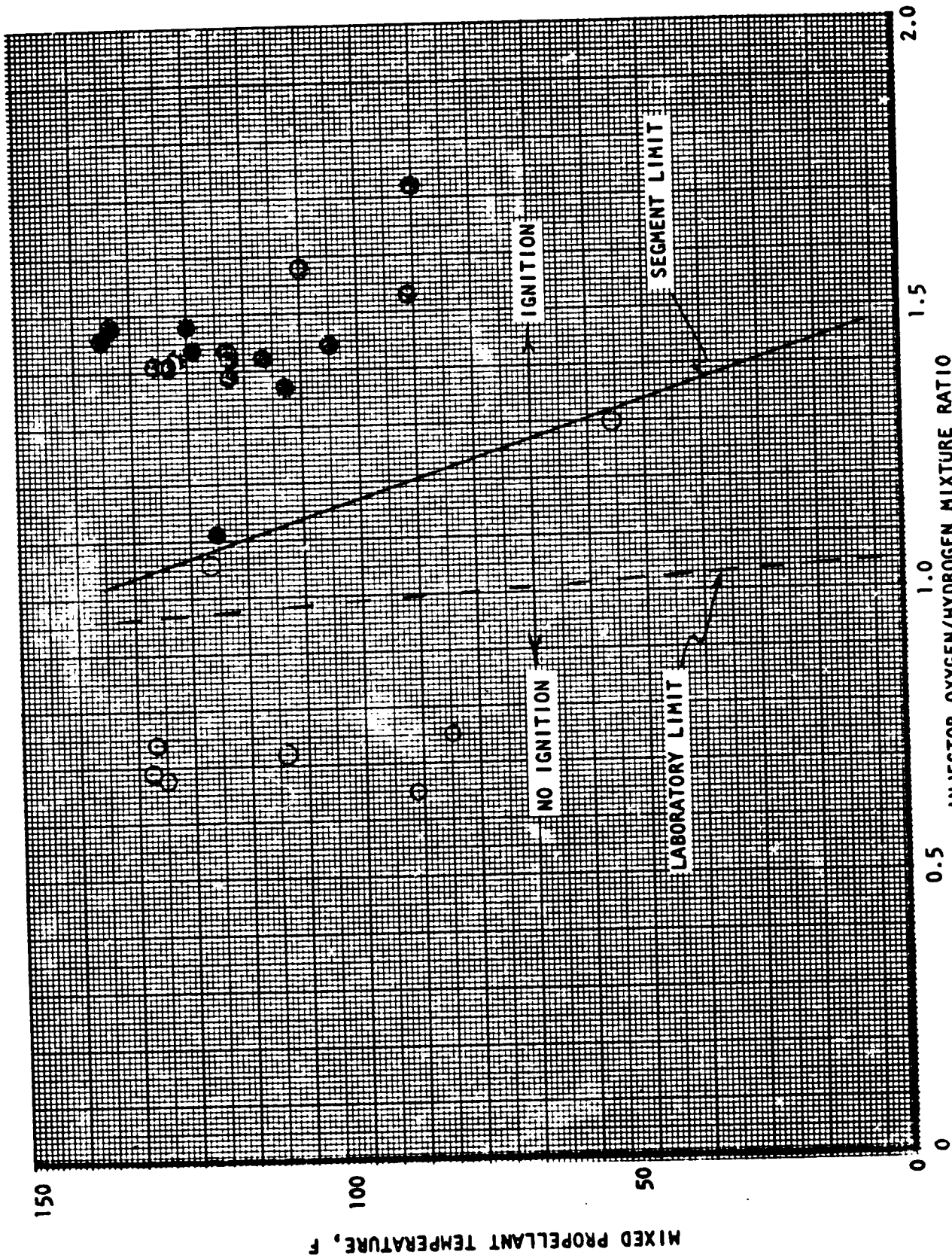


Figure 86. Fluorine Ignition, Oxygen/Hydrogen Ignition Limits

Combustion Wave Ignition System

During the period of July to December 1971 a significant amount of research and component development was conducted on the combustion wave ignition system. Enough successful results were obtained to commit this advanced ignition system for use on test bed No. 1. A single spark, generated from an integrated spark plug/exciter, initiates a single combustion wave which branches to the desired number of combustors (20 for test bed No. 1 and 10 for test bed No. 2). The wave ignites a H_2/O_2 pilot which, in turn, ignites the main combustors. Figure 87 schematically portrays this ignition sequence. No pilot failures were encountered when initial conditions are proper.

Component testing was conducted to develop an ignition system capable of being interchangeable with the fluorine system on test bed No. 1. The component work conducted during this period was performed in three phases:

- Phase I. Effort conducted at the Rocketdyne Propulsion Research Area on single elements, 10 elements, and 20 elements.
- Phase II. Effort conducted at the Rocketdyne CTL test area on the multi-segment (three-segment) test hardware.
- Phase III. Effort conducted at the LAD Thermodynamics Area on 20 pilot elements.

Phase I Objectives. The following objectives were established:

1. Evaluate the capability of the "triaxial" element to ignite under standard sea level backpressure conditions.
2. Evaluate the capability of propagating a combustion wave through a 0.050-inch-diameter tube, a 0.040-inch-diameter tube, and a 0.026-inch-diameter tube, and, in turn, igniting a pilot fed with GO_2 in an inner annulus and GH_2 in an outer annulus under simulated tank-head start conditions.
3. Determine the effects of induction lengths of 3 to 9 feet.

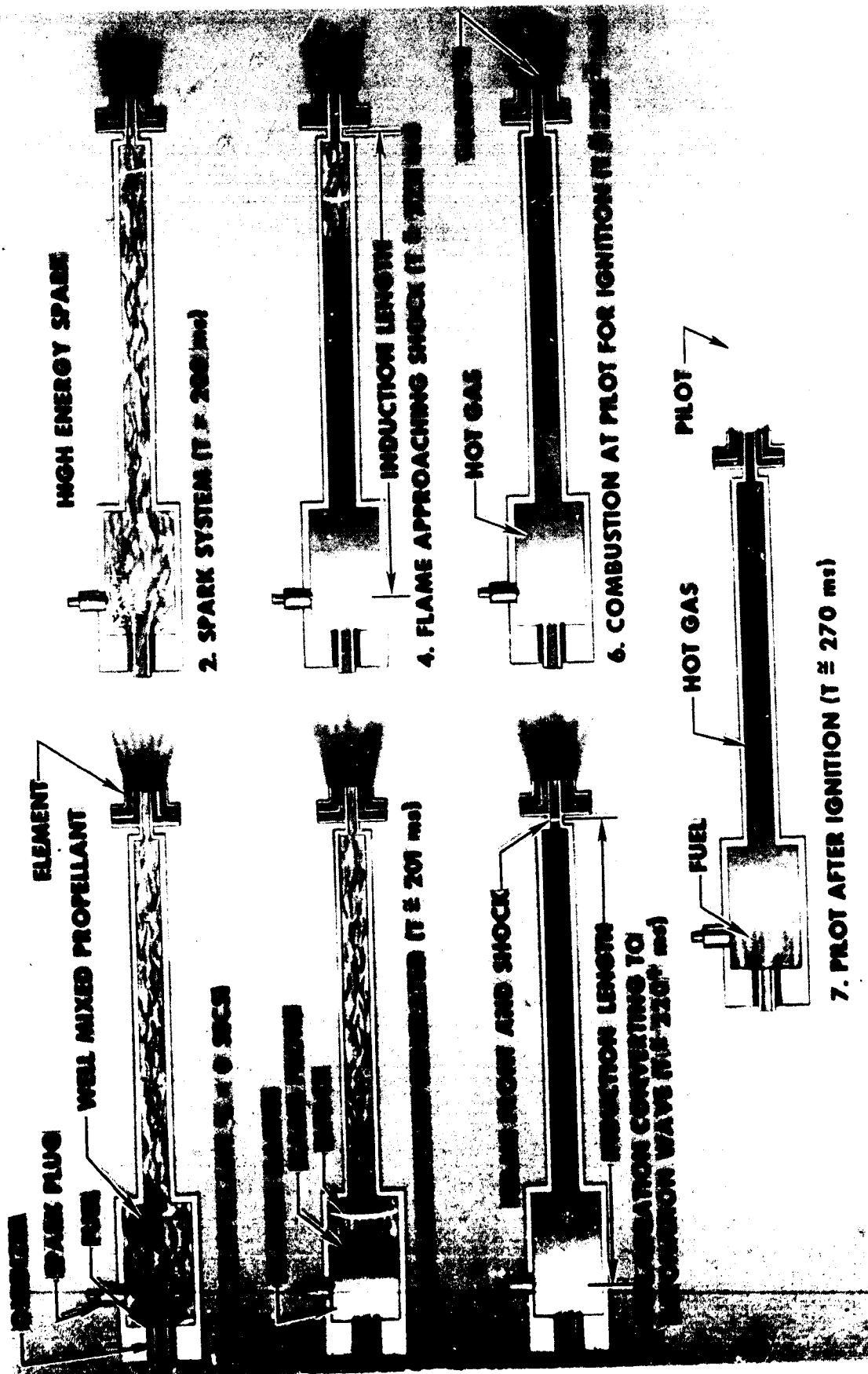


Figure 87. Combustion Wave Ignition Sequence

4. Evaluate the capability of igniting three igniter pilots by initiating a single combustion wave and branching through three 0.040-inch-diameter tubes.
5. Evaluate the capability of igniting 10 igniter pilots by initiating a single combustion wave and branching through 10 0.040-inch-diameter tubes.
6. Evaluate the capability of igniting 20 igniter pilots by initiating a single combustion wave and branching through 20 0.040-inch-diameter tubes.
7. Evaluate the capability of the "triaxial" element to operate with durability under mainstage conditions.
8. Provide sufficient test data on the 0.040-inch igniter element to map about the operating point of the test bed No. 1 configuration to commit the igniter element for Phase II effort.

Phase II Objectives. On the multisegment assembly:

1. Demonstrate the capability of generating a combustion wave under tank-head start conditions.
2. Demonstrate the capability of igniting three combustors simultaneously from a single combustion wave source when the combustors are flowing propellants from a simulated tank-head start.
3. Provide a partial map of the acceptable range of operation for combustion wave ignition under simulated tank-head starts.

Phase III Objectives. On 20 elements in a laboratory environment:

1. Evaluate the effects of backpressure on pilot ignition.
2. Evaluate the effects on generation of a combustion wave by inclusion of a check valve into the wave flow line.
3. Evaluate a newly designed mixer for use on test bed No. 1.
4. Determine the minimum delivered energy from a spark source required to generate a combustion wave.

5. Evaluate an integrated sparking unit designed for use on test bed No. 1.
6. Evaluate the capability of a dual or multiple priming and sparking system.
7. Provide a mapping of inlet pressures required for use by the combustion wave ignition system mixer.

Phase I Testing. All three test phases performed were conducted on elements designed for use with manifold fed pilots. Four igniter configurations were tested in this phase of the test program. Igniter elements (Fig. 88) that were used in all tests have a configuration capable of inclusion into the fluorine system presently used in test bed No. 1. Figure 89 depicts the interchangeable combustion wave/fluorine ignition system. Hardware was utilized in this series of tests duplicating the element spacing, manifold arrangement, and supply from the mixer.

All igniter elements considered are of the "triaxial" configuration. The inner annulus requires oxidizer flow and the outer annulus requires fuel flow. The igniter element, which is compatible with the fluorine system, has annular flow supplied from the main injector's fuel and oxidizer manifolds (Fig. 90). To provide simulated flow conditions, an igniter housing assembly (Fig. 88) was used for all tests.

To evaluate the "triaxial" element configuration during mainstage tests, a combustion chamber was used in conjunction with the igniter housing and igniter element (Fig. 88). A separate ignition source was provided to allow for element flow as obtained in mainstage tests.

Figure 91 shows the test setup for 20-element tests. Thermocouples are mounted at the element exit for ignition detection, manifolds are used to provide pilot annular flow, and a J-2 spark plug and exciter is used to initiate the combustion wave in a high efficiency mixing unit.

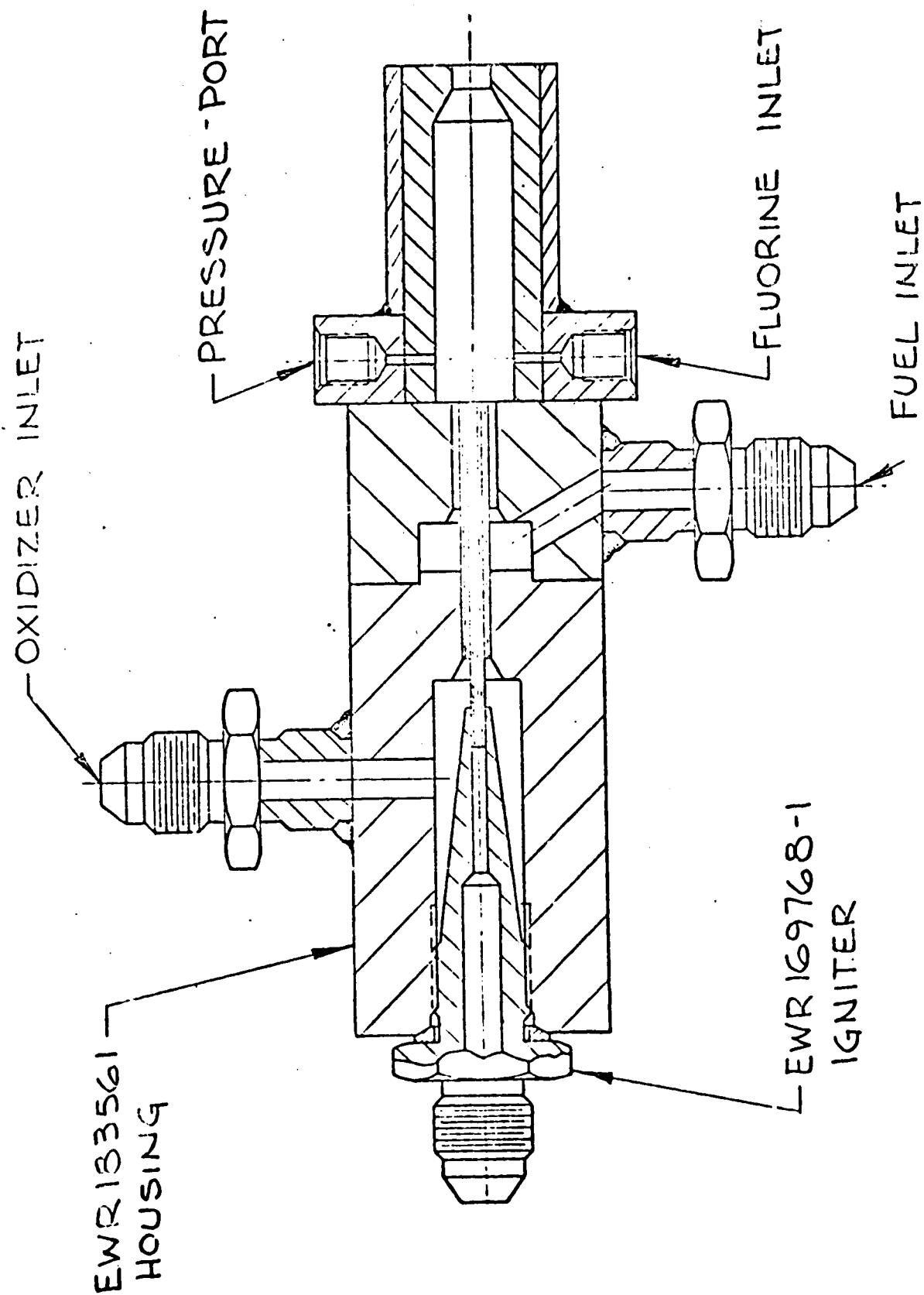
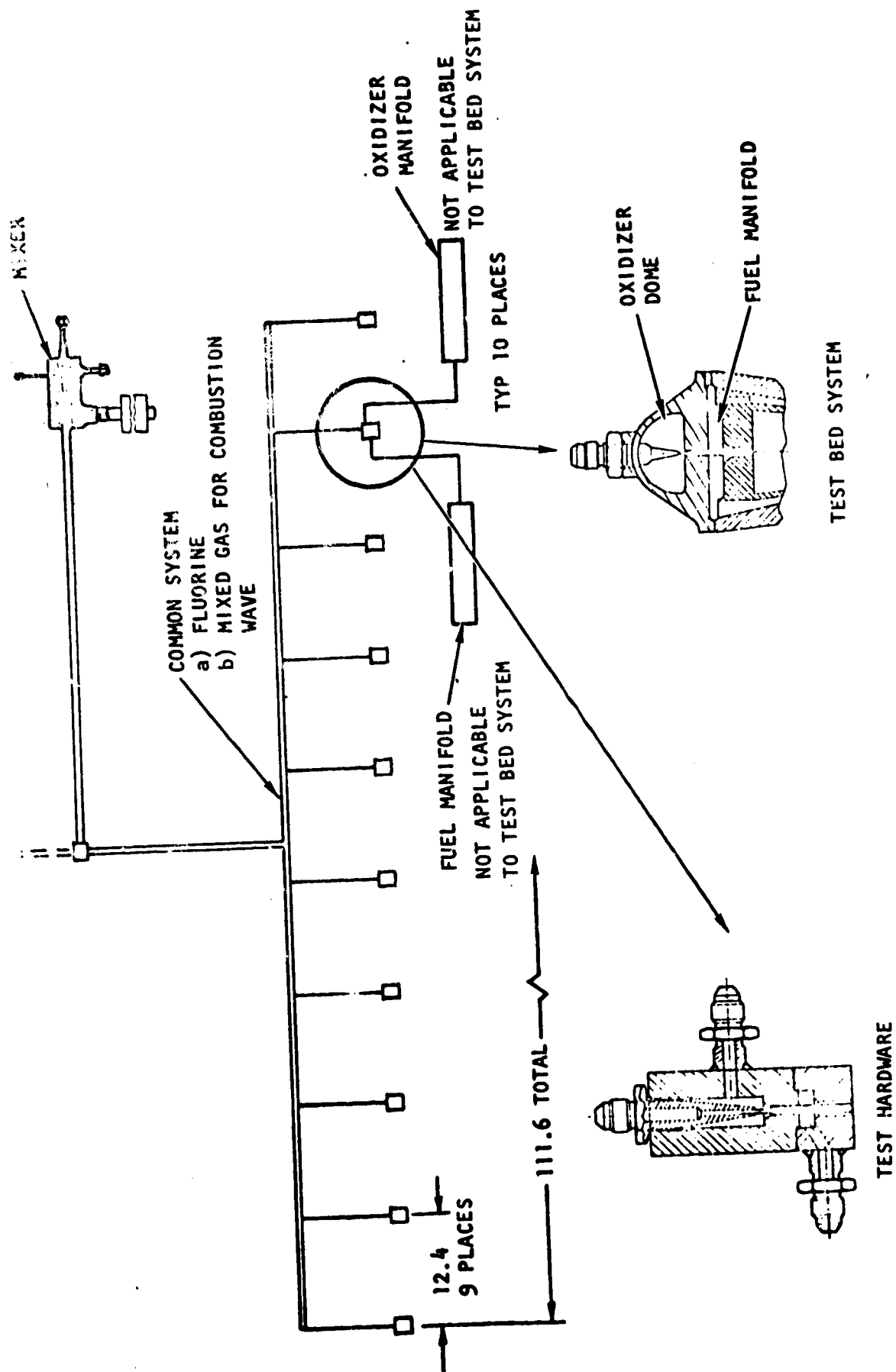


Figure 88. High-Pressure Test Fixture



R-9049

Figure 89. Fluorine-Combustion Wave Interchangeable Ignition System

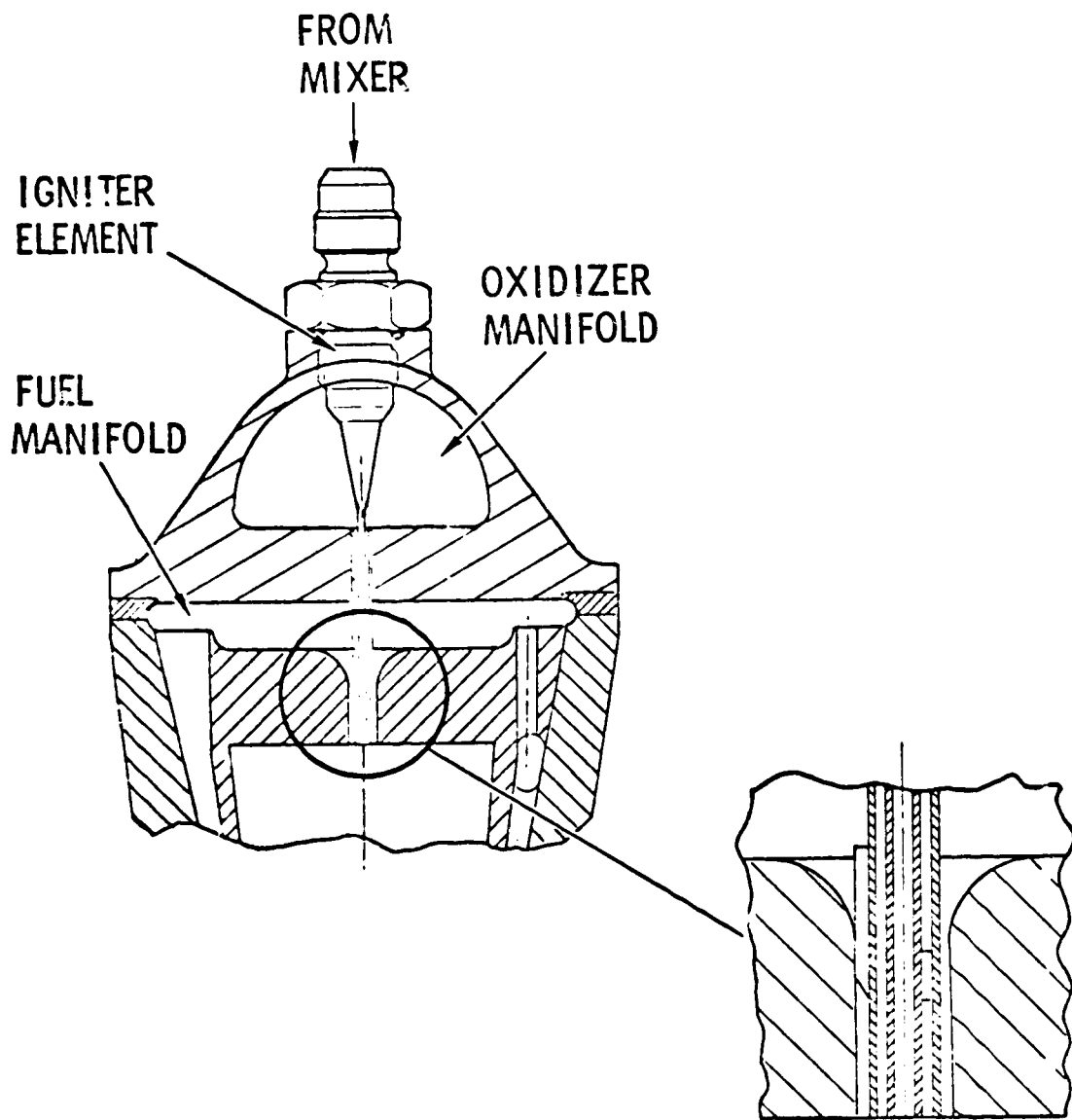
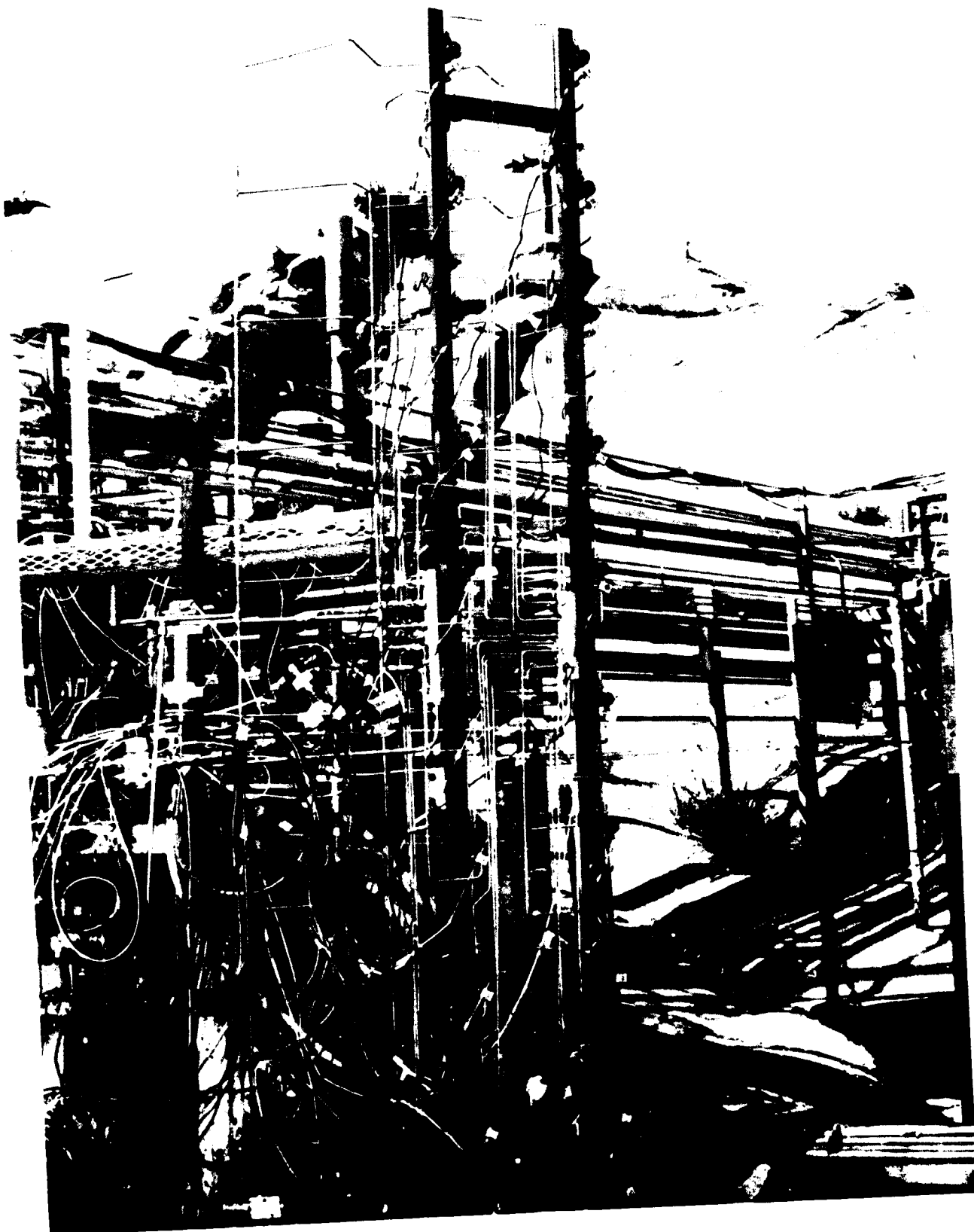


Figure 90. Combustion Wave Igniter Configuration for Segment Testing



5AA21-8/2/71-S1

Figure 91. Combustion Wave Ignition System Test Setup

R-9049
190

Phase II Testing. Three of the 20 elements tested in Phase I were used in the multisegment hardware. The 20-element development mixing unit and J-2 spark plug exciter used in Phase I was also used in this phase. No hardware differences existed between this phase and Phase I except for a coiled hard line providing approximately 7 feet of induction length.

Phase III Testing. The 20 elements and holders mounted on unistruts used in Phase I were installed into a vacuum can at the NAR Los Angeles Division Thermodynamics Laboratory for some additional component tests. The development and a newly fabricated mixer fashioned after the development mixer provided the H_2-O_2 flammable mixture. A newly fabricated spark igniter unit was fabricated for test use. This component was prepared by combining a J-2 type spark plug with an inductive discharge exciter unit. The J-2 spark plug has an 0.050-inch doped, recessed, single gap. The durability of this recessed gap plug is improved over a surface gap due to less exposure to hot combustion gas products. The J-2 plug provides proved high-pressure internal seals (required for engine level testing) which augmented the selection of this plug for use in this application. The spark igniter electrical circuit chosen for use on this unit operates on the principle of storing and transferring electrical energy to the spark plug gap by simple transformer action (inductive discharge circuit).

Direct current input is changed to square wave pulses to finite duration by an oscillator to control a solid-state switch. During the switch "on" period, current flows in the primary winding of the energy storage transformer, the resultant magnetic field storing energy in the transformer's core. When the switch is turned off by oscillator output pulse decay, the transformer winding voltages reverse and increase until sufficient amplitude occurs on the secondary winding to cause spark gap breakdown. The reflected voltage on the primary is limited by a protective diode from exceeding switch breakdown limits. The energy stored in the transformer is then transferred to the spark gap until all energy is dissipated (a portion of it in the transformer, due to residual flux and I^2R winding losses). The cycle repeats at 200 pulses/second.

The smaller and slower changing current of the inductive system circuit (compared to a capacitive discharge system) enables lower power consumption and reduces radiated and conducted RFI. Fewer series circuit elements of this system minimize losses, thus providing a higher efficiency which further permits low input power. It was anticipated that spark discharges of 100- to 1000-microsecond duration would be more likely to ignite the H_2-O_2 mixture at more effective temperature and pressure conditions with lower energy content than the shorter spark discharges (10 to 50 microseconds) utilized in a capacitive discharge system. (Tests performed in Phase III confirm the capability of low-pressure, ambient propellant ignition with this circuit design.) The delivered energy of this circuit has been determined to be 12 millijoules.

Figure 92 depicts this unit. The physical dimensions are ~1.5 pounds, ~2.1 inches in diameter, and 7.5 inches long.

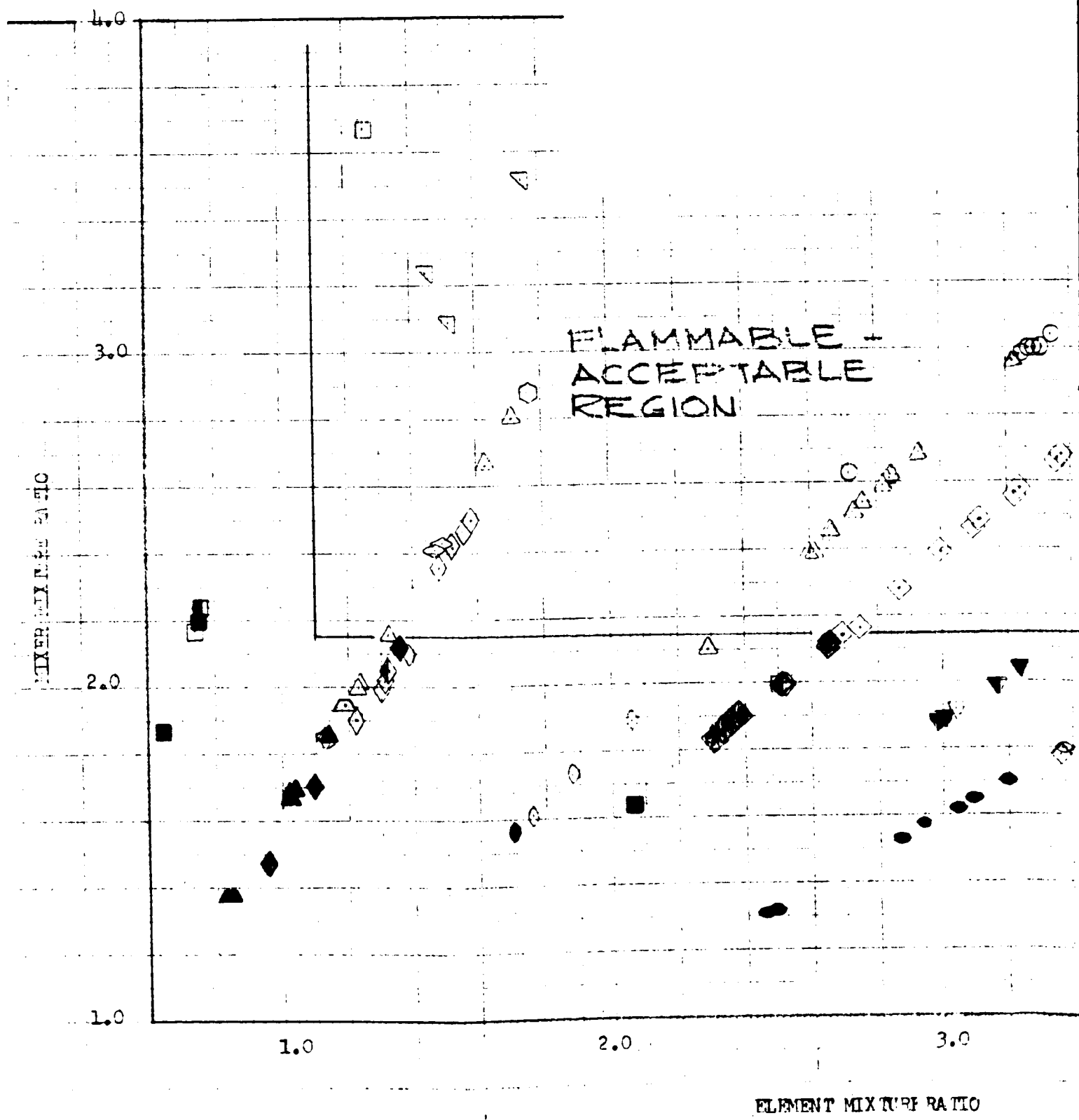
Phase I Results. A total of 142 tests was conducted in this phase to obtain qualitative data. It was necessary to determine ignition or no ignition for various potential configurations for use in test bed No. 1. As a result, no serious attempt was made to provide precise pressure data in this phase. However, Fig. 93 presents the flammable-acceptable region of mixer mixture ratios based on sonic flow measurements. Mixer mixture ratios of 2.15 and greater ignite successfully without exception. Mixer mixture ratios of 1.6 to 2.14 had results of ignition, partial ignition, and no ignition. Mixer mixture ratios less than 1.6 would not establish a combustion wave.

Propagation of a combustion wave was successfully demonstrated through flow passages as small as 0.026 inches. Three tests were conducted on this size element with ignition of a pilot occurring on the two attempted ignitions. The third test indicated wave generation, but no pilot flow was used. No difficulties were noted in these three tests. However, many difficulties were encountered in fabricating an eccentric 0.026-inch element and no operational differences were noted between this configuration and a 0.040-inch element tested under similar conditions as the 0.026-inch element. As a result, nominal 0.040-inch elements, which also demonstrated successful wave generation in many additional tests were selected for use.

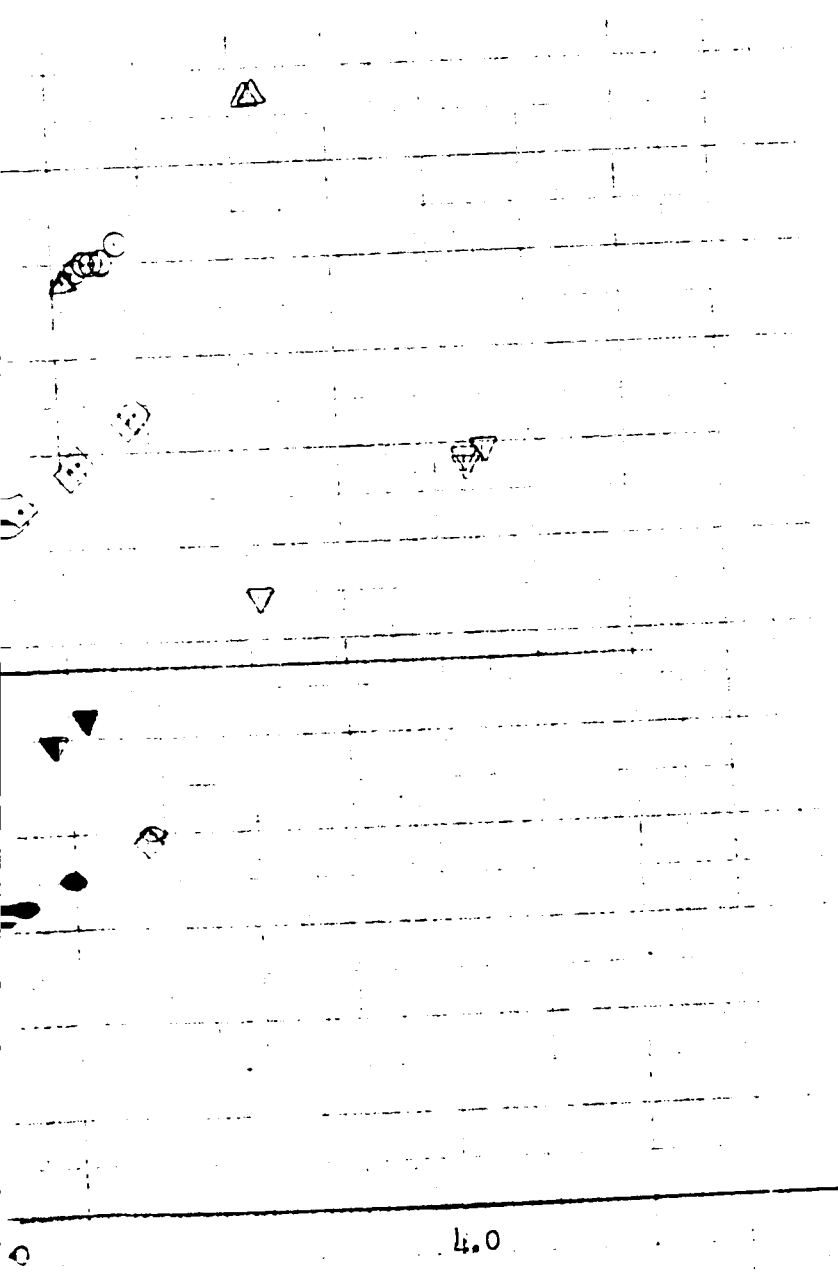


ICT61-8/24/71-C1

Figure 92. Combustion Wave Ignition System Spark Igniter Unit



FOLDBOUT FRAME



RUNS

- ◇ 28-29
- △ 30-62
- ◇ 63-87
- ◇ 88-89
- △ 103-104
- ◇ 90-94
- ◇ 95-102
- ◇ 106-132
- ▽ 133-142
- ▽ 144-149
- 153-161
- 162-169

Shaded Symbols = No Ignition
Partial Shaded Symbols = Partial Ignition

Figure 93. Research Area Test Data, Mixer Mixture Ratio Versus Element Mixture Ratio, Combustion Wave Igniter

R-9049

Three elements with a 0.040-inch center core were tested at various operating points to ensure successful operation in Phase II testing. Sufficient data were obtained to provide assurance of successful pilot ignitions in multisegment testing under tank-head start pressure conditions. No attempts at simulating chilled propellants were made.

The proposed line configuration of the ignition system for test bed No. 1 is shown in Fig. 89. Induction lengths of approximately 4 to 9 feet are presently on the engine as used in the fluorine ignition system. Tests were conducted to evaluate the effects of induction length from 3 to 9 feet. All lengths were determined to be compatible with this combustion wave ignition system.

Three high-pressure tests were conducted to evaluate the durability of the tri-axial element configuration. Element cooling is provided by propellant flow through the three flow passages. The heat flux at the element tip is a function of the combustor pressure and these tests were performed to simulate this heat flux for a duration of approximately 1 second. Fluorine was injected to provide an ignition source, and propellants were flowed at simulated mainstage conditions. No deterioration was noted in the combustion wave element.

Simultaneous ignition of 10 elements (as programmed for test bed No. 2) was demonstrated. Ten elements were mounted on a unistrut as shown in Fig. 94. A spark plug discharging at ~200 sparks/second provided the source for establishment of a flame. All tests indicated wave initiation on the first spark. Figure 95 provides the qualitative test results of this test series. The first frame (right or top) shows no evidence of flame. The second or middle frame (5 milliseconds after the first frame) shows flame on all 10 pilots. In addition, the overboard dump, which was utilized to simulate the 10 additional elements which were not used on this series of tests, shows burning of the exhaust gases. The third frame (an additional 5 milliseconds after the second frame) shows pilot operation on all 10 elements, whereas the flame on the overboard dump has extinguished. This sequence of photos indicates that, in addition to achieving simultaneous pilot ignitions from a single combustion wave,

FOLDOUP MARKER

0 Time

+5 MS

+10 MS



Time

Figure 94. Combustion Wave Ignition System Simultaneous Ignition, 10 Elements

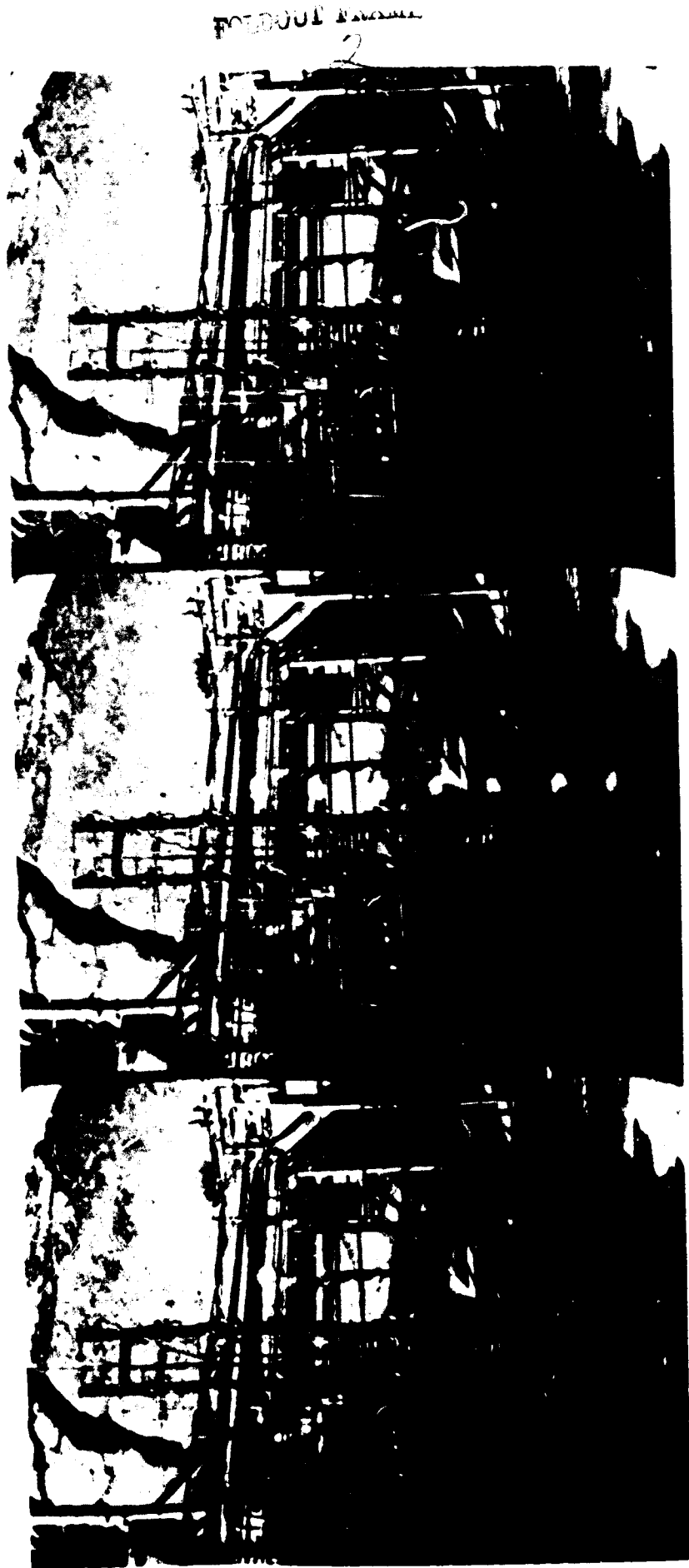
0 Time

+5 MS

+10 MS



FOLDO



Time

Figure 95. Combustion Wave Ignition System Simultaneous Ignition, 20 Elements

a pilot is not needed when a preprimed combustor is to be fed a combustion wave. This sequence was employed in test bed No. 1.

Simultaneous ignition of 20 elements (as programmed for test bed No. 1) was demonstrated. Two unistruts, 10 elements each, were mounted in a test facility as shown in Fig. 91. Sparking was identical to all previous tests. Figure 95 provides the qualitative test results that all 20 elements ignite simultaneously from generation of a single combustion wave. The photo sequencing is the same as described for the 10-element tests and the results are identical.

Testing conducted in preliminary tests at the NAR Los Angeles Division on the combustion wave igniter indicated that a backpressure of approximately 4 psia is required at the pilot for ignition. However, testing conducted to arrive at this conclusion provided the necessary backpressure with a pilot combustor. The effects of the backpressure device on the pilot ignition could not be evaluated and it was unclear what results might occur at ambient backpressures on the pilot without backpressure devices. Tests in this phase confirmed the result that ambient backpressure is sufficient for pilot ignition when flammability levels are correct.

Phase II Results. Thirteen tests were conducted at the Rocketdyne CTL-3 test facility to map acceptable inlet pressures (under tank-head start) for combustion wave ignition followed by combustor propagation. GH_2 and GO_2 were supplied to the test hardware by dropping liquid propellants to the facility main valves. Figure 90 depicts the combustion wave ignition system integrated into test bed No. 1. Integration of the combustion wave ignition system into the multisegment test hardware was identical to this configuration. It can be noted that the sparking does not occur until a minimum of 0.8 second after opening of the main oxidizer valve. The fuel main valve had opened 1 full second prior to this event. This timing ensured adequate pilot and combustor priming time.

Table 14 presents the test results pertinent to the multisegment combustion wave test series. These tests (084-095) were conducted for ignition characterization only. The results are similar to data received from prior multisegment ignition

TABLE 14. COMBUSTION WAVE TESTS ON MULTISEGMENT HARDWARE

TEST NO.	TANK PRESSURES		MIXER CONDITIONS*				COMBUSTOR CONDITIONS						RESULTS		
	OXID	FUEL	W_o	W_f	M.R.	P_c (PSIA)	P_{o_i}	T_{o_i}	P_{f_i}	T_{f_i}	W_o	W_f		M.R.	P_c
975-084	46.0	51.5	.0066	.0021	3.10	21.8	25.5	19.1	19.1	61	.159	.077	2.07	16.1	Satisfactory ignition in all 3 combustors
975-085	44.3	49.2	--	.0018	--	21.3	28.5	18.7	18.7	82	.186	.073	2.55	17.1	Satisfactory ignition in all 3 combustors
975-086	39.1	47.8	.0049	.0020	2.39	20.8	25	19.5	19.5	89	.149	.076	1.96	--	Satisfactory ignition in all 3 combustors
975-087	39.5	53.9	.0055	.0023	2.41	20.8	18.9	20.2	20.2	55	.087	.084	1.03	--	No ignition in all 3 combustors
975-088	51.4	49.7	.0065	.0022	2.99	21.8	31.5	18.5	18.5	92	.223	.070	3.18	17.5	Satisfactory ignition in all 3 combustors
975-089	51.4	44.8	.0065	.0017	3.87	21.8	31.2	17.6	17.6	91	.211	.065	3.20	15.9	Satisfactory ignition in all 3 combustors
975-090	39.8	51.6	.0049	.0023	2.14	20.8	24	20.0	20.0	91	.146	.080	1.8	33.7	Slow ignition in all 3 combustors
975-091	44.7	49.8	.0046	.0017	2.77	29.8	33	19.0	19.0	85	.228	.075	3.0	--	Satisfactory ignition in all 3 combustors
975-092	51.8	50.8	.0060	.0014	4.30	31.8	37	21	21	110	.268	.085	3.14	--	Satisfactory ignition in all 3 combustors
975-093	39.4	50.0	.0026	.0016	1.57	28.8	18.5	19.2	19.2	80	.080	.075	1.07	--	No ignition in all 3 combustors
975-094	40.8	50.3	.0029	.0021	1.36	28.8	20	18.8	18.8	50	.098	.075	1.3	13.6	No ignition in all 3 combustors
975-095	43.8	50.2	.0036	.0021	1.74	29.8	22	19.0	19.0	37	.122	.0767	1.59	14.4	Satisfactory ignition in 2 combustors - no ignition in the third
975-096	44.4	49.8	.0039	.0014	2.89	29.8	28.5	18.6	18.6	67	.186	.073	2.55	14.7	Satisfactory ignition in all combustors

*Mixer propellant inlet temperatures nominally at 555 R for all tests

tests. Combustor mixture ratios greater than 1.1 ignited in all cases where the combustion wave had sufficient energy for pilot ignition. Mixer data indicated the generation of a combustion wave in all tests. Test 094 did not ignite at a combustor mixture ratio of 1.3. The strength of the combustion wave was insufficient to light the main combustors (low MR in the mixer). Testing conducted in Phase III determined the existence of a narrow band on mixture ratio in the premix where a combustion wave is generated but is insufficient to ignite a H_2-O_2 pilot. This condition might have also existed in test number 095 (the calculated mixture ratios in the mixer for both tests 094 and 095 are near to the questionable region determined in Phase III); the mixture ratio of the combustors also was low and either condition might have caused ignition failure.

The capability of the combustion wave igniter to ignite three segments simultaneously was adequately demonstrated. Ignition delays of greater than 1 millisecond were not detected as typically shown on the oscillograph trace from test 085 (Fig. 96).

Phase III Results. A total of 126 tests was performed at the NAR/LAD thermodynamics laboratory on the 20 combustion wave igniter elements used in Phase I. Of these tests, 87 successfully ignited all intended elements, 31 were conducted outside the ignition limits, and 8 were performed to demonstrate the combustion wave without pilot operation.

The mixer utilized in all previous tests was tested at varying inlets; when nominal inlet conditions were encountered, $P_{O_i} = 44$ psia, $P_{f_i} = 50$ psia, the conditions were such that no ignition was obtained. Figure 97 presents the map of this mixer. A new post was fabricated to extend the safe ignition zone. This modification resulted in satisfactory ignition at nominal inlet conditions (Fig. 98).

Mixture ratios in the mixer of 1.6 to 1.9 had unpredictable results; combustion wave generation was successful but pilot ignition was not attained. However,

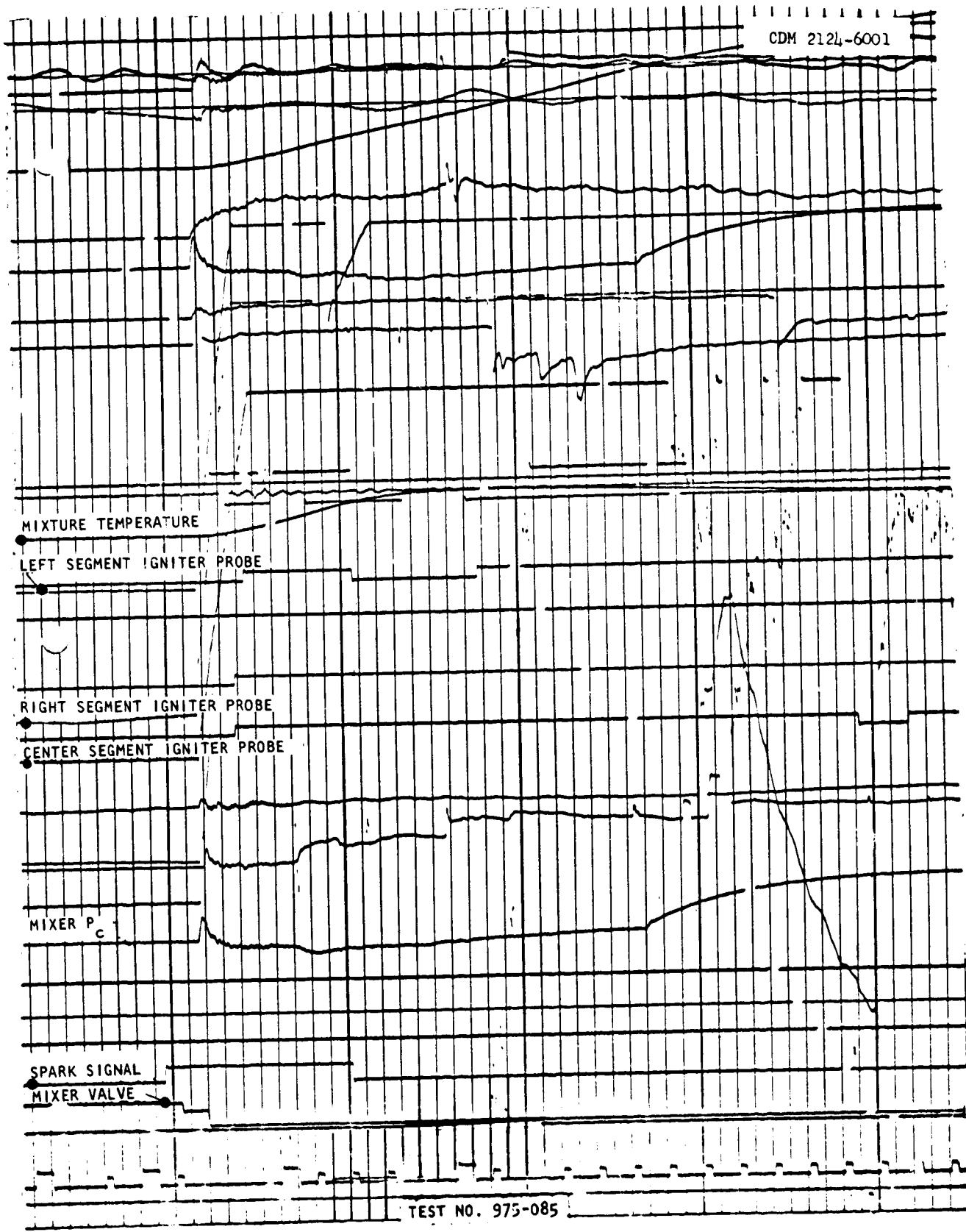


Figure 96. Oscilloscope Trace, Test No. 975-085

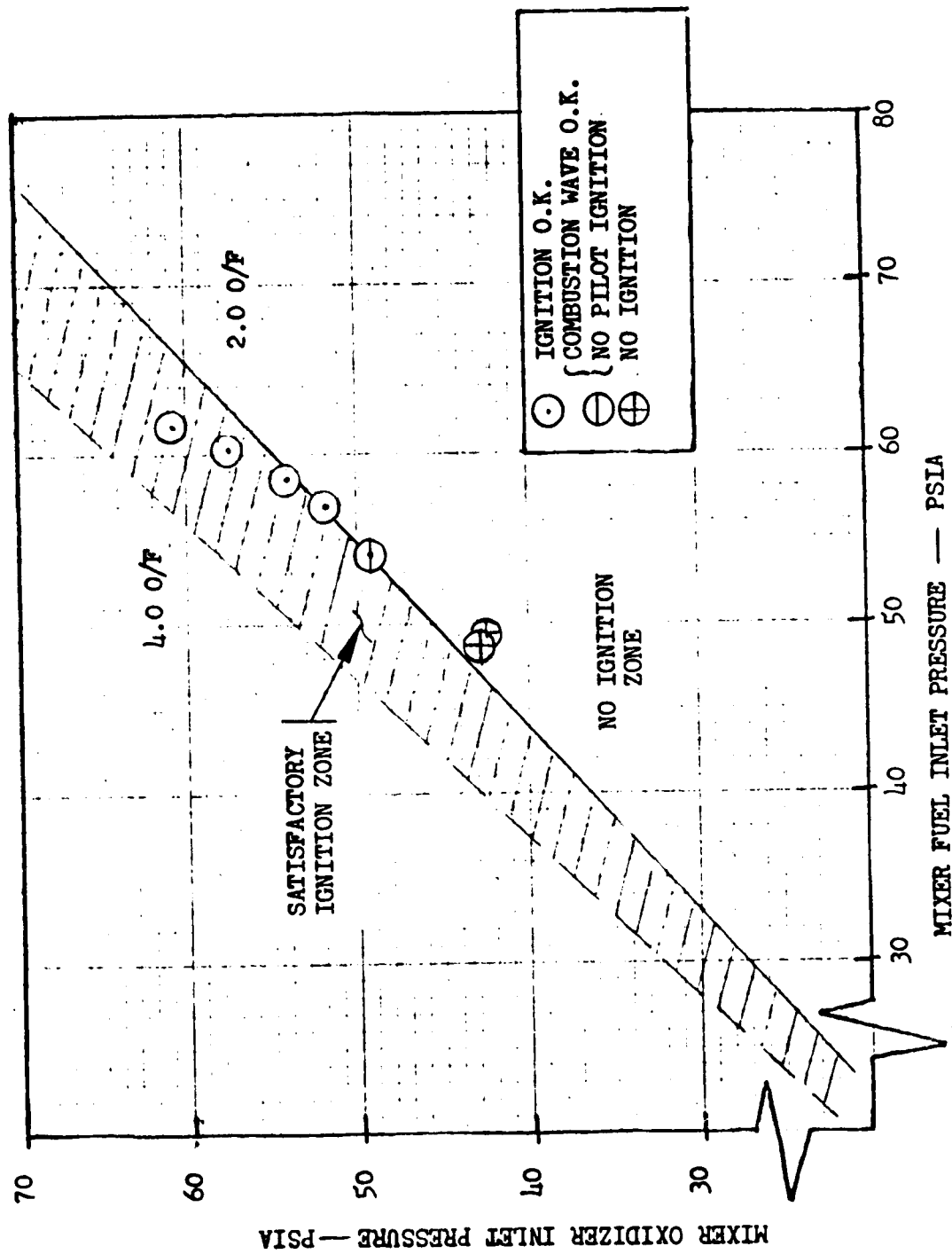


Figure 97. Operating Region for the Development Model Mixer

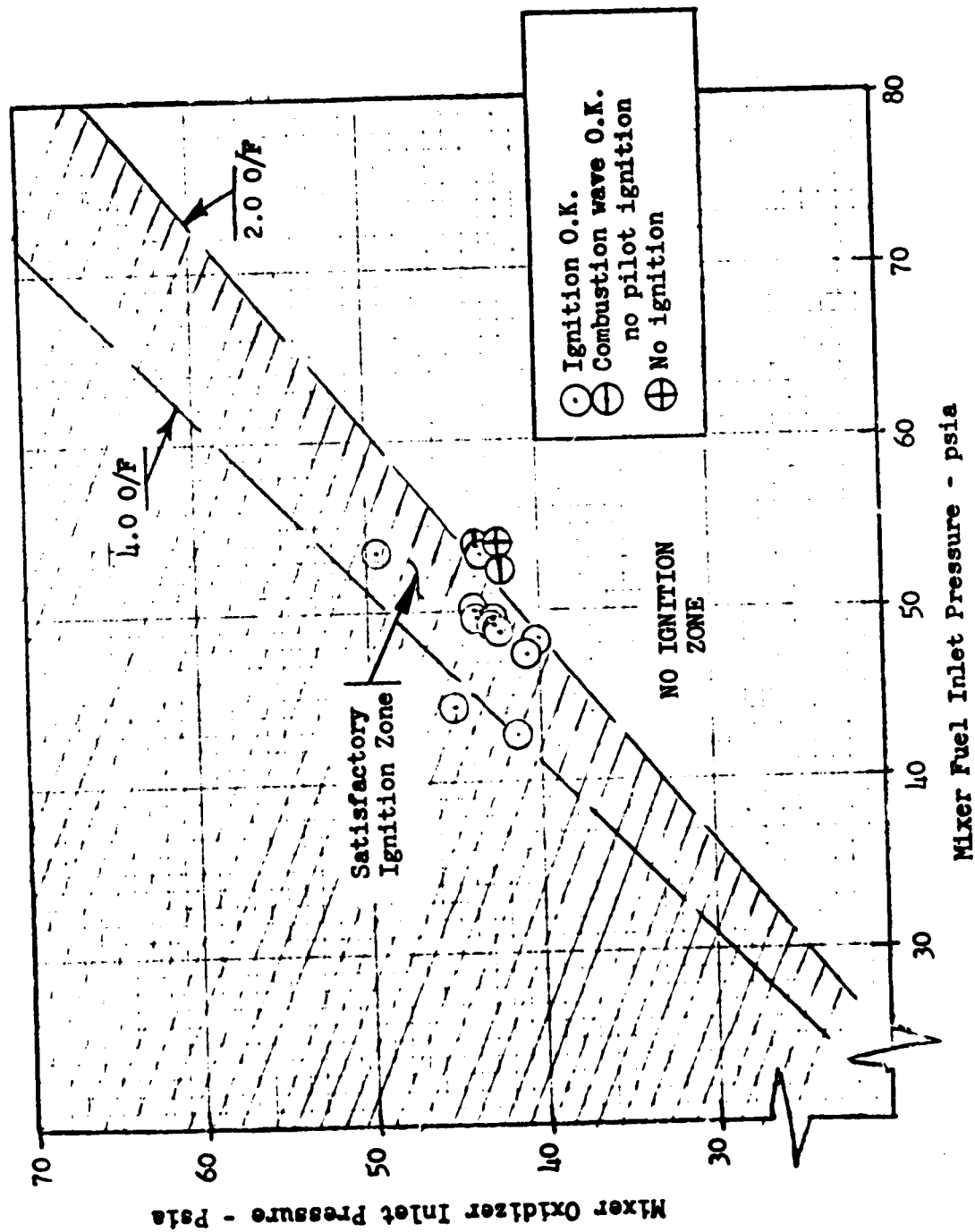


Figure 98. Operating Region for the Breadboard No. 1 Mixer (20-Element Mixer)

mixture ratios in the mixer of greater than 1.9 always ignited all element pilots regardless of pilot operating conditions. Mixture ratios less than 1.6 would not be sufficient for wave generation in all cases.

Ignition was found to occur on the first spark generated by the integrated spark unit. A 10-to-11-millisecond delay exists between the application of 28 vdc to the spark igniter and the first spark generation. This delay was measurable on the data trace of a monitor circuit provided in the exciter circuit. This monitor circuit is closed when current flows across the spark plug.

Backpressure tests were conducted to determine the minimum atmospheric condition for pilot ignition. Earlier combustion wave igniter work indicated some positive pressure was required. Tests in this phase determined that an absolute level of 1.6 psia and greater is sufficient for pilot ignitions of configurations such as those employed in this series.

The combustion wave ignition system concluded sufficient component testing to be considered usable on test bed No. 1. An operating regime map of acceptable inlet pressures to the mixing unit is presented in Fig. 98 and provides all acceptable safe operating points for engine use. Multisegment tests provided data that main combustor and/or pilot operation of mixture ratios of ~ 1.25 or greater provide an ignitable mixture when ignited from either fluorine or combustion wave igniters.

SINGLE-SEGMENT C01 TESTING

The C01 assembly was tested at CTL-3, Cell 18. The C01 combustor assembly was designed to duplicate the breadboard test bed configuration in all respects including the full-length tubular nozzle. In addition, the hot-gas fences employed at each end of the assembly nozzles were installed as part of the C01 assembly. The installation of the segment in CTL-3 was arranged so that the total thrust vector would be oriented horizontally at 1200-psi chamber pressure. The axial centerline of the combustor was canted about 43 degrees below the horizontal.

Cast combustor C01 was one of the initial units in the manufacturing cycle. It was suspected pretest that the unit had a marginal copper bond and therefore marginal structural integrity. The unit was scheduled for component engine firing only. A modified proof pressure test was specified, and two proof pressure series were performed. The initial series consisted of five 2-minute, 800-psig pressurization cycles of all fuel channels. The second series consisted of pressurization cycles of all nozzle fuel channels aft of a plane 0.5 inches above the throat. The first test was targeted for the operating point expected on the engine assembly at minimum PU setting. The second test was targeted for the operating point expected at a nominal PU setting. A list of stabilized test conditions is presented in Table 15. A portion of the combustor wall fractured during start of the second test and no further proof testing was conducted.

Test 975-097 was the first test on the C01 assembly. It was a 10-second test which stabilized at 932-psia chamber pressure and a mixture ratio of 4.86. Table 15 indicates the magnitude of stabilized conditions at various manifolds in the C01 assembly. The nozzle of this assembly also contained several thermocouples and pressure measurements for mapping the nozzle operating characteristics during mainstage. All of these special measurements appear to have functioned properly.

Test 975-098 was the second and last mainstage test with the C01 assembly. Target conditions were 1080 chamber pressure and 5.3 mixture ratio. At about 120 milliseconds after 90-percent chamber pressure, a 2- by 3-inch piece of the NARloy liner blew out of the outer combustor wall nozzle surface, interrupting the normal progress of the test. The piece extended from 7/8 to 2-7/8 inch from the left side plate and from the throat to the exit of the combustor assembly. The test was allowed to continue by the test observer since only several small, short-duration streaks were observed. The streaking did not continue as the test proceeded. The scheduled duration of 50 seconds was accomplished with the assembly in a failed condition. The exposed area of the combustor assembly was film cooled by the reverse flow of hydrogen from the fuel injection manifold through the channels to the throat. The discharge of approximately 20 hydrogen jets was sufficient to protect the uncooled surface.

TABLE 15
STABILIZED TEST CONDITIONS

<u>Parameter</u>	<u>Test 097</u>	<u>Test 098</u>
Slice Time	22.001-23.031	25.009-26.039
Time from 90% P _c	9	10
P _{CIE} , psia	932	789
MR	4.86	11.8
Nozzle Inlet P, psia	1774	1302
Nozzle Inlet T, °F	-384	-390
OCW Inlet P, psia	1639	936
OCW Inlet T, °F	(N.G.)	(N.G.)
Fuel Injection P, psia	1122	830
ICW Outlet T, °F	105.8	-68.6
OCW Outlet T, °F	113.8	-12.6
LOX Orifice D/S P, psia	1068	903
Fuel Inlet flowrate, lbm/sec	3.44	6.96
Fuel Injection Flowrate, lbm/sec	same as inlet	1.72 (based on 097 resistance)
LOX Inlet flowrate, lbm/sec	16.71	20.305
Fuel Tank P, psig	1849	2088
LOX Tank P, psia	1958	1591
Target Conditions		
P _c , psia	940	1080
MR	4.8	5.3
Fuel Tank P, psig	1860	2100
LOX Tank P, psig	1960	1600
Fuel Venturi Dia., in	.399	.399
LOX Venturi Dia., in	.298	.349
Fuel Injection ΔP, psi	188.5	40.5
Fuel Cup ΔP, psi	48.1	-
LOX Injection ΔP, psi	135.8	113.8
LOX Cup ΔP, psi	54.4	-
η_{C*} (P _c)	96.46	N.A.

The failure was caused by a separation in the electroformed copper layers which serve as a barrier to hydrogen contact with the electroformed nickel. The purpose of the barrier is to prevent hydrogen embrittlement of the electroformed nickel.

Secondary damage was sustained by the C01 assembly in test 098. This damage is evaluated to be a result of the major failure of the combustor assembly nozzle wall and not as a result of normal operation. Several areas of distress were observed: (1) the nozzle tube bundle below the failed patch sustained eight major tube splits, several more minor tube splits, and minor hot-gas wall erosion; (2) the left fence sustained several small surface erosions on the hot-gas surface and several "pin-hole" openings to the coolant surface on the tube crowns at the eroded places; and (3) the left fence sustained minor erosion of the last two fence support tips due to "rollover" of the combustion gas over the edge of the fence. All these areas of distress are ascribed to the disturbance of the hot-gas flow field from three sources: (1) the initial blowout and blow away of the failed piece, (2) the disturbance of the supersonic hot-gas flow field by the discharging hydrogen from the exposed channels, and (3) the disturbance of the flow field by the hydrogen jets emanating from the outer combustor wall inlet manifold orifices traveling at nearly right angles to the primary flow field. The NARloy liner exhibits several overheated areas and probable cracks at grain boundaries in the upper combustion zone above the failed nozzle wall. These areas resulted from the interruption of the hydrogen cooling during the time of wall failure and the subsequent operation at elevated mixture ratio.

Stabilized data are presented in Table 15 for test 098 at a time corresponding to the data from test 097. It will be observed that all assembly temperatures and pressures are lower than anticipated for normal operation. Redline device settings, normally maximums, were not exceeded during the 50 seconds of mainstage duration which followed the failure.

As a result of the liner wall failure in the nozzle section, the overboard dump fuel caused an injector mixture ratio of about 12. The break in the wall was located on the outer contour wall below the throat. The hydrogen which was dumped through the opening came from several sources. First, six of the outer contour wall manifold discharge holes to the fuel passage inlets were exposed directly to the hot-gas stream which had a very low static pressure. Most of the fuel dump came from the manifold through these holes (an area of 1.7 in.²). The second source of fuel came from cross flow from the adjacent channel inlet manifold (an area of 0.036 in.²). It is estimated that 5.24 lbm/sec of hydrogen was dumped into the hot-gas stream in the area of the failure. Most of this was dumped in a direction transverse to the local flow field direction. The total hydrogen flowrate of 6.96 lbm/sec passed through the tubular nozzle, about 1.9 lbm/sec passed through the liner cooling channels, and about 1.72 lbm/sec passed through the injector face and participated in combustion.

The nozzle gas-side heat transfer coefficient was increased by mixture ratio and reduced by chamber pressure for a net reduction in gas-side heat transfer from nominal design point. The nozzle cooling side heat transfer coefficient was substantially increased by more than twice the nominal coolant flow. As a result, the nozzle was overcooled and underheated compared to the nominal operating point.

The combustor walls were cooled without failure at the mixture ratio of 12 and the reduced chamber pressure of 789 psia. No surface oxidation on the liner wall was observed after the high mixture ratio operation for 50 seconds.

INJECTOR ELEMENT MIXING TESTS

The obvious alignment and general nature of the combustor erosions experienced during engine tests suggested that the erosions were a function of the injector element liquid mixing conditions. Single-element, cold-flow mixing tests were performed in an effort to define the general constraints of the mixture ratio on the combustion gases next to the combustor walls. Test conditions simulating

breadboard operating points during the ignition phase, LOX dome prime transient to mainstage, and mainstage operation were conducted. Tests simulating typical mainstage operation of the multisegment also were performed. Table 16 is a summary of the test and test conditions performed.

Figure 99 is a schematic of the test setup used. Water was used as a simulant for the liquid oxygen; helium was used to simulate the hydrogen fuel. The simulants were flowed through an actual injector element into a pressurized container with a pressure-regulating device to maintain the chamber pressure at predetermined specific values. Test conditions were established to simulate injection density and velocity at the injector element LOX post tip. Mass flux measurements of the helium were obtained by traversing the element flow field with a stagnation pressure probe to measure local total pressure. The local liquid mass flux was measured by collecting the liquid flow through the probe for a specific interval of time. Samples were taken from the center of a flow field radially outward in increments of 0.1 inch.

Figures 100 through 105 show the results of liquid-gas mass flux and resultant mixture ratio as a function of distance of centerline of the injector element. Figure 100 displays results of a test simulating breadboard engine operation at a chamber pressure of approximately 1200 psi. This test condition produces a zone of low mixture ratio in the outer periphery of the spray field next to the combustor wall.

Figure 101 displays the results of tests simulating the breadboard test conditions at a P_c of approximately 900 psi. As can be seen, the outer zones next to the combustor walls operate at a mixture ratio significantly higher than the injected mixture ratio. Approximately 18 percent of the injected mass is contained within this outer zone.

Figure 102 displays the results from a test simulating the same chamber pressure but with a lower injection velocity similar to that observed in the multisegment testing. The mass is concentrated in the center of the injection spray field with a very low outer zone mixture ratio.

TABLE 16. SUMMARY OF COLD-FLOW TESTS CONDUCTED

Run No.	Hot-Fire Test Conditions Simulated (LOX/GH ₂)				Cold-Flow Test Conditions (H ₂ O/He or He-GN ₂ mix)*						Comments
	P _c , psia	MR, \dot{w}_{Ox}/\dot{w}_f	V _f , ft/sec	V _{ox} , ft/sec	V _{f/V_{ox}}	P _c , psia	MR, \dot{w}_g/\dot{w}_g	V _g , ft/sec	V _g , ft/sec	V _{g/V_g}	
1	680.5	3.43	1746	39.1	44.7	393	3.43	1743	45.2	38.5	Main stage condition
2	905.7	4.35	1650	56.6	29.1	482	4.35	1646	65.8	25.0	Main stage condition
3	567	4.77	1716	49.5	34.7	320	4.77	1712	51.4	33.3	Transition phase condition
4	340	1.65	1745	62.2	28.1	284	1.65	1742	15.8	110.5	LOX dome prime phase condition
5	322	1.68	2402	55.8	43.0	172	1.68	2397	14.7	163.9	LOX dome prime phase condition
6	122	0.23	3450 (sonic)	205	168.5	180	0.23	2867	2.8	1038	Ignition phase condition
7*	905.7	4.35	1168	56.6	20.6	482	4.35	1168	65.8	17.8	Main stage condition; define effect of fuel velocity on mixing; compare with Run No. 2
8	567	4.77	1209	49.5	24.4	486	4.77	1209	51.4	23.5	Transition phase condition; define effect of fuel velocity on mixing
9	567	4.77	1510	49.5	30.5	379	4.77	1510	51.4	29.4	Transition phase condition; define effect of fuel velocity on mixing
10	567	4.77	1912	49.5	38.6	286	4.77	1912	51.4	37.2	Transition phase condition; define effect of fuel velocity on mixing
11	567	4.77	1716	49.5	34.7	328	4.77	1712	51.4	33.3	Transition phase condition; define effect of fuel velocity on mixing
12**	567	4.77	1716	49.5	34.7	328	4.77	1712	51.4	33.3	Define effect of liquid post recess on mixing; compare with Run No. 11**
13	1238.6	6.96	1673	86.4	19.4	519	6.06	1669	100.4	16.6	Main stage condition
14	905.7	4.35	1650	56.6	29.1	482	4.35	1647	65.9	25.0	Tests conducted to define test data repeatability and gas molecular weight (etc.) effects on mixing
15	905.7	4.35	1657	56.6	29.1	321	4.35	1647	65.9	25.0	Tests conducted to define test data repeatability and gas molecular weight (etc.) effects on mixing

* Cold-flow simulants were H₂O/He in all runs except No. 7 and No. 15. An He-GN₂ mixture (65.5 weight percent He) was used to simulate the GH₂ in runs No. 7 and 15.

** Liquid post recess = 0.196 inch. For all other tests, liquid post recess = 0.151 inch.

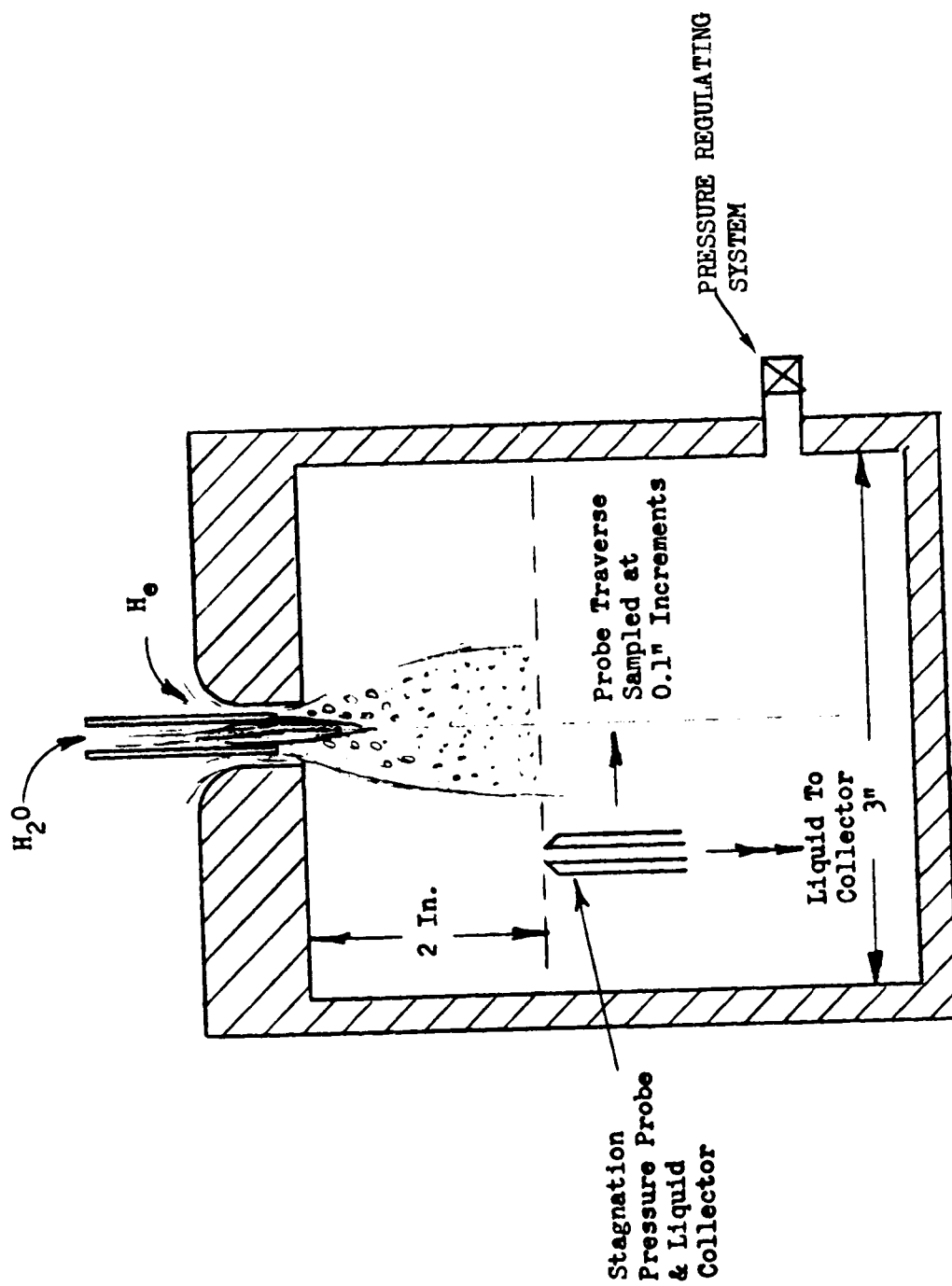


Figure 99. Element Mixing Test Apparatus

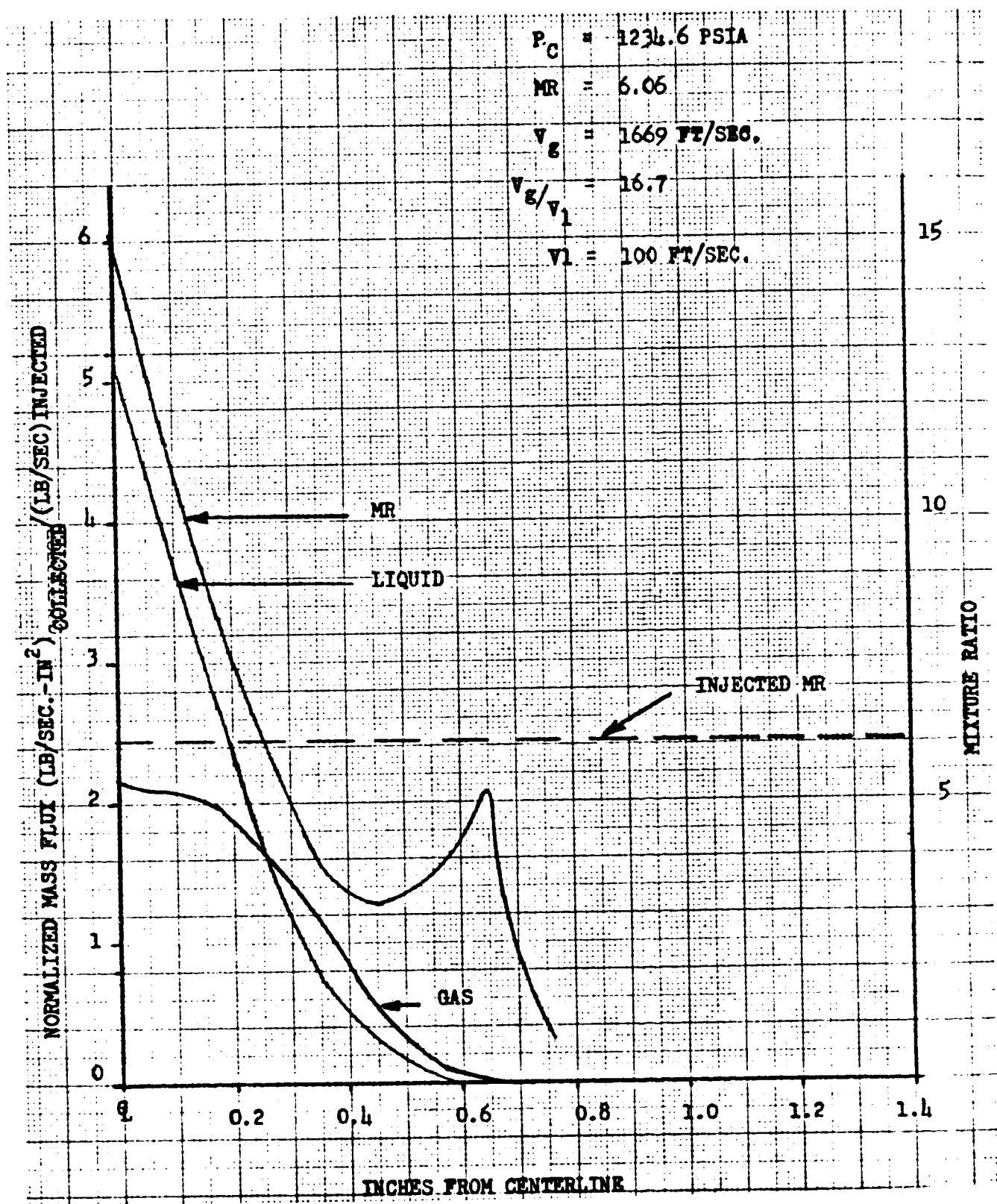


Figure 100. Normalized Mass Flux vs Inches From Centerline
(Run No. 13)

R-9049

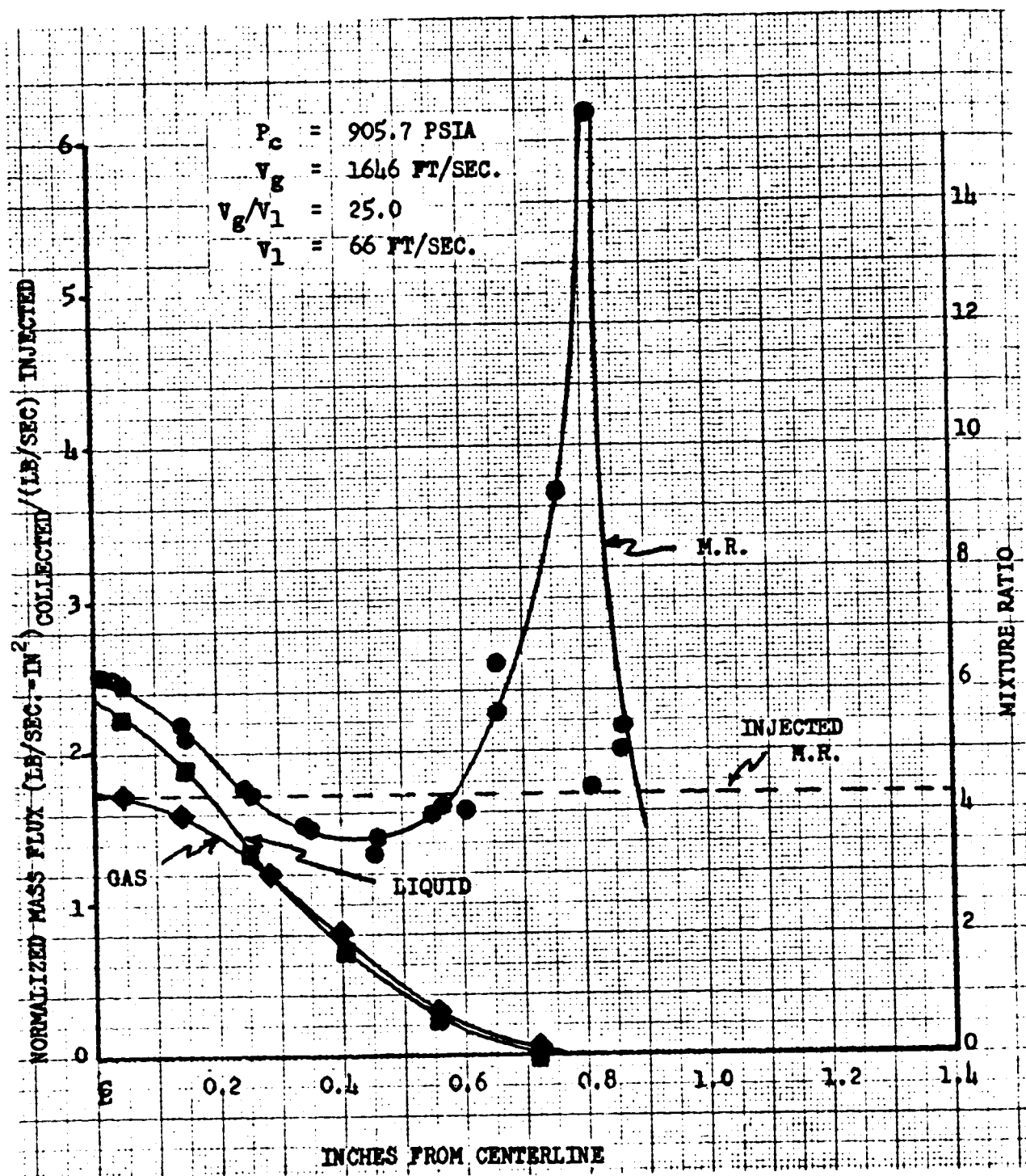


Figure 101. Normalized Mass Flux vs Inches From Centerline

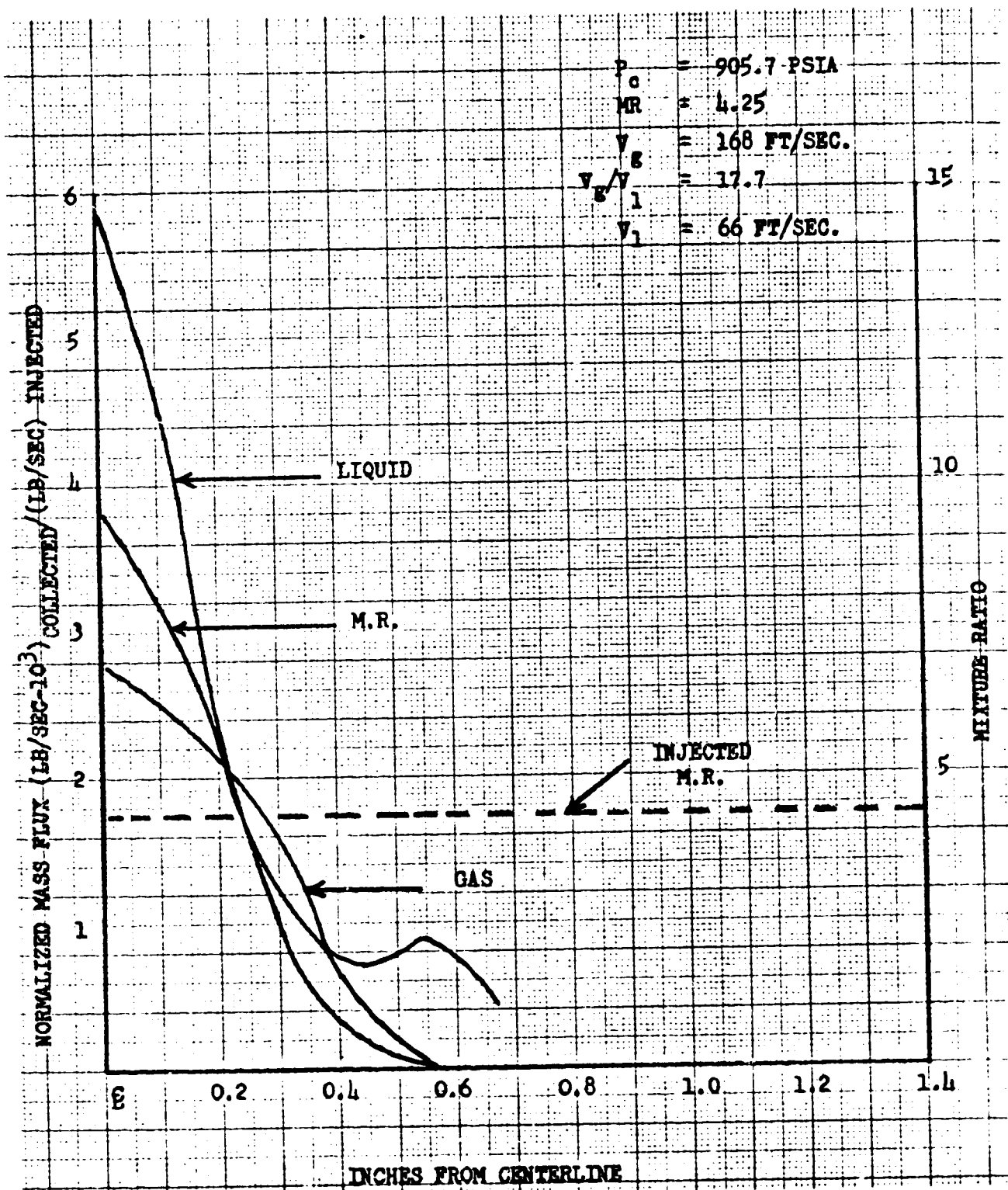


Figure 102. Normalized Mass Flux vs Inches From Centerline
(Run No. 7)

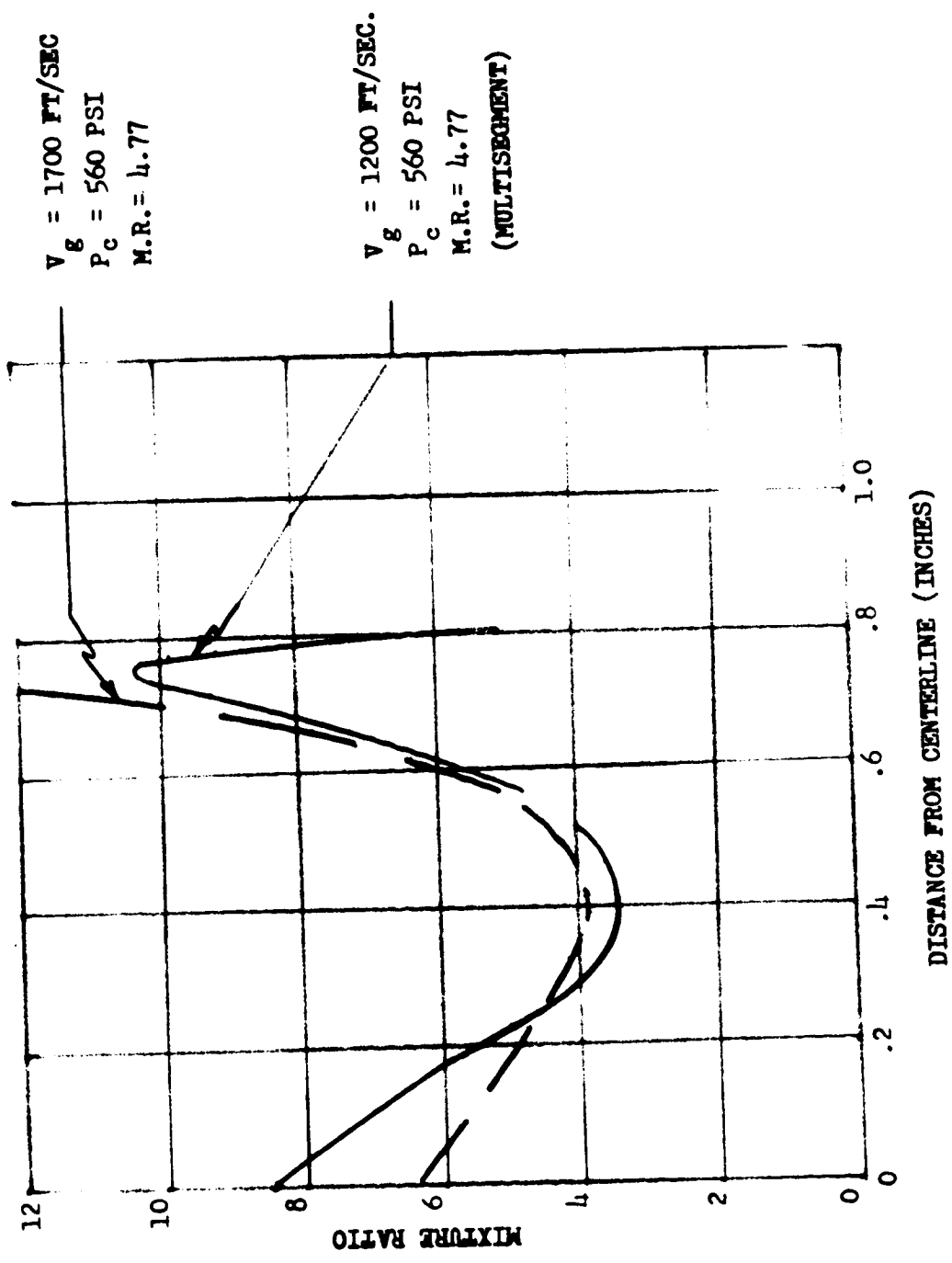


Figure 103. Effect of Fuel Velocity on Mixture Ratio Distribution (Transient Conditions)

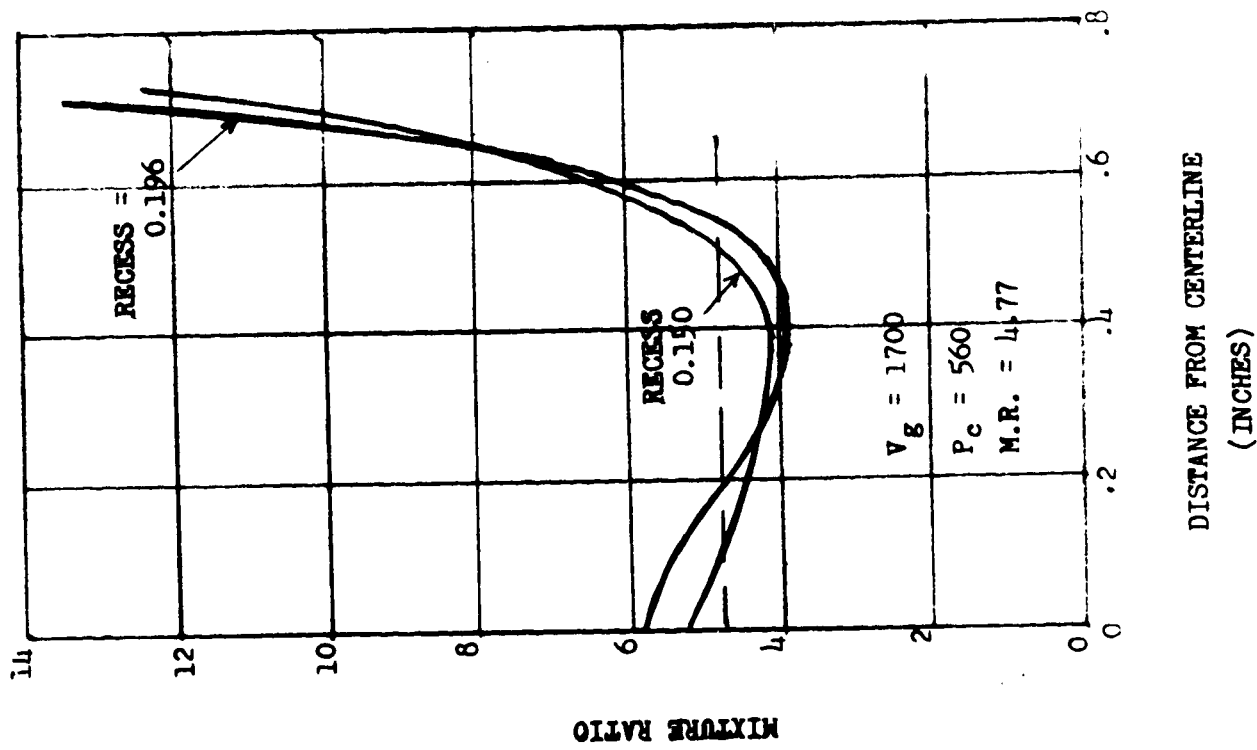


Figure 104. Effects of Recess on Mixture Ratio Distribution

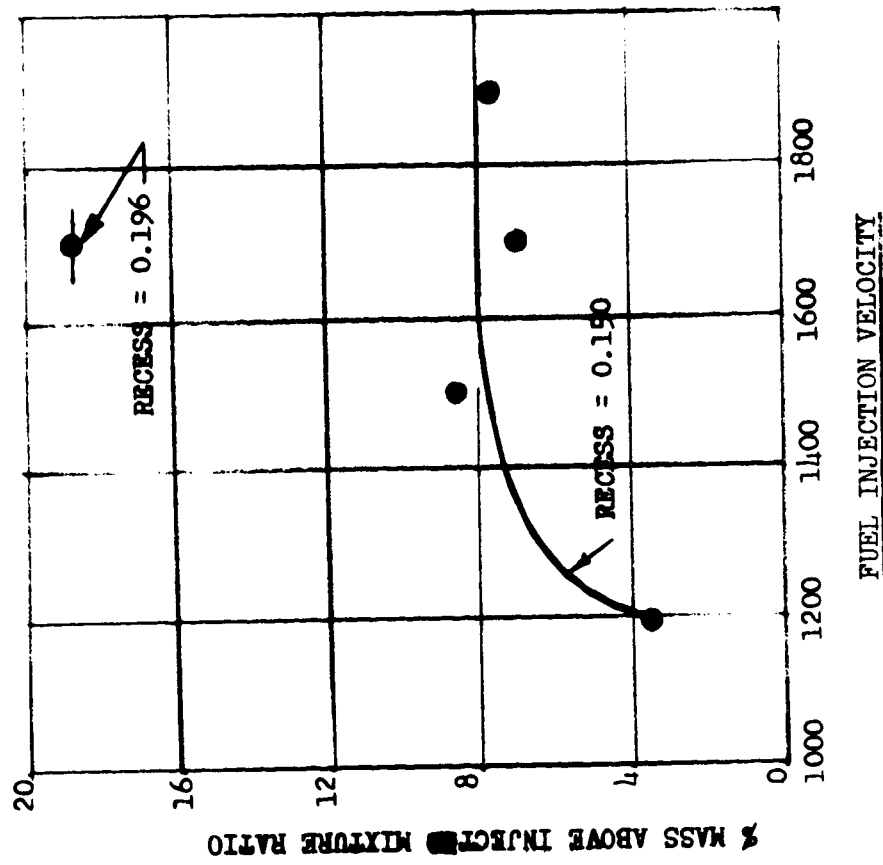


Figure 105. Mixing Results, Transient

Figure 103 displays the results of a test simulating conditions representative of the transition from LOX-dome prime to mainstage of the breadboard engine. The outer zone mixture ratio is quite high under these conditions. Figure 104 displays the results of the same test conditions with the exception that the oxidizer post recess is varied from the nominal position of 0.150 to 0.196 inch. The mixture ratio distribution did not vary significantly between the two conditions.

Figure 105 displays the results of several tests performed for this transient engine operating condition, and displays the percent of the injected mass which was above the injected mixture ratio in the outer zone as a function of fuel injection velocity. The percent mass in the outer zone was nearly constant at 8 percent for fuel velocities in excess of 1500 ft/sec at the nominal recess. Increasing the recess to 0.196 inch increased the mass in the outer zone to 18 percent.

Testing performed at conditions simulating conditions prior to LOX dome prime did not exhibit any tendency for high outer zone mixture ratios.

Summary

The single-element, cold-flow mixing test indicates a strong tendency for the oxidizer to migrate to the combustor walls creating a high mixture ratio content adjacent to the walls during LOX dome prime and transition to mainstage. The steady-state operating conditions of the breadboard engine indicate a similar condition for steady-state operation near 900-psi chamber pressure. Chamber pressures of 1200 psi would have a low outer zone mixture ratio. Lower fuel injection velocities representative of the multisegment test conditions did not produce a tendency for high mixture ratio near the combustor walls. The tests indicate the reverse to be true.

C06 SINGLE-SEGMENT TEST PROGRAM

A single segment (C06) for the breadboard test bed was tested at CTL-3, Cell 18a, to demonstrate its operational capability. These tests were the first tests of

the breadboard configuration segment assembly. The segment was hot-fired without a tubular nozzle, and required conditioned hydrogen (335 R) at the combustor inlet. A summary of the test program is presented in Table 17. All test objectives were satisfactorily achieved.

C06 Single-Segment Hot-Fire Testing

Test 975-039 was a fuel blowdown and fluorine/hydrogen ignition test was conducted to evaluate (1) gas and liquid facility resistance characteristics, (2) automatic sequence checkout, and (3) hydrogen gas/liquid mixing system characteristics. The test was conducted as programmed and all objectives were achieved.

Test 975-040 was primarily a repeat of test 975-039 to determine if an amplifier change and a gain adjustment in the control circuitry would eliminate the pressure oscillations of the gas-liquid mixing system. All test objectives were satisfactorily achieved and the controller modifications stabilized the servocontrol system.

Test 975-041 was the initial mainstage test was performed on component engine C06 on 9 June 1971. Test duration was scheduled for 1 second. The test was terminated at 330 milliseconds by an erroneous chamber pressure redline cut. The hardware was in excellent condition posttest.

Test 975-042 was the initial long-duration test (~40 seconds was attempted on this test). The test was aborted due to failure to achieve ignition detection. The ignition detection thermocouple probe was blown out of the effective fluorine-hydrogen plume during the fuel lead. The ignition detection thermocouple probe was removed and the sequence logic modified in preparation for the next scheduled test because satisfactory ignition under mainstage conditions was demonstrated on test 975-041.

For test 975-043, the objectives were to evaluate performance, stability, and hardware durability as a function of mixture ratio. The mixture ratio was varied by

TABLE 17. SINGLE SEGMENT TEST SUMMARY, SSFL, CTL-3, CELL 18A

Test No.	Test Date	Test Duration (Sec)	Chamber Pressure (psia)	Mixture Ratio (O/F)	Accumulation Test Time		Comments
					Cycles	Seconds	
Blowdown	3 June 71	-	-	-	-	-	Oxidizer System Calibration
975-039	4 June 71	-	-	-	-	-	Ignition Checkout
975-040	7 June 71	-	-	-	-	-	Gas Mixer Servo Control Calibration
975-041	9 June 71	.330	843.8	3.5	1	.330	Erroneous HI-Pc Cutoff
975-042	10 June 71	-	-	-	-	-	Abort-No Ignition Detect Signal
975-043	10 June 71	38.0	877 to 885	3.9 to 4.5	2	38.33	Varied Inlet Temp & MR
975-044	16 June 71	-	-	-	-	-	Abort-MFV failed to open
975-045	16 June 71	10.5	1116.7	4.83	3	48.83	Satisfactory Test
975-046	18 June 71	20.5	1200.5	5.71	4	69.33	Satisfactory Test
975-047	21 June 71	10.5	1192.1	5.62	5	79.83	LOX post Inserts Installed Satisfactory Test
975-048	21 June 71	30.6	1194.3	5.63*	6	110.43	LOX cavitating Venturi Removed. Satisfactory Test

*Estimated

means of increasing the combustor fuel inlet temperature during the test with the hydrogen gas/liquid mixing system. The test duration was 38 seconds. The combustor inlet temperature varied from -120 F to approximately zero F which varied the mixture ratio from 3.9 to 4.6. All test objectives were satisfactorily achieved. Analysis of the test data indicated that:

1. All parameters exhibited 7.5-Hz oscillations
2. During the test, an observer appeared to see one corner of the trailing edge of the outboard side of the left segment glow bright

Posttest leak checks revealed that a copper/nickel bond joint associated with the inner contour wall welded manifold separated. The segment was removed from the test stand and weld repaired in the Engineering Lab at Canoga.

The hydrogen gas-liquid mixing system 7.5-Hz oscillations was determined to be caused by a low resistance in the hydrogen liquid system resulting in a pressure coupling of the gas/liquid system. A sharp-edge orifice (0.422) was installed in the hydrogen liquid system to increase the resistance.

Test 975-044 was programmed to evaluate the engine operating characteristics at 1100-psig chamber pressure and M/R = 5.0, for a duration of 10 seconds. A secondary objective was to determine if increasing the resistance of the hydrogen liquid system would eliminate the pressure oscillations associated with the gas-liquid mixing system. Test 044 was aborted at start because the main fuel valve failed to open.

Test 975-045 was a repeat of test 975-044 and was conducted to evaluate the engine operating characteristics and the gas-liquid mixing system characteristics. The test was satisfactory in all respects and a programmed cutoff was achieved at 10.5 seconds. The feed system coupling experienced on test 975-043 (7.5 Hz) was eliminated by increasing the resistance of the liquid hydrogen feed system. The weld repair of the NARloy to copper bond separation withstood the test environment, and no further damage was experienced in this area or in the nozzle section of the combustor.

1

Test 975-046 was conducted to evaluate linear engine C06 operating characteristics at 1224-psia chamber pressure and an MR of 5.88. The duration of the test was 20.5 seconds, and the test results were satisfactory in all respects. A chamber pressure of 1200 psia was achieved, and no further damage was experienced in the weld repair bond area.

Tests 975-047 and 975-048 were conducted to evaluate linear engine C06 operating characteristics with the 12K-Hz LOX post inserts installed in 67 elements. Test 975-047 was conducted for 10.5 seconds at 1191-psia chamber pressure and an MR of 5.63. The test duration was programmed and the results were satisfactory in all respects.

Test 975-048 was conducted for 30.6 seconds at 1194-psia chamber pressure and an MR of 5.63. This test was conducted without the oxidizer cavitating venturi installed in the facility feed system. The 12K-Hz LOX post inserts remained installed in the injector. The results of the test were satisfactory and all test objectives were achieved.

Test data analysis indicates that the 12K-Hz LOX post inserts and removal of the LOX feed system cavitating venturi reduced the hardware g level in the 12K-Hz frequency range.

HIGH-FREQUENCY STABILITY ANALYSIS

Analysis of the high-frequency data for segment, multisegment, and test bed tests has been conducted in an attempt to fully understand stability characteristics.

SEGMENT AND MULTISEGMENT

A typical segment component test may be characterized by a brief period (transition and early mainstage) with rapidly changing oscillations as equilibrium is sought in propellant properties and hardware temperatures. During this period of time, oscillation frequencies range up to approximately 10 KHz but with primary oscillation content near 6000 Hz. Amplitudes in this period averaged approximately 200 psi peak to peak, while the maximum amplitude recorded during any burst was 600 psi peak to peak. These oscillations are transient in nature and are not of great concern.

This period is usually followed by extended periods of 12- to 14-KHz oscillations, which for the most part do not subside prior to shutdown. These oscillations have been identified as being feed-system coupled with the first hydraulic resonance within the oxidizer injection element. Average amplitudes ranged from 200 to 400 psi peak to peak. The 13-KHz oscillations have not been known to cause any hardware detriment, but were considered an area of concern due to the uncertainty as to their long-term effects.

Accelerometer instrumentation have indicated similar frequencies and also have shown 20- to 24-KHz frequency content. These higher frequencies are probably hardware resonances and are of no concern.

Indications of transverse acoustic oscillations have been observed in some tests, but these have been confined to start transients and tests at extreme off-nominal operating or hardware conditions. These oscillations are not a problem to testing with breadboard linear engine hardware at normal operating conditions.

Throughout the period of segment testing, the 13-KHz oscillations were a prime interest, and several hardware modifications were made in an attempt to cause attenuation and decoupling. These oscillations were thought to be coupled between a hydraulic resonance within the oxidizer injection element and the combustion process within the fuel cup recess. Modifications attempted consisted of retuning of the oxidizer element hydraulic response through the use of oxidizer post inserts, elimination of a potential feed system driver in the flow metering cavitating venturis, and retuning of the frequency of maximum combustion gain through elimination of the fuel cup recess.

Early multisegment tests were inconclusive in determining the effect of oxidizer post inserts on the 13-KHz oscillations, but later tests with both two and single segments firing indicated the inserts were effective in reducing oscillation amplitudes in oxidizer injection pressure by as much as an order of magnitude.

It was thought that the flow metering cavitating venturis could be generating noise within the oxidizer feed system which, in turn, could be supplying all or part of the energy driving the element hydraulic resonance. Removal of the venturis, however, proved ineffective in attenuating the 13-KHz oscillations.

DISCUSSION

In this section, the high-frequency test results from a typical linear multisegment component test are characterized. The oscillation phenomena and hardware variations identified as being the most significant have been given detailed analysis and are discussed. Because of the significant hardware configuration differences in the 001 segment, results from this series of tests are discussed separately.

CHARACTERIZATION OF STABILITY FOR A TYPICAL TEST

Test No. 975-008 was selected for detailed analysis, as it represented an instance in which three segments were run simultaneously at nearly nominal operating

conditions. This test is considered to represent the oscillation content for the normal linear engine including any interaction effects between the segments, while excluding any effects of subsequent stability aids or off-nominal operating conditions.

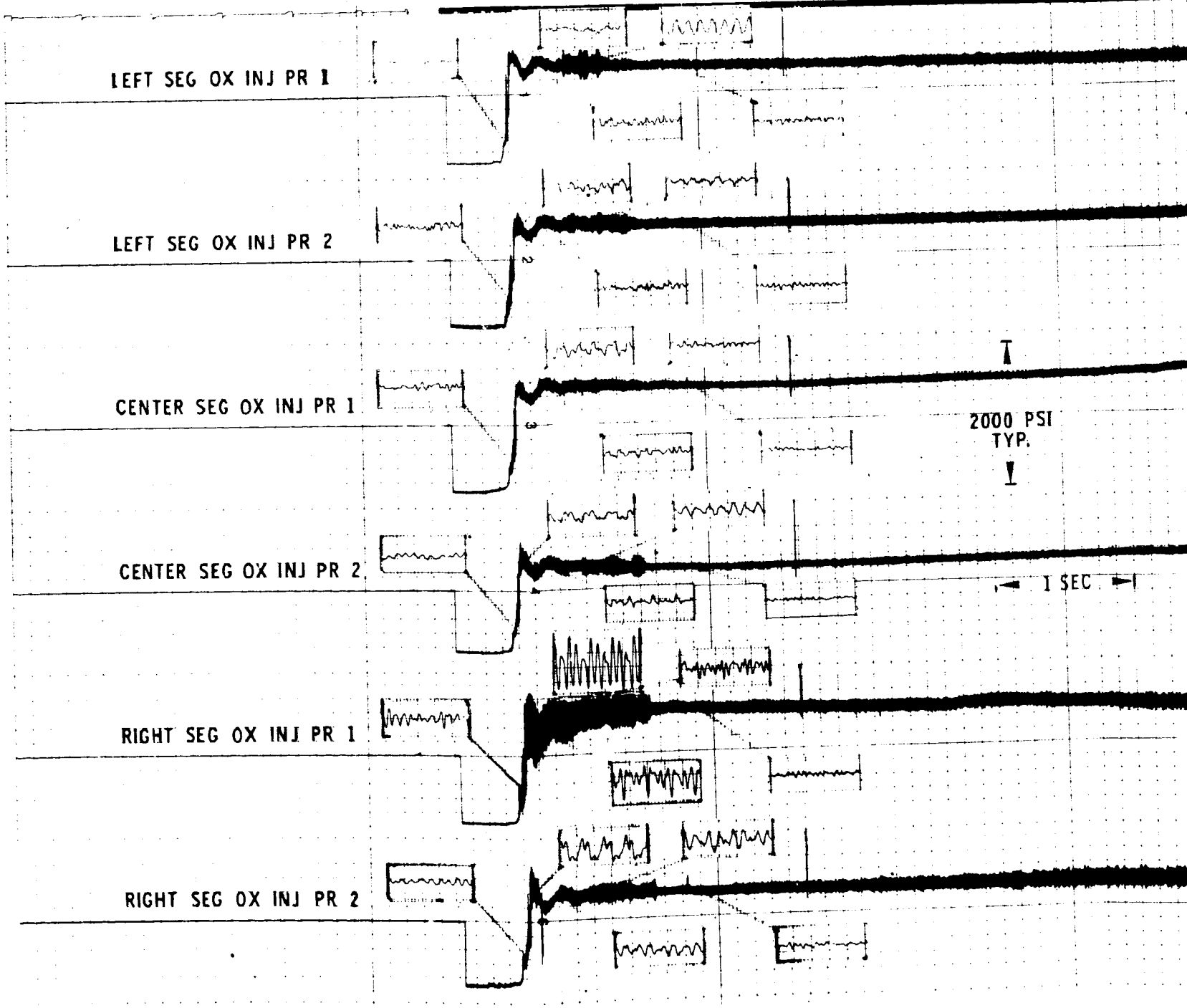
The oscillation profile of test No. 008 may be best typified by its lack of consistency during approximately the first second of operation. The oscillation profile for this test is shown in Fig. 106. The time scale has been greatly compressed in this figure to allow presentation of an overall view of the oscillation amplitude for the entire test. Because there are normally no direct dynamic chamber pressure measurements in the linear hardware, the oxidizer injection pressures are used as the best indication of oscillation content within the individual combustors. These pressure measurements have been provided at both ends of the oxidizer dome in each segment. The lack of consistency mentioned earlier is readily observed in Fig. 106, as short expanded sections of records are shown for each of the parameters at several times during the test.

The first expanded section shown is during the start transient when the segments had reached approximately 25 percent of full chamber pressure. At this time, all of the segments showed 8 to 10 KHz of fairly low amplitudes; however, the oscillations were somewhat higher in amplitude and coherence in the right segment. As the engine progressed into mainstage, the right segment indicated a stronger burst of oscillations with primary frequencies of 3000 and 9500 Hz. The center segment had oscillations of lower amplitudes at 3000 to 4000 Hz, while the left segment displayed less coherence. The oscillation content in each of the segments continued to change until approximately 0.9 second after the achievement of full chamber pressure. Frequent bursting with a primary frequency of 6000 Hz was noted in all of the segments during this time. Average amplitudes during the early part of mainstage were approximately 200 psi peak to peak, while maximum amplitudes during any short burst were 600 psi peak to peak.

FOLDOUT FRAME

FOLDOUT F

BRUSH INSTRUMENT



FOLDOUT FRAME

BRUSH INSTRUMENTS DIVISION, GOULD INC. CLEVELAND, OHIO PRINTED IN U.S.A.

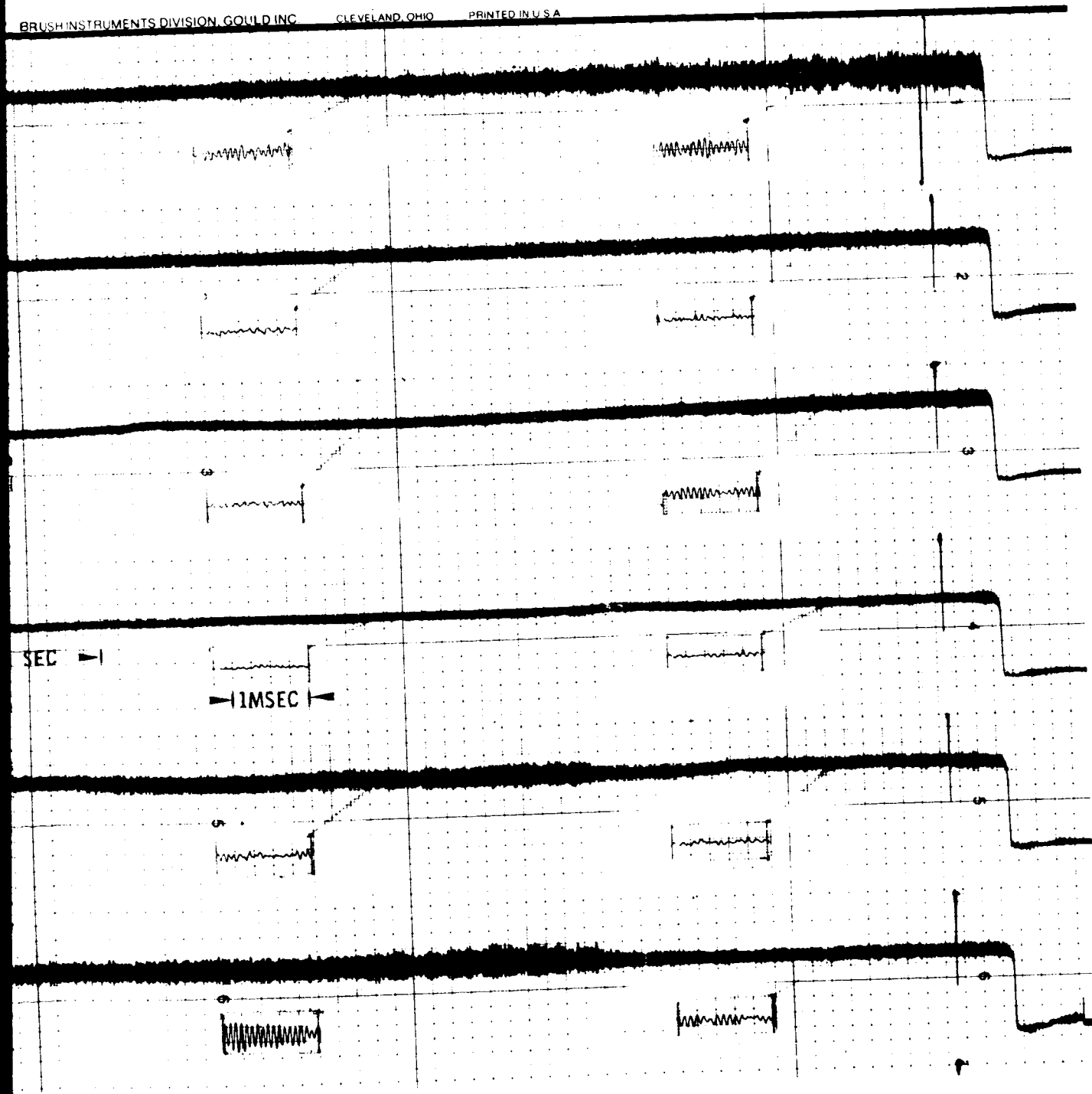


Figure 106. Stability Characteristics, Multisegment Test 975-008

At 0.9 second, rapid damping of these oscillations was evident in the traces from each of the segments. From that time to cutoff, the left and center segments indicated a very gradual growth of oscillation level from nearly negligible amplitudes to as high as 400 and 200 psi peak to peak, respectively, just prior to engine cutoff. During this same period, the frequency increased from 12 to 14 KHz. This same phenomenon was occurring in the right segment until approximately 7.5 seconds into the test, at which time the oscillation amplitude greatly reduced. This was accompanied by an indicated reduction in resistance for both the oxidizer and fuel injection elements and is thought to be a result of the flame moving outside the fuel cup recess. This flame position and its relation to the 12- to 14-KHz oscillations will be discussed more fully in the section of this report concerned with high-frequency, feed-system-coupled oscillations.

FEED-SYSTEM-COUPLED OSCILLATIONS

The primary mode of oscillation in the linear segment hardware in the multisegment and single-segment testing was a sinusoidal oscillation at frequencies of 12 to 14 KHz. It was quickly recognized that this frequency corresponded to the first resonance of the oxidizer injection element, and an investigation was pursued to identify the complete mode (feedback loop) of the oscillations and to effect a solution for their elimination.

The 13-KHz mode of oscillation was thought to be similar to the 4400-Hz oscillation phenomenon experienced during development of the J-2S engine, and is shown graphically in Fig. 107. In this schematic, a chamber pressure perturbation causes a change in injected flowrate as dictated by the response of the oxidizer injection element, which may or may not result in a change in gas generated by the combustion process, depending on the response characteristics of the combustion process. If the combustion chamber has sufficient response, a subsequent pressure wave is generated which then may cause the process to repeat. For the oscillation to grow, each box within the schematic must have sufficient gain and proper phase shift so that the total loop gain will be greater than unity and that the pressure is fed back with the proper phase shift for reinforcement of the subsequent cycles.

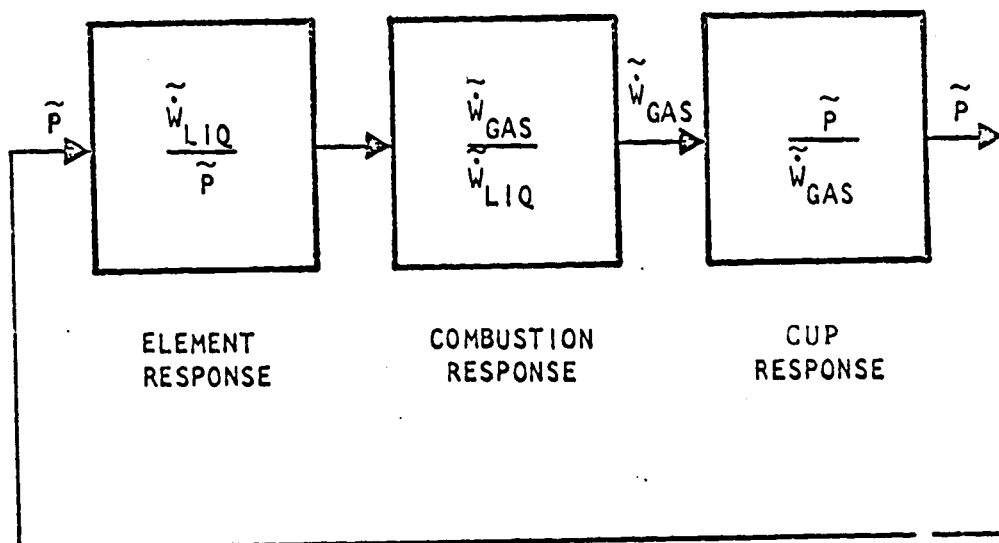


Figure 107. Injector Element Feedback

In the J-2S 4400-Hz phenomenon, the small amount of combustion within the cup recess was sufficient to cause completion of the feedback loop and, hence, main chamber combustion and acoustic response were not required. This provided a combustion process with a short enough time delay to support the relatively high frequency, and an algebraic chamber (cup) response.

The combustion response for a typical linear segment test is shown in Fig. 108. This figure shows that the combustion response in the cup region is capable of supporting oscillations in the region of 5000 to 23,000 Hz. The cup break frequency is above 14 KHz and, hence, pressure is generated in a steady-state (linear) manner to support these oscillations. Conversely, the entire chamber combustion response is at frequencies below 3000 Hz, thus excluding the main chamber from the 13-KHz oscillations.

From an analytical standpoint, the 12- to 14-KHz linear segment oscillations fit the model of the J-2S 4400-Hz phenomenon. Further substantiation of the 12-KHz mode of oscillation was found in the right segment in multisegment test No. 975-008. At approximately 7.5 seconds into the test, a slight step upward in chamber pressure was experienced while the indicated resistances across both the fuel and oxidizer elements decreased. A significant reduction in 12 to 14 KHz was noted in that segment at the same point in time, while the oscillation content appeared unchanged in the other segments. This phenomenon can be seen quite clearly in Fig. 106 and 109. In the second figure, frequency from 5 to 15 KHz is shown along the abscissa, while amplitude is shown as a vertical deflection. Each horizontal line represents a subsequent time slice during the test. It is apparent that oscillations of 12 KHz initiated early in the test in all segments and, as operating conditions changed, these oscillations progressed to a frequency of 14 KHz. These oscillations then greatly reduced in the right segment at 7.5 seconds, but continued in the center and left segments. This phenomenon is thought to be indicative of the flame moving outside the cup region, causing a reduction in cup ΔP and a concurrent shift in the cup combustion gain in that segment. The result is a large reduction in oscillation amplitude. (Conditions within the linear engine

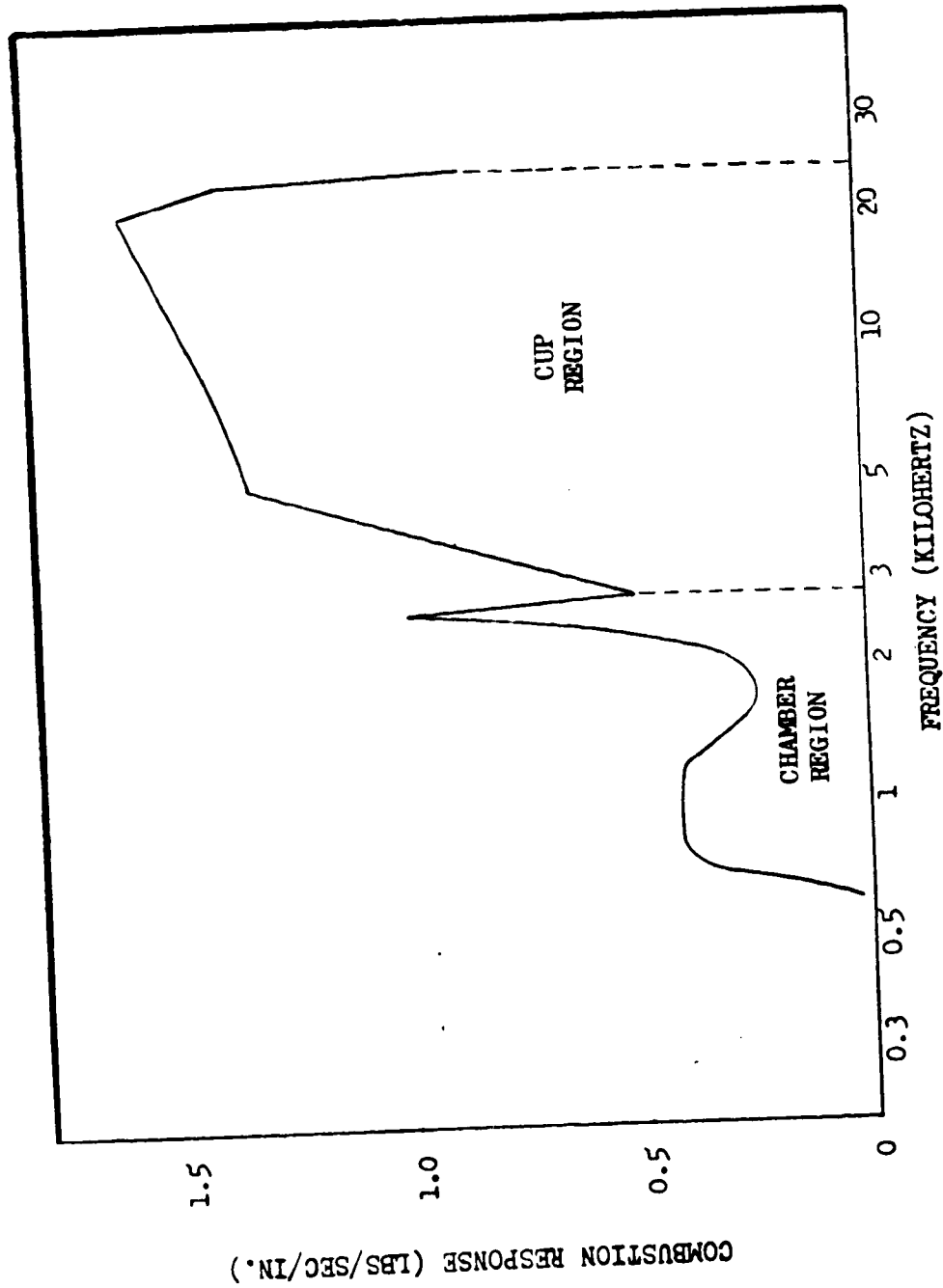
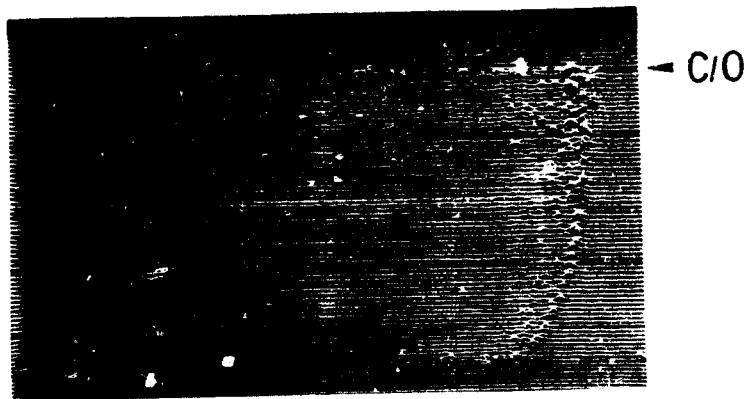
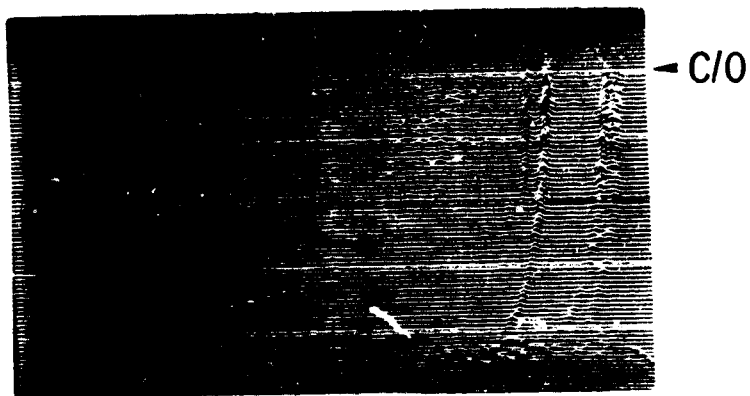


Figure 108. Linear Engine Combustion Response

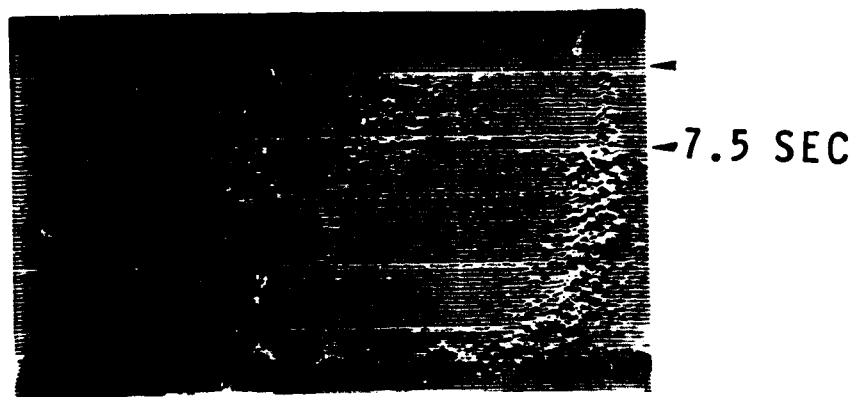
LEFT SEG



CENTER SEG



RIGHT SEG



5 10 15
FREQUENCY (KHZ)

Figure 109. Oxidizer Injection Pressure, Test No. 975-008

cup recess are marginally conducive to sustained burning and, therefore, this observed shift in "flame position" may not be totally unexpected.)

There are several approaches toward elimination of oscillation phenomena of the type represented by the linear segment 12- to 14-KHz oscillations. Each of these attempts involved reducing the gain of the coupled feedback loop by either detuning (changing the resonant frequency) of the oxidizer elements or combustion process, by adding dissipative resistance (ΔP) to the loop, or combination of both.

Oxidizer Post Inserts

In approaching oscillation phenomena of this type, the gain of the feedback loop may be decreased below unity by sufficiently reducing the gain of any of the elements combined to form the complete loop.

The J-2S oscillations were approached with success by changing the response and resistance of the oxidizer injection elements (posts) to reduce the gain at 4400 Hz. This same approach was taken during the multisegment testing by placing inserts within the oxidizer posts. The effective change in the post response is shown in Fig. 110 .

Results of early testing with oxidizer element inserts during the multisegment program indicated that there was an improvement in stability in the frequency range of 12 to 14 KHz, but a quantitative assessment was not obtained due to general instrumentation difficulties of measuring oscillations of relatively low amplitudes and very high frequencies while interpreting interaction effects between the segments.

A definitive evaluation of the effect of oxidizer post inserts was obtained during subsequent multisegment testing in tests No. 975-081 and -082. The left segment was not run for these tests, as the fuel cups had previously been flared to produce zero oxidizer post recess and would have served only to obscure the data from the unmodified elements. Test No. 975-081 was conducted with inserts

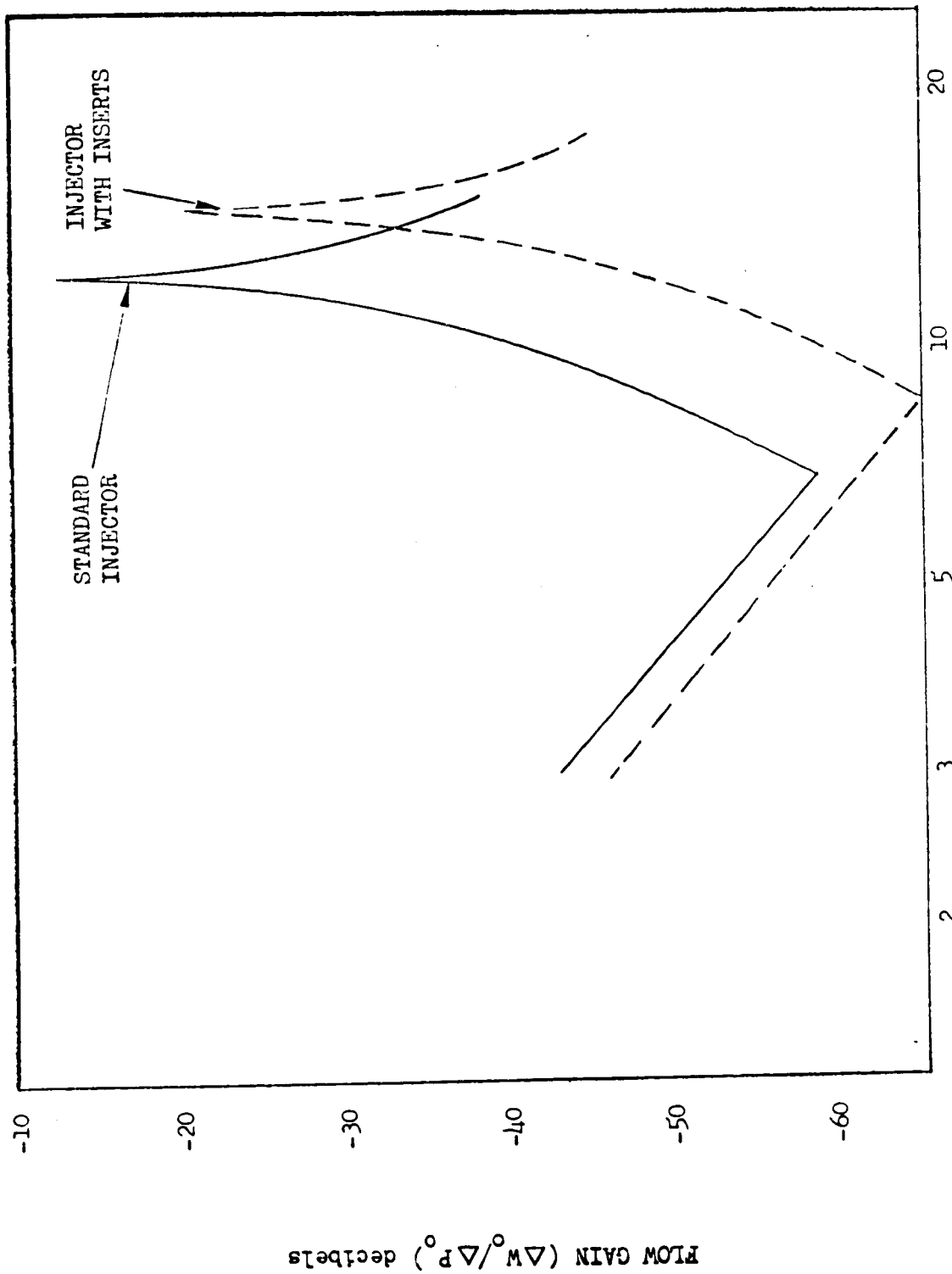


Figure 110. Hydraulic Response

installed in both of the active segments, while the inserts were removed from the right segment for test No. 975-082. The results of these tests are shown in Fig. 111, where it may be noted that neither segment showed significant oscillations with the inserts installed. When the inserts were removed from the right segment for test No. 975-082, significant coherent oscillations with a predominant frequency of 13.5 KHz were observed in both oxidizer injection pressure measurements in the right segment, while the center segment (which had oxidizer element inserts) indicated no significant oscillation content. Oscillation amplitudes within the right segment oxidizer manifold reached a maximum of approximately 400 psi peak to peak when the inserts were removed.

Further quantitative evaluation of the effect of oxidizer post inserts was obtained during the linear engine C06 component tests.

High-frequency data from tests 975-043 and -045 through -047 were reviewed to determine the effect of oxidizer post inserts on high-frequency oscillations in the range from 10,000 to 15,000 Hz. Tests 043 and 045 were conducted at chamber pressures varying from approximately 880 to 1120 psia and mixture ratios from 3.9 to 4.8. Tests 046 through 048 were conducted at approximately 1200 psia and mixture ratios of 5.6 to 5.7. Inserts were installed in the injector oxidizer posts prior to test 047.

The data from these tests (and test 048 in which the oxidizer feed system venturi was removed) were subjected to sonic spectral analysis. The data from tests 046 through 048 were analyzed using real time spectral analysis techniques, where the frequency spectrum of interest is presented as nearly continuous function of time (Fig. 112). Frequency is scaled from 10,000 to 15,000 Hz along the abscissa. Vertical deflections represent the relative amplitude of the frequency component. Each line progressing up the ordinate represents approximately 0.5 second of test duration.

The predominant oscillation frequency tended to increase from test to test in tests 043, 045, and 046. Chamber pressure was increased progressively in each

LEFT SEG. OXID. PRES. #1 (INACTIVE)

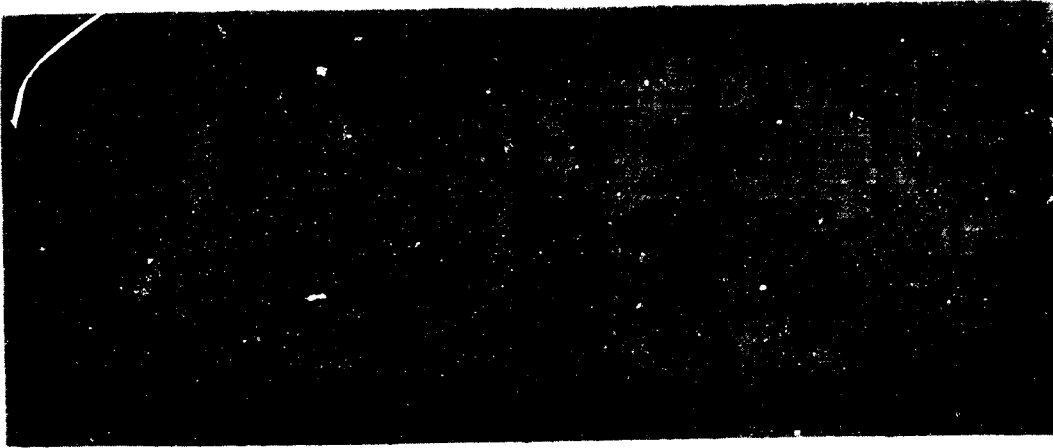
LEFT SEG. OXID. PRES. #2 (INACTIVE)

RIGHT SEG. OXID. PRES. #1

CENTER SEG. OXID. PRES. #1

RIGHT SEG. OXID. PRES. #2

CENTER SEG. OXID. PRES. #2



T/N 975-082-071

INSERTS IN CENTER SEG. ONLY



T/N 975-081-071

INSERTS IN CENTER & RIGHT SEGS.

Figure 111. Effect of Oxidizer Post Inserts

FOLDOUT FRAME

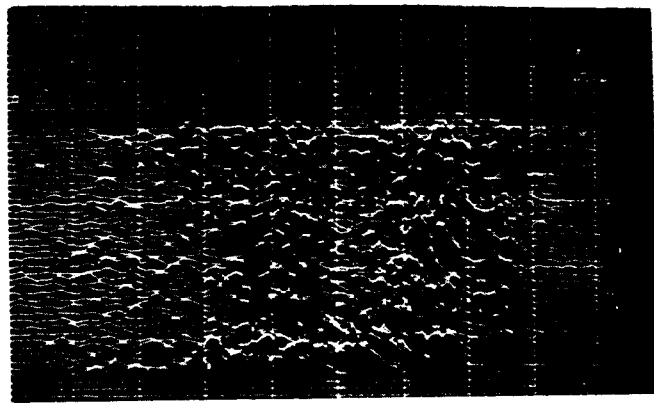
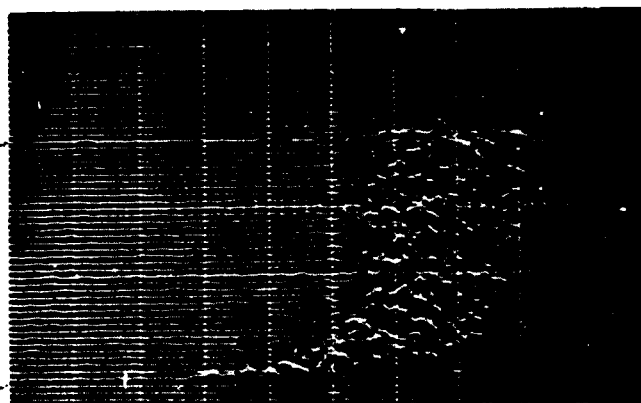
OXIDIZER INJECTOR PRESSURE

HORIZONTAL ACCELERATION

TEST 046

CUTOFF →

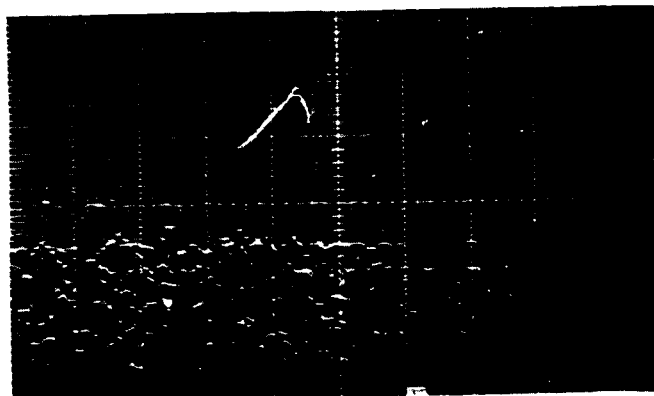
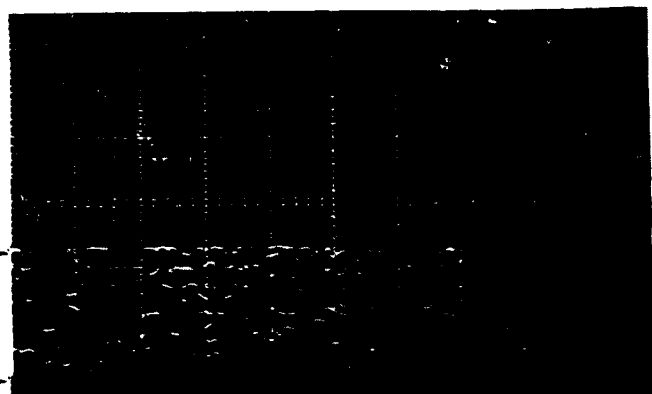
START →



TEST 047

CUTOFF →

START →



GAIN RELATIVE TO TEST 046 →

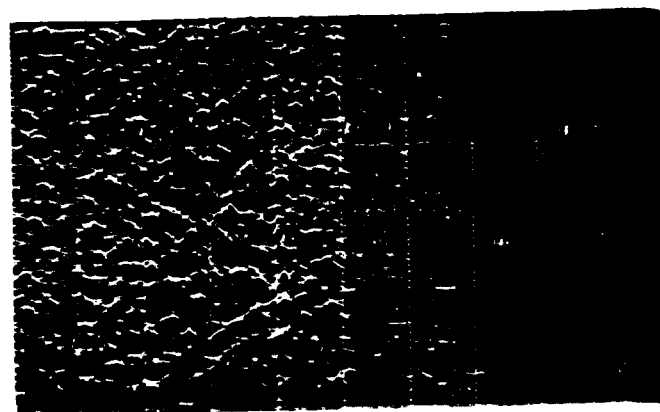
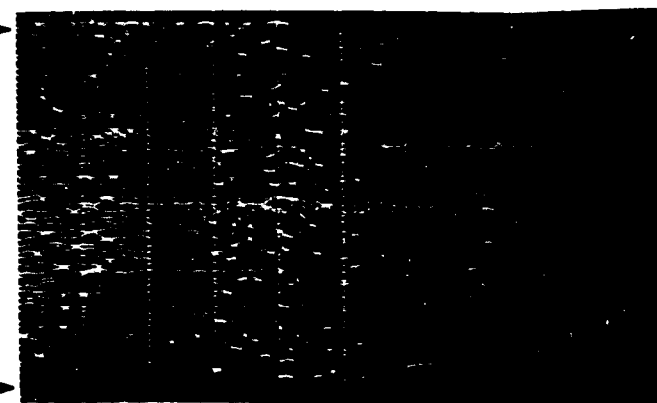
X10

X3

CUTOFF →

TEST 048

START →



GAIN RELATIVE TO TEST 046 →

X10

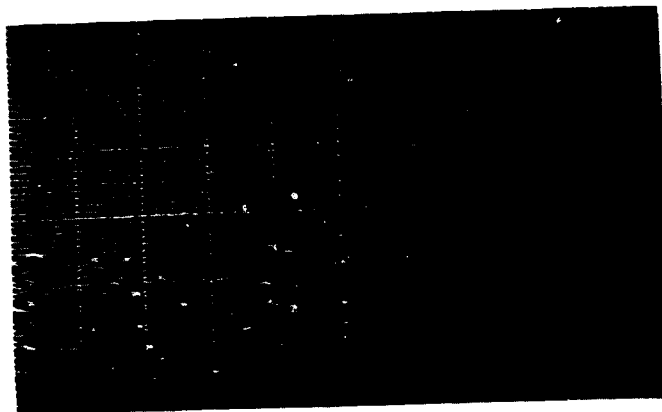
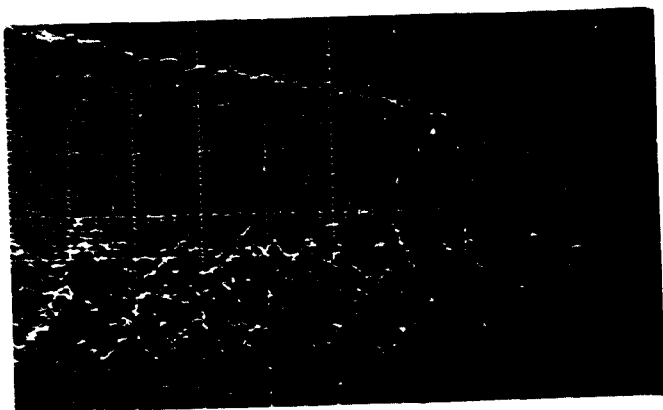
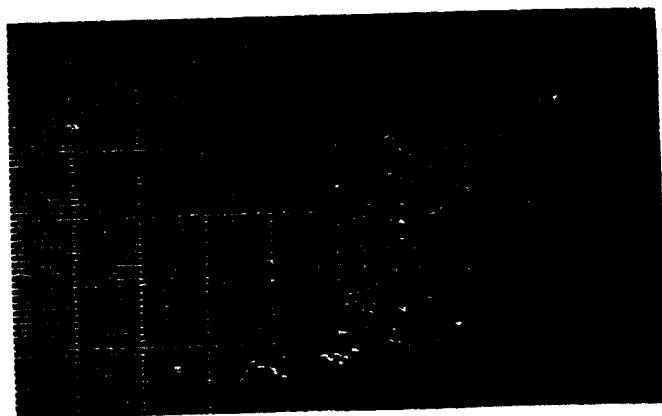
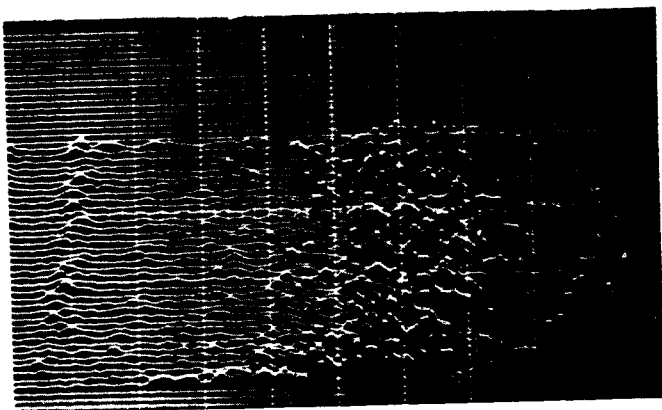
X3

FOLDOUT FRAME

2

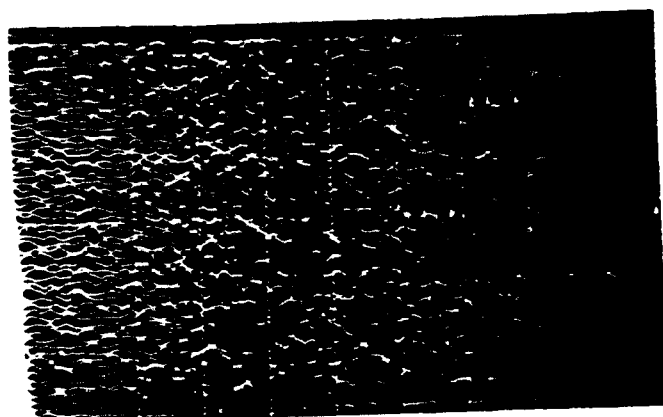
OXIDIZER DUCT PRESSURE

OXIDIZER DUCT ACCELERATION



X10

X6



X10

X6

Figure 112. Real Time Spectral Analysis

R-9049

234

test. The increase in oscillation frequencies is attributed to the chamber pressure increase, a trend observed during the multisegment test series.

An upward sweep in frequency during the early seconds of test 046 (Fig. 112) was a result of changing oxidizer temperature as the warm LOX in the ducting was replaced by colder fluid from the tank. The frequency range corresponds to the first resonance of the oxidizer post, and the change in frequency relates directly to the increased acoustic velocity of the colder oxidizer. This trend also was observed during the multisegment testing.

The effect of the oxidizer post inserts on the high-frequency oscillations in the range of 10,000 to 15,000 Hz was determined in tests 046 and 047. These tests differed in that the inserts were installed for test 047. Significant oscillation amplitudes were observed in all high-frequency measurements on tests 043, 045, and 046, which were conducted without LOX post inserts. Test 047 data are presented for comparison with test 046 (Fig. 112). The coherent high-amplitude oscillations of test 046 were reduced significantly in test 047 by the installation of the LOX post inserts. In particular, sonic analysis indicated the oxidizer pressure oscillations were reduced by an order of magnitude from 110 psi peak to peak to approximately 10 psi peak to peak. The hardware-mounted horizontal and axial accelerometers indicated residual amplitudes of approximately 200 g peak to peak, but these are thought to be structural resonances and may well have been masked by the high-amplitude data of the previous tests. Complex amplitudes for chamber parameters were reduced by a factor of approximately 2 to 4 with inserts.

Acoustic Oscillations

The presence or absence of transverse combustion chamber acoustic oscillations was difficult to ascertain for the majority of tests due to the lack of high-frequency chamber pressure measurements. As a result, the identification of possible occurrences of first transverse oscillations was made strictly by observance of the proper frequency in the oxidizer injection pressures and accelerometers.

1

For the most part, occurrences of possible first transverse oscillations were confined to start transitions or tests duplicating part of the start transient. The oscillation frequencies were in the range of 2200 to 3000 Hz and are thought to vary as a function of operating condition. The observed frequency was not correlated to operating conditions due to the transient character of most of the data.

Multisegment test 975-020 was conducted at engine start conditions with segment chamber pressures ranging from 270 to 310 psia and mixture ratios of 0.6 to 1.1. The test was a cycle evaluation with four 10-second-duration sections of mainstage interrupted by 2-second sections during which the engine was shut down. Indication of 2200-Hz oscillations was noted in the right segment at about 5 seconds into the third section of mainstage. At 9.5 seconds, the oscillations increased in amplitude and grew to 220 psi peak to peak in oxidizer injection pressure prior to cutoff. During the fourth section of mainstage, these oscillations were present to approximately 120 psi peak to peak in the center segment and 260 psi peak to peak in the right segment. These oscillations are thought to be the first transverse acoustic mode in the major combustor axis, but cannot be verified other than by frequency.

A possible instance of mainstage oscillations was noted in the left segment between 4 and 6 seconds into multisegment test 975-024. In this instance, 3000-Hz oscillations were noted to 400 psi peak to peak in oxidizer injection pressure No. 1, but were not readily apparent in the other oxidizer injection pressure. This segment had previously had the fuel cup recess removed in an attempt to decouple the 13-KHz oxidizer injection element hydraulic-coupled oscillations, and is not indicative of the linear breadboard hardware.

In general, it is thought that transverse acoustic oscillations are confined to start transients and tests at extreme off-nominal operating or hardware conditions. These oscillations are not considered a problem to testing with normal breadboard linear engine hardware and normal operating conditions.

001 SEGMENT STABILITY RESULTS

Segment 001 was modified for increased performance and tested at Propulsion Research Area NAN stand on tests 001 through 033, in 1971. The modification of high hydrogen velocity, low oxidizer velocity, and minimum oxidizer post thickness and deeper recess was designed to provide high cup atomization and subsequently higher η_{c*} .

With the higher relative velocities, it was expected that stability (at least in chamber acoustic modes) would be benefited. With the increased cup length and increased atomization, some possibility of high-frequency coupling action between the LOX post and cup was indicated. Inserts were installed to raise the oxidizer post hydraulic frequency and increase the damping.

Contrary to intention, the test results indicated lower η_{c*} , apparently because of increased burning within the cup. However, this cup burning did not result in any indications of combustion coupling phenomena.

Of the 33 tests, 001-006 were aborts, as were 008 through 010. Mainstage was achieved on tests 007, 011 through 017, and 033 with tests 018 through 032 designed to simulate engine start transients.

The instrumentation consisted of a horizontal and axial accelerometer, two LOX dome Photocons, and a Kistler chamber pressure measurement. Detail review of the oscillographs from tests 007 and 011 through 017 revealed no oscillation phenomena of importance.

The acceleration amplitudes were as high as 350 g peak to peak in mainstage, but levels as high as 265 g peak to peak were noted pretest and posttest. Both of these levels are considered high, but it should be noted that much of the frequency content was greater than 20 KHz, and there is little experience in this frequency regime to define what is normal. As the real concern with vibration is the physical displacement of parts (which is an inverse function of the

frequency squared), 350 g at 20 KHz is equivalent in displacement to only about 22 g at 5 KHz, or 56 g at 8 KHz, and these are demonstrated levels on the F-1, J-2, and J-2S engines. Thus, the accelerometer levels noted on these tests are deemed acceptable.

Pressure amplitudes in the LOX dome were 100 to 150 psi peak to peak, with pre-run and postrun noise levels of 60 psi peak to peak. Thus, they are comparable with existing and acceptable levels of LOX/hydrogen engines. The predominant frequency was 120 Hz which is attributable to electrical noise. There was also significant energy at 1800 Hz, 7 KHz, 10 KHz, and 15 to 20 KHz. The 1800-Hz appears to be the first mode of the oxidizer dome. The 7 to 10 KHz has been observed to shift with oxidizer temperature, and apparently is also a mode in the LOX manifold and/or feed system. The 15 to 20 KHz is probably the first mode of the oxidizer posts.

In all tests, the Kistler was judged to be yielding erroneous pressure data. The frequency content and amplitude variations closely resembled those of the accelerometers, while the dome pressures were exhibiting clearly different oscillations. Thus, the Kistler data were disregarded.

All amplitudes were acceptable levels and no sustained frequencies of oscillations were noted. Based on the mainstage tests, the engine is judged satisfactory with respect to its oscillation characteristics.

BREADBOARD NO. 1 HIGH-FREQUENCY RESULTS

The high-frequency characteristics of each of the test bed segments were monitored with a dome-mounted accelerometer, mounted so that the sensitive axis was along the major transverse axis (horizontal direction) of the individual segments. In addition to the accelerometer instrumentation, Photocon transducers monitored the high-frequency oscillations in the oxidizer domes of segments 1, 5, 15, and 20 and the fuel injection pressures in segments 1 and 5.

High-frequency data were reviewed in detail for mainstage tests 624-009 through 624-013 and are considered typical. Surveys were made on the other tests. Acceleration levels for the complex waves were 100 to 300 g peak to peak. Pressure amplitudes were in the range of 20 to 200 psi peak to peak. The lower level was typical. Occasional bursts exceeded these values.

Several frequencies occurred intermittently throughout the tests. The primary frequencies were 13 KHz (discussed earlier), which is associated with fluid resonance within the oxidizer injection elements, and two other frequencies of approximately 6 KHz and 8 KHz, which are thought to be associated with the propellant feed systems.

Test 624-012 was reviewed in particular detail, as it was an extended duration test of 100 seconds at 1130-psia chamber pressure with PU valve excursions.

Segment 1 showed the most consistent 13-KHz oscillation content with average complex amplitudes of 270 to 400 g peak to peak in the horizontal accelerometer and 100 to 250 psi peak to peak in oxidizer injection pressure. The fuel injection pressure indicated 6-KHz oscillations to approximately 100 psi peak to peak. Nearly all segments had at least some indication of 13-KHz content.

Segment 14 indicated some clear bursting at 13 KHz during the middle portion of the test, while segments 2 and 18 had sporadic 13-KHz oscillations during approximately the first 20 seconds of the test. Clear 13-KHz oscillations also were evident in segment 2 during the final 15 seconds of the test.

Nearly all segments had indications of 6-KHz oscillation content at some time during test 012; however, several segments (in particular, segment 13) had indications of 6 KHz throughout most of the test.

Eight-KHz oscillations were particularly evident in segments 3, 5, and 15.

The PU valve was actuated from the null to the maximum position at approximately 20 seconds and back to the null position 85 seconds into test 012. These PU valve position changes were evident to some extent in high-frequency oscillation content. While the effect was not apparent in all of the segments, segment 2 exhibited clear 13-KHz oscillations during the first 20 seconds of the test. When the PU valve was cycled to the maximum position, these oscillations became less clear until the PU valve was cycled back to the null position.

The effect of PU position is a function of its imposed variation in the operating conditions of the individual segments, which are essentially individual chambers.

Oscillations at frequencies of 10 to 13 KHz were present in all segments during the cutoff transients of tests 624-010 through 624-013. These oscillations occurred as the chamber pressure dropped below approximately 50 percent, and were present to 500 g peak to peak in acceleration and 200 psi peak to peak in oxidizer injection pressures. Similar oscillations were noted during the start transients in some segments.

Some 400 Hz, feed-system-coupled buzz oscillations were noted to amplitudes of 200 psi peak to peak in the early part of transition into mainstage.

The primary frequencies observed during the testing of the test bed were the same as those noted during the previous segment and multisegment tests. Amplitudes were considerably lower. These oscillations, in particular the 12 to 13 KHz, appeared to be less well defined in the test bed. This may be due to a difference in fuel injection velocity between the segment tests and those with the test bed. The nominal fuel injection velocity for the segment tests was approximately 1200 to 1300 ft/sec and 1650 to 1900 ft/sec for the test bed. This difference was due to a higher fuel injection temperature and slightly lower mixture ratio for the test bed tests.